DOCUMENT NO. 665D4201
20 JANUARY 1966

GRAVITY GRADIENT STABILIZATION SYSTEM for the APPLICATIONS TECHNOLOGY SATELLITE

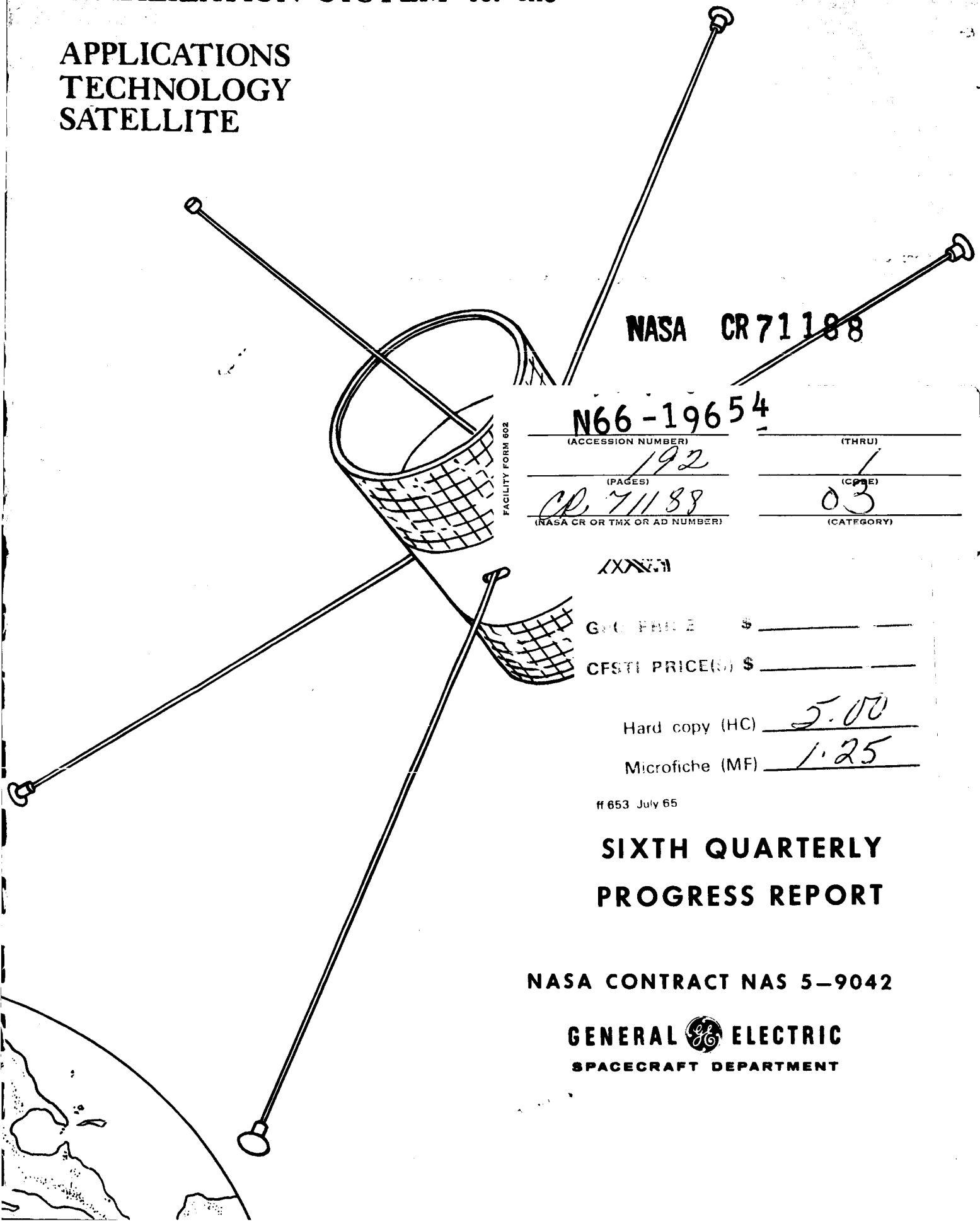

SIXTH QUARTERLY PROGRESS REPORT

NASA CONTRACT NAS 5-9042

GENERAL ELECTRIC
SPACECRAFT DEPARTMENT

DOCUMENT NO. 66SD4201

20 JANUARY 1966

SIXTH QUARTERLY PROGRESS REPORT
FOR THE
APPLICATIONS TECHNOLOGY SATELLITE
GRAVITY GRADIENT
STABILIZATION SYSTEM

1 OCTOBER THROUGH 31 DECEMBER 1965

CONTRACT NO. NAS 5-9042

FOR THE

NATIONAL AERONAUTICS AND SPACE ADMINISTRATION
WENDELL SUNDERLIN
ATS TECHNICAL OFFICER

APPROVED BY _____

R. J. KATUCKI, MANAGER
PASSIVE ATTITUDE CONTROL PROGRAMS

GENERAL ELECTRIC

SPACECRAFT DEPARTMENT

A Department of the Missile and Space Division

Valley Forge Space Technology Center

P. O. Box 8555 • Philadelphia, Penna. 19101

TABLE OF CONTENTS

TABLE OF CONTENTS (Cont)

TABLE OF CONTENTS (Cont)

LIST OF ILLUSTRATIONS

LIST OF ILLUSTRATIONS (Cont)

LIST OF ILLUSTRATIONS (Cont)

LIST OF ILLUSTRATIONS (Cont)

LIST OF TABLES

ABSTRACT

The status of the Attitude Determination Program (ADP) is presented in Section 2.2. Discussions with the NASA/Goddard Data Processing group has resulted in changes to the ATS data formats specification. Other investigations in the ADP were coordinated with NASA/Goddard during the reporting period. The progress in updating each of the sections of the preliminary flight evaluation plan is tabulated in Section 2.3. The list contains those portions of the flight evaluation plan that require changes in addition to the status of each task. The current philosophy of gravity-gradient orbit test requirements was documented in preliminary form in ATS System Memo No. 068. Copies of the memo will be included on the agenda of the NASA design review scheduled for early January, 1966 at General Electric.

Test firings of the ball-lock mechanism were successfully completed. This device was selected to replace the cable cutter mechanism for release of the damper boom tip masses. The new mechanism is described and illustrated in Section 3.2.

A summary of the engineering testing performed at GE on the first primary boom (Engineering Unit T-1a) is included in Section 3. The unit was exposed to pre-environmental testing, including deployment on the 150-foot track facility at GE. However, engineering evaluation of the primary boom was suspended pending installation of retrofit kits to correct problems noted in the postvibration functional test.

The major effort in the Combination Passive Damper (CPD) area was devoted to assembly of Engineering Unit 1. The difficulties encountered during assembly of this unit were found to be due to the exacting and time consuming adjustments.

Throughout the assembly of the CPD Engineering Unit 1, recommendations were made that proved to be of great assistance in the assembly of Engineering Unit 2 and the Prototype units. Detailed photographs are included in Section 4 of the Engineering Unit 1 assembly sequence. These photographs clearly illustrate the complexity of the CPD.

The encoder disc in the boom angle indicator broke in a number of places during vibration testing of the CPD Engineering Unit 1. This failure was the cause of improving the encoder disc both from the physical and material standpoint. A beryllium-copper disc was successfully subjected to vibration tests which exceeded qualification requirements.

A series of test setups was completed on the Low Order Force Fixture (LOFF). Pictures are included in Section 4 which demonstrate the versatility of this unique test equipment.

Results of a thermal analysis, that was completed for the TV Camera System and an evaluation of corona effects under conditions of evacuation, are presented in Section 5. As part of the engineering evaluation, the TV Camera System was exposed to temperature and solar-vacuum environments. The data obtained in these tests were analyzed, and the results are presented in Section 5.

Results of the PCU environmental tests are presented in Section 5 along with the latest schematics of PCU functions.

The performance of the Solar Aspect Sensor (SAS) was verified in a series of tests in direct sunlight. These tests are described together with an analysis that was completed of the index of refraction.

Ground test activities are presented in Section 6 under the categories of engineering evaluation tests, qualification tests, and flight acceptance tests. In accordance with the program schedule, the gravity-gradient system engineering units were subjected to a prescribed series of functional performance and environmental tests. This series is aimed at an evaluation of design adequacy and a comparison of performance of each unit before and after exposure to qualification-level environments. A summary of these engineering evaluation tests conducted to date is presented in Section 6.1.

The latest revision to the parts qualification program is presented in Section 6.2. The Group A and Group B parts are updated in Tables 6-1 and 6-2 from the corresponding data presented in the Fifth Quarterly Progress Report. The status of these parts is presented in Table 6-3.

Three reliability analyses are reported in Section 10. The first is a determination of the desirability of including limit-switching in the emergency mode of the primary boom operations. The second study is a preliminary assessment of the CPD boom angle indicator, and the third reports failure-mode risk assessments of the primary boom subsystem.

Two items are reported as new technologies which have resulted from development of the passive stabilization system for the NASA Applications Technology Satellite (ATS). The items were developed as part of implementing the Combination Passive Damper. The first item concerns the damper boom angle indicator readout device. The principle on which this device operates was first reported as a new technology in the Fourth Quarterly Progress Report. The second item describes the CPD clutch mechanism that is used for transferring either one of the two damper systems to the damper boom.

The GE Gravity Gradient System Prototype Field Test Plan, Revision A to GE document 65SD4499, was delivered to NASA/GSFC during December. This document contains the GE input to the Hughes Aircraft Company (HAC) System Qualification Test Plan. The information is intended for use during the system environmental tests to be conducted by HAC. These tests are required to establish mechanical and electrical compatibility of the prototype components of the Gravity Gradient Stabilization System with the ATS spacecraft. Suggested directions are included in the report for aligning the component axes to the spacecraft principal axes, and detailed procedures are given for checking component performance when commanded through the HAC telemetry system.

SECTION 1
INTRODUCTION

1-1 PURPOSE

This report documents the technical progress made during the period from 1 October to 31 December 1965, toward the design and development of Gravity Gradient Stabilization Systems for the Applications Technology Satellites.

1.2 PROGRAM CONTRACT SCOPE

Under Contract NAS 5-9042, the Spacecraft Department of the General Electric Company has been contracted to provide Gravity Gradient Stabilization Systems for three Applications Technology Satellites: one to be orbited at 6000 nautical miles (ATS-A), and two to be orbited at synchronous altitude (ATS-D and ATS-E). Each system will consist of primary booms, damper boom, damper, attitude sensors and the power conditioning unit. In addition to the flight systems, GE will provide a thermal model, a dynamic model, an engineering unit and two prototype units. GE will also supply two sets of aerospace ground equipment.

SECTION 2

SYSTEMS ANALYSIS AND INTEGRATION

2.1 EVENT SUMMARY

Events having a significant bearing on the course and direction of ATS systems analysis efforts during the past quarter are summarized as follows:

5 October	GE reported (by TWX) on the sensitivity of ATS-D/E yaw errors to the frequency of application of station-keeping thrust. The error (due to thruster effects only) was reported as 15 degrees for a 7-day-on/7-day-off cycle and 6.3 degrees for a 3-hour on/ 3-hour-off cycle.
8 October	Typewritten drafts of the ATS System Requirements Specification were forwarded to NASA for review.
14 October	ATS capture studies were completed and issued as PIR 4174-030. Results included upright capture for ATS-A as well as constraints for ATS-D/E capture.
19 October	Letter to NASA/GSFC providing GE's rationale in planning the use of orbit parameters rather than world map data, in GE's Attitude Determination Program.
22 October	Letter to NASA/GSFC delineating GE's requirements for non-GE telemetry data. Included in the letter was GE's rationale for requesting the data.
27 October	NASA/GE data processing interface meeting and working session at GE. The major portion of outstanding action items were resolved and summarized in minutes of the meeting published the same date.
27 October	In response to a NASA action item, GE submitted six copies of a PIR entitled "Motion of Rod End Mass Relative to Center Body Rotation."
28 October	In response to a NASA action item, GE published data on the "Response of ATS to a Solitary Impulse (PIR 4174-032). For a given attitude determination capability, the results provide the impulse required (on either the pitch, roll, or yaw axis) to produce a measureable response in pitch, roll, and yaw. For example,

assuming a 1-degree measurement system capability and the applied impulse about the yaw axis, 0.0075 lb-ft-sec is sufficient to produce a measureable yaw response, 0.075 lb-ft-sec for a measureable pitch response, and 0.090 lb-ft-sec for a measureable roll response. The 1-degree capability is a partial function of orbital position and will therefore introduce a constraint on orbital position for the corresponding test package of the Orbit Test Plan.

28 October — The analytical model for simulation of the hysteresis damper in the ATS Mathematical Model was outlined in PIR 4174-033.

29 October — PIR's were published on effects of rod misalignments and unequal solar absorptivities (PIR 4174-034 and PIR 4174-023 Rev A).

1 November — The analytical approach to be used for real-time attitude determination during a pitch inversion maneuver was investigated and summarized in PIR 4424-055. The technique uses sun sensor data only with the assumption of planar inversion in a plane of known orientation.

4 November — NASA response to GE's request for non-GE telemetry data (ATS Systems Memo No. 066).

5 November — NASA contacts were established in the boom thermal bending analysis and test areas; plans were established for the conduct of GE thermal bending tests in the NASA/GSFC test facility; first tests (with an instrumented, seamless rod) are scheduled for early January.

10 November — An ATS Data Formats Specification (SVS-7429) was completed and submitted to NASA/GSFC for signature approval. The specification includes all data formats used for the interchange of flight data between GE and NASA.

18 November — GE received a revised version of the Gravity Gradient Interface Specification (S2-0401-1) for review and comment.

29 November — Based on data formats of ATS Data Formats Specification SVS-7429, requirements for a modified data simulation program were generated. This program will be used for a preliminary simulation of the NASA data tape for checkout of the data reduction module of the Attitude Determination Program.

13 December — GE submitted (to NASA) comments, additions, and changes to the Gravity Gradient Interface Specification (S2-0401-1) received on 18 November.

15 December — Analytical studies of ATS-A pitch inversion, based on a predetermined timing sequence, were completed and documented as PIR 4174-042.

20 December — First results of investigations using the Attitude Determination Investigation Program (ADIP) were published as PIR 4424-061, "Sensitivity Coefficients and Estimation of ATS Attitude Angles."

30 December — ATS Systems Memo No. 068, "ATS Gravity Gradient Orbit Test Philosophy," was completed and prepared for publication. Points of contention will be reviewed with NASA at the ATS Program Review on 6 January 1966.

2.2 ATTITUDE DETERMINATION PROGRAM

Since the first issue of "ATS Data Formats," Specification SVS-7429, 10 November 1965, several aspects of the data specification have been under discussion with NASA/Goddard Data Processing, particularly pertaining to the GE Raw Telemetry Data Tape (RTDT). By mutual verbal agreement between GE and the Goddard Data Processing organization, several changes to the RTDT format have been made primarily concerning bit formats for the two telemetry modes. Since SVS-7429 has not yet been officially approved by the cognizant NASA organization, these changes to the document are expected to be made prior to the official approval.

Other data formats described in this specification are:

- NASA Attitude Data Tape(ADT)
- TV 35 mm film
- Quick Look TTY data to and from GE

The Gerber scanner that is to be used to read the 35 mm TV film has been shipped to the manufacturer for modification to handle the film. On the last day of this reporting period

the modified scanner has been returned to GE but no checkout or inspection of the equipment has been performed.

A Data Simulation Program (DSP) was programmed during this quarter and is to be used in the investigations of attitude determination. Using a simplified orbital model, the spacecraft is perturbed sinusoidally in any and/or all axes. The resultant outputs are the sensed direction cosines to the earth and sun read by the appropriate IR and Solar Aspect Sensors. This data is inputted to the ADIP for analytical studies. Antenna polarization data is also determined in the DSP. The DSP was then further modified to output the RTDT format specified in SVS-7429 by simple simulations of all other telemetry functions. The simulated RTDT data will be used to check out the Data Reduction Program which will perform diagnostic processing for Gravity-Gradient Subsystem evaluation from telemetry data.

The ADIP was programmed and used during this quarter to perform several analytical investigations. At present, the ADIP requires approximately 11.5k word core storage in the IBM 7094 computer.

The ADIP was used to generate direction cosine sensitivity coefficients for SAS and IR sensors. An analytical investigation was also performed to show that these coefficients can be used to compute spacecraft attitude, by hand, to an accuracy of 1/2 degree or less, when the pitch, roll, and yaw angles are less than 10 degrees. The sensitivity coefficients have been published in a tabled format such that the spacecraft attitude can be calculated by knowing: (a) SAS direction cosines assuming zero attitude angles in all axes, (b) SAS direction cosines received from telemetry, and (c) IR direction cosines received from telemetry.

The NASA/Goddard orbit model computer program was received from NASA and converted by GE from FORTRAN II to FORTRAN IV.

2.3 FLIGHT EVALUATION PLAN

In continuing efforts toward completion of a final version of the ATS Flight Evaluation Plan, an outling indicating areas of particular need has been established. The progress in updating each of the pertinent sections of the Preliminary Flight Evaluation Plan (PFEP) is indicated in Table 2-1.

Primary emphasis to date has been placed on establishing details of the weekly analysis operation. In this effort specific philosophy, task definition, and specification of formats, to be used in data presentation, are being set.

2.3.1 ATTITUDE DETERMINATION

In order to optimize the weekly processing of flight data for return to NASA/GSFC, a survey of input data will be performed prior to its use in attitude calculations. This survey will be directed toward verifying the accuracy and continuity of various sensor outputs and determining the usefulness of any redundant data inputs. The actual scan of data will be performed on raw data prior to any compression, integration, or smoothing. The results of this input data survey will be incorporated into a set of instructions to the ADP, indicating useable data inputs as noted and the corresponding data quality.

In addition to examination of input data, ADP operation will be monitored through surveillance of intermediate outputs and confidence check parameters to be generated in calculating attitude angle data. Also, the output data being prepared for return to NASA/GSFC will be available for examination and quick evaluation.

TABLE 2-1. OUTLINE FOR UPDATING
PRELIMINARY FLIGHT EVALUATION PLAN

PFEP SECTION	TITLE	AREA REQUIRING UPDATING	STATUS
2	General Description	Operational definition and support planning	Awaiting further integration with Orbit Test Plan; further update will come with generation of Orbit Test Handbook
3	Measurement System	Antenna polarization	Awaiting technique definition; format specification for data transmission has been completed (see Section 2.2)
		Supplementary information	Nominal calibration data has been acquired on most telemetry functions; completion and further updating needed is underway. Vehicle date and on-orbit information be be required is being defined
5	Data Reduction and Processing	Data system checkout	Preliminary data simulation tape and engineering unit interpretation have been generated in conjunction with the attitude date simulation program output (see Section 2.2)
6	Flight Analysis and Evaluation	Analysis philosophy	Specific analysis approach philosophy and task lists are being established for the various phases of analysis (see text).
		Data requirements	Detailed specification of formats to be used for data presentation is being generated (see text)

2.3.2 VEHICLE ATTITUDE PERFORMANCE

ADP output data will be used in conjunction with gravity-gradient configuration knowledge and orbit information to evaluate vehicle attitude performance. The primary aims of this analysis will consist of flight data comparison with ATS Math Model predictions, using amplitude excursions, frequency components, and transient decay characteristics as parameters. Subsequent evaluation will include consideration of contributing influences such as vehicle position, disturbance torques, and operational effects.

2.3.3 DIAGNOSTIC (SYSTEM HARDWARE)

Telemetry data will be scanned by computer on a file-by-file (i.e., station pass) basis. Summarized results will be presented in one of several "survey" formats. This summary will give initial status (system and subsystem operating configuration) of the vehicle at acquisition and will indicate any subsequent change in this status during the contact period. Diagnostic functions (temperatures, voltages, etc.) will be surveyed and summarized, with any out-of-limit function being noted. Complementing these survey formats will be detailed subsystem formats, available for more comprehensive presentation of data pertinent to a particular system or subsystem:

a. X-boom
- Configuration (lengths, scissor angles, rod extension, clutch positions)
- Environment (temperature, pressures)
- Tip data availability (TV on/off)

b. Damper
- Configuration (damper in use, boom angle, squib monitors)
- Environment (temperatures)

c. PCU
- Voltages
- Command monitors

d. Earth Sensor - Outputs (all axes)
- Status (on/off, sun in view)
- Environment (temperatures, voltages)

e. Solar Aspect - Outputs (angles, detector number)
- Status (on/off)
- Environment (temperatures)

f. Television - Status (on/off)
- Environment (currents, voltages, temperatures)

(A special format will be established for presentation of data derived from television pictures.)

These formats will be available on an as-requested basis.

2.4 ORBIT TEST PHILOSOPHY

The current philosophy of gravity-gradient orbit test requirements has been documented in ATS Systems Memo No. 068. This document summarizes the major constraints, as well as the major points of contention, in the accomplishment of gravity-gradient orbit test objectives. Mission objectives are defined and categorized in Table 1 of the memo and a specific test sequence is proposed, with reservations, in Table 2 of the memo. Each test in the second table is keyed to mission objective categories presented in the first table and the specific philosophy of each separate test is discussed. A preliminary version of the Orbit Test Plan is being documented in "package" format; each package representing a separate and distinct test of the Orbit Test Plan.

2.5 REVISED SYSTEM ERROR BUDGET

A complete error budget is being prepared for both the ATS-A and ATS-D. The primary sources of error (thermal bending, magnetics, etc.) have been evaluated in the past.

These error sources are being updated. Added to those,will be error sources due to manufacturing tolerances, uncertainties, etc. Spring null shift, short rods, unequal reflectivities of rod and vehicle, etc., will be evaluated and listed. Most of the error sources have been identified, and hand calculations as well as computer runs have been used to estimate the errors.

2.6 BOOM THERMAL BENDING ANALYSIS

The effort to improve the thermal bending model for the booms consists of two main tasks. One being an analytic approach, the other an empirical approach.

In the analytic area, a rigorous solution to the shell equations was programmed for the digital computer and results obtained. These results are being evaluated at the present time. The shell equations, solution, numerical evaluation, and technique for correcting boundary conditions are being assembled into a coherent report. This report is to be completed by 31 January 1966. Concurrent with this effort, a lumped parameter description of the rod was undertaken and solutions obtained. These solutions will be used as approximations to check the results from the rigorous analysis.

A trip was made to NASA/Goddard to confer with H. Frisch and become acquainted with his efforts in the area of boom bending. An evaluation of his analysis and comparison with our current analysis is underway. The thermal test facility at NASA/Goddard was reviewed with their people. We are planning to use this facility to perform thermal bending tests on sample rods.

The first test will be performed with a control rod. It is a 1/2-inch-diameter seamless, stainless steel tube which is currently being instrumented with thermocouples. We have been successful in welding 5-mil Chromel-alumel thermocouples to this material. The purpose of this test is to verify our ability to control rod environment, predict temperature distribution, and correctly measure temperatures. Upon the successful completion of

the control test, a series of tests on bare BeCu rods will be undertaken. Rod samples are available and we have been successful in welding 1-mil iron-constantan thermocouples to them.

A test plan has been prepared for the above series of tests.

The end fitting for the control rod is currently being drawn up for manufacturing.

2.7 BOOM DYNAMICS

Work during this quarter has been devoted to obtaining numerical results from the equations shown in Section 2.9 of the Fifth Quarterly Progress Report.

The equations described for the order 42 system exceed the capacity of the existing computational system, thus some reduction has been necessary. This reduction in the scope of computations has taken the form of: (1) restriction to a circular orbit, (2) restriction to body rotation about a single axis, and (3) reduction of the size of the mathematical description of the satellite to 24 coordinates. Debugging of the computations has to date resulted in a partial processing of data, but a run to completion has not yet been accomplished. The effects of the reduction in order are assessed as follows:

a. Restriction to a circular orbit - This is felt to be a minor restriction and is not estimated to have a significant effect on results.

b. Restriction to body rotation about a single axis - This restriction will not affect significantly, the computation of thermal "twang" inversion and scissoring computations. Rod extension cases may be affected significantly. Further work to reduce this restriction will be attempted after successful processing with the restricted system is obtained.

c. Reduction of the number of vehicle coordinates - The size of the representation of the system has been accomplished by eliminating the rotational coordinates of the masses at the ends of the booms as follows.

If the stiffness matrix is considered partitioned so that the coordinates to be eliminated are indicated by the subscript 2 and those retained are designated by the subscript 1

$$\begin{bmatrix} K_{11} & K_{12} \\ K_{21} & K_{22} \end{bmatrix} \begin{bmatrix} X_1 \\ X_2 \end{bmatrix} = \begin{bmatrix} F_1 \\ F_2 \end{bmatrix} \tag{2-1}$$

$F_2 = 0$ since when the coordinate is eliminated no external force may be applied to it.

Then

$$K_{11} X_1 + K_{12} X_2 = F_1$$

$$K_{21} X_1 + K_{22} X_2 = 0 \tag{2-2}$$

From the second equation

$$X_2 = K_{22}^{-1} K_{21} X_1 \tag{2-3}$$

Substituting this in Equation (2-1) and combining terms yields

$$K X_1 = (K_{11} - K_{12} K_{22}^{-1} K_{21}) X_1 = F_1 \tag{2-4}$$

The resulting representation uses the total representation of the elastic characteristics, but permits no application of either inertial or externally derived forces. Therefore, if the sums of these terms are actually small order terms, relative to the inertial forces at the coordinates retained, the representation can be considered

adequate. Due to the small I_o of the end masses, compared to the total rotational moment of inertia of the system, the reduction indicate is felt to be acceptable. Evaluation of this effect, in a computational procedure which does not include orbital forces, is presently underway.

SECTION 3
BOOM SUBSYSTEM

3.1 KEY EVENTS

5 October	Engineering Unit T-1 Damper Boom Assembly shipped back to deHavilland for retrofit.
8 November	Initial engineering testing on T-1a Primary Boom Assembly completed at GE.
23 November	Detail drawings for Primary Boom Assembly resolution received from deHavilland.
4 December	Retrofitted Engineering Unit T-1 Damper Boom Assembly received at GE.
8 December	Engineering testing started on retrofitted T-1 Damper Boom Assembly at GE.
15 December	T-1a Primary Boom parts rework completed at GE for installation of deHavilland retrofit kit.
26 December	Retrofit kit for T-1a Primary Boom Assembly received at GE.

3.2 DAMPER BOOM TIP MASS RELEASE

The Avdel ball-lock mechanism, deHavilland plunger and lever arm, and Holex linear actuator (squib/thruster) combination selected to replace the original Conax bolt cutters for the Damper Boom tip mass release, have undergone functional testing during assembly testing at GE with the use of Engineering Unit T-1. The ball-lock mechanism (Figure 3-1) and plunger (Figure 3-2) are integral parts of the Damper Boom Assembly (Figure 3-3), and the linear/actuator and lever arm are mounted on the baseplate of the CPD as shown in the test setup in Figure 3-4. The two receptacles shown at the ends of the ball-lock mechanism in Figure 3-2 provide the coupling between the tip mass housing and the central body when the Damper Boom is in the stowed position. At deployment, the plunger (Figure 3-4) travels through the slot in the center of the ball-lock assembly and contacts the two spindles which permit the balls to depress inside the housing and release the receptacles. The plunger movement is initiated by either or both the electroexplosive squib-linear actuator devices.

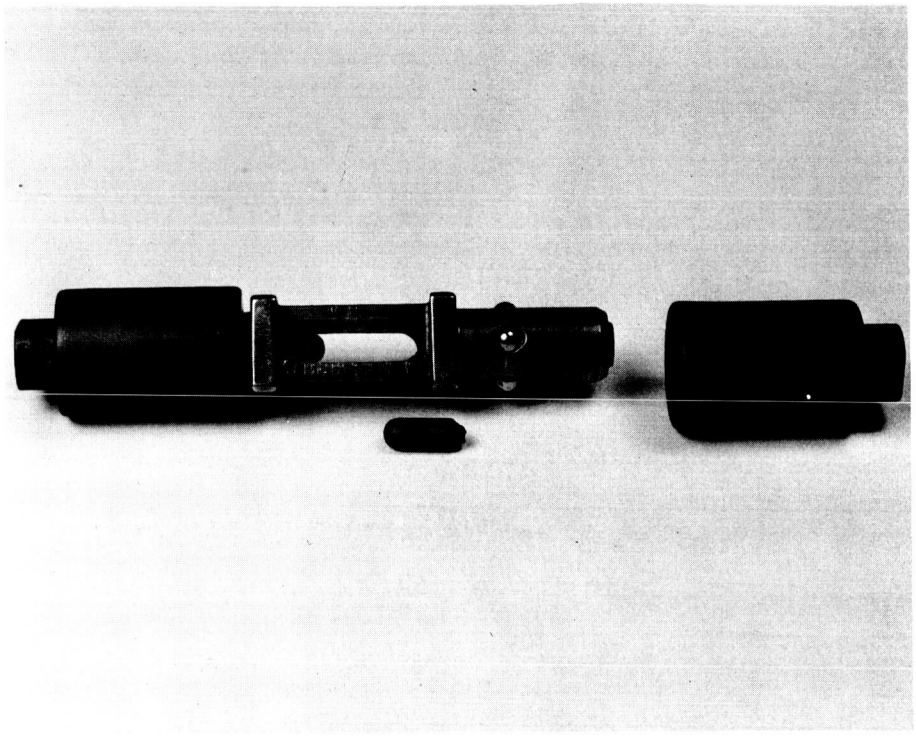

Figure 3-1. Avdel Ball-Lock Mechanism

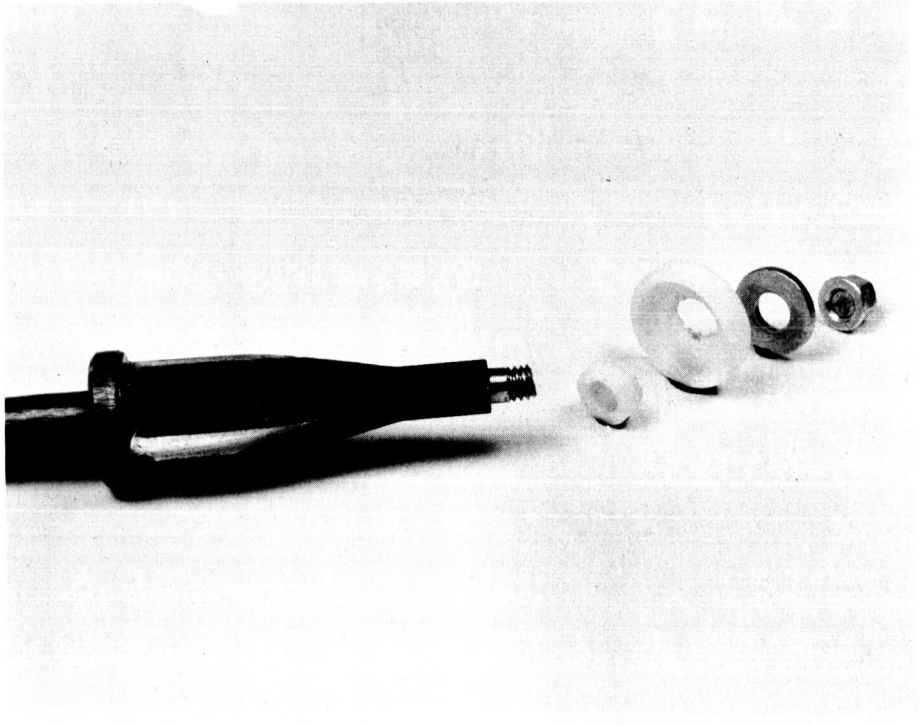

Figure 3-2. Plunger Shown With Spacing Hardware

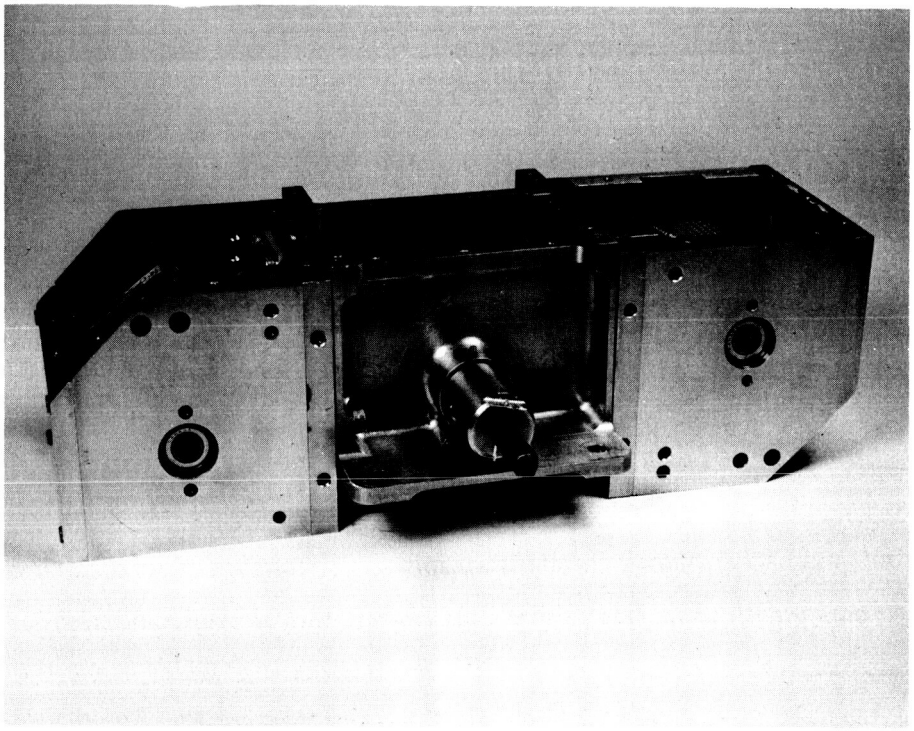

Figure 3-3. T-1 Damper Boom Assembly

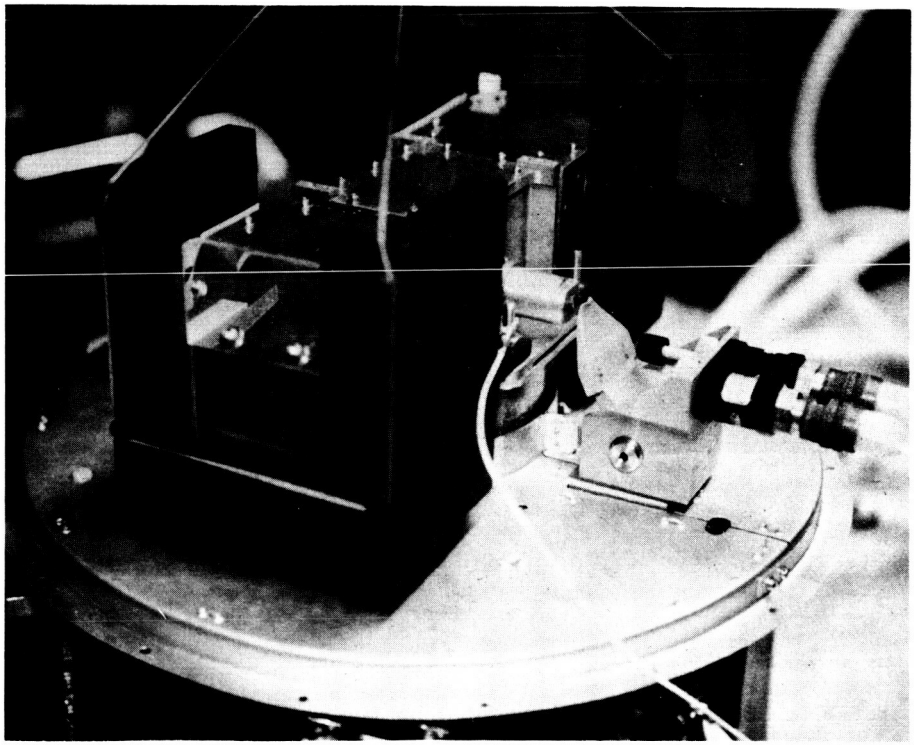

Figure 3-4. Squib Firing Test Setup, T-1 Damper Mounted to CPD

The tip masses then separate from the central body in a manner similar to that illustrated in Figure 3-5. In the actual system, the end of each tape is secured to the central body. The spring shown at the end of the central body provides the initial separation force and the three guide pins ensure coaxial separation.

Details of the tip mass are shown in Figure 3-6. The tape storage is clearly shown in the illustration together with the lever arm which provides tension against the tape.

The adequacy of this combination for accomplishing the release of the tip masses has been proven by functional tests. Although the above combination has proven adequate for releasing the tip masses, individual parts have experienced secondary failures during accomplishment of the releases.

Two Avdel ball-lock mechanisms were used during the tests. Each mechanism was subjected to one single and one double squib/thruster firing. The mechanism subjected to a single firing first showed no visible abnormal spindle damage after the first firing, but sustained one broken spindle (as seen in Figure 3-1) during the second (double) firing. This mechanism also underwent two mechanical releases at deHavilland prior to shipment of the T-1 Damper Boom Assembly. The mechanism subjected to a double firing showed no visible abnormal spindle damage after the first firing but sustained two broken spindles during the second single firing. The spindles from both of these expended ball-lock mechanisms are presently under analysis. Consideration is being given to treating this mechanism as a "one-shot" device, similar to the squib/thruster, and concurrently a spindle material change is being investigated to ensure that the spindles will be intact after this "one-shot."

Six Holex linear actuators (squib/thruster) were used during the tests. Each actuator was fired only once. There were two single firings and two double or simultaneous firings. The second double firing only resulted in breakage of one piston at the end of its travel.

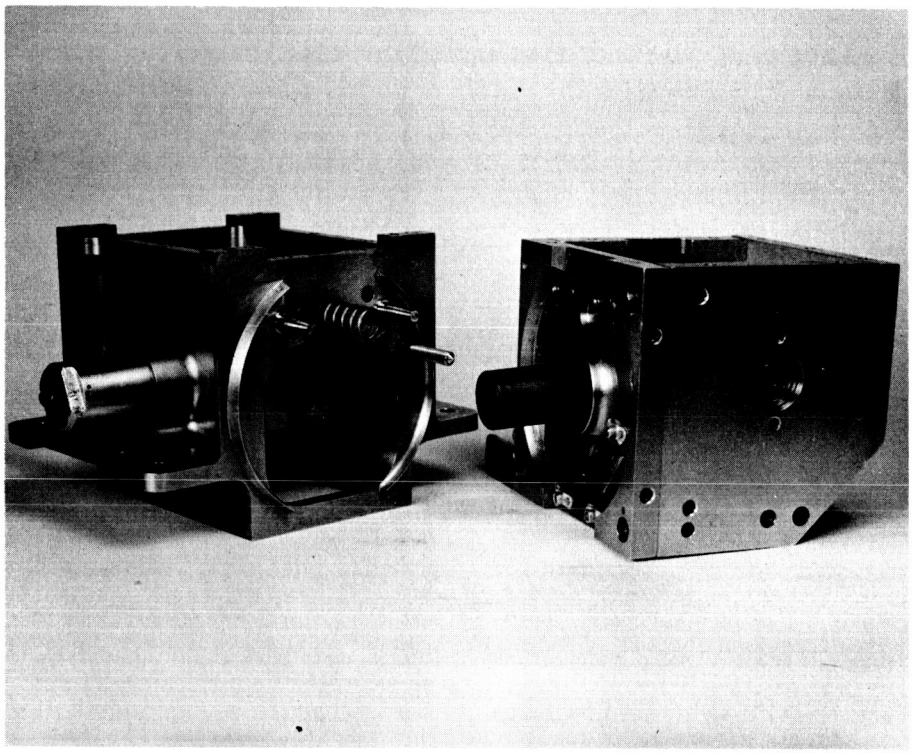

Figure 3-5. Damper Boom Central Body (Left) and Tip Mass

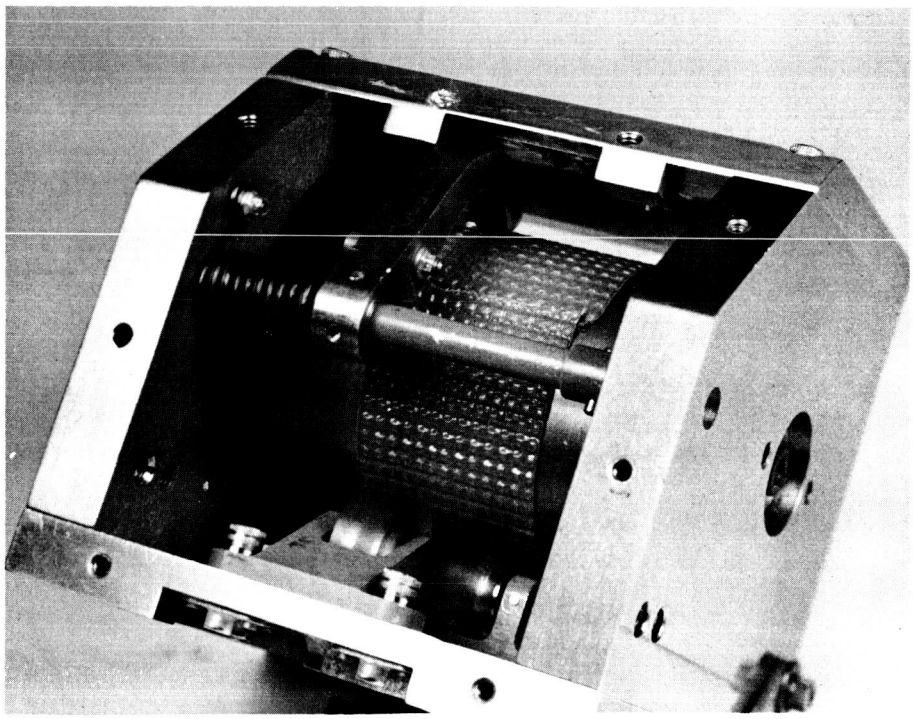

Figure 3-6. Damper Boom Storage Drum Details

None of the other firings resulted in any noticeable abnormal piston damage. Simultaneous firing of both linear actuators is a system requirement but cannot be absolutely guaranteed from a pyrotechnic standpoint. Redesign of the thruster piston is underway to prevent piston failure when fired into no load as,may occur with simultaneous firing of two linear actuators.

Only one deHavilland plunger has been used during the tests. During the first single firing, the threaded end, protruding through the ball-lock mechanism and its nylon guide, was damaged when the plunger contacted the overlapping support arms of the GE tip-mass catcher at the end of the plunger travel. These unnecessary overlapping support arms were cut off before the second firing to eliminate this plunger damage at the end of its travel. During the second firing (double) the damaged plunger end failed and the other two firings were conducted with no guide on this portion of the plunger. Based on these two successful tip mass releases, without the guide and the guiding prior to and within the ball-lock mechanism, this back guide could be eliminated. Adequacy of this guide elimination will be determined during future planned vibration testing.

Only one deHavilland lever arm has been used during the tests. No noticeable abnormal damage resulted from the first firing (single). During the second firing (double),the lever arm overtraveled and became wedged beneath the end of the plunger protruding from the Damper Boom Assembly. Uncaging of the damper within the CPD released the lever arm and allowed it to return to its normal fired position. The top edge of the lever arm was damaged and the roll pins in the lever arm and its mechanical stop were bent. The other two firings were conducted with a spacer placed beneath the actuator assembly to compensate for lever arm overtravel. Redesign of the lever arm and its mechanical stop are underway at deHavilland. The lever arm will be made longer and stronger and its mechanical stop will become an integral part of the actuator housing.

3.3 ENGINEERING UNITS

3.3.1 T-1a PRIMARY BOOM

3.3.1.1 General

This section is a summary of the tests performed at GE on the T-1a Primary Boom Assembly. These tests include all of those performed up until testing was postponed pending retrofit of the unit to overcome problems discovered during vibration testing. Upon completion of the retrofit, the unit will again be subjected to vibration testing. A second engineering unit (T-1b) is also being manufactured by deHavilland to incorporate the retrofit definition. Complete engineering tests will be conducted on the T-1b Primary Boom Assembly and may supersede additional testing of the T-1a assembly, if the overall engineering test schedule can be improved by such action.

3.3.1.2 Conclusions:

The T-1a Primary Boom Assembly, which is the first engineering model of the ATS Primary Boom System, performed satisfactorily at ambient conditions with regard to tip mass release, boom deployment and retraction rates, scissor rates, repeatability of boom extension and scissor positions, telemetry functions, and standby mode operation. Deficiencies were found in the unit with respect to its ability to endure the vibration environment specified. These deficiencies have necessitated the redesign effort that is now underway.

3.3.1.3 Background

The T-1a Primary Boom Assembly was bought-off at deHavilland and shipped to GE on 17 September 1965. It was bought-off even though lengths, scissor angle range, clutch operating voltage, and pressurization did not meet the specification requirements. The

performance data collected at the time of buyoff is presented in Section 3.3.1 of the Fifth Quarterly Program Report.

3.3.1.4 Specimen Identification

It is assumed that the reader is already familiar with the concept of the STEM-type booms and the basic components of the ATS Primary Boom Assembly Package. The Storable Tabular Extendable Member (STEM) concept is described in the Section 2.2 of the Second Quarterly Progress Report, dated 16 October 1964. The purpose of this discussion is to provide better definition of the general arrangement of the Primary Boom Assembly. Figure 3-7 illustrates the fully assembled T-1a Primary Boom Assemblies . Two such assemblies make up a Primary Boom System for one satellite. The black anodized portion of the assembly constitutes the basic structure.

The face of the structure nearest the camera is the upper base plate. Directly opposite this face is the lower base plate. The upper and lower base plates are almost identical.

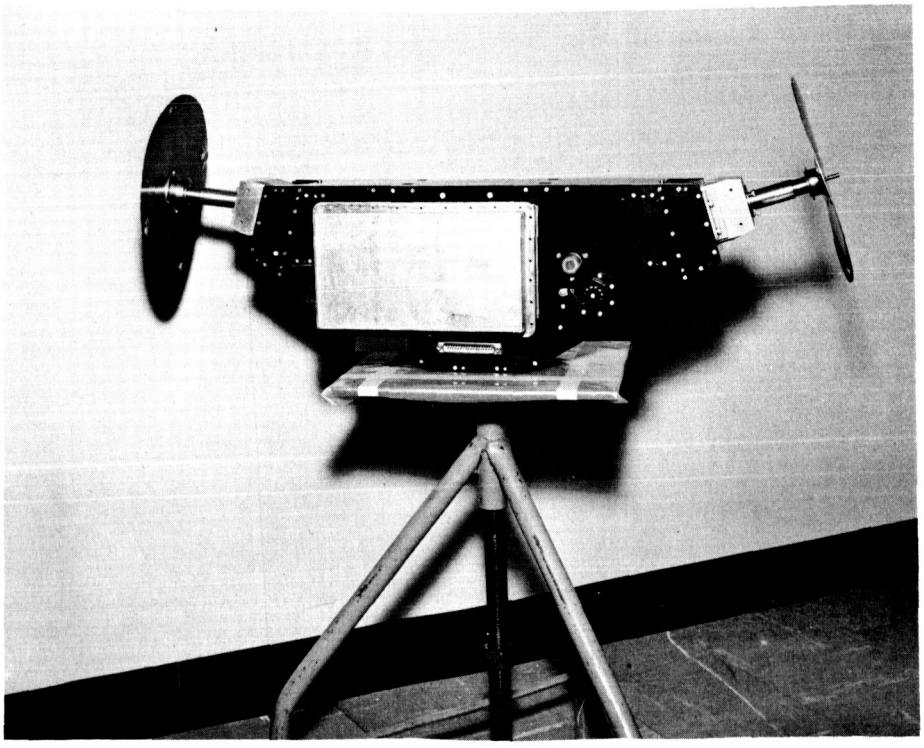

Figure 3-7. Engineering Unit T-1a Primary Boom Assembly

The Primary Boom Assembly is attached to the satellite structure through three 1/4-inch mounting holes in the upper base plate. The steel-gray box structure located directly above the upper base plate is the transmission housing. Two primary boom erection units are mounted to the structure interior. The two aluminum colored blocks at each end of the structure are tip weights. The tip weights are attached to the ends of each assembly. The standoffs mounted on each of these blocks are mounted for the TV targets. TV targets are the circular discs at the end of each standoff. The line of deployment of each primary boom is approximately colinear with the axis and the standoffs. The boom which deploys colinear with the standoff at the left of the picture is identified as Primary Boom 1 and the opposite boom is identified as Primary Boom 2. The vehicle harness interface connector, a flex-pivot mount, and the ascent pressure vent valve are also readily recognizable in the picture. Figure 3-8 is a photograph of a partially disassembled unit. This picture shows the position of one of the two erection units inside the structure assembly.

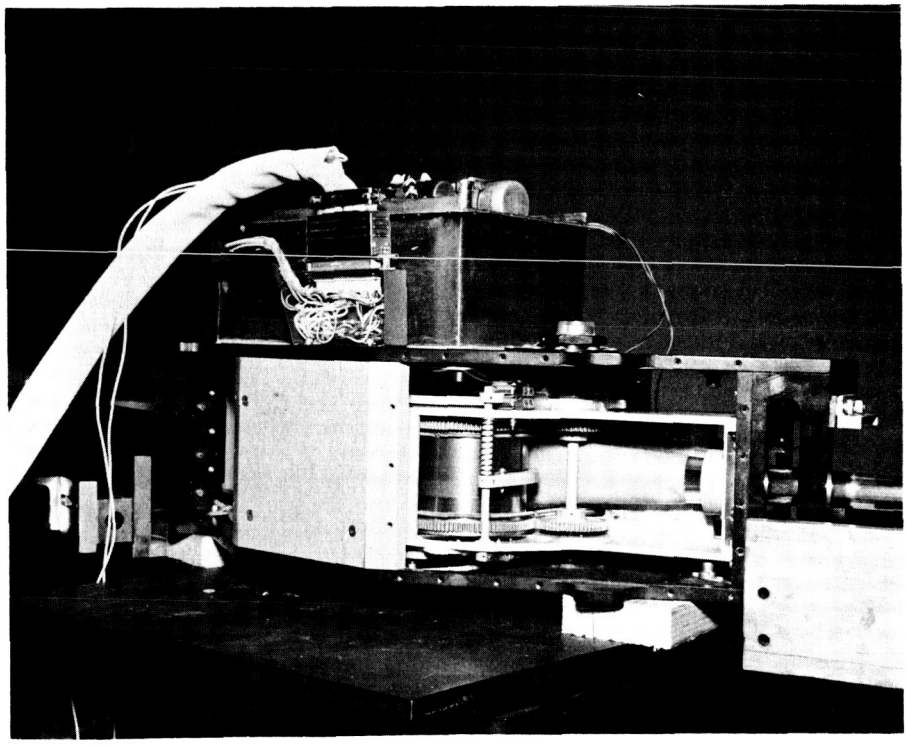

Figure 3-8. Partially Disassembled T-1a Primary Boom Assembly

3.3.1.5 Pre-Environment Testing at GE

A complete circuit isolation, continuity, and dc resistance check, completed at GE prior to performance testing, disclosed a short between -5 vdc and the chassis. Troubleshooting traced the problem to a damaged wire insulation at the extension potentiometer hold-down strap. Switch relocation being undertaken for subsequent units will eliminate repetition of this problem.

A helium "sniffer" pinpointed the pressurization leak at the center (not near any weld) of the stainless steel scissor bellows on the No. 2 erection unit side of the assembly. This leak was attributed to handling damage since the assembly had been successfully sealed prior to teardown to correct other problems at deHavilland. Redesign is now under way to incorporate bellows of beryllium copper in subsequent units, instead of the presently used stainless steel bellows.

At the beginning of initial performance tests at GE, the test console telemetry indicated unexpected off-scale current readings from the internal (scissor motor) temperature sensor (thermistor). Subsequent voltage measurements indicated that the voltage through the internal thermistor was 5 vdc while the voltage through the external thermistor was 3.5 vdc. Both were at room temperature. The problem turned out to be confusion, on the part of deHavilland, concerning what size resistor GE required to be wired in parallel with the thermistor. The precise resistor size, as well as the specific thermistor specification required, have been specified in subsequent directions to deHavilland. All other wiring was found to meet specification.

After the above checkout, the unit was brought to the boom deployment area shown in Figure 3-9. As shown, the unit is mounted at the intersection of a long (150 foot) section of track and a short (10 foot) section. Figure 3-10 shows the tip weight of one boom (excluding target) mounted to a trolley which travels along the 150-foot section. The other boom is connected to a special boom take-up mechanism. In this way, one boom

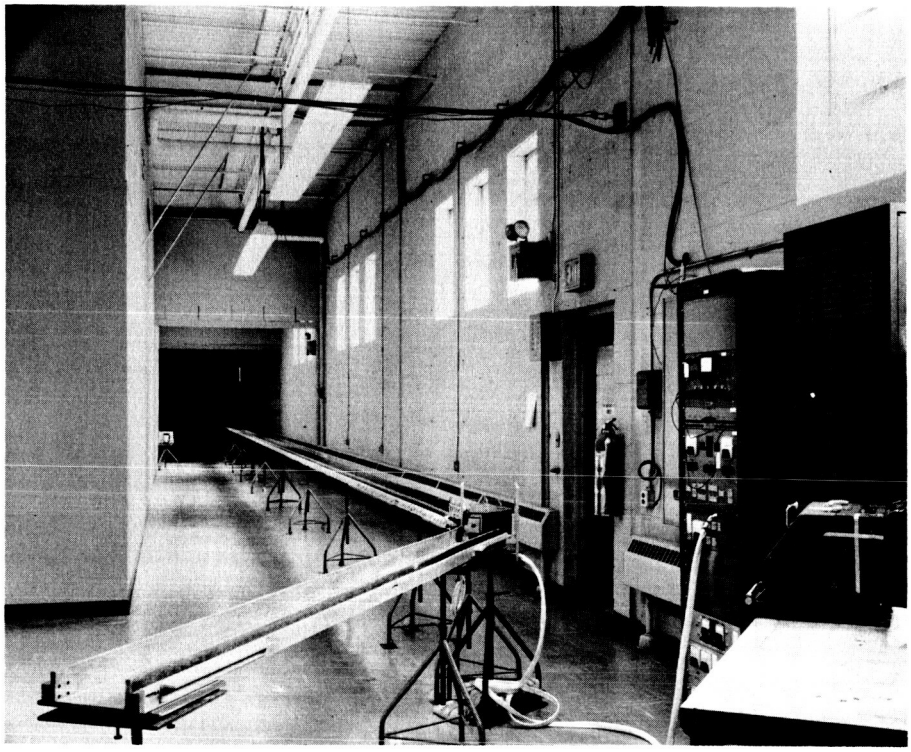

Figure 3-9. Boom Deployment Area

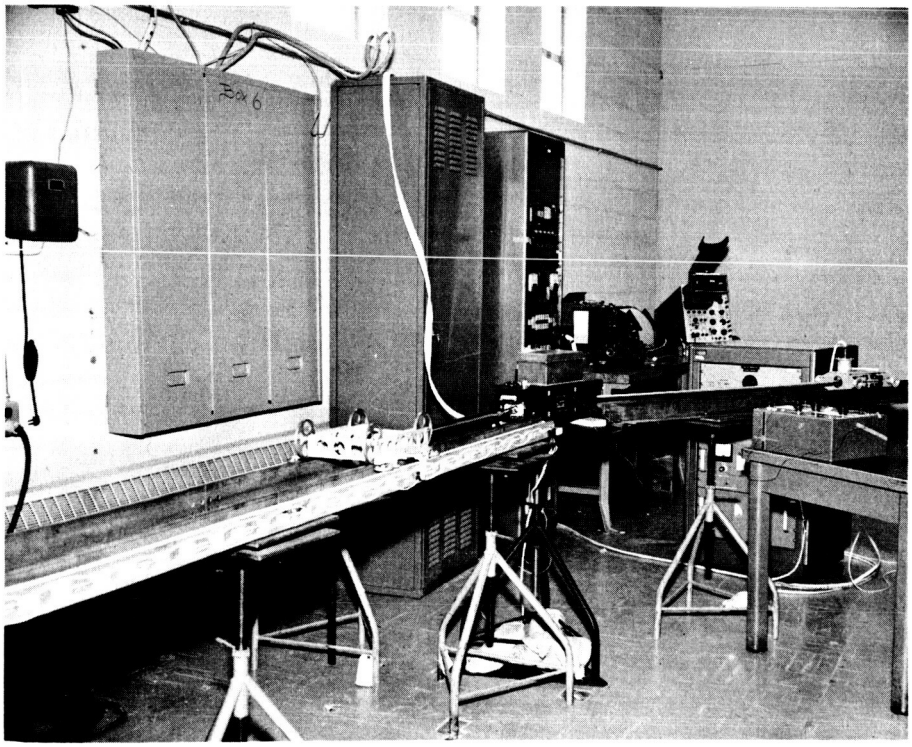

Figure 3-10. T-1a Primary Boom Assembly Mounted on Test Track

can be fully deployed while the other boom is reeled-up by the take-up mechanism (this reducing the required total test area). Figure 3-11 shows the power controller unit used to synchronize the action of the take-up unit with the component under test. Figure 3-12 shows the take-up mechanism at close range. Note that the unit is mounted on wheels to minimize the amount of load which could be transmitted to the boom due to poor synchronization of the two units.

Initial performance tests were hampered when slight missynchronization of take-up and extension motor speeds resulted in loading of the boom tape, rather than loading on the wheel-borne take-up mechanism. This problem with the test equipment was overcome when the nylon wheels, provided by the manufacturer, were replaced with the ball bearing mounted, stainless steel wheels shown in Figure 3-12.

Table 3-1 of the Sixteenth Monthly Progress Report, contains a tabulation of the data from the initial performance tests. Table 3-2 of the same report contains a tabulation of the calibration data for both scissor and extension potentiometers. Similar calibration data will be furnished for each unit delivered. Initial testing revealed that extension motor no-load armature current were now substantially higher than those experienced at deHavilland. Extension at -22 vdc was marginal at best, while retraction at -22 vdc was not possible at all. Subsequent application of G300 grease to the accessible portions of the gear train made the -22 vdc operation satisfactory and reduced the extension motor no-load armature currents to previous levels experienced at deHavilland.

In addition to deployment and scissoring performance, other pre-environment tests performed on the T-1a Primary Boom Assembly included a preliminary magnetic dipole test and boom electrical isolation. The dipole test indicated a well defined dipole of approximately 152 pole-cm with tip masses removed. The skewed orientation of the dipole axis with respect to component principle axes appears to result from the location of permeable materials in the motors, motor gearhead, clutching solenoid, and sealed drive unit. The specification limit of 80 pole-cm has not been met; however, calculations

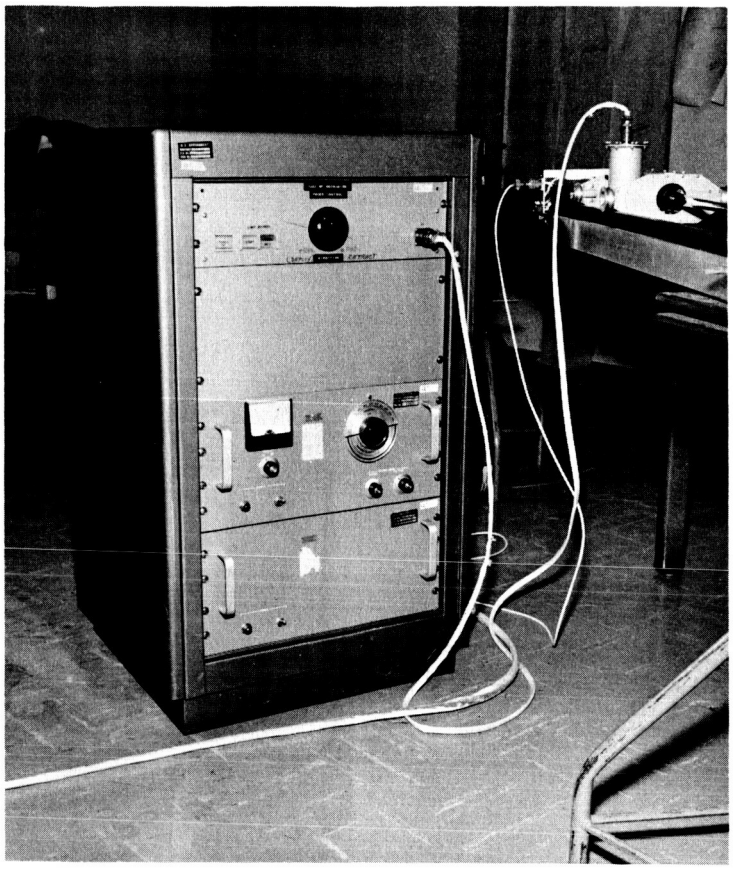

Figure 3-11. Take-up Mechanism Power Controller

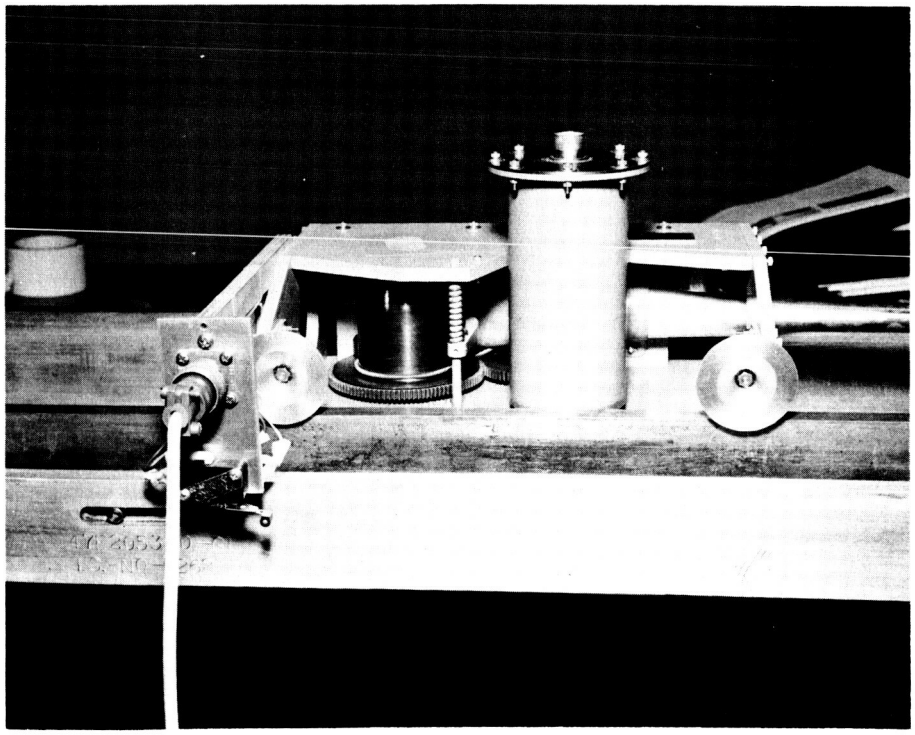

Figure 3-12. Boom Take-up Mechanism

indicate that a fully magnetized 0.25 x 0.25 x 0.75 inch bar magnet, suitably positioned should reduce the net dipole to within specification limits. The tip mass dipoles are 13 pole-cm each. The test data shows some lack of correlation about different axes. The final test fixturing for performing this test will provide more accurate test data. The test will be repeated on Engineering Unit T-1b using updated fixturing and procedure.

3.3.1.6 Vibration Testing

Vibration tests were conducted at GE on the T-1a Primary Boom Assembly using the C-125 shaker facility. The component was mounted in the vibration fixture as shown in Figure 3-13. In this figure, as well as all figures in this section, the structural side plates have been removed to provide a clear view of the component interior. The side plates were replaced for all high level vibration tests. Figure 3-14 shows the component and fixture mounted on the slip table of the C-125 shaker facility.

The internal erection unit covers have been removed to provide a view of accelerometer mounted inside the unit. The component axes definition used during the test can be seen marked on the fixture. Due to an error in marking the fixture, this axis definition does not exactly correspond to the vehicle axes definition and the following table should be used to correlate vehicle axes to axes definition used in this report.

TABLE 3-1. PRIMARY BOOM/VEHICLE AXES RELATIONSHIP

COMPONENT AXIS	VEHICLE AXIS
Z - Z	Z - Z
X - X	Y - Y
Y - Y	X - X

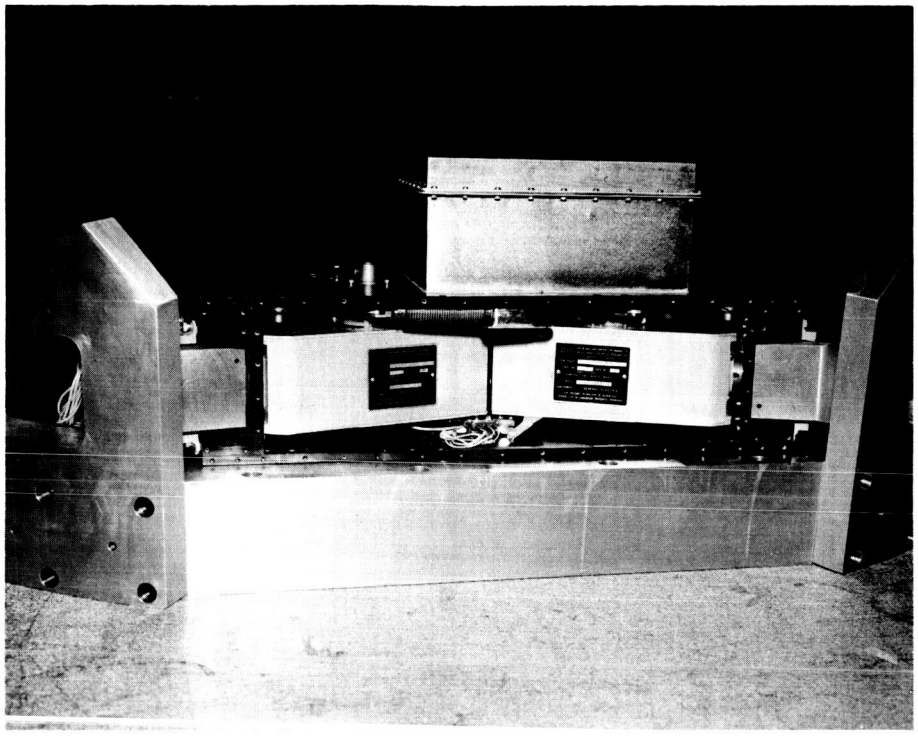

Figure 3-13. T-1a Primary Boom Assembly Mounted on Vibration Fixture

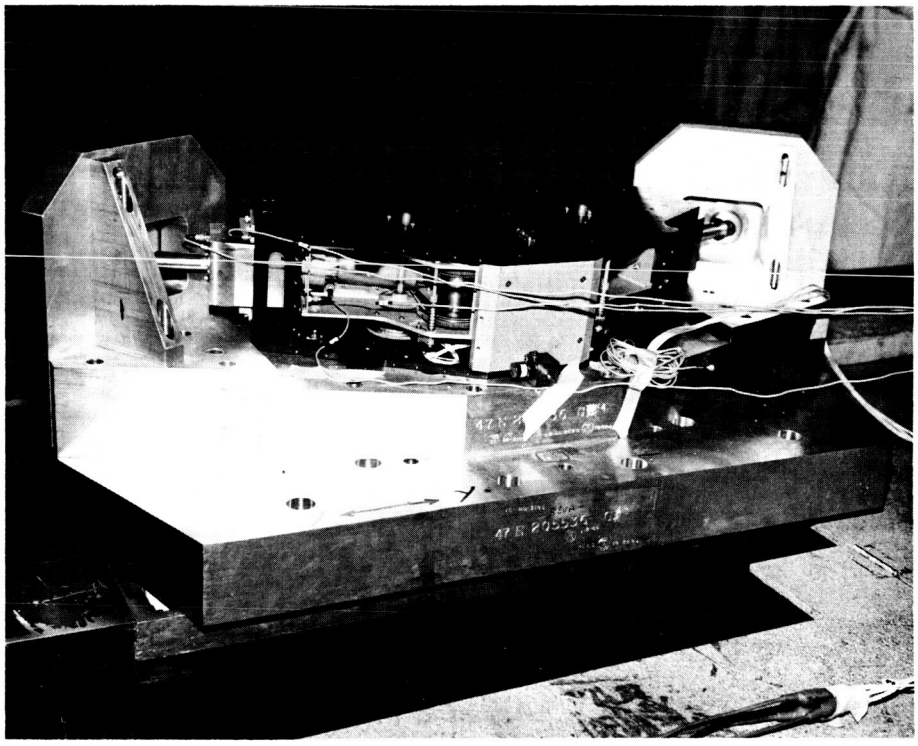

Figure 3-14. Axis Definition and Accelerometer Locations, T-1a Primary Boom Assembly

Also visible in Figure 3-14 are:

a. The control accelerometer for input in the Y-Y axis (mounted on the aluminum cube at the center of the figure).
b. Accelerometers sensing the Y-Y axis on the tip weight, end bulkhead adjacent to the tip weight, and internal of the erection unit (one each).
c. An accelerometer sensing the X-X axis mounted internal to the erection unit.

The above mentioned accelerometer locations were approximately duplicated for each of the three axes.

Initial resonance search at 1.5g in the Z-Z axis resulted in the tip mass on Boom 1 becoming uncaged. Subsequent troubleshooting pinpointed the cause at the external (to erection unit) drive gear set screws. Replacement set screws of a slot head configuration had been previously installed and were found not properly seated. This screw allowed the gear to drop out of engagement and the spool to rotate, thereby moving the boom and uncaging the tip weight. The installation of the proper allen-head set screws retained these gears in position during further resonance testing. This initial search indicated a resonance for the entire unit at 175 cps and other resonances of the erection unit and tip mass at 70 cps and 500 cps.

The initial sinusoidal vibration was started in the Z-Z axis and was initiated at one-half of the qualification vibration levels (approximately three-fourths of the acceptance vibration levels). At the 5.8g level, both of the tip masses became uncaged at 39 cps. After removal of all access covers, the exact cause of uncaging was not readily discernible. However, the carbofil gears did show indications of possible rotation and vibration hammering on faces. Also, the erection unit polycarbonate housings showed signs of crazing at the mounting holes. In an effort to pinpoint the exact nature of the uncaging, resonance searches were again conducted, but with all the access covers removed for observation with a strobotac. During the 2.5g resonance search, movement of boom tape on the spool was detected. Subsequent marking of relative positions on tapes, spools,and gears

confirmed suspicions that boom stacking, and not gear rotation, was the cause of uncaging. During vibration the boom tape tends to tighten up on the spool and resultant end cap movement is sufficient to allow the tip weight to become uncaged.

After defining the uncaging problem, resonance searches were completed in the Z-Z, X-X and Y-Y axis at 1g and 2.5g levels by artificially restraining the end caps from moving during vibration. Redesign efforts were begun to make uncaging of the tip weights in future units independent of boom tape movement on the spool. Upon completion of resonance searches, normal mode performance tests were conducted and the unit was still functionally operative. Since resonance searches in all three axes revealed no problems other than those stated, sinusoidal vibration testing was undertaken with plugs placed in the tip target standoffs to restrain the end caps from moving during vibration.

Vibration of the T-1a was conducted in the Y-Y, Z-Z and X-X axes in the following sequence:

a. 1g resonance search - one-half qualification sinusoidal run (shaped spectrum).
b. 1g resonance search - full qualification sinusoidal run (shaped spectrum).
c. 1g resonance search - full qualification random run.
d. 1g resonance search

Performance testing after vibration in the Y-Y axis was limited to tip weight uncaging which was satisfactory. Performance testing after vibration in the Z-Z axis was limited to tip weight uncaging and partial deployment (about 3 feet). Both operations were satisfactory; however, an inspection revealed several cracks at two separate locations on each boom (at attachment to end cap and at drum support rollers). Performance testing after vibration in the X-X axis (after retrimming booms) was limited to uncaging, partial deployments (about 3 feet and 56 feet), and normal and standby scissoring. All operations were satisfactory; however, inspection of both booms during the 3-foot deployment revealed that Boom 2 was cracked again at the drum support rollers while Boom 1 sustained only wrinkles. Both booms showed evidence of cracking at the attachment to the end cap.

Figure 3-15 shows a typical crack at the drum support roller (note the evidence of chafing on the roller just adjacent to the crack). Cracks at the end cap were less severe (1/8 inch maximum).

The other partial deployment with Boom 2 on the test track trolley and Boom 1 in the take-up mechanism resulted in a dramatic Boom 2 element failure. At a deployed length of 56 feet, the trolley stopped its forward motion. When power was removed from the unit, inspection revealed that the element had split from both edges diagonally toward the center at the entrance to the guide within the erection unit and had reverse wound approximately one-half turn on the storage drum. Inspection after removal of Erection Unit 2 from the assembly revealed that the storage drum support bearings had hung up in the kidney-shaped guide slots. Resulting damage to the element is shown in Figures 3-16 and 3-17.

Inspection of the deployed portion of both booms reveals a regular pattern of creases starting at the erection unit and gradually decreasing in severity until they disappeared at approximately 20 feet away from each erection unit. The patterns can be seen developing in the guidance as shown in Figure 3-18. These patterns suggested the possibility of a condition of unnatural deployment developing on both booms, which gradually worsened as more boom was deployed. Figure 3-19 shows a typical length of this pattern on an erected boom. Disassembly of the unit subsequent to the above failure revealed the following:

a. The storage drums of both booms were found to be hung-up in the kidney slots in a position consistent with zero extended boom length. Figure 3-20 shows a side view of the erection unit with the storage drum bearing in a "boom-deployed" condition. The line at the edge of the kidney slot is the position of the bearing center in the "hung-up" condition. Figure 3-21 is a close-up of the condition immediately after disassembly and shows the approximately 0.15-inch displacement between the point of hang-up and the position of the bearing that corresponds with a boom deployment of 56 feet.

b. The thin spacer under the bearing flange (visible in Figure 3-22) was found to be badly deformed in the area where it is contacted by the bearing flange.

c. A bearing stress failure of the side plate material was found in the area just under the bearing flange (in booms-stowed position). Fretting corrosion is also visible in the area contacted by the spacer (See Figure 3-22).

d. This bearing stress failure was found to have moved metal in a feather-edge fashion into the kidney slot, thereby reducing its width (See Figure 3-23). This reduction in bearing slot width was found to restrict motion of the bearing along the kidney slot, resulting in the hang-up.

Both sideplates of the disassembled erection unit (Boom 2) were found to be similarly affected. The Boom 1 drum bearings were found to be hung-up in a like manner but this unit was not completely disassembled at the time.

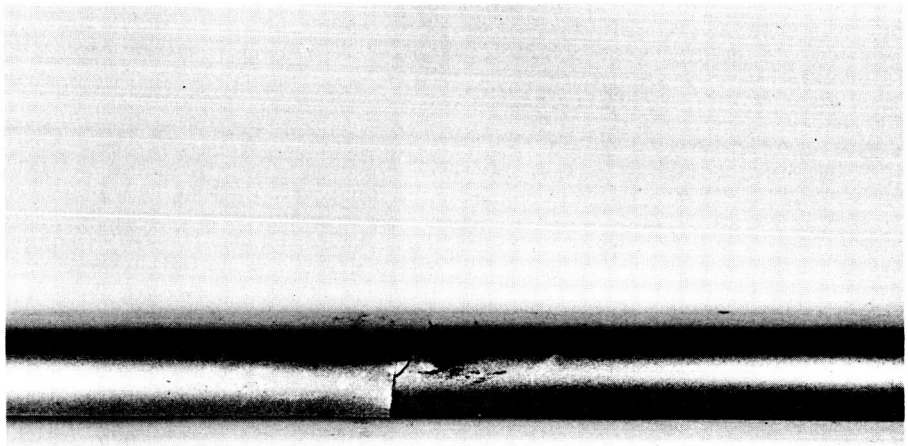

Figure 3-15. Typical Boom Crack at Drum Support Roller

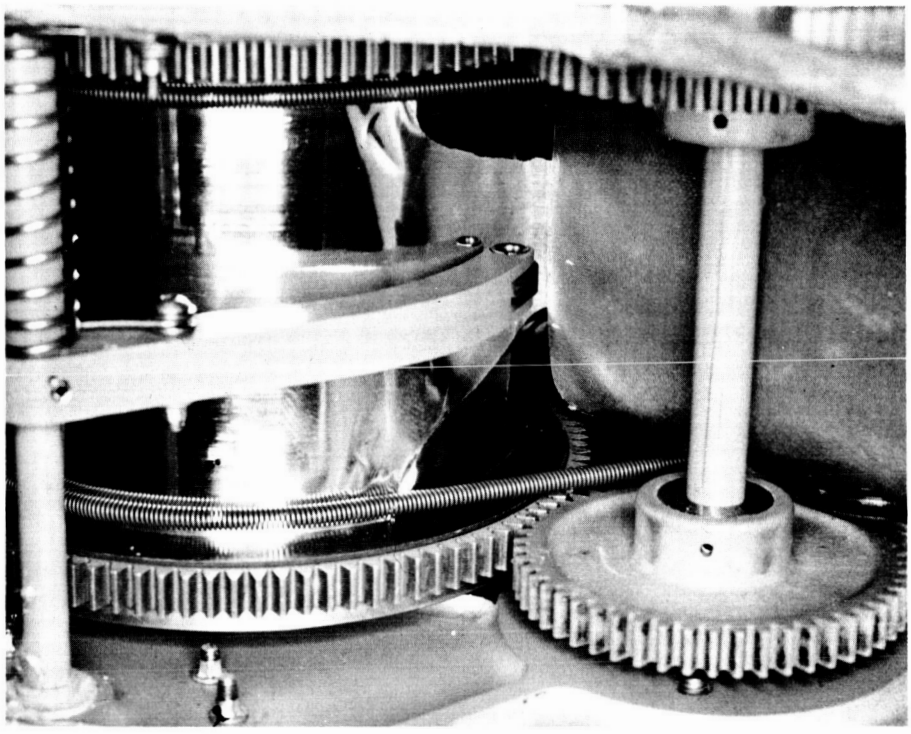

Figure 3-16. Erection Unit 2 Boom Element Failure, T-1a Primary Boom Assembly

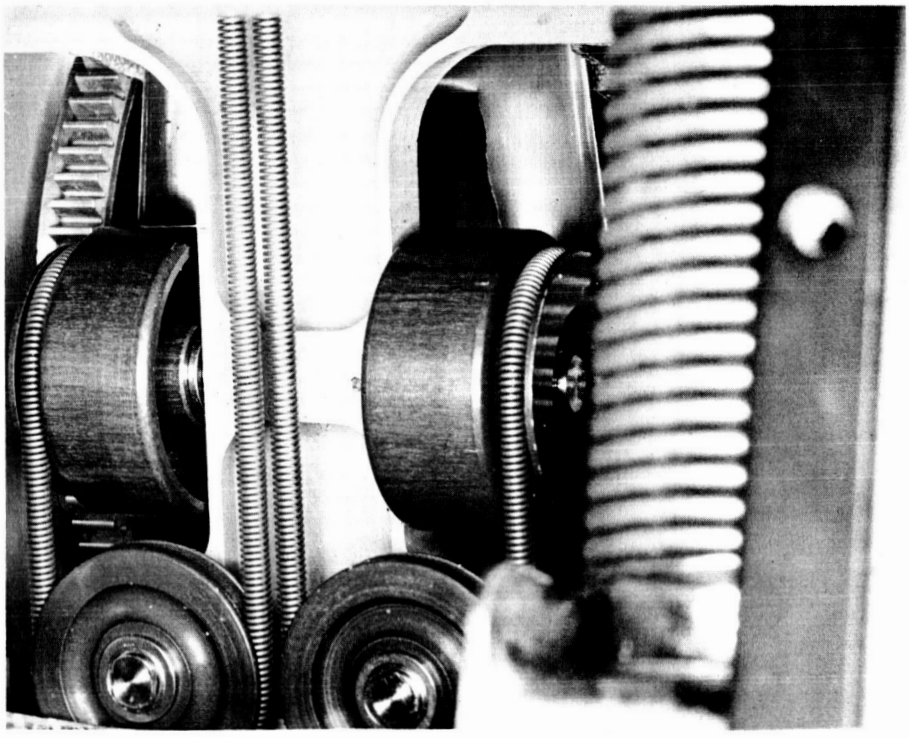

Figure 3-17. Erection Unit 2 Boom Element Failure, Reverse Side

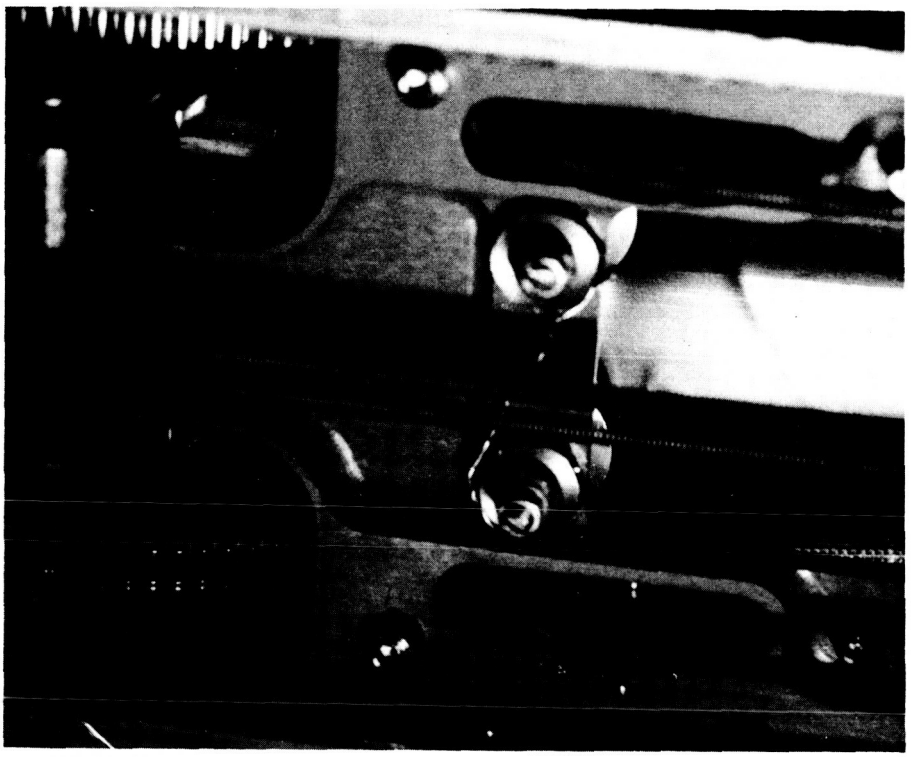

Figure 3-18. Wrinkle Pattern Developing in Boom, Internal to Guidance

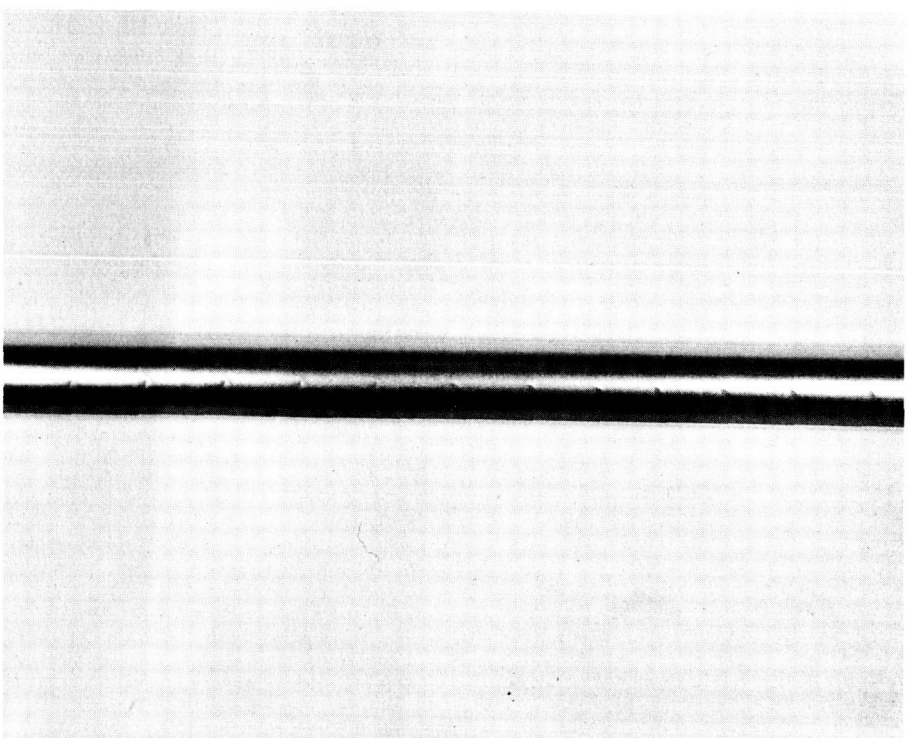

Figure 3-19. Boom Wrinkle Pattern

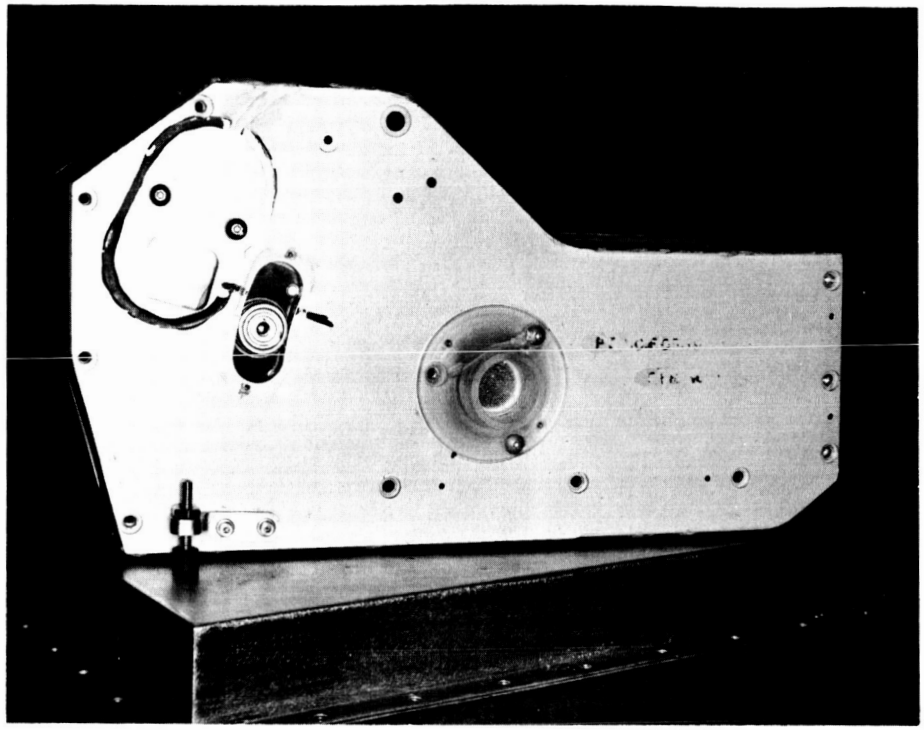

Figure 3-20. Side View of Erection Unit Showing Bearing Hang-up

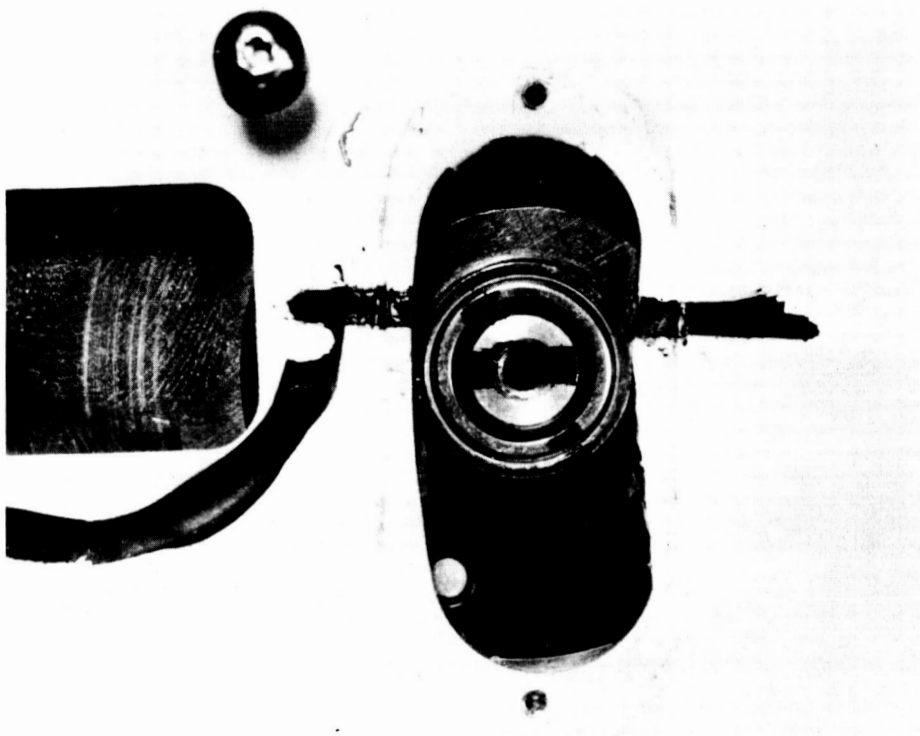

Figure 3-21. Close-up of Bearing Hang-up

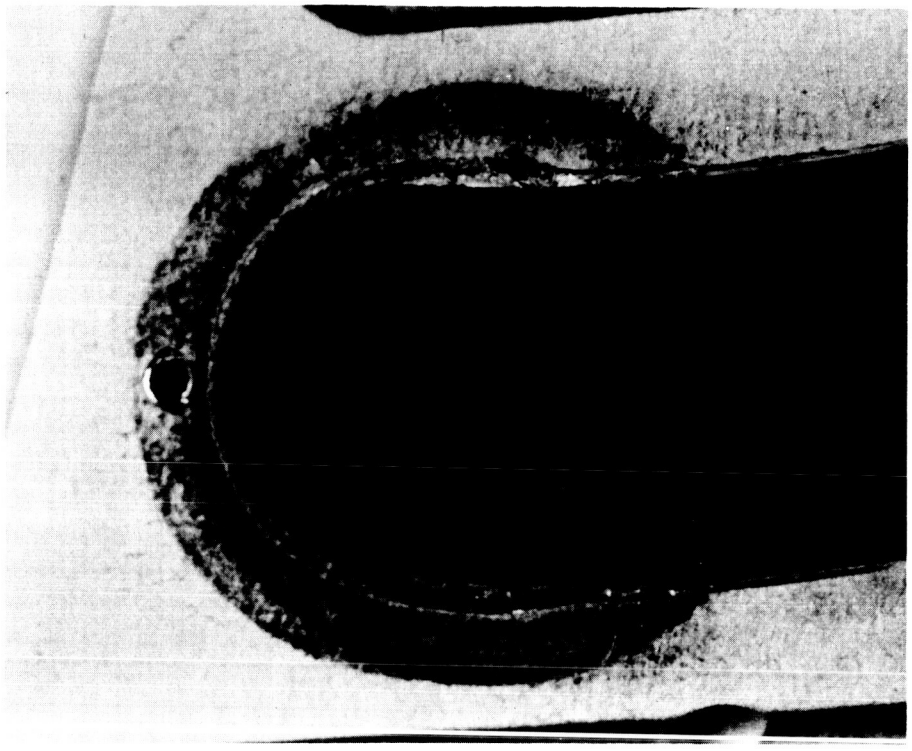

Figure 3-22. Bearing Stress Failure of Kidney Slot

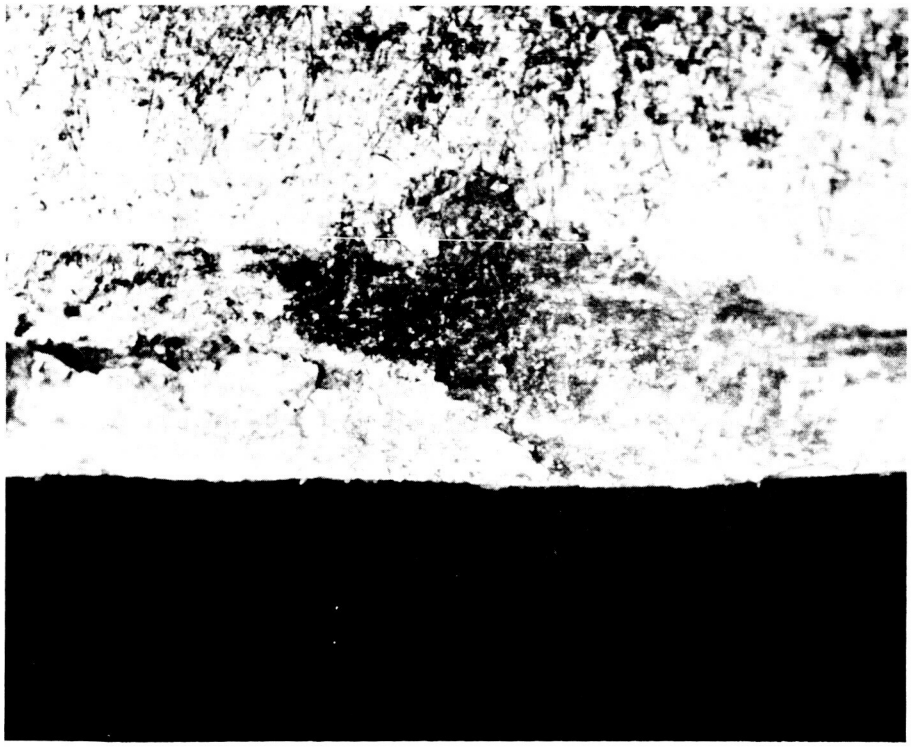

Figure 3-23. Magnified View of Bearing Stress Failure of Kidney Slot

Since speculation existed that the reverse wind type failure experienced by Boom 2 might not be entirely due to the drum hang-up, an attempt was made to repeat the failure on Boom 1 in a manner conducive to close observation. Accordingly, the unit was set up at the test track and the drum drive gear was manually driven, while disconnected from the drive motor. Figures 3-24 through 3-31 show the results of this test. The sequence is as follows:

a. Wrinkles at both edges of boom tape developed due to misalignment of drum that is tangent with entry to guide (approximately 65 feet of boom deployed) (See Figure 3-24).
b. Wrinkles jammed against guidance entry. Tape begins to bulge toward viewer as torque continues to be applied to drum (See Figure 3-25).
c. Bulge more perceptible. Tape begins to reverse wind at end of bulge nearest drum (See Figure 3-26).
d. Reverse wind more evident. Bulge is drawn tight around edge of guidance (See Figure 3-27).
e. View from opposite side of erection unit. Reverse wind evident for about a quarter turn. Edge of reverse wind catches under sping belts (See Figure 3-28).
f. Second bulge begins to develop (See Figure 3-29).
g. Second bulge more pronounced (See Figure 3-30).
h. View from opposite side of erection unit. Reverse wind has progressed to same point as that on Boom 2. Drum can no longer be manually turned due to excessive resistance (See Figure 3-31).

The results of the attempted failure repetition are:

a. The reverse-wind failure was duplicated with no unit discrepancies except drum/guidance misalignment due to kidney slot hang-up.
b. No edge damage (crack) was evident before or after test.
c. The ductile tear as in Boom 2 was not duplicated but this could be attributed to the vast difference in deployment speeds.

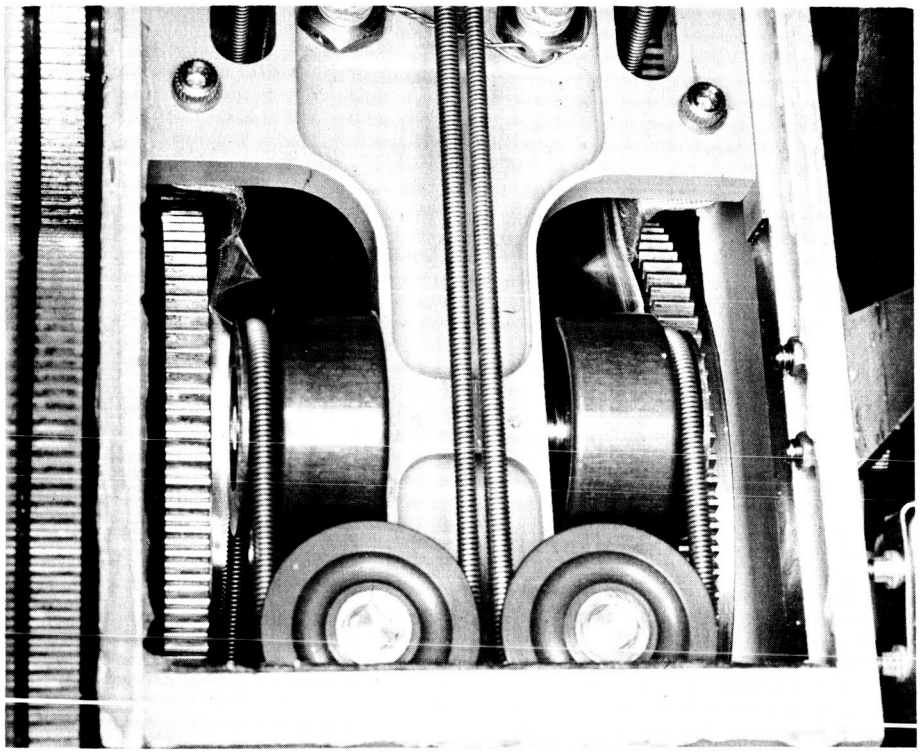

Figure 3-24. Results of Boom 1 Reverse-Wind Type Failure, Shot a

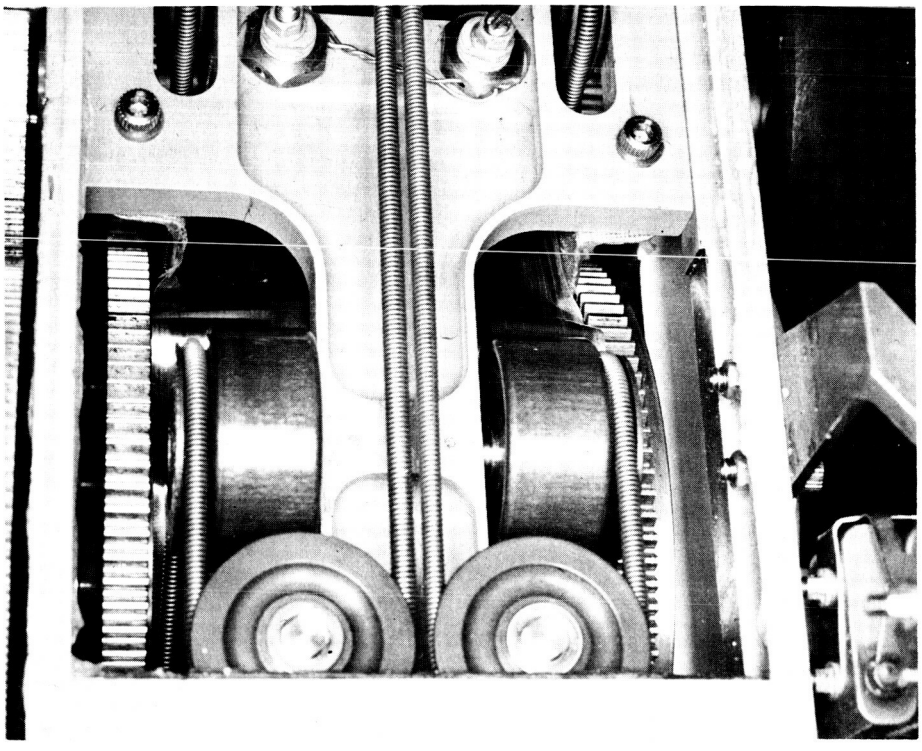

Figure 3-25. Results of Boom 1 Reverse-Wind Type Failure, Shot b

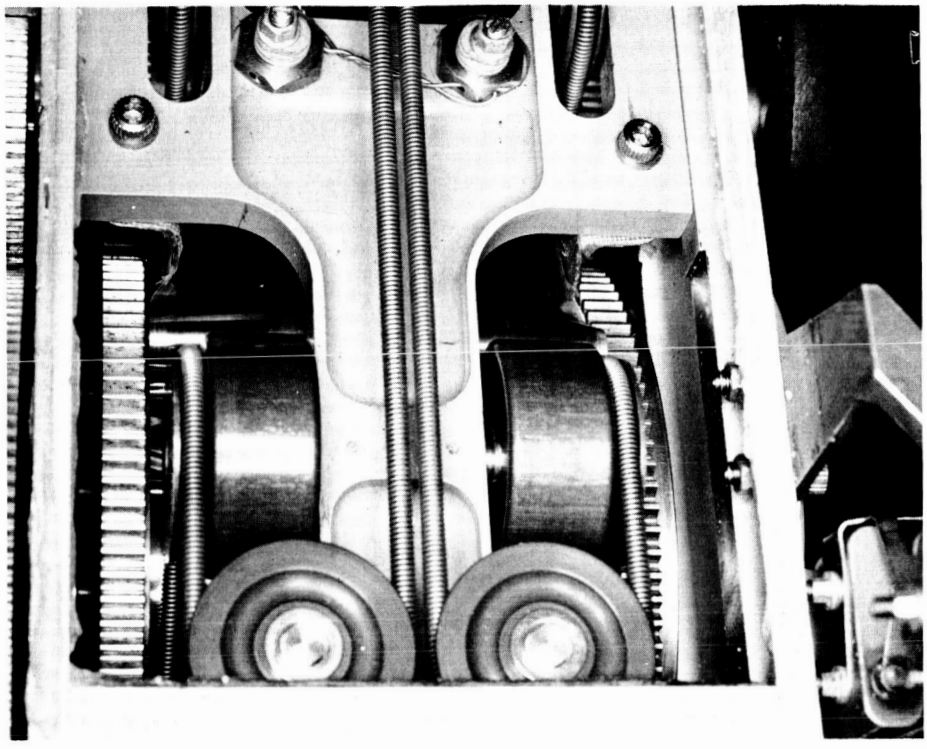

Figure 3-26. Results of Boom 1 Reverse-Wind Type Failure, Shot c

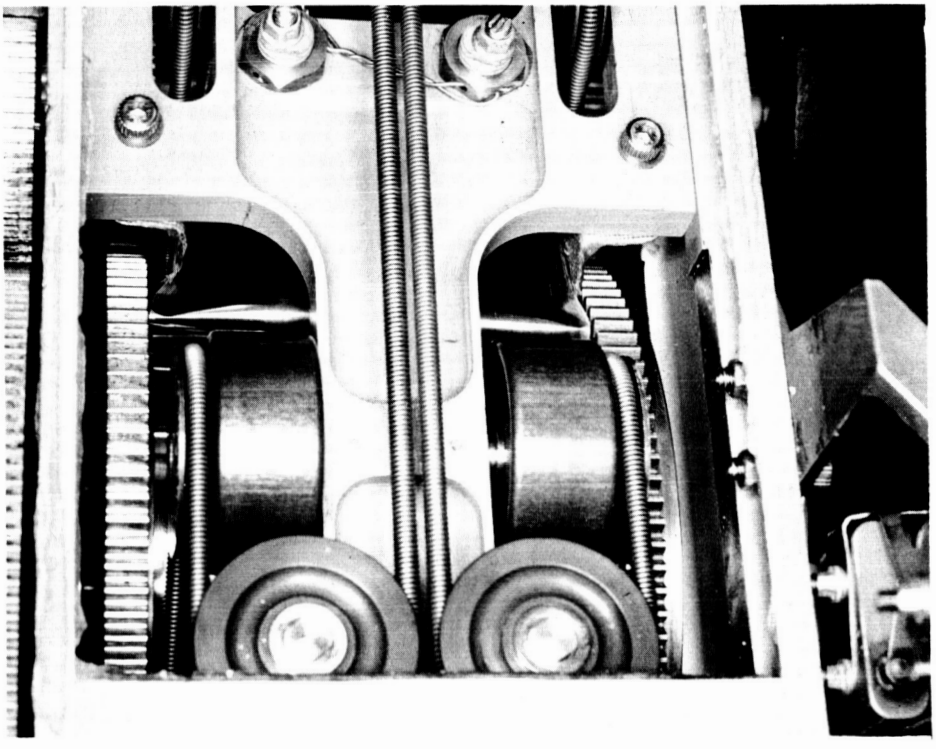

Figure 3-27. Results of Boom 1 Reverse-Wind Type Failure, Shot d

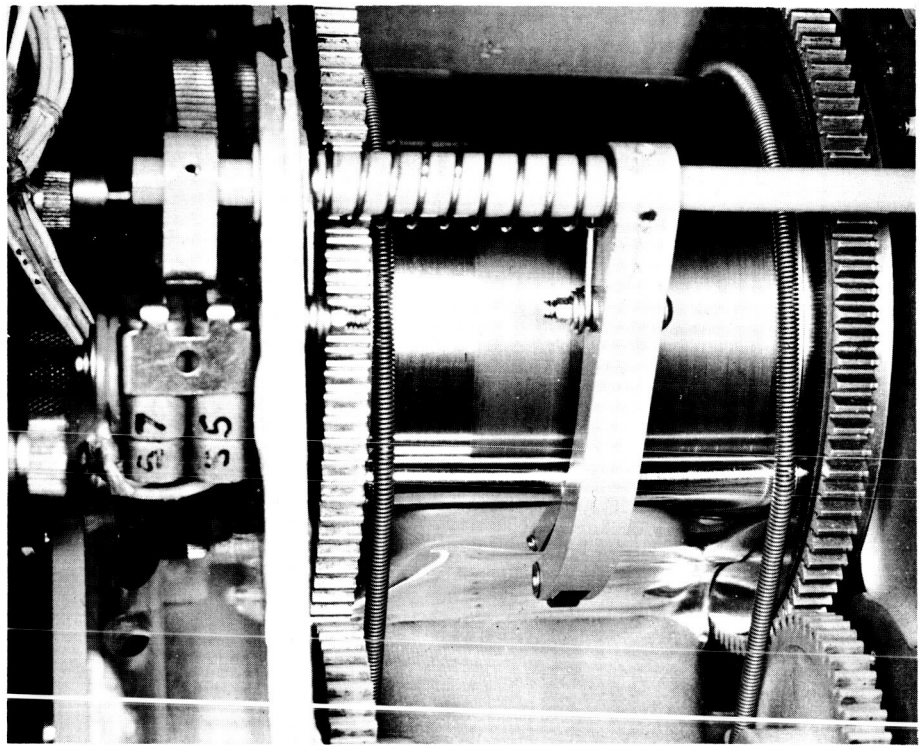

Figure 3-28. Results of Boom 1 Reverse-Wind Type Failure, Shot e

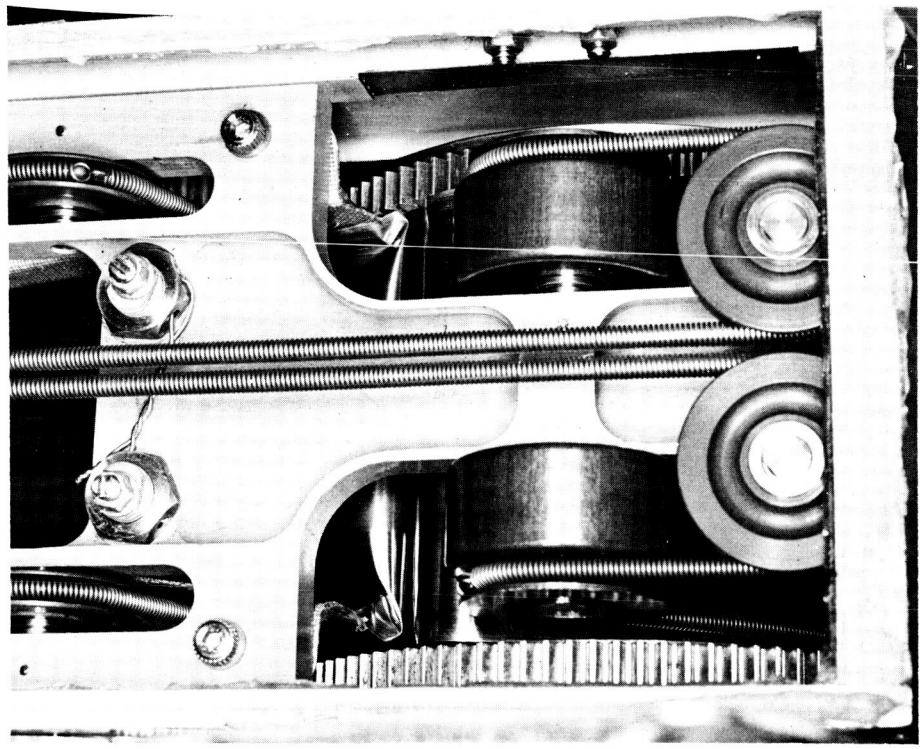

Figure 3-29. Results of Boom 1 Reverse-Wind Type Failure, Shot f

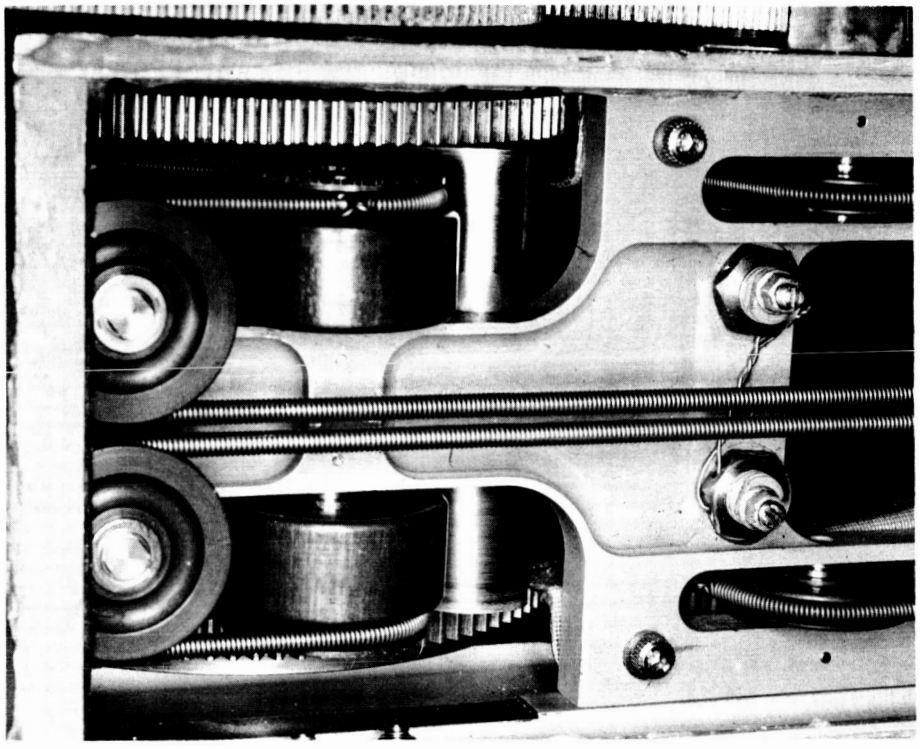

Figure 3-30. Results of Boom 1 Reverse-Wind Type Failure, Shot g

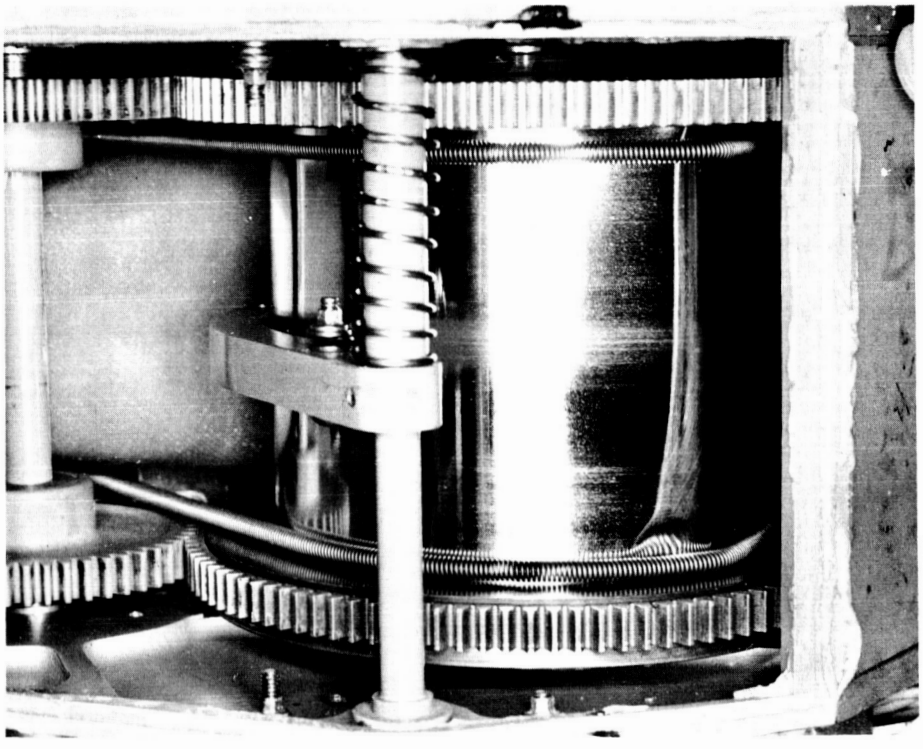

Figure 3-31. Results of Boom 1 Reverse-Wind Type Failure, Shot h

d. The wrinkle pattern (as in Boom 2) was found on the deployed position of the boom but not on the undeployed portion, indicating that misalignment between drum and guidance caused the wrinkling.

It was therefore concluded that the kidney slot hang-up (and resultant misalignment) is the problem to be attacked in precluding the reverse-wind failure. The redesign for this condition is to provide a much larger bearing area under the flange and a chamfer as shown in Figure 3-32.

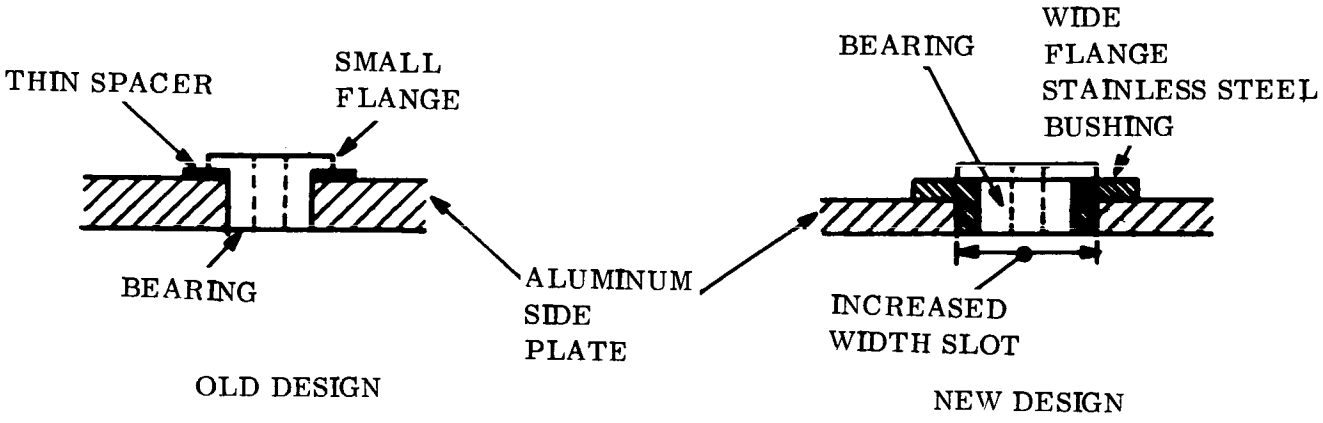

Figure 3-32. Redesign of Flange to Correct Reverse Wind Failure

3.3.1.7 Summary of Vibration Induced Failures and Fixes

Concurrence on the resolution of the four vibration induced problem areas has resulted in the submittal of detailed drawings by deHavilland for rework of T-1a parts. A retrofit kit will be provided by deHavilland and existing T-1a parts will be reworked by GE. The retrofit will be reflected in T-1b and subsequent units.

In summary, the problems and fixes are:

a. Tip weight uncaging resulted from "stacking" of the element on the drum during vibration. Essentially the element became more tightly wound on the drum and this tightening resulted in enough movement of the end cap so that the caging springs were disengaged from the locking grooves within the tip weights, thus releasing the tip masses. The basic problem is that tip weight uncaging is directly dependent upon boom element movement. The fix will incorporate a flexible latching cable which ensures that tip weight uncaging is independent of element movement due to "stacking". The flexible cable will be inserted into the unit through the end of the tip weight and guided to a special worm gear attached to the internal polycarbofil drum drive gear. Engagement will be accomplished by screwing the cable into engagement with the special gear and locking in place. Disengagement will occur only with rotation of the drum drive gear.

b. Element cracking at the drum support rollers was a direct result of insufficient element stored on the drums. The original design specified 150-foot booms and the kidney slots were designed for this capacity. However, the length was subsequently changed to 132 feet. The fix to compensate for the difference in design capability and actual capability will be to incorporate a kidney guide slot "snubber." This snubber will fill up the kidney slot to reduce the effective drum-support bearing movement to that anticipated at 150-foot capability.

c. Bearing hang up in the kidney slot resulted from inadequate kidney slot bearing surface for the drum-support bearings. The fix for this inadequacy will be the incorporation of a hardened bearing support bushing around the bearings. This bushing will do the bearing within the kidney slot and provide a larger, more adequate bearing surface to react axial loads.

d. Element cracking at the attachment to the end cap is a direct result of the method of attachment. The present semicylindrical mounting plate forces the element to assume its circular shape faster than it would under natural circumstances. This unnatural restraint results in excessive "scissoring" of the

element edges at the point of attachment. The fix would incorporate a flat mounting plate to allow the element to assume the circular shape at a more natural rate thereby reducing the scissoring and resultant cracking. As a result of the reverse-winding failure and cracking at the drum-support roller, a metallurgical analysis was performed. The results are included in Appendix A of this report.

3.3.2 T-1 DAMPER BOOM ASSEMBLY

The retrofitted Engineering Unit T-1 Damper Boom was received at GE on 4 December. The basic retrofit consisted of a new center-body to accomodate the new tip mass release mechanism, new brake lever arms, new spools with new boom elements, and all the associated modifications. The Damper Boom has since been subjected to additional engineering tests which are described in Section 6.1.3.

SECTION 4

COMBINATION PASSIVE DAMPER

4.1 EVENT AND SPECIFICATION STATUS SUMMARY

4.1.1 SUMMARY OF MAJOR EVENTS DURING REPORTING PERIOD

25 October	Final assembly of Combination Passive Damper (CPD) Engineering Unit 1 started.
28 October and 18 November	CPD alignment problems discussed at a meeting with NASA representatives at GE.
5 November	CPD Thermal Unit returned from HAC to GE because vehicle thermal tests were deleted.
22 November	CPD Engineering Unit 1 was delivered to test area from final assembly. First firing of pyrotechnic devices was successfully accomplished.
23 November	CPD Dynamic Unit shipped to (HAC) per NASA request.
7 December	Updated Specification SVS-7331 for Passive Hysteresis Damper was signed off by NASA and released.
10 December	CPD Engineering Unit 1 completed vibration test. Fired squibs.
14 December	CPD Engineering Unit 1 completed acceleration test successfully. Fired squibs.
16 December	CPD Engineering Unit 1 completed humidity test with slight corrosion of magnesium parts. Fired squibs.
18-19 December	CPD Engineering Unit 1 in solar vacuum test. Test setup unsatisfactory.
28 December	CPD Engineering Unit 1 re-entered solar vacuum chamber with improved test setup.
28 December	CPD Engineering Unit 2 assembled and available for test or other utilization.

4.1.2 CPD SPECIFICATION STATUS

Table 4-1 lists the status of specifications directly applicable to and generated for the CPD.

TABLE 4-1. CPD SPECIFICATION SUMMARY

SPECIFICATION TITLE	SPECIFICATION NO.	STATUS
Combination Passive Damper	SVS 7314	Issued 4 June 1965 and reissued on 7 December 1965.
Passive Hysteresis Damper	SVS 7331	Revised to incorporate changes in design and testing requirements that have occurred since original issue on 5 March 1965.
Electroexplosive Pressure Cartridge and Cable Cutter	SVS 5292	Issued 10 May 1965
Solenoid	R 4612	Revised and reissued 7 July 1965.
Semiconductor Photo-Transistor, Silicon, NPN	R 4615	Issued 10 July 1965.
Pyrolytic Graphite Simple and Complex Shapes	171A4211	Revised and reissued 22 January 1965.
Flexible Epoxy Adhesive	171A4402	Issued 17 September 1965.
Dispersion, Carbonyl Iron-Epoxy	171A4411	Issued 27 December 1965; torsional restraint pattern for Eddy-Current Damper.

4.2 DESIGN DEVELOPMENT EFFORT

4.2.1 GENERAL

The majority of the effort during this period was spent in the activities associated with manufacturing the first engineering units of the CPD. These activities included subassembly

of various portions of the CPD including in-process testing and adjustment of the eddy-current, torsional restraint and suspension magnet elements.

Assembly of Engineering Unit 1 started on 25 October in a "clean tent" at the final assembly area of the GE Valley Forge Facility to minimize contamination of the unit by foreign matter, particularly magnetic particles. A preliminary handling document was prepared and issued which outlined precautions to be taken in handling the CPD with respect to magnetic particle contamination. Because this unit was the first assembly of a functional CPD package, a number of problem areas were uncovered in planning, assembly fixturing and parts utilization. These difficulties were expected as a part of the normal learning curve and they were recorded as they occurred and were evaluated to determine the changes required to drawings and planning to simplify the assembly of Engineering Unit 2 and subsequent units.

Assembly of Engineering Unit 1 was completed on 21 November and the unit was immediately available for engineering evaluation testing. This evaluation was conducted in accordance with the "Engineering Test Plan for CPD" which was published in PIR 4076-085 (Revision A), dated 27 July 1965. Functional tests were performed on the Low Order Force Fixture (LOFF) and the Advanced Damping Test Fixture (ADTF), as appropriate. A measurement of the magnetic dipole was also made in the applicable environmental test area. All test facilities are located in the GE Space Technology Complex at Valley Forge, Pennsylvania. These engineering evaluation tests include:

a. Functional tests
b. Vibration
c. Acceleration
d. Solar vacuum
e. Humidity
f. Thermal functional

Requirements for each environment are in accordance with the provisions of the Combination Passive Damper Specification, SVS-7314. All tests, except the thermal functional test, were completed on Engineering Unit 1 by the end of the reporting period. The results of these tests are summarized in Section 6 of this report.

4.2.2 COMBINATION PASSIVE DAMPER PACKAGE

A detailed description of the CPD was included in the "Fourth Quarterly Progress Report" (Pages 4-4 through 4-10) and a summary description repeated in the Fifth Quarterly Progress Report (Pages 4-4 through 4-7). For ease of reference, a drawing of the CPD package is shown in Figure 4-1 of this report. Figure 4-1 is identical to Figure 4-1 of the Fifth Quarterly Progress Report except that the thermal shield has been modified as requested by NASA, and the transient suppression diodes (item 62 of Figure 4-1) have been added to the CPD. Previously, they were included within the Power Control Unit. As in the previous reports, Sheet 1 of Figure 4-1 shows the details of the Passive Hysteresis Damper which are included in the CPD; Sheet 2 is a cross section of the CPD which delinates the various functional elements of the CPD; and Sheet 3 is a detailed view of the baseplate of the CPD showing the caging elements and the attachment of the Damper Boom. A summary of the parts and their function is given in Table 4-2.

4.2.3 ENGINEERING UNIT 1

4.2.3.1 Design Effort

During fabrication and assembly of Engineering Unit 1, problem areas associated with assembly and adjustment of the complete CPD were identified and in conjunction with manufacturing, engineering, and planning, corrective techniques were established and incorporated as changes in manufacturing techniques or as design modifications for the assembly of Engineering Unit 2 and subsequent units. It was found that some very close tolerances which were previously thought to affect the functional performance of the CPD could be relaxed as a result of experience gained during the assembly of Engineering Unit 1. Such changes were implemented by drawing changes,where appropriate. The assembly procedure was further developed and, as a result, fasteners were redefined in some cases while in other areas, the need for specialized wrenches and other tools became evident.

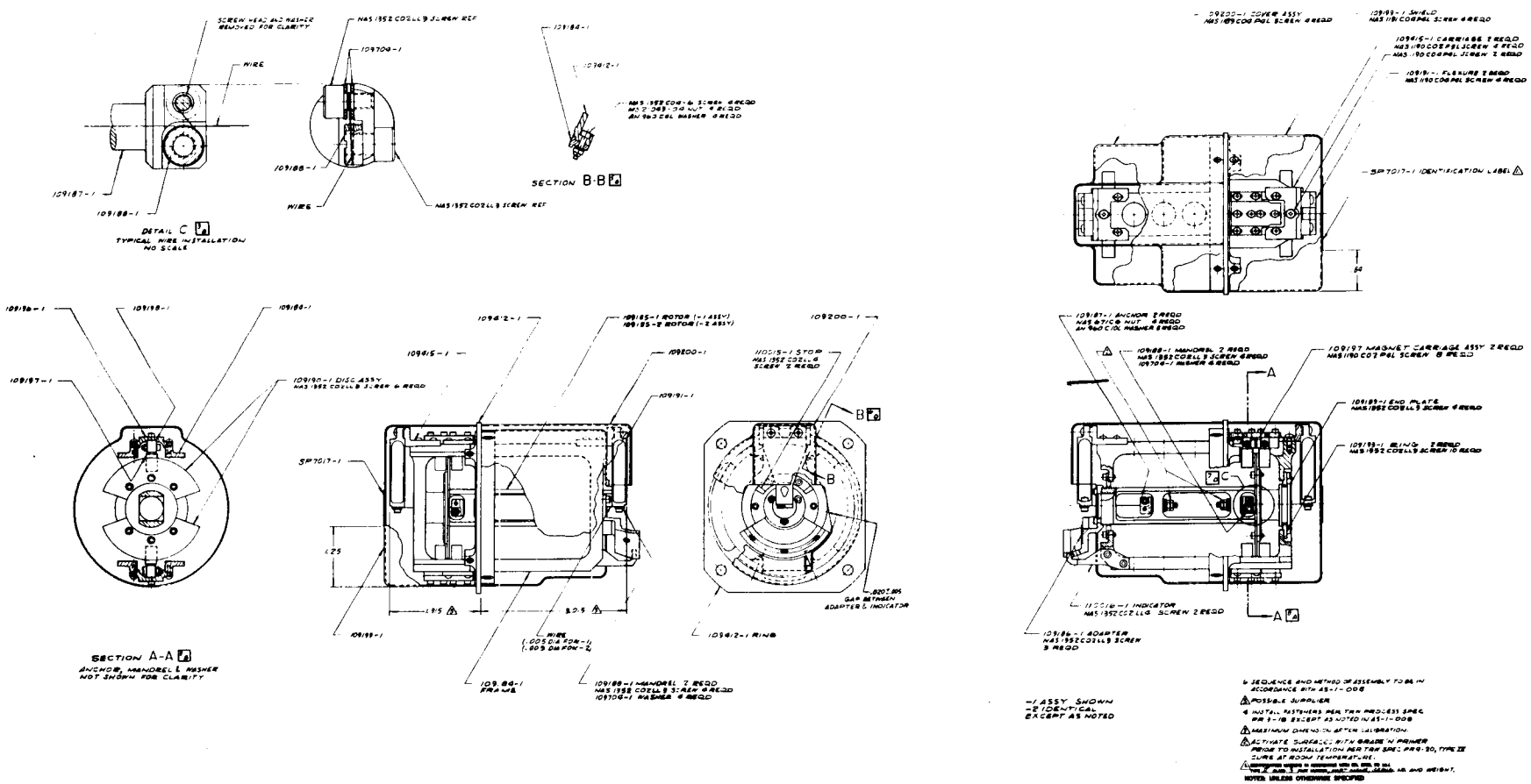

Figure 4-1. Combination Passive Damper Package (Sheet 1 of 3)

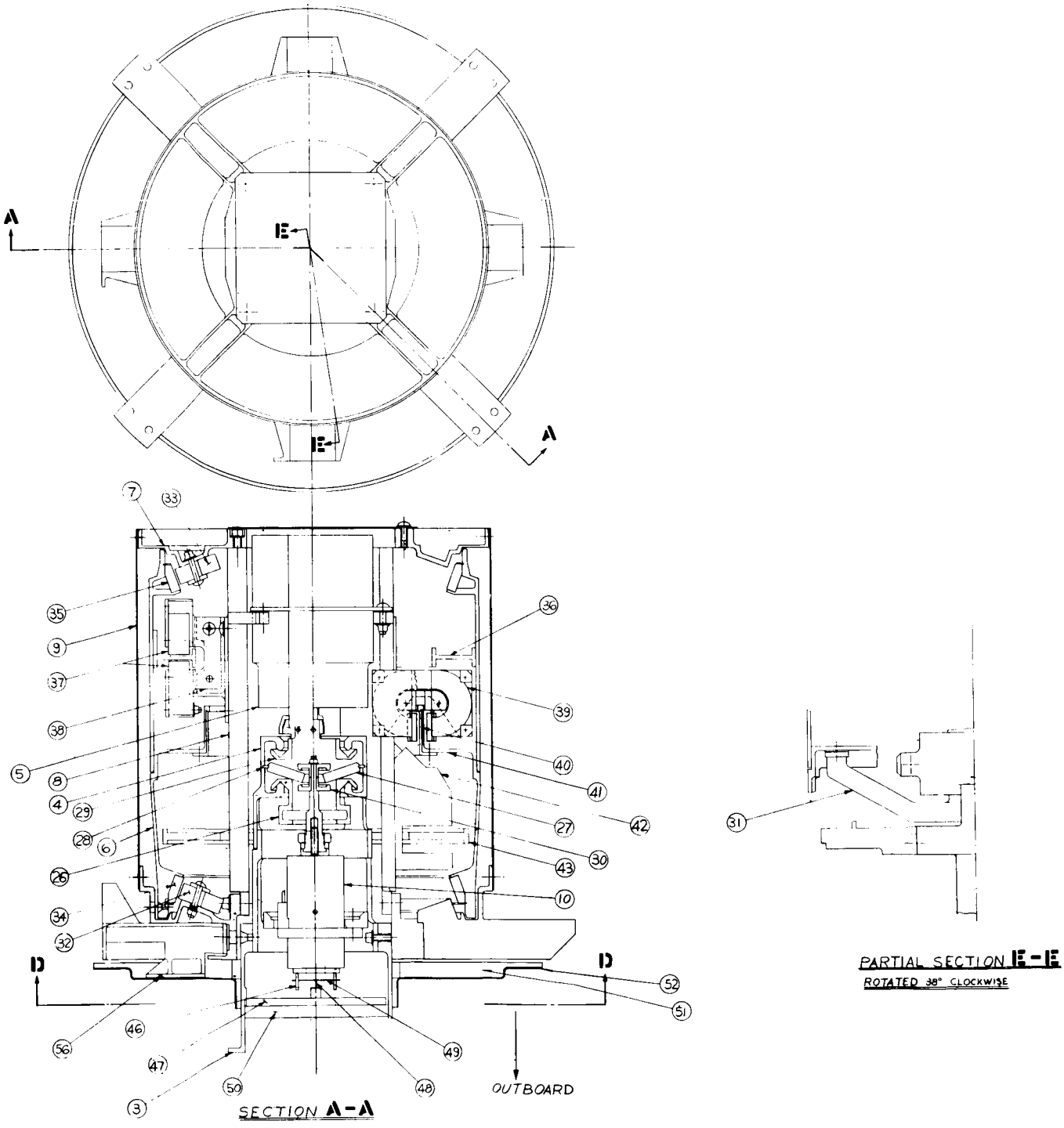

Figure 4-1. Combination Passive Damper Package (Sheet 2 of 3)

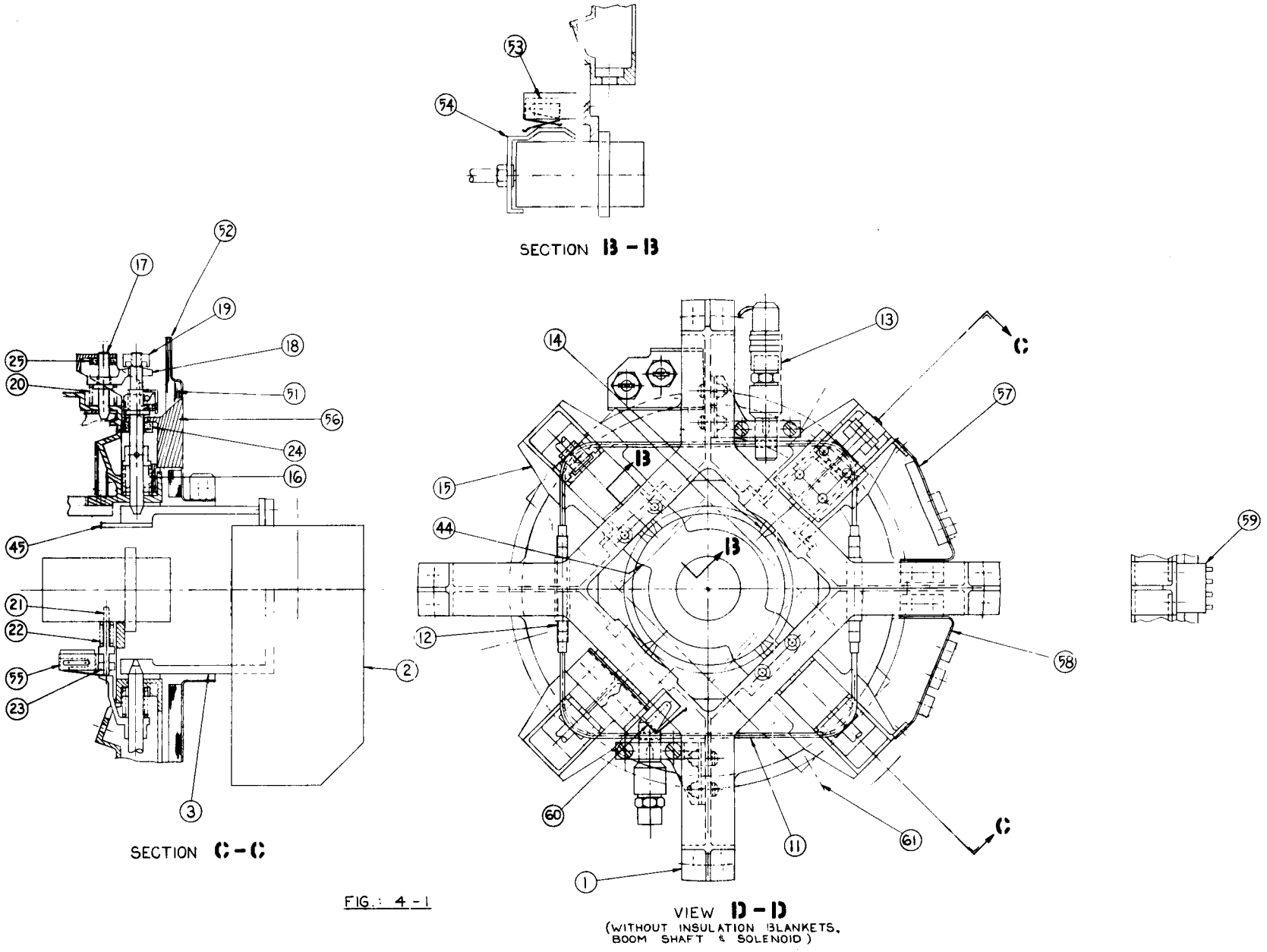

Figure 4-1. Combination Passive Damper Package (Sheet 3 of 3)

Some of the difficulty in assembly was found to be due to the very exacting and time consuming adjustments that must be made. These adjustments have been delineated on Drawing No. 47A207480 and included in manufacturing and quality control planning. Adjustments are included on the drawing for the following elements:

a. Clutch plates and hysteresis damper location
b. Solenoid and actuator rings
c. Caging pin switch
d. Boom switches
e. Solenoid switches
f. Boom shift caging
g. Soft stop adjustment
h. Angle indicator alignment
i. Pyrolytic graphite rings
j. Suspension magnets
k. Eddy-current rotor nominal position
l. Torsional restraint pattern
m. Torsional restraint magnets
n. Eddy-current magnets.

All adjustments require careful work at certain specific stages of assembly. If for some reason, the CPD must be partially disassembled, the adjustments must be repeated at reassembly. To meet the design requirements, the suspension and damping magnets must operate with close clearance. Setting of the "hard stop" position requires accurate adjustment. Caging of the damper boom and eddy-current damper requires that a certain routine be carefully followed. Accurate alignment of the clutch and solenoid are required to give adequate clearance and force. The angle indicator operates with close clearances. The "soft stop" is a relatively intricate device that operates through only 5 degrees of mechanical rotation, resulting in the need for careful accurate adjustment. It was found in making the adjustments on Engineering Unit 1, that a considerable amount of time was required from the very competent mechanics who did the assembly work.

The CPD clutch test fixture (GE dwg 47E209676) was designed and the drawing was released to manufacturing on 16 November. The parts for this test are now being fabricated. A proposed vacuum test procedure was written. The purpose of this procedure was to check that the Belleville washer in the clutch will not cold weld or seriously bind on the molybdenum pivot ring as the clutch is exercised under space environmental conditions.

TABLE 4-2. COMBINATION PASSIVE DAMPER PARTS AND FUNCTIONS

COMPONENT	FUNCTION
1. Base plate	Main structural member
2. Damper boom package	Shown in stowed position. Stores the 90-foot damper boom
3. Damper boom shaft	Couples clutch housing to damper boom
4. Clutch housing	Clutches between damper boom and selected damping element
5. Hystereses damper	Hysteresis damping mode
6. Eddy-current damper	Eddy-current damping mode
7. Inboard plate	Inboard suspension magnets
8. Posts	Connects Inboard & Base plates Internally
9. Cover	Connects Inboard & Base plates Externally
10. Solenoid core	Used to actuate clutch on command
11. Cable, 0.125-in. diameter	Retains caging pins
12. Turnbuckle	Provides tension to cable
13. Guillotine	Shears cable to uncage dampers. Squib actuated
14, Main Caging Pins	Cages damper boom to CPD framework
15. Pin Bracket	Supports caging pins
16. 49-pound Spring	Retracts boom caging pins in base plate
17. Pin	Cages eddy-current damper to framework
18. Fork	Restrains eddy-current caging pin
19. Nut	Loads boom caging pin
20. 25-pound Spring	Retracts eddy-current pin
21. Pin	Cages solenoid core
22. 10-pound Spring	Retracts solenoid caging pin
23. Guide	For solenoid caging pin
24. Buna-S Rubber Cushions	Absorb energy of boom and eddy-current caging pins, respecitvely
25. Buna-S Rubber Cushions	
26. Eddy-Current Clutch Plate	Couples eddy-current damper to boom
27. Coned Diaphragm	Holds selected clutch plate in contact with clutch housing
28. Pivot Ring	Absorbs reaction of force holding clutch faces in engagement and acts as pivot for coned diaphragm
29. Hysteresis Clutch Plate	Couples hysteresis damper to boom
30. Activator Spool	Pushes diaphragm over center when activated by solenoid
31. Arm	Attachs eddy-current rotor to clutch plate

COMPONENT	FUNCTION
32, 33 Suspension Magnets (20)	Supports eddy-current rotor
34. Pyrolytic Graphite rings	Diamagnetic material used in conjunction with suspension magnets to support eddy-current rotor
35. Pyrolytic Graphite rings	
36. Eddy-current damping ring	Actual eddy-current damping element
37. Eddy-current Magnets	Energy storage elements for eddy-current damper
38. Brackets	Attaches eddy-current magnets
39. Magnets	
40. Torsional Restraint Pattern	Provides torsional restraint element for eddy-current damper
41. Cylindrical Flange Extension	
42. Angle indicator head	Provides read-out of angular relationship between damper boom and framework of the CPD (i.e., the spacecraft)
43. Angle indicator discs	
44. Faces (on solenoid support bracket)	Constitutes "hard" stop on rotation of damper boom
45. Arms	
46. Pins (2)	Fixed portion of soft stop
47. Spider	Supports insulation pad and rotating part of soft stop
48. Torsion Wire	Contracts pins and provides required restraining torque for soft stop
49. Crossbar	
50, 51 Insulation Blanket (2)	Provide thermal shield for CPD
52 Aluminum Sheet	
53. Switches (2)	Signals position or solenoid (i.e., damping mode in use)
54. Ramp	
55. Switch	Indicates uncaging of damper
56. Bracket	Mounting for catcher bracket from damper boom
57. Bracket	Holds electrical connectors for catcher guillotine
58. Bracket	Mounting for all other connectors
59. Electronic Module	Provides telemetry processing circuits for CPD
60. Switches (2)	Indicate when damper booms have extended
61. Pin	Provides manual caging of eddy-current rotor during handling and testing of CPD
62. Transient Suppression Diodes	

4.2.3.2 Fabrication and Assembly

Engineering Unit 1 was assembled in a "clean tent" which was ventilated with constantly filtered air. All parts were cleaned ultrasonically before they were brought into the tent. Personnel were required to wear white coats, hats, boots, and white gloves before entering the clean area. Nonmagnetic tools were used as much as possible during the assembly process. Test results have shown no discrepancies which were traceable to the lack of cleanliness.

The CPD was partially assembled then disassembled several times in order to arrive at the best fabrication procedure. All of these changes were recorded and used as the basis for change notices to the procedures for assemblying subsequent CPD units.

Reference to Figures 4-2 through 4-10 will aid in visualizing the various elements of the CPD as fabricated for Engineering Unit 1.

Figure 4-2 shows the assembly with the cover and thermal shield removed as it is instrumented for vibration testing. The electrical wiring in the right of the picture was used for accelerometer and strain gage connections which were used in the vibration testing evaluation. The T-1 Damper Boom package is in place on the CPD. The switches that indicate damper boom extension, together with the actuator, are shown adjacent to the Damper Boom tip masses. The baseplate at the CPD is resting on the assembly stand. The upper magnet mounting plate is pictured at the bottom of Figure 4-2, and the rotor support of the eddy-current damper is also shown.

Figure 4-3 shows the eddy-current rotor and upper magnet mounting plate from a different angle than that shown in Figure 4-2. The nominal clearance gap (0.040 inch) between the eddy-current rotor and upper magnet mounting plate can be seen at the bottom of Figure 4-3. The eddy-current damping magnets on each side of the damping disc are shown together with the end of the torsional restraint magnet. The clutch housing is also shown, and the edge of the angle indicator encoder disc support is seen above the clutch housing.

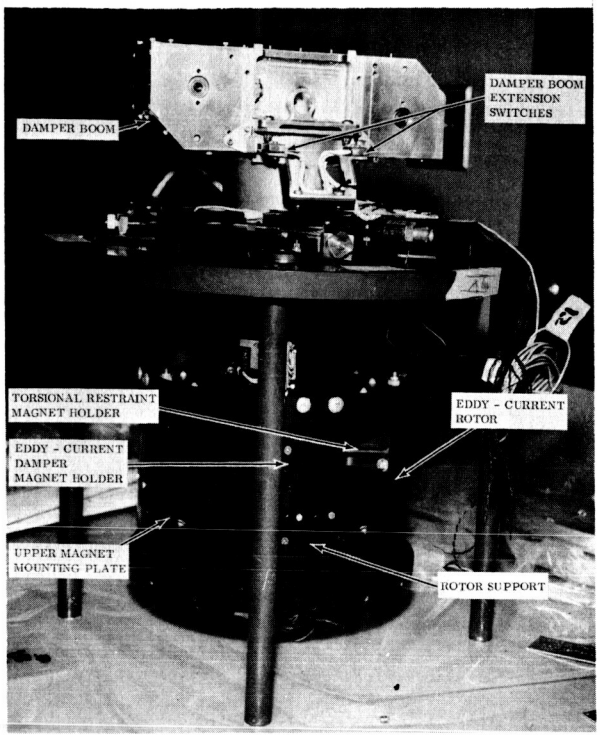

Figure 4-2. CPD Engineering Unit Assembled (Cover Removed) and T-1 Damper Boom Package in Place

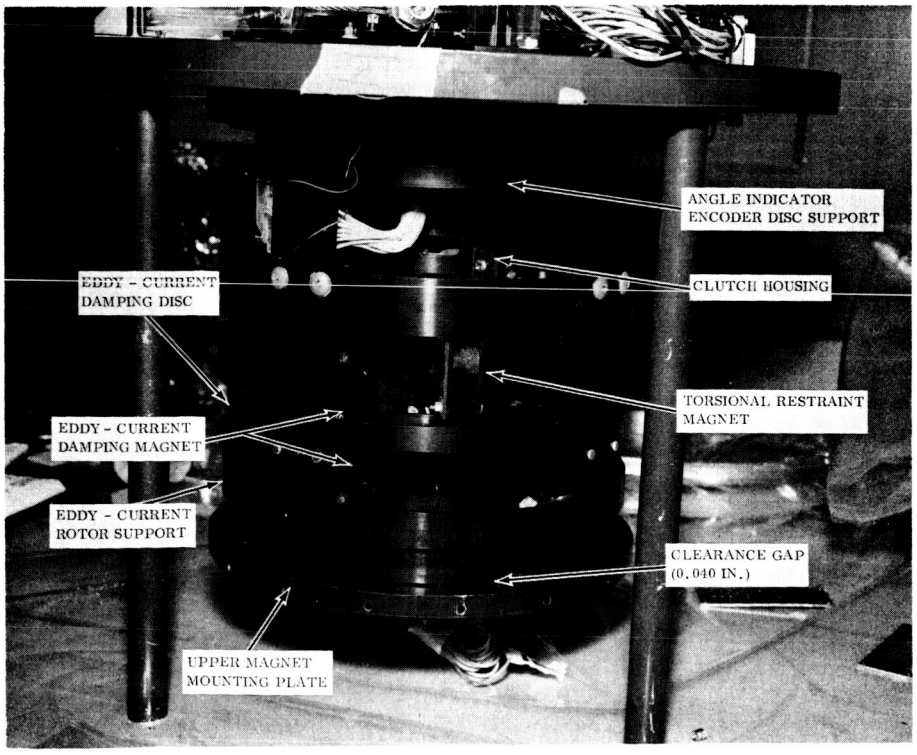

Figure 4-3. Details of CPD Engineering Unit 1

Figure 4-4 clearly shows the attachment of the Damper Boom package to the boom shaft on the CPD and the boom release mechanism which is attached to the caging pin bracket on the baseplate. The boom shaft and eddy-current damper caging cable is shown in the tensioned (caged) position with the pyrotechnic device, boom shaft caging pins and eddy-current caging pins evident.

In Figure 4-5 the major wiring run to the electrical connectors is prominent. Smaller wires (Wire Gauge No. 24 as compared to No. 20) will be used on future models to increase the clearance between the caging cable and the electrical wiring. Again, the caging cable and pins are evident as is the pyrotechnic cable cutters.

Figure 4-6 is a detail of the assembly of the suspension magnets to the upper magnet mounting plate. The magnets are adjusted to a ring fixture and clamped by the screws shown. The epoxy fillet seen around the magnets augment the frictional forces of the clamping screws to hold the magnets in place.

The lower magnet mounting plate is shown in the assembly fixture in Figure 4-7. The suspension magnets, primary structure weldment and solenoid support are also shown in this figure.

Figure 4-8 shows the lower half of the eddy-current rotor with the pyrolitic graphite ring in place. The part that is marked with an "A" is one-half of the torsional restraint pattern holder.

The first test performed following assembly of Engineering Unit 1 was an uncaging exercise. The guillotine cable cutters were electrically detonated. Figure 4-9 shows that all strands of the caging cable were completely cut by the uncaging guillotine. The right-hand part of the caging cable was placed on top of the baseplate especially for this picture: it is normally threaded through a clearance hole in a web of the baseplate. The connector on the right with its white power leads and dark ground wire was disconnected from the pyrotechnic device at the time the picture was made. When connected for firing,

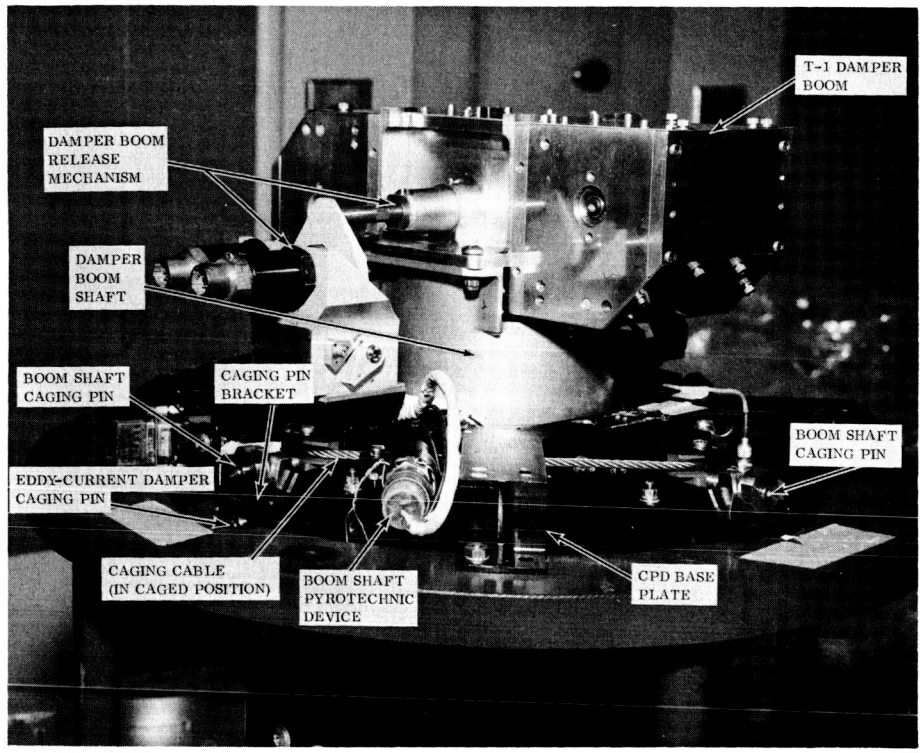

Figure 4-4. Baseplate and Caging Mechanism of CPD Engineering Unit 1 with Damper Boom Package in Place

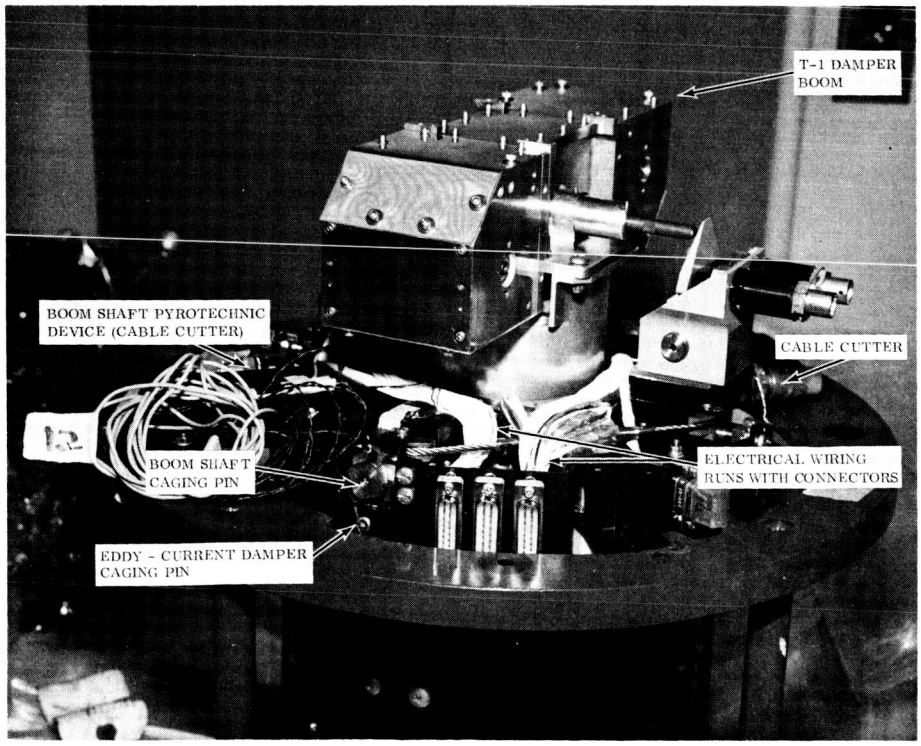

Figure 4-5. Baseplate General Arrangement, CPD Engineering Unit 1

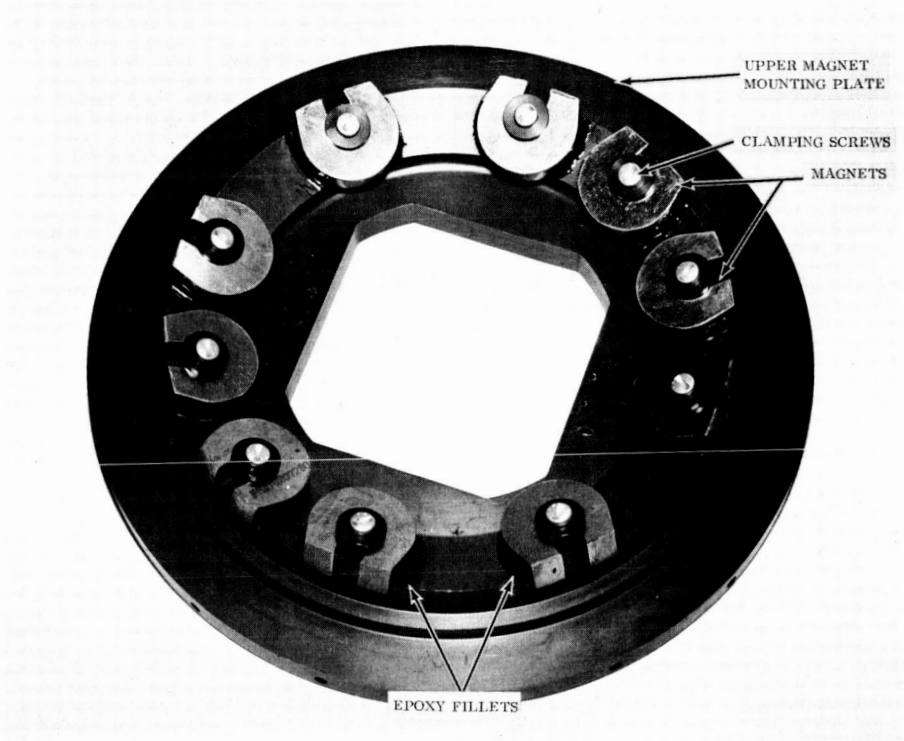

Figure 4-6. Upper Magnet Mounting Plate of Eddy-Current Damper, CPD Engineering Unit 1

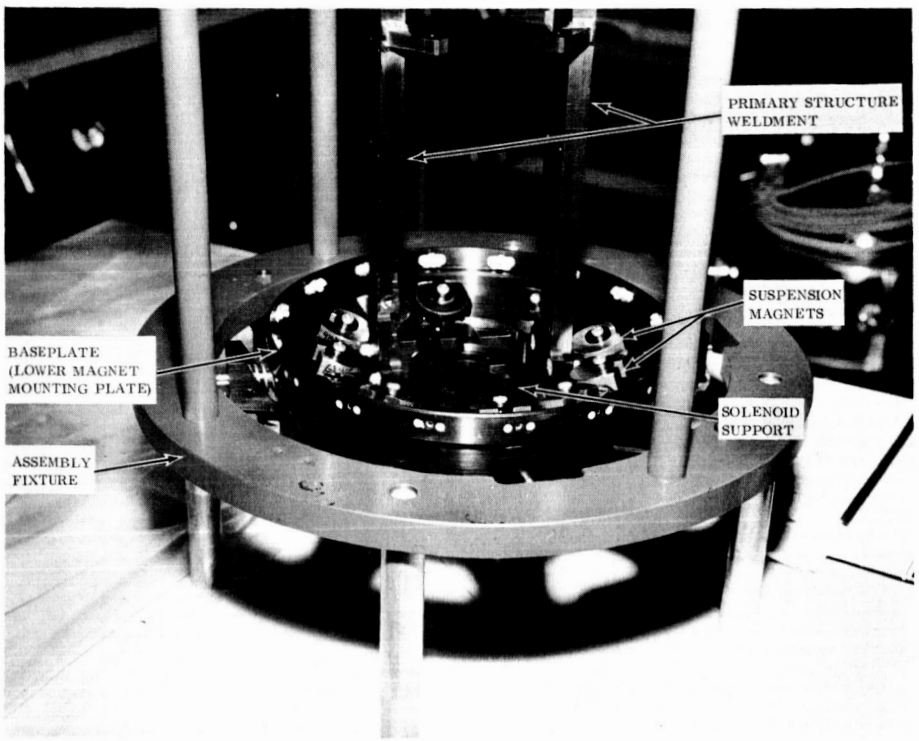

Figure 4-7. Lower Magnet Mounting Plate of Eddy-Current Damper, CPD Engineering Unit 1

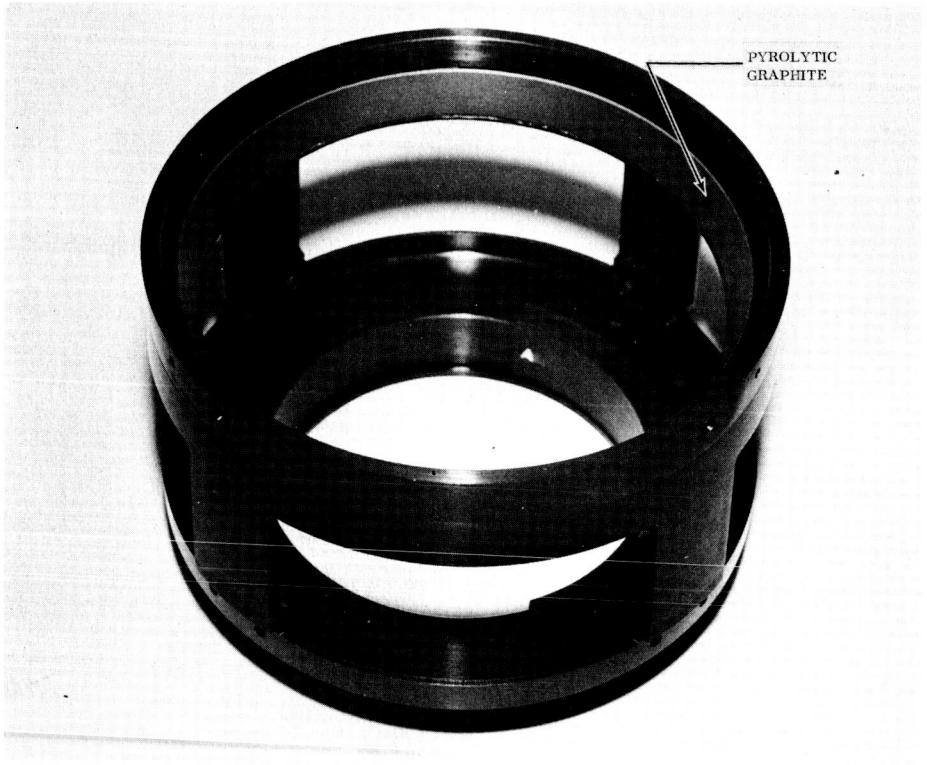

Figure 4-8. Lower Half of Eddy-Current Rotor, CPD Engineering Unit 1

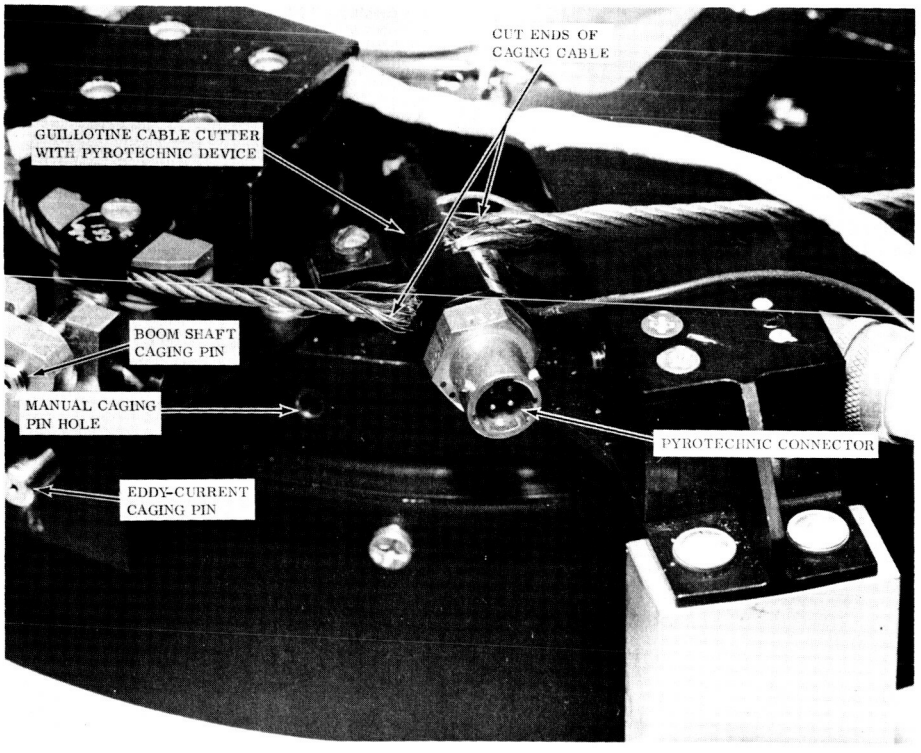

Figure 4-9. Caging Cable (at Pyrotechnic Device 1) After Uncaging Operation, CPD Engineering Unit 1

this connection would normally be inserted into the bayonet end of the pyrotechnic device shown at the center of the picture. (Figure 4-4 shows connector mated.) The bracket with four holes (shown in left of picture) is used for the boom release mechanism. The boom mechanism release is shown in Figure 4-4. The square nut, at the left-hand edge of Figure 4-9, is on the end of the boom caging pin and is used to adjust the force on the eddy-current caging pin which, in turn, is located just below. The open hole, identified in Figure 4-9, is used for the manual caging pin.

Figure 4-10 shows the opposite caging cable again completely severed. The wiring (along with the conformal coating which holds the wiring), the connectors, and the boom extension switches are also shown. The thermal insulation in the center of the boom shaft can be seen at the top center.

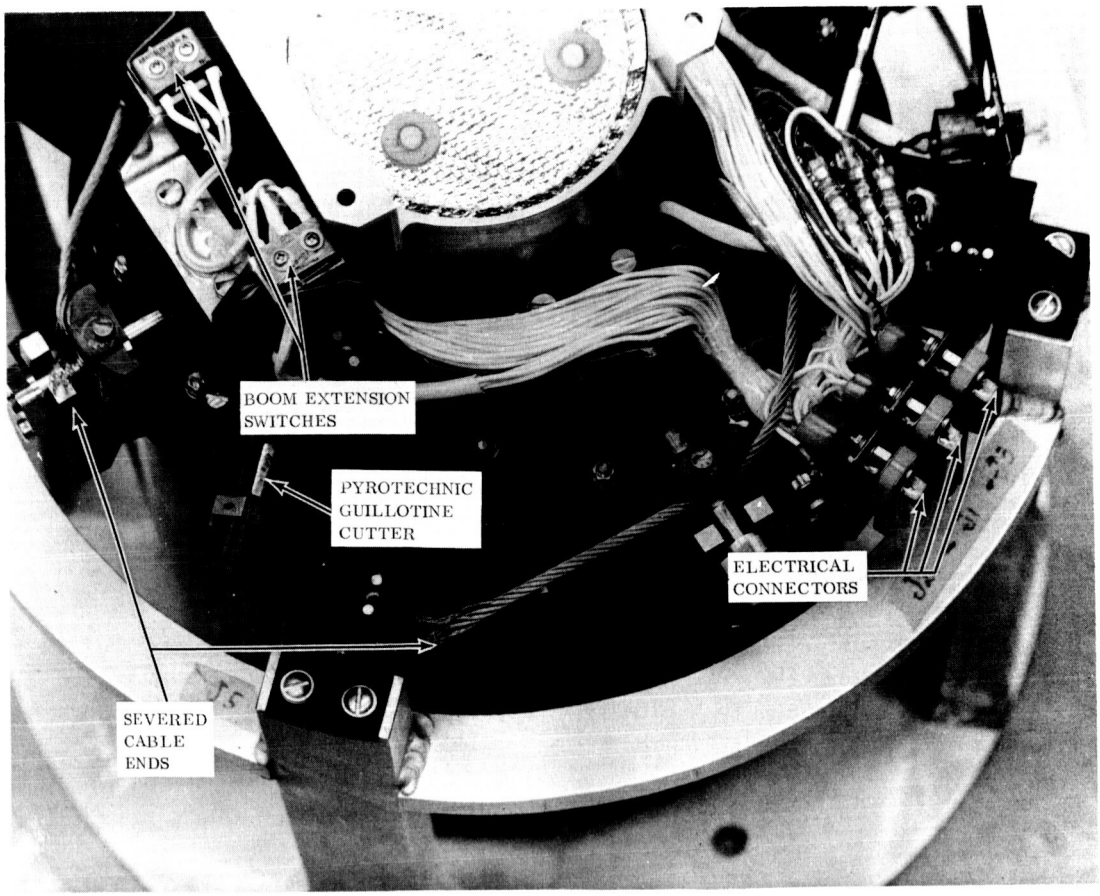

Figure 4-10. Caging Cable and Baseplate (with Pyrotechnic Device 2) After Uncaging Operation, CPD Engineering Unit 1

4.2.4 ENGINEERING UNIT 2

4.2.4.1 Design Effort

Procedures and tools developed for Engineering Unit 1 materially assisted in the assembly of Engineering Unit 2. A tool designer was available during the assembly of Engineering Unit 2 and additional tools were designed as required. The general problem during assembly of Engineering Unit 2 was to design specially shaped screw drivers and wrenches to be able to reach all of the fasteners and to allow adequate torquing.

4.2.4.2 Fabrication and Assembly

The assembly of Engineering Unit 2 was completed on 28 December. The assembly went much easier than Engineering Unit 1. Very little engineering liaison with manufacturing was required during the assembly of this second unit. Again, as on Engineering Unit 1, a number of out-of-tolerance conditions in fabrication and assembly, that would not affect the functioning of the CPD, were accepted. A survey of the problems encountered during assembly of both units was made and analyzed. This information was used as a basis for changes in the assembly of Prototype 1 and subsequent units, to facilitate fabrication, and to improve the quality of the CPD.

4.2.5 CPD PROTOTYPE UNITS

4.2.5.1 Design Effort

A considerable number of design changes have been reviewed, studied and documented during this reporting period. These changes were to correct design errors; to facilitate procurement, fabrication, and/or assembly; and, in a few cases, to improve functional performance. A number of these changes are a relaxation of tolerances. From experience in the fabrication, assembly, and testing of Engineering Unit 1, it was found that parts which had been accepted with out-of-tolerance conditions worked satisfactorily. Some of

these tolerances were relaxed, as well as others which were found to be tighter than necessary. A few of the more significant changes are discussed below.

The angle indicator head attachment to the structural weldment was changed. The angle indicator bracket and the structural weldment were altered to allow a two-bolt attachment in place of the three-bolt method which was previously used. The bolts were arranged in the new design for easier access and adjustment. One of the previous three bolts was covered by the angle indicator head, making adjustment difficult.

After considerable development effort on the welding of the structural weldment, a design was achieved that produced welds which meet the electron beam welding specification. Previous welds had been too porous. The final design uses external pads which act as heat sinks, and balance internal heat flow paths which are created by the "pads" used for bolt attachment. The external pads are cut off after the weld is completed.

The interchangeability requirement for the boom shaft was relaxed to allow line reaming of the caging pin holes. It was questionable whether true interchangeability was being achieved. The new arrangement ensures better alignment of the holes for each caging pin. A boom shaft could still be replaced by using a boom shaft piece which had not been drilled and then line-reaming it in place using the base plate assembly as a guide for the line-reamer.

The use of smaller diameter electrical wire simplified the placement of the wires on Engineering Unit 2. Because the electrical current carried is so small, the No. 24 gauge wire now being used is more than adequate.

A new thermal shield was designed for incorporation on Prototype Unit 1 and subsequent units. The redesign was necessary to meet HAC configuration requirements.

4.2.5.2 Fabrication and Assembly

The fabrication of parts for Prototype Unit 2 has progressed much more smoothly than the previous models and with fewer problems. The following factors have contributed to this condition: experience, relaxation of tolerances, availability of special tools, clarification of drawings, and emphasis on quality. The assembly of Prototype Unit 2 has not yet been started.

4.2.6 EDDY-CURRENT DAMPER - MAGNETIC TORSIONAL RESTRAINT MATERIALS INVESTIGATION

The investigation of carbonyl iron powder dispersed in an epoxy substrate, described on page 4-20 of the Fifth Quarterly Progress Report, was continued. Improvements in the formulation technique resulted in the production of uniform magnetic dispersions which are essentially free of voids and other imperfections. The effect of material thickness, magnet flux, air gap, and percentage of iron were investigated to arrive at a near optimum pattern configuration for both the ATS-A and ATS-D/E applications. A final configuration was selected which meets all performance requirements and which has no measurable hysteresis loss when tested on equipment capable of measuring as little as 1 dyne-cm of hysteresis torque.

Consequently the previously selected Eastman sound recording tape, Type A303 has been replaced by this new material on all CPD units. Engineering Unit 1 has a 20% carbonyl iron magnetic dispersion material, 0.015 inch thick. Engineering Unit 2 has a 5% carbonyl iron magnetic dispersion material 0.0075 inch thick. Further development of the material and pattern configuration has led to the selection of one pattern design for all prototype and flight units. This pattern contains 5% carbonyl iron by volume and is 0.010 inch thick. The desired magnetic torque for either ATS-A or ATS-D/E is obtained by adjusting the magnet flux.

With the 5% carbonyl iron pattern 0.010 inch thick, nominal performance is obtained as shown in Table 4-3.

TABLE 4-3. TORSIONAL RESTRAINT MATERIAL NOMINAL PERFORMANCE

	ATS-A	ATS-D/E
Torque, dyne cm/deg (2 patterns)	23.1 ± 10%	3.85 ± 10%
Lateral Force, dynes/mil (2 patterns)	9 max	1.5 max
Hysteresis, dyne cm	None	None
Linearity, % of max torque	6% Max Variation	6% Max Variation
Angular Magnetic Travel, deg	± 48° min	± 48° min
Nominal Magnet Flux, gauss	1350	550

Tests were conducted with the carbonyl iron patterns over a range of oscillation amplitudes from ± 50 degrees down to ± 2 degrees of angular travel. No hysteresis was measurable at any of these amplitudes.

Elevated temperature testing of the carbonyl iron patterns indicate a variation in torque of less than 0.4% between room ambient and 150°F. Therefore, a maximum variation in torque of less than 1% is anticipated due to thermal effects over the operating temperature range of the CPD.

A material specification for the carbonyl iron-epoxy magnetic dispersion has been prepared and issued, drawing changes have been issued, and the required number of torsional restraint patterns have been made and magnetically inspected to supply all prototype and flight units.

A discussion of the development of carbonyl iron powder for use as a torsional restraint material is reported in Section 11.

4.2.7 PASSIVE HYSTERESIS DAMPER

4.2.7.1 Subcontract Activities

TRW, Inc. delivered Prototype Unit 2 during this quarter. GE authorized TRW to begin work on the three flight units. It is anticipated that delivery will be made in January 1966.

TRW completed the first portion of the ATS-D wire qualification program. The first wire passed four qualification level vibration tests in the thrust axis while installed in the Passive Hysteresis Damper Development Model. It then passed 140,000 torsional oscillations at $\pm$ 60 degrees with no apparent degradation. The second wire broke during the second vibration test. It was then decided to review the qualification program and revise it to subject the wire to a difficult test but a more realistic one. An increase in the number of samples to be tested was made, and the number of vibration tests to which the sample was subjected was reduced.

4.2.7.2 In-House Activity

Damping and torsional restraint tests were performed on both engineering units. GE results agreed with the results obtained by TRW.

4.2.8 ANGLE INDICATOR

4.2.8.1 Design Status

During the assembly of the angle indicator heads for Engineering Units 1 and 2, several areas of difficulty were uncovered that needed rework in order to improve the units from both a manufacturing and reliability standpoint. Most of these changes were of a minor nature and were incorporated into Engineering Unit 2. One of the two remaining areas is in the manufacture of the module, which is presently being reworked, and offers no problem. The second difficulty is in mounting the phototransistors. At present the five phototransistors

in each head are mounted directly into the head. During manufacture, it was observed that this method presents an opportunity for major mistakes to be made. Direct mounting also creates a hazard because damage can be done to the phototransistors and unwanted foreign material may be included with the phototransistors. In addition, the replacement of a phototransistor presents major problems. The approach now being studied is to premount the phototransistors in a metallic sleeve and perform various subassembly operations on the unit (e.g., place sleeving on leads, form and bond leads, bond phototransistor to sleeve). These subassemblies could then be bonded into the angle indicator head.

The fiber optic assemblies used in Engineering Units 1 and 2 are of the 250-bundle randomized version as reported in the November and December Monthly Progress Reports. These units show a marked improvement over the old units in uniformity of light transmission, but the total light transmission on these units, although adequate, is somewhat lower. The units to be used for prototype and flight have been tested and have shown an increase of approximately 10% in transmission over those used in Engineering Units 1 and 2.

During the vibration test of Engineering Unit 1, the encoder disc broke at a number of places as shown in Figure 4-11. The possibility of this happening had been considered and a new disc of a different temper and thickness was being built; however, it was not possible to install it into Engineering Unit 1 in time to meet the engineering test schedule of the unit. Because of the number of the fractures in the first disc, a program is now underway to improve the design from both a materials and physical standpoint. The improvements being investigated include:

a. The pattern is being repositioned to eliminate inadequately supported sections.
b. Corner radii are being increased to reduce stress concentrations.
c. Material is being changed to improve fatigue strength.

The new discs will be subjected to a qualification level vibration test prior to installing it into future units. The design shown in Figure 4-12 incorporates the changes mentioned

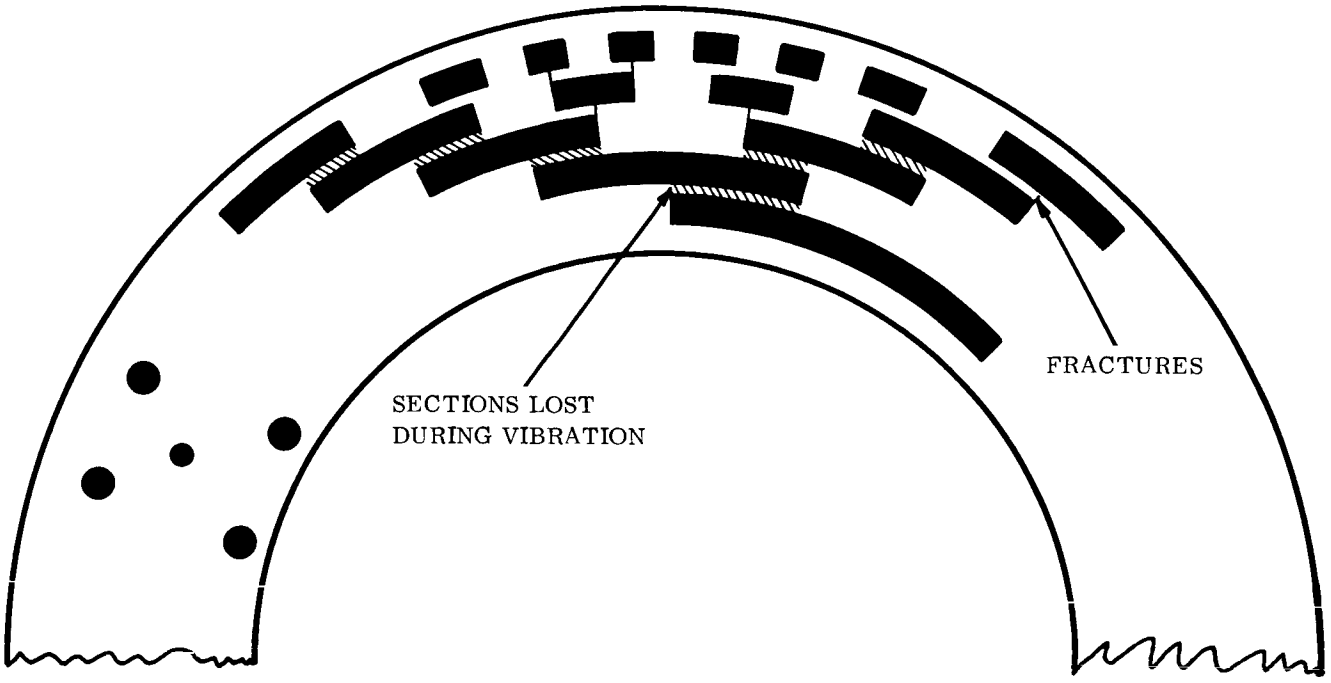

Figure 4-11. Original Encoder Disc Design

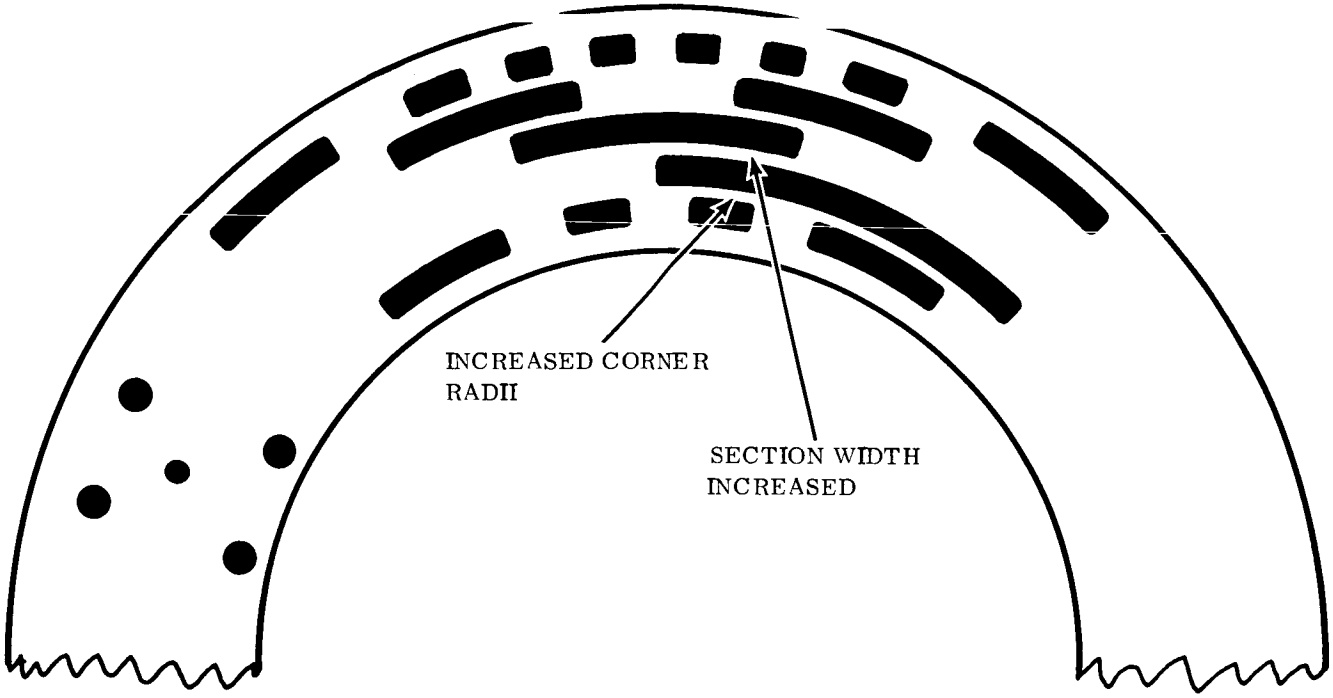

Figure 4-12. New Encoder Disc Design

in (a) and (b) above and this design is being fabricated in several materials for test evaluation. Comparison of Figures 4-11 and 4-12 will reveal that there has been some transposition of the various bits. These transpositions provide more physical support of all cut-out sections. The increased corner radii are also readily apparent in Figure 4-12.

4.2.8.2 Testing

Temperature tests of the angle indicator module were performed to determine the sensitivity of threshold levels (i.e., the input current value at which the output changes from a "0" state to a "1" state or vice versa) to temperature. The results of the test, as plotted in Figure 4-13, show that the "0" threshold of the module is well below the nominal design maximum for this threshold. It should be noted that these nominal threshold values have been chosen so that a considerable degradation can occur in the threshold (i.e., current required can increase significantly) without affecting the performance of the angle indicator. The data also show that the "1" threshold is considerably higher than the minimum design value at all temperatures.

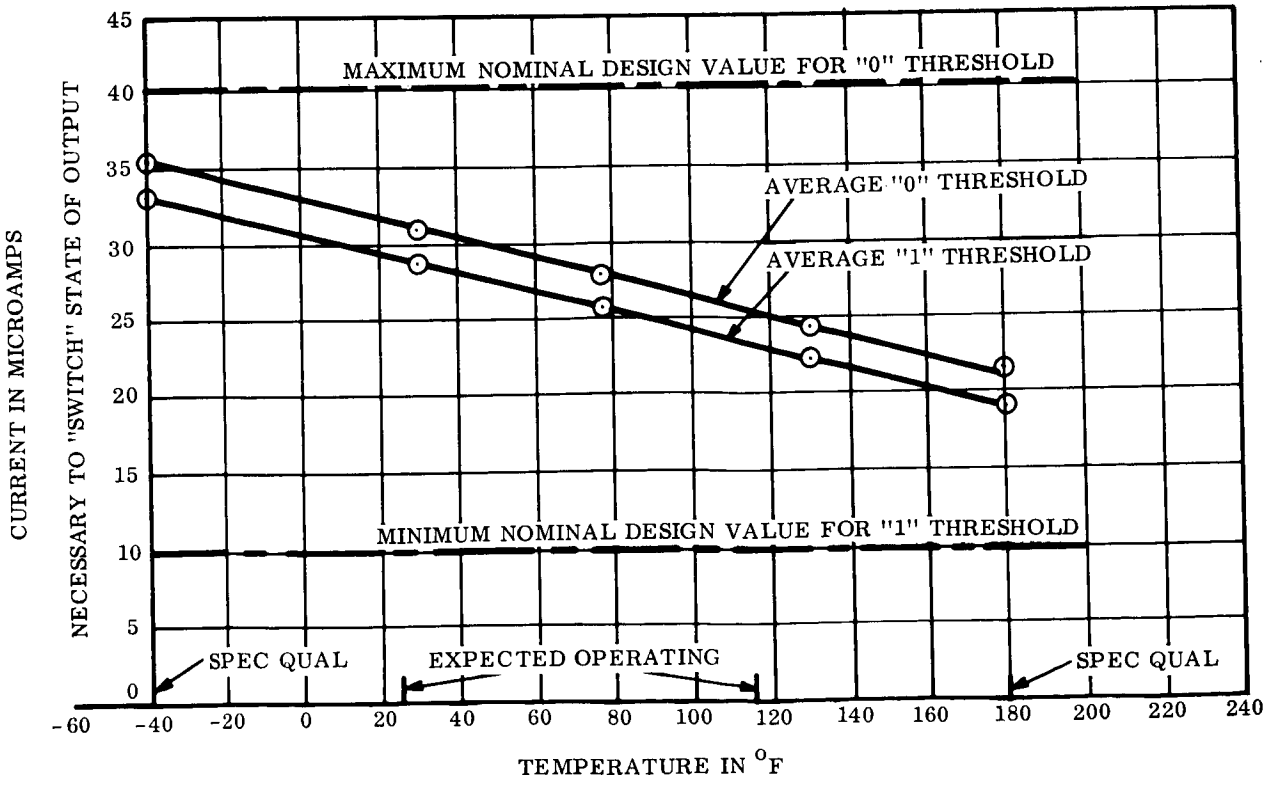

Figure 4-13. ATS Angle Indicator Thermal Test Results (Average of Two Modules)

Five lamps are on an accelerated voltage life test (6.3 volts as compared to a nominal voltage of 5.7 volts). Test time to date is equivalent to 163 days in orbit. No significant changes have occurred to date.

A comprehensive test program is in process to completely evaluate the angle indicator as a unit by itself. This testing consists of temperature and humidity effects as well as simulated degradations due to radiation and end-of-life considerations. Results of this testing will be used to verify end-of-life design margins and variation of angular accuracies under the above mentioned environments and conditions.

4.2.9 SOLENOID

The engineering evaluation program conducted by GE on the first two units was successfully completed. The two prototype units were delivered to GE, along with one spare unit, by Koontz-Wagner. Koontz-Wagner started the qualification program on the six qualification solenoids. The first two units that were vibration tested failed when the shaft broke at the end of the thread. The problem was traced to a notch at the break point. These threads were made differently than the engineering units. Two additional qualification units were reworked to eliminate this notch and both passed vibration tests successfully. The three units delivered to GE are to be returned to Koontz-Wagner for rework.

4.3 TEST EQUIPMENT

All mechanical test equipment, cables and consoles have been completed and were used for Engineering Unit 1 and 2 in-process and final component testing, with the exception of the thermal chambers for the LOFF and for the ADTF. The LOFF chamber has been completely fabricated and is in the process of being checked for proper operation. The ADTF chamber is 75% complete. Availability of these ovens will not delay the CPD testing schedules.

A series of setups was completed on the LOFF and ADTF equipment using the dynamic model of the CPD as a mockup of the completed CPD. These exercises gave the test personnel an opportunity to verify test procedures which were to be used with Engineering Unit 1 in advance of actual tests. The test arrangement for measuring radial force is shown in Figure 4-14. The axial force test setup is shown in Figure 4-15. The overturning torque test setup is shown in Figure 4-16.

Air bearing manometer accumulators were designed to protect the air bearing from possible water damage in the event of a large bearing pressure differential and the resultant manometer blowover. These units were fabricated and installed on all air bearings.

A close-up view of the console panels is shown in Figure 4-17. The top panel controls the functions of the angle indicator (detector). The lower panel contains the controls for the CPD functions.

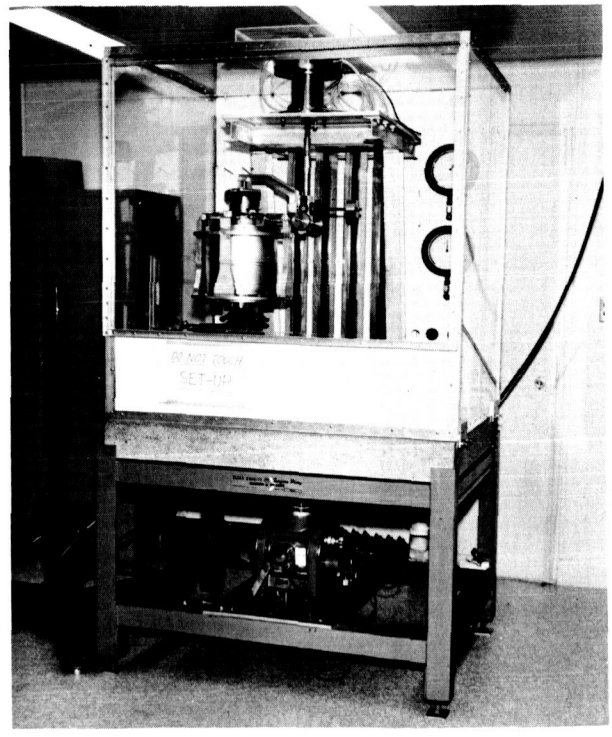

Figure 4-14. Radial Force Measurement Test Setup on LOFF

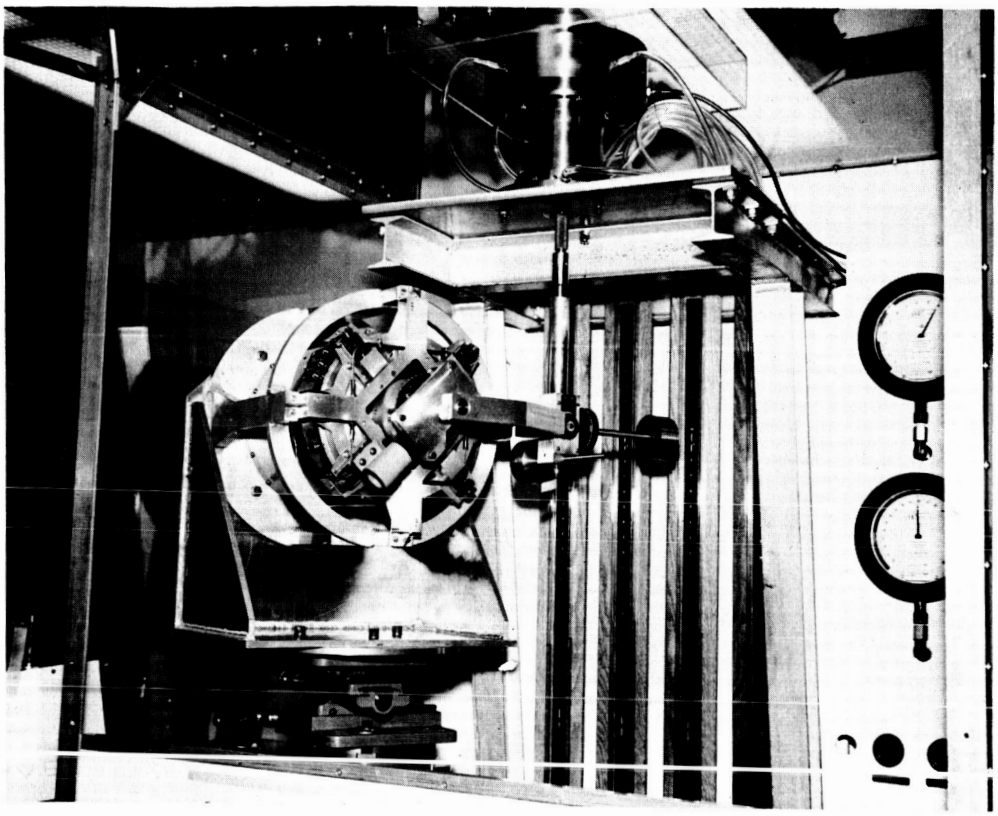

Figure 4-15. Axial Force Measurement Test Setup on LOFF

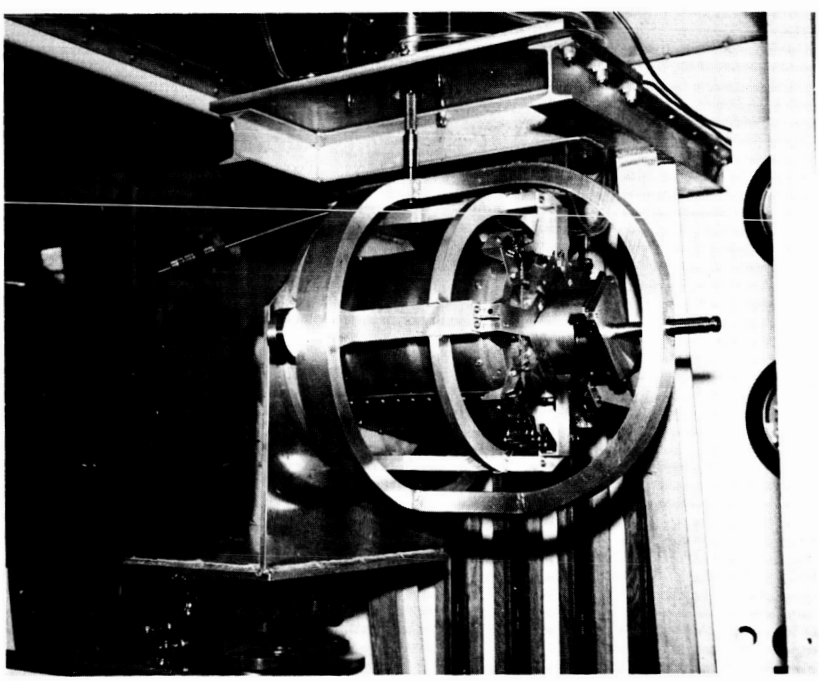

Figure 4-16. Overturning Torque Test Setup on LOFF

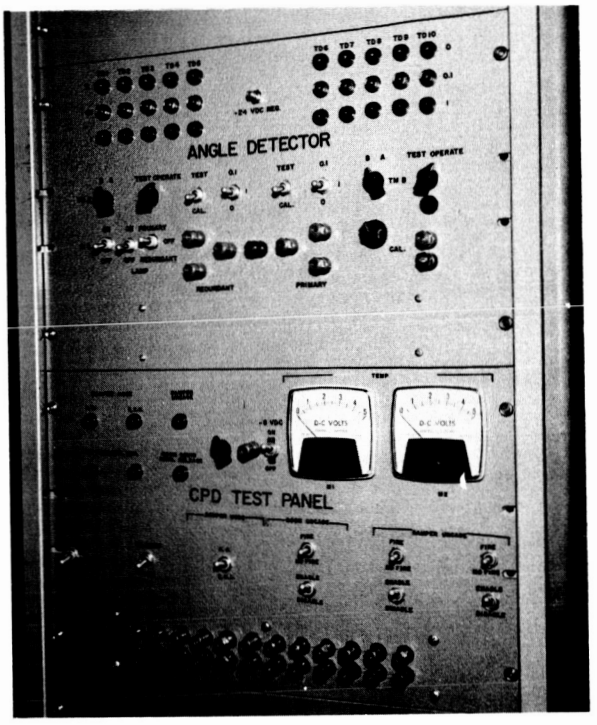

Figure 4-17. CPD Test Panels

SECTION 5
ATTITUDE SENSOR SUBSYSTEM

5.1 SUBSYSTEM DESCRIPTION

The latest electrical configuration of the ATS Gravity Gradient Stabilization System is shown in Figure 5-1. Since there have been no major conceptual changes in the last quarter, it is similar to the configuration shown in the Fifth Quarterly Report. The only exception is that the encoder and decoder identification letters, A and B, were revised to agree with the ATS-A Interconnection Diagram (GE drawing 47J207481), which is published monthly by GE in the Monthly Interface Reports. Although no changes to the general block diagram of the ATS Gravity Gradient Stabilization System are contemplated at this time, the latest electrical configuration can be obtained during the interim between quarterly progress reports by consulting the interface documents referenced above.

5.2 TV CAMERA SUBSYSTEM

5.2.1 THERMAL ANALYSIS

A detailed thermal analysis of the TV Camera was completed in November 1965. In-orbit temperature profiles were calculated for equilibrium conditions of maximum and minimum solar heating at synchronous altitude. Figures 5-2 and 5-3 present incident solar flux levels as a function of time in orbit. This data corresponds to special case orbits which occur at the Vernal or Autumnal equinox for maximum heating and at the summer solstice for the case of minimum solar heating.

Wherever possible, design data was taken from a layout drawing of the lens package as provided by Revere-Wollensak division of Minnesota Mining and Manufacturing Co. In addition, some dimensions of the lens package were measured directly from an engineering model. An extensive disassembly of the camera was not permitted to preserve the

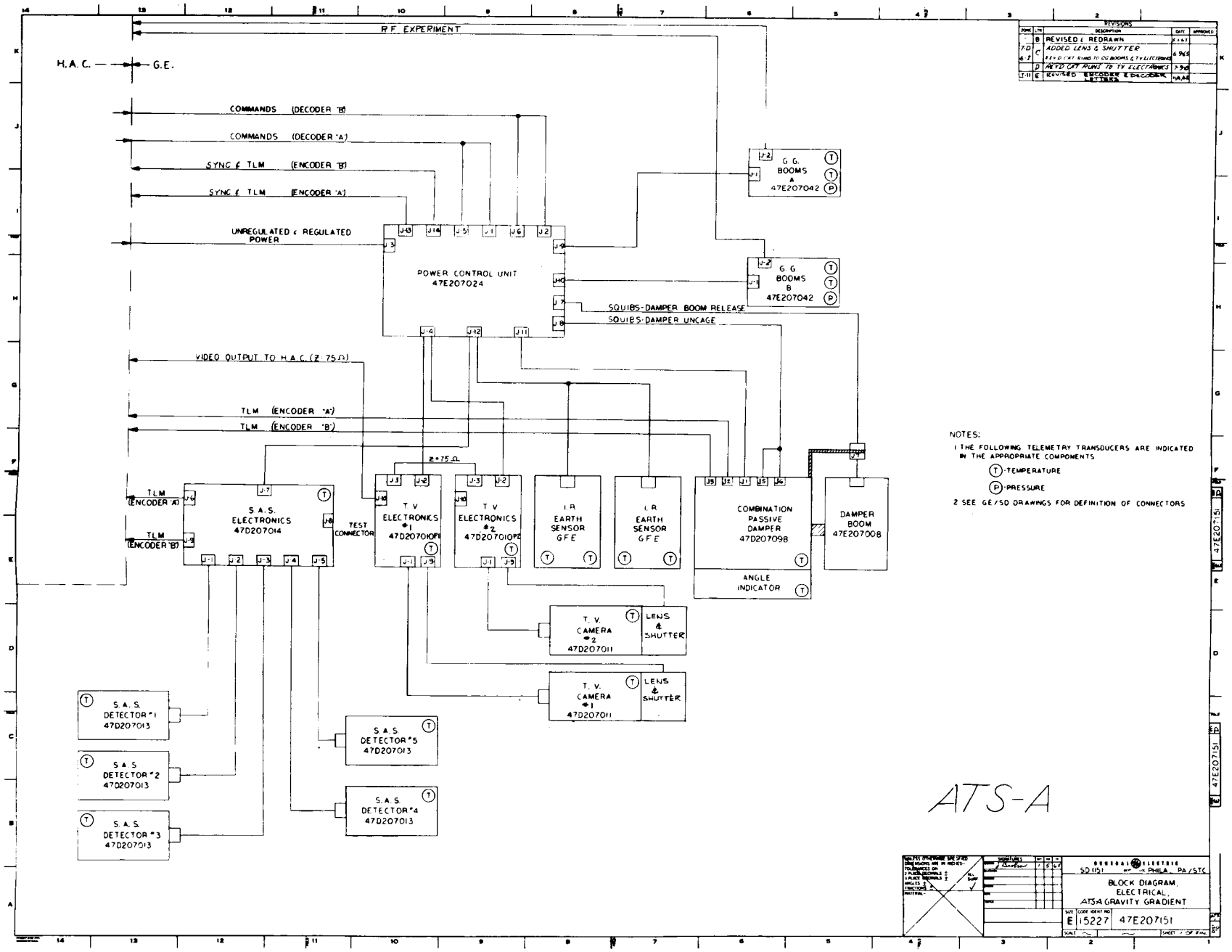

Figure 5-1. GE/HAC Electrical Interface (GE Drawing 47E207151)

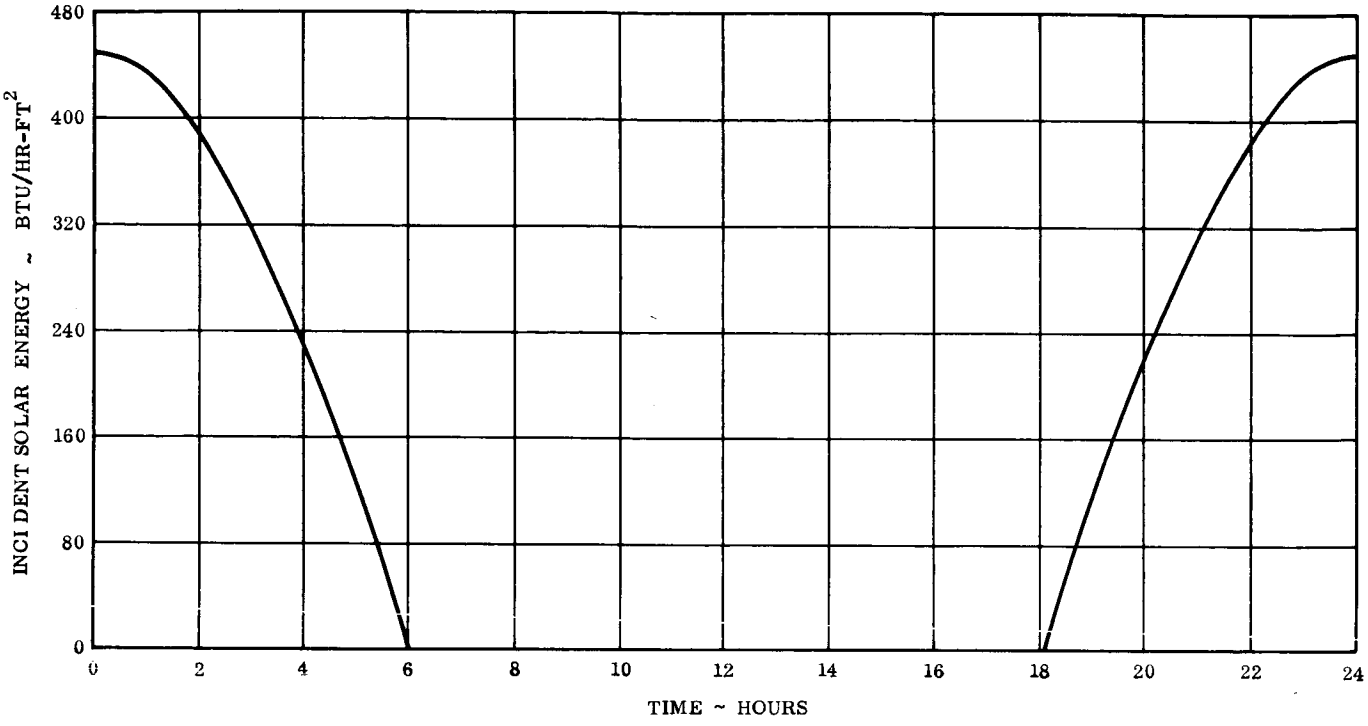

Figure 5-2. Orbit of Maximum Incident Flux on TV Camera

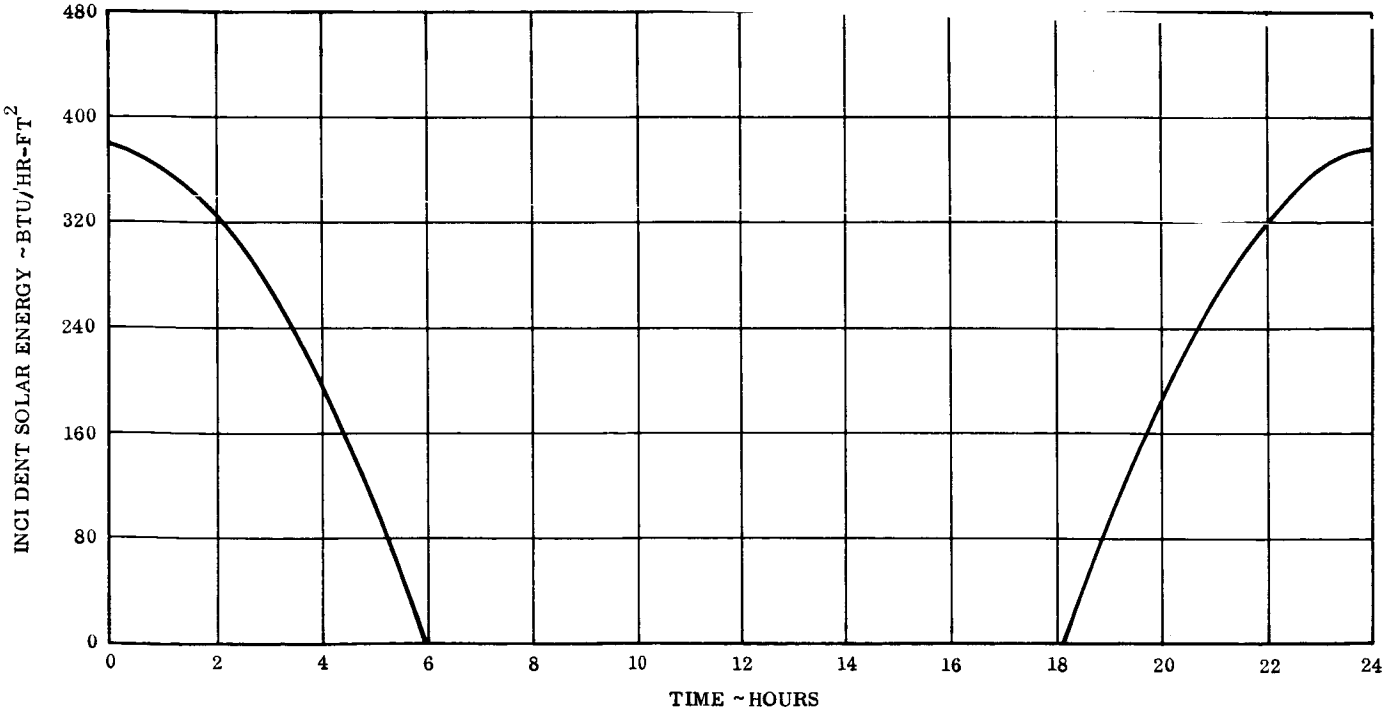

Figure 5-3. Orbit of Minimum Incident Flux on TV Camera

integrity of the assembled model. Other details relative to the vidicon tube and camera electronics were obtained from the cognizant component engineer. Information regarding the internal vehicle environment for the camera was not available. Accordingly, assumptions were made to define the radiation sink temperatures surrounding the camera and to incorporate a measure of the effectiveness of the camera mounting surface which will be provided by the Hughes Aircraft Company.

The following assumptions were made as a basis for the analysis:

a. For the quartz filter - reflectance = 0.25
   - transmittance = 0.28
   - absorptance = 0.47

b. Camera wall thickness = 0.125 inch

c. Camera shutter closed for solar cone angle < 44 degrees

d. Vidicon heater dissipation = 0.9 watt

e. Temperature at camera mounting lugs = +110°F maximum
   = + 35°F minimum

f. Camera exchanges heat by radiation with EME experiment - Temperature of experiment package = +120°F maximum
   = + 40°F minimum

g. Geometric view factor to EME experiment package = 0.65

h. Camera exchanges heat by radiation with thrust-tube - temperature of thrust tube = +100°F maximum
   = + 40°F minimum

Results of the analysis are presented in Figures 5-4 through 5-13. Despite the conservative estimates of assumptions (e) and (f), the anticipated maximum temperature of the vidicon face plate is well below the recommended maximum operating temperature of +140°F.

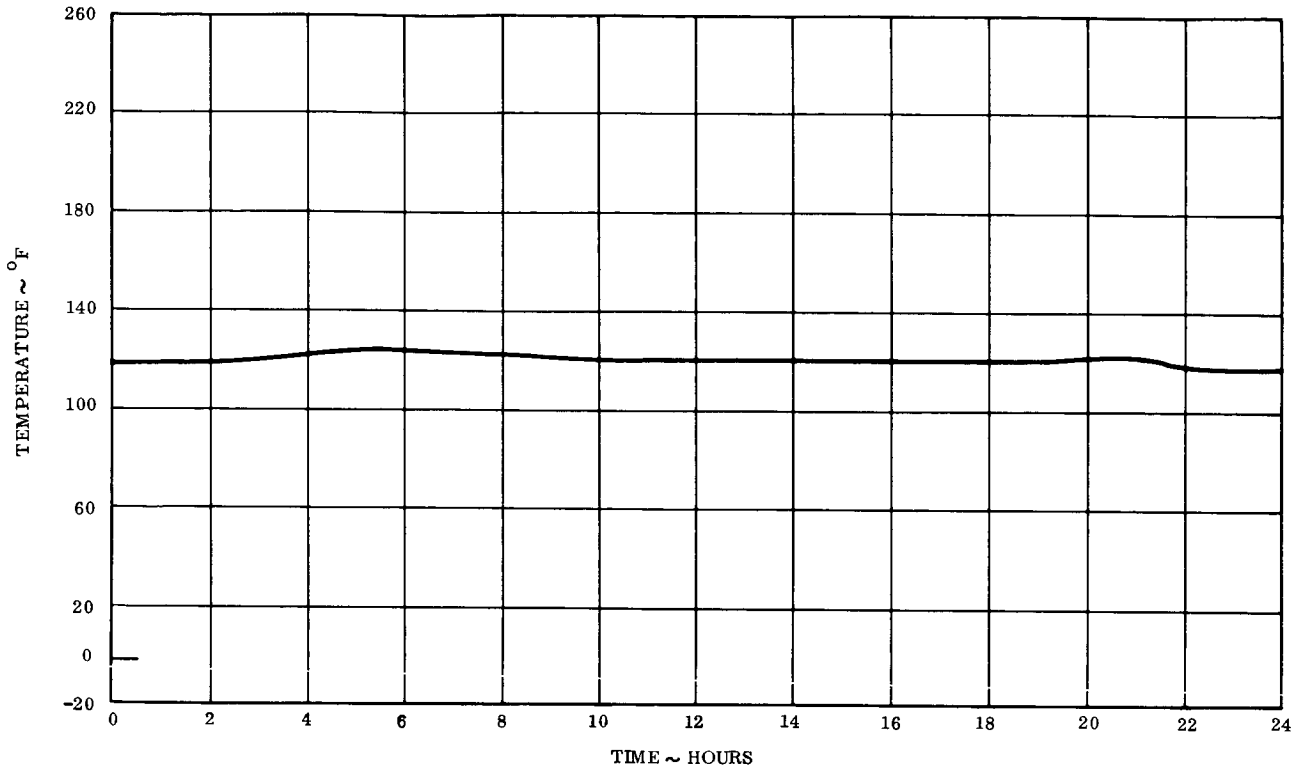

Figure 5-4. Temperature Profile in Maximum Flux Orbit for Vidicon Face Plate

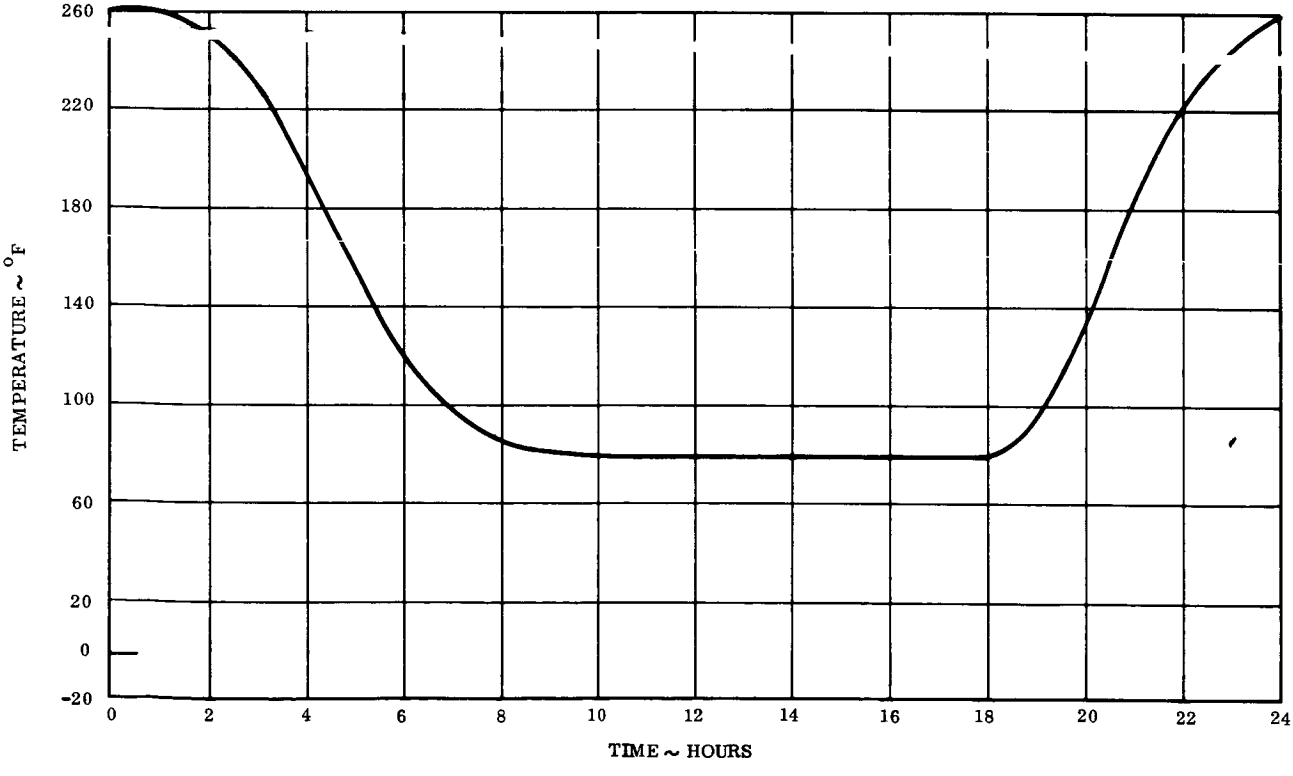

Figure 5-5. Temperature Profile in Maximum Flux Orbit for Solar Shutter

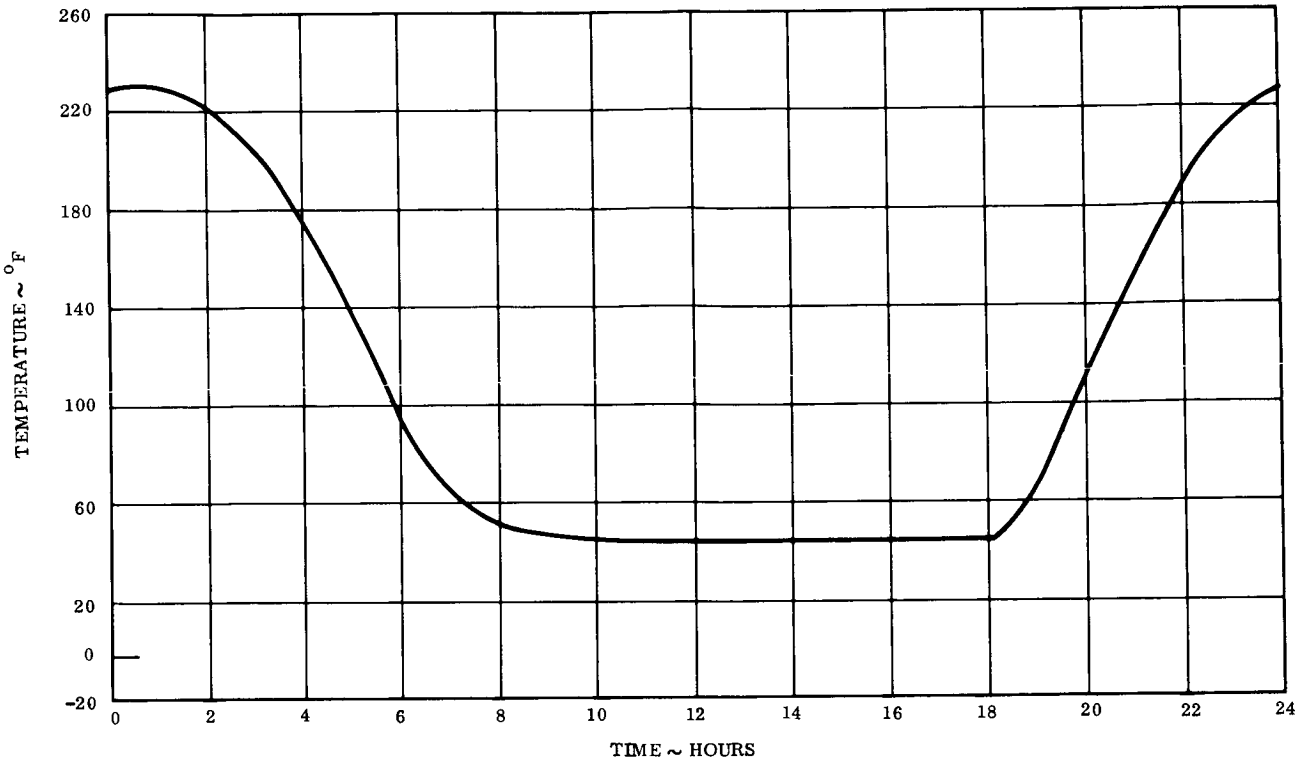

Figure 5-6. Temperature Profile in Maximum Flux Orbit for Quartz Filter

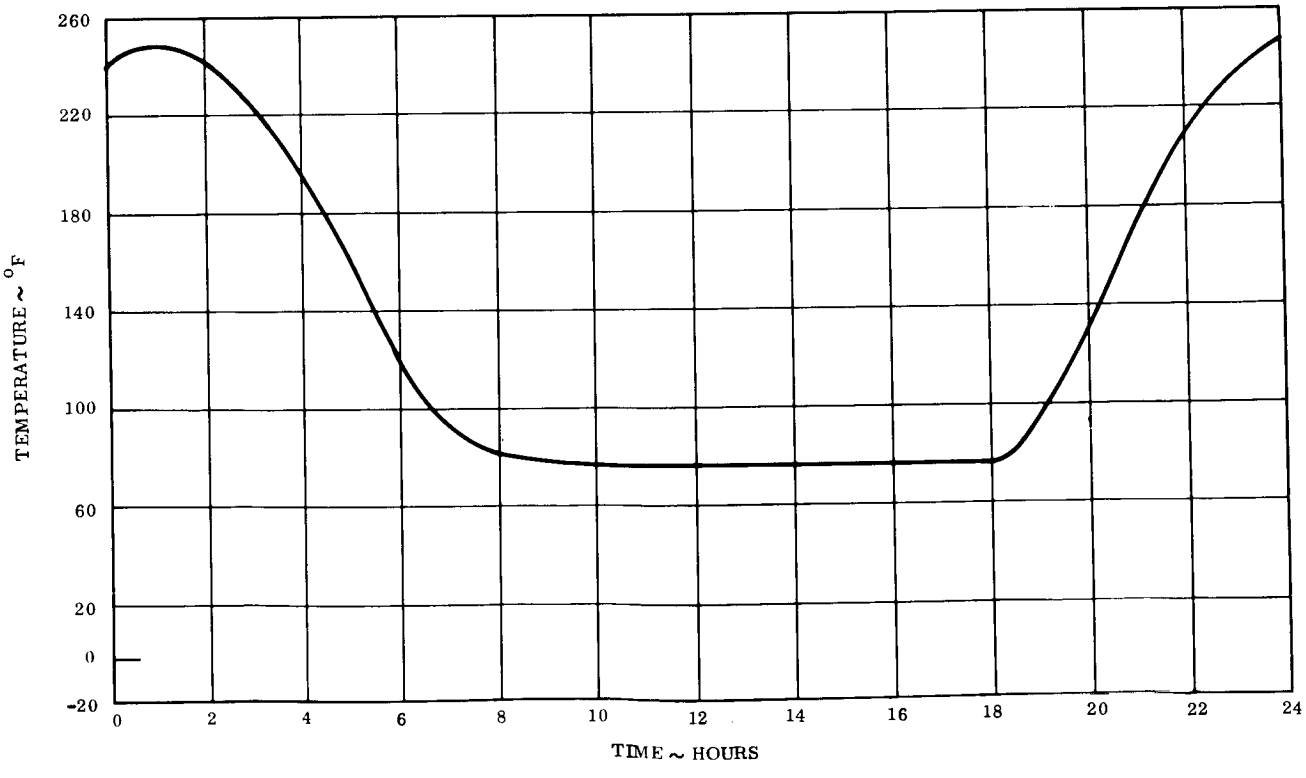

Figure 5-7. Temperature Profile in Maximum Flux Orbit for Filter Support Structure

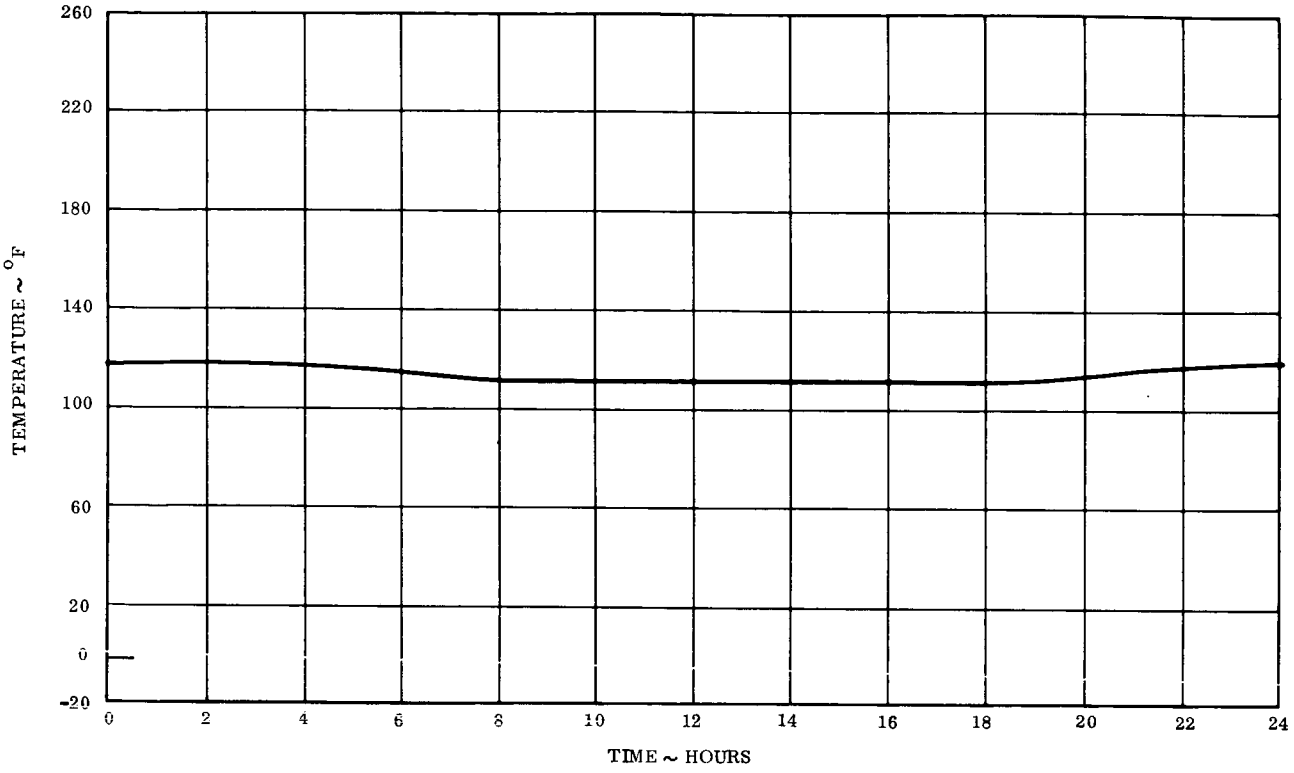

Figure 5-8. Temperature Profile in Maximum Flux Orbit for Camera Case

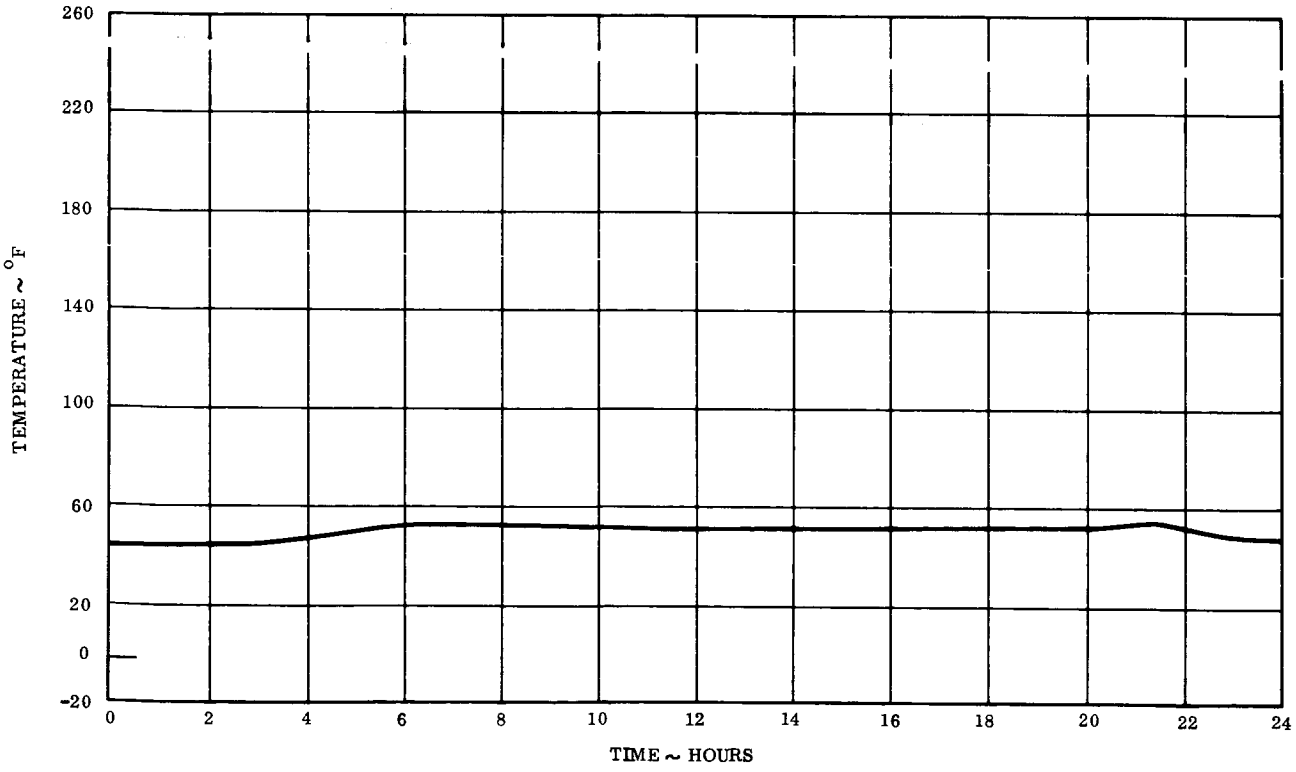

Figure 5-9. Temperature Profile in Minimum Flux Orbit for Vidicon Face Plate

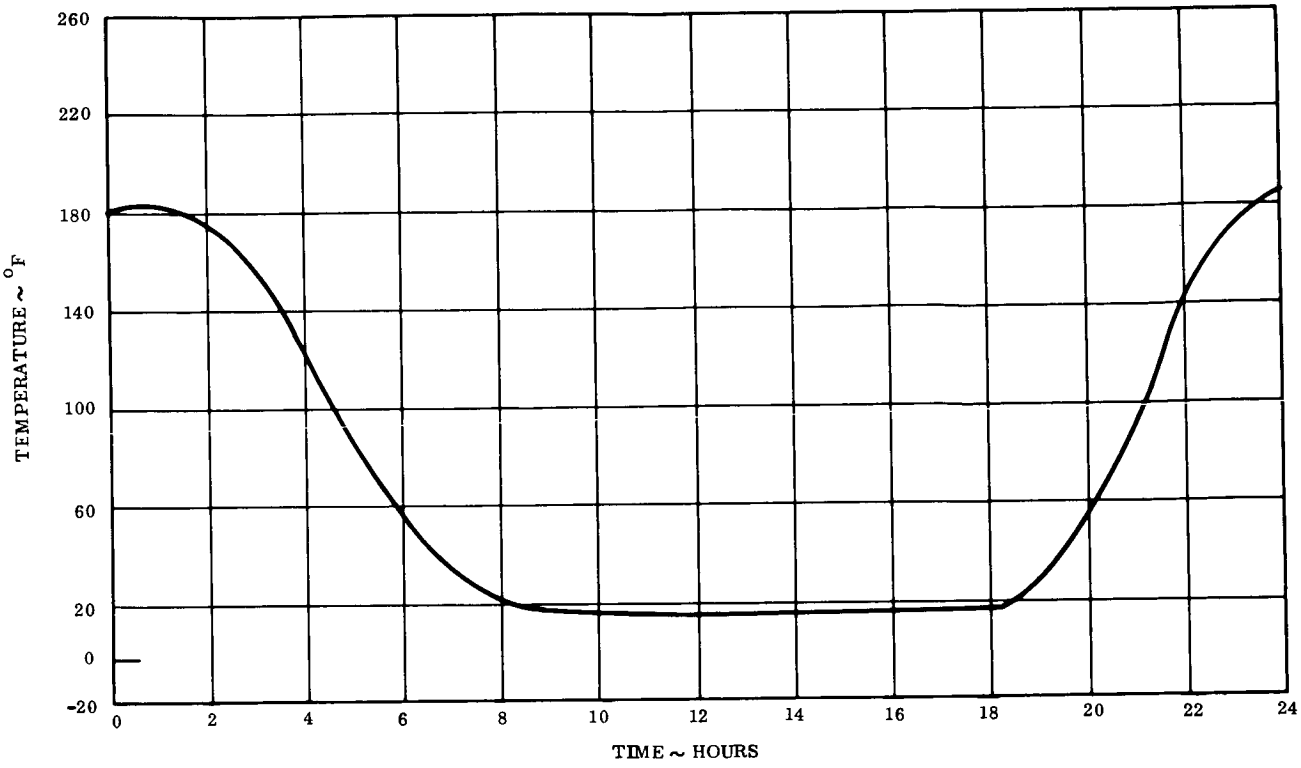

Figure 5-10. Temperature Profile in Minimum Flux Orbit for Solar Shutter

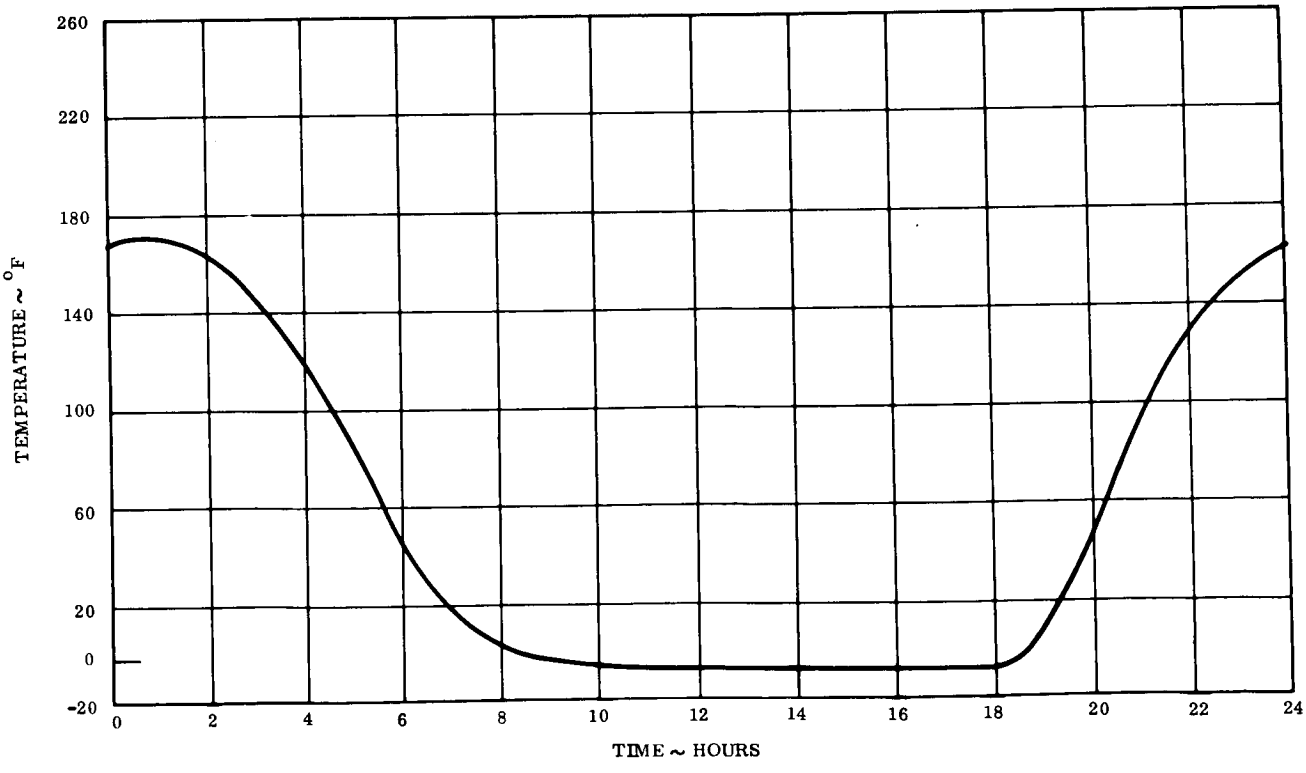

Figure 5-11. Temperature Profile in Minimum Flux Orbit for Quartz Filter

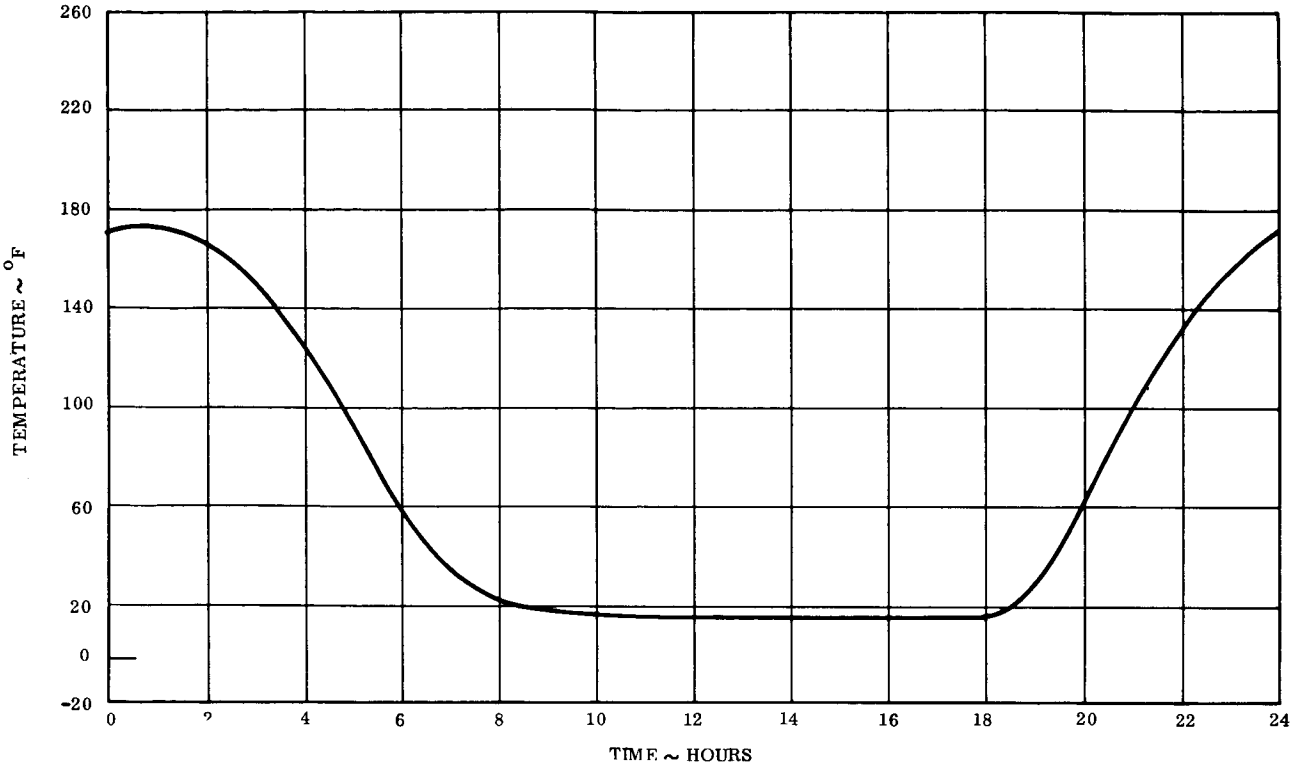

Figure 5-12. Temperature Profile in Minimum Flux Orbit for Filter Support Structure

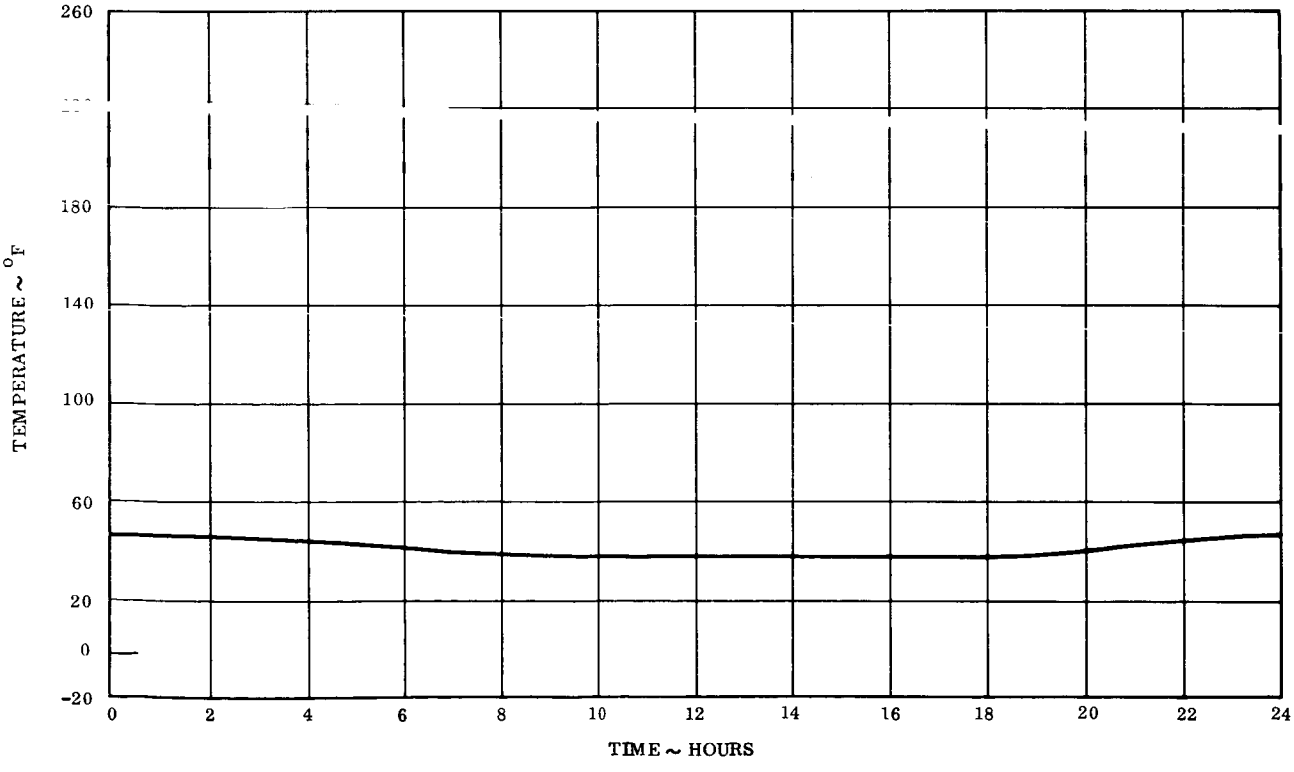

Figure 5-13. Temperature Profile in Minimum Flux Orbit for Camera Case

5.2.2 CORONA TESTING

The second TV Camera System (Engineering Model SN-5102) was subjected to a corona test in a 2-foot by 2-foot vacuum chamber. For this test, five channels of Sanborn 150 recording were made which included the four telemetry channels of the TV Camera Subsystem and a wide band (30-15,000 kc), Field Intensity Meter, NM-40A, No. IC WK-016. Telemetry channels are: 1) vidicon heater current, 2) vidicon target supply voltage, 3) vidicon faceplate temperature, and 4) power inverter temperature. Channel 6 was the RFI meter. The current probe for this receiver was placed surrounding the multiconductor cable that interconnects the camera and control units.

The sequence of test events are listed as follows. Operation of the TV Camera Subsystem was verified by observing the monitor and oscilloscope traces of the composite video signals. The recorder was calibrated. The telemetry voltages number 1, 3 and 4 were checked by the VTVM on the test console. The chamber platen thermostat was set to $80^{o}F$.

Pump down was started at 1200 hours. By 1208 hours the chamber pressure was approximately 2 mm Hg and first indications of malfunction were observed. In these observations and those that followed, malfunction was observed as a momentary loss of picture and as a noise pulse in the RFI meter. After malfunction occurred, the TV Camera Subsystem was turned off and chamber pumping was stopped. The supply voltage was then reduced from 24 to 20 volts. Malfunction was again observed when the camera was turned on.

Chamber pumping was resumed and at a chamber pressure of 300 microns, the platen thermostat was reset from $80^{o}F$ up to $120^{o}F$. This was done in order to accelerate any outgassing. When a pressure of 10^{-4} mm Hg was obtained the pressure gage indicated abrupt changes in pressure. These irregularities were interpreted as evidence of outgassing.

At 1344 hours (104 minutes after the test started) the chamber pressure was 1.2×10^{-5} mm Hg. The TV Camera Subsystem power supply voltage was lowered to 20 volts and the power was turned on. The vidicon heater current was somewhat low (65 ma whereas 85 ma is nominal). All other readings appeared within expected range. The power supply voltage was then raised to 24 volts. Heater current came up gradually to 81 ma. Chamber pumping was then stopped. Faceplate temperature was measured as $101^{o}F$. Platen temperature was reset from $120^{o}F$ to $80^{o}F$ and dry nitgrogen was slowly bled into the chamber. The TV Camera Subsystem was operating as the pressure was increasing in order to find the rising pressure at which breakdown would occur. No indication was observed until a pressure of 3×10^{-4} mm Hg was obtained. The TV Camera Subsystem was turned off whenever repeated indications were obtained. These occurred again at 3.7×10^{-4}, 4.5×10^{-4} and 7×10^{-4} mm Hg. After the last indication the TV Camera Subsystem was kept off until ambient pressure was obtained. When turned on at ambient pressure, no TV picture was obtainable.

The following conditions were determined immediately after test. Heater current and target supply voltage were apparently normal. Input current dropped from 330 ma to 320 ma. Horizontal sync was present.

Subsequent testing revealed that a 2N598 transistor (Q12) in the camera had a partial short from collector to emitter. This transistor is driven by the horizontal deflection voltage and couples to a hold-off circuit which keeps a protective bias from cutting off vidicon beam current so long as horizontal deflection is present. Failure of this transistor caused the vidicon beam current to be cut-off and absence of TV picture.

Difficulties with corona were not experienced to the extent anticipated. The present vent holes proved to be adequate for the TV Camera Subsystem operated normally at 1.5×10^{-5} mm Hg chamber pressure at 104 minutes after pumping started.

Outgassing was observed at three different pressures during pump down. Since normal operation was obtained after initial outgassing, a vacuum soak of 24 hours at elevated temperature now appears to be unnecessary and a shorter soak time should be considered. A 4-hour soak at a pressure of 10^{-5} mm Hg and a platen temperature of 120^{o}F will be used.

The use of the RFI meter (Stoddart Aircraft Model NM40A) was satisfactory for use on the recording chart. It gives a relative amplitude indication which the TV monitor does not do acceptably.

A simulated launch profile was constructed from the corona test data, as shown in Curve A of Figure 5-14, by converting the chamber pressure into altitude per the 1959 Standard Atmosphere. Operational tests were deliberately conducted in the vicinity of the corona region. The measured unsafe corona region is indicated on the graph to lie between altitudes from 40 to 49.5 kilometers. Allowing a safety factory of two for time and ten for pressure, it can be stated that the TV Camera Subsystem will operate without corona within 60 minutes after launch provided that the pressure around the component is not greater than 0.03 mm Hg. The unsafe region is that indicated under the dashed curve (B) in Figure 5-14.

5.2.3 THERMAL-VACUUM TESTS

Vacuum testing of the second engineering model (SN-5102) was performed from 25 October to 27 October 1965. Much new information was obtained about the TV Camera Subsystem although the complete set of qualification environment was not obtainable. The order of tests will be described, the environmental levels that have significance will be reviewed and the camera system performance will be discussed.

The TV Camera System was installed in a 4-foot by 5-foot vaccum chamber. The camera was mounted on a platen and faced the chamber view port. The camera case was wrapped in a mylar sheath and thermocouples were placed on the sun shutter housing and on the

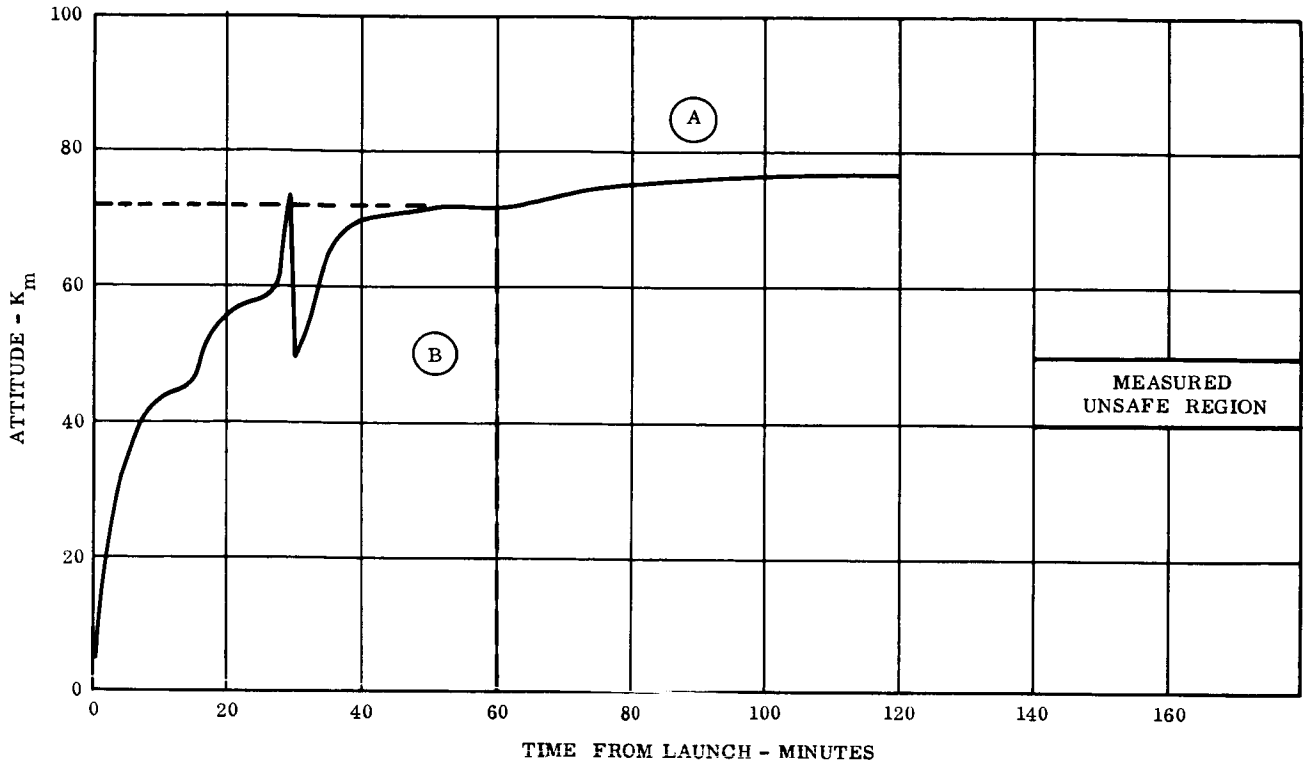

Figure 5-14. Corona Pressure Results During Simulated Launch

camera barrel near the connector. A strip heater was placed around the periphery of the housing for the optical window. The control unit was placed below and forward of the camera unit on a separate platen. It was also wrapped in a mylar sheath. Three thermocouples placed on the housing were combined for a single readout.

The purpose of the mylar sheaths around the camera case and control unit case was to be able to bring these to different temperatures with respect to the optical window.

A RETMA television resolution chart was hung on a remotely movable panel in front of the optics of the camera at a distance of 18-1/4 inches from the front edge. The chart could be raised out of the field sufficiently to allow use of the chamber window for sighting or introducing simulated sunlight. The chart was illuminated by two floodlamps, one on each side of the camera. Because of limited working area, the chart was rotated 90 degrees from its usual upright position and the camera was also rotated 90 degrees so that the nominally horizontal portions of the chart appeared horizontal in the video display as seen on the monitor.

The lamps for illuminating the chart were powered through a Variac. The brightness was held at an arbitrary value of 53 on a 0-100 scale. This was later changed to 60 when another Variac was submitted.

A performance test of the TV Camera Subsystem was made and the chamber was pumped down to a vacuum of 1.0×10^{-6} mm Hg. A second performance test was then made. The peak-to-peak video signal dropped from 1.1 to 1.03 volts. It was assumed that the vidicon target voltage had shifted (automatic target control) since the reticle cross amplitude as well as peak white amplitude from the RETMA chart had dropped from 0.66 to 0.56 and 0.76 to 0.68 volt, respectively. The assumed change in target voltage may have been due to a change in vidicon faceplate temperature which had dropped from 96.5 to 87°F according to the telemetry.

Power was removed from the TV Camera Subsystem and the temperature of the chamber was dropped. The second performance test was made when the key thermocouples read as follows:

a.	Camera case (rear)	16°F
b.	Camera optics	-20°F
c.	Control unit	30°F

At this time some changes in performance were noted:

a. Relative resolution had dropped from 450 to 400 lines.
b. Vertical blanking time dropped from 1240 to 1080 microseconds, resulting in 18 horizontal pulses per vertical blanking interval instead of 20.
c. Vidicon current telemetry reversed polarity and indicated a heater current value of 62 ma compared to 87.3 ma at ambient.

d. Peak-to-peak video signal dropped to 0.6 volt.

e. The video presentation gave the appearance of the chart being illuminated less brilliantly.

Items (b), (c), and (d) indicated out-of-specification conditions. Items (a) and (e) indicate some deterioration of picture quality and reason to suspect out-of-specification conditions. It is possible that the resolution was affected by the illumination level. Reviewing the tests that were performed, it is also realized now that there is a reasonable doubt that the illumination level was constant for two reasons. One, the Variac used on the lamps was replaced with a different Variac. This was done with the precaution of measuring the voltage level with the original Variac used and setting the same voltage on the substitute Variac. The new relative reading was 60. In addition, to relieve the transient strain on the lamp filaments, the Variac was wound up and down rather than switched. The other questionable condition is whether the lamps continue to develop the same illuminance regardless of bulb temperature. The test was not instrumented for absolute control of chart illumination. As a result, lamp bulb temperature was monitored but not recorded. It is known that this temperature tracked the chamber temperature in a broad sense.

At this point, it was decided that the provisions made for controlling the temperature of the optics of the camera were not adequate. In addition, the motor for raising the chart was frozen. Rather than soak the TV Camera Subsystem for 24 hours at the wrong temperatures for qualification level, and since the chart could not be moved to expose the optics to the cold, it was decided to attempt the stabilization at the high temperature qualification levels. These were to have been 138°F at the camera and 118°F at the electronics. Unfortunately, the chamber temperature overshot and peak temperatures of 145°F and 130°F, for camera and control unit respectively, were recorded. It is considered that this overshoot invalidated some of the test data; nevertheless, these data were recorded shortly after these peak temperatures were reached.

The most obvious condition was the appearance of the graduated reticle in the video presentation as beginning to "melt" into the vidicon faceplate. Also, the loss in resolution was such that less than 200 lines (relative) could be distinguished. In addition, line start jitter increased from 0.2 to 1.0 microsecond. Interlace was poor in the upper one-fifth of the raster and a sinusoidal type of vertically-oriented interference was evident in the lower left quarter of the raster. This interference had a frequency, roughtly estimated at 200 kc. Vidicon heater current telemetry, when converted, indicated a value of 106 ma. Vidicon faceplate temperature telemetry was indicating a temperature of 170°F.

It was known that vidicon damage would ensue if the vidicon faceplate exceeded a temperature of 140°F for several minutes and the telemetry of this temperature was under constant watch during this critical time. Chamber heat was turned off when chamber temperature was 92°F, because the chamber being used had only manual controls for this.

It was decided to repeat the functional test closer to the proper qualification levels. This was done at the following values:

a.	Camera case (rear)	118°F
b.	Camera optics	116°F
c.	Control unit	114°F

There was some recovery evident. Resolution was again read as 400. Line start jitter recovered to 0.6 microseconds. Vidicon faceplate temperature telemetry indicated 140°F. On the other hand horizontal sync pulse width dropped from 5.2 to 4.8 microseconds (still within specification). There were now 21 horizontal pulses per vertical blanking interval (1290 microseconds). The interlace was restored and the sinusoidal type of vertically oriented interference disappeared. However, the graduations on the reticle were not restored and it was concluded that the vidicon upper temperature limit had been exceeded.

5.3 POWER CONTROL UNIT

Tests were performed on the engineering Power Control Unit (PCU) according to the issued Engineering Test Plan No. 4172-091. This test plan calls out voltages, temperature variations, and loads in excess of those stated in the PCU Specification SVS7307. Therefore, those few readings which exceed the specification limits were directly traced to the overstressed inputs or loads.

The first set of performance readings were taken with the -30 volts set to -24 volts; the -24 volts set to -23 volts; and the input command signal set below its specified low limit. A second set of performance readings were taken with the -30 volts set to -36 volts, the -24 volts set to -25 volts, and the input command signal set below its specified low limit. The third set of performance readings were taken and in this case, the input signal voltage was increased to +30 volts while the other voltages were set to normal.

Performance tests were made with the temperature set to $-30^{\circ}C$ and three runs were made with the voltages set as explained previously. Then the temperature was increased to $70^{\circ}C$ and three more voltage variation runs were performed. During the temperature test, several failures occurred. A field driver module was accidently grounded causing the module to become inoperative. Rod A solenoid driver became inoperative; the trouble was later traced to a defective transistor. The delay time on the squib driver was longer than the specifications allow, but this variation was due to a much lower command pulse than normal. All other tests were within the tolerances specified.

The thermal-vacuum test was performed at a pressure of less than 1×10^{-6} mm Hg, with a temperature of -20 and $60^{\circ}C$ and high, low, and nominal voltages. This test was performed without the rod A field driver, which was overstressed during the temperature test. All readings were within the component specifications except as noted previously.

All drawings were updated and reissued under new drawing numbers. Several changes were made as a direct result of tests performed on the engineering unit and to facilitate manufacturing. The principle improvements include: a change to the power bus supplying the motor driver module, the addition of terminals for selected parts, an inhibit circuit in the motor driver module, and changes in the power runs. The latest schematics of the PCU for the prototype and flight assemblies (GE drawing 417J207904) are shown in Figure 5-15.

5.4 SOLAR ASPECT SENSOR (SAS)

5.4.1 DETERMINATION OF THE EFFECTIVE INDEX OF REFRACTION TO BE USED FOR SAS DATA REDUCTION

The transfer function of the SAS was derived for monochromatic incident light. Since the detector contains a block of quartz, the index of refraction of quartz appears in the transfer function. Solar illumination, however, is obviously not monochromatic, and the index of refraction of quartz varies sufficiently over the range of wavelengths of the detector response so that an effective index of refraction must be found and incorporated.

Graphs of the solar spectrum in the region of interest, silicon solar cell response and the index of refraction of fused quartz as a function of wavelength, are shown in Figures 5-16, 5-17 and 5-18. From these graphs, it is evident that a monochromatic index of refraction is not satisfactory. Specifically, this is shown by differentiating the transfer function (for simplicity the one valid in the planes of the two slits) with respect to the index of refraction, n.

$$\theta = \text{arc sin}\left(\frac{nd}{\sqrt{t^2 + d^2}}\right)$$

where θ = angle of incidence

d = distance from the center at the bottom of the quartz reticle

t = thickness of the quartz reticle = 0.4480 inch

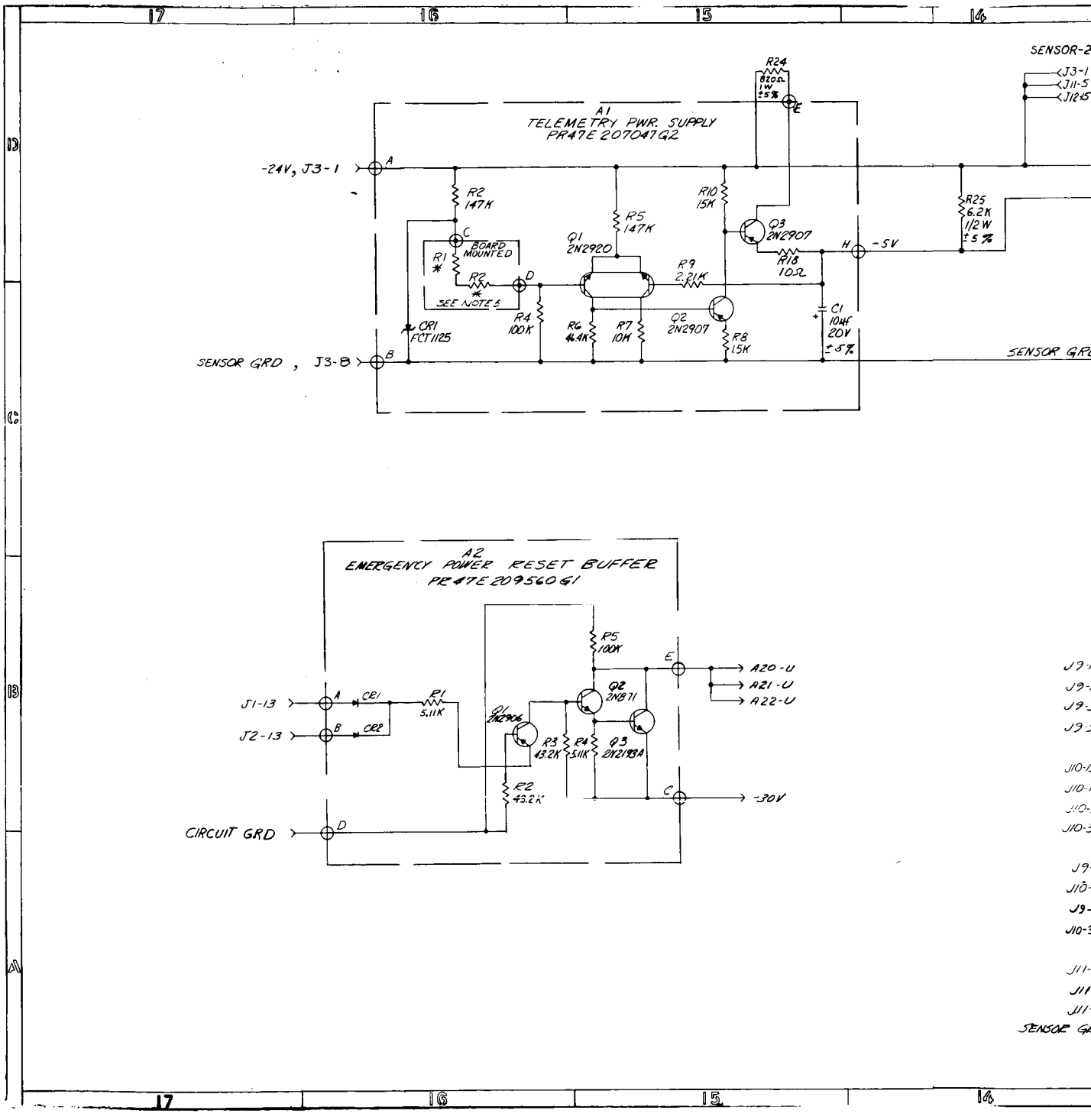
A1
TELEMETRY PWR. SUPPLY
PR47E207047G2
-24V, J3-1
SENSOR GRD , J3-8
R24
820Ω 1W ±5%
R2 147K
R5 147K
R10 15K
R25 6.2K 1/2W ±5%
R18 10Ω
-5V
Q1 2N2920
Q3 2N2907
Q2 2N2907
R9 2.21K
R1 *
R2 *
BOARD MOUNTED
SEE NOTE 5
R4 100K
R6 44.4K
R7 10M
R8 15K
C1 10μF 20V ±5%
CR1 FCT1125
SENSOR-2
J3-1
J11-5
J12-5
SENSOR GRD
A2
EMERGENCY POWER RESET BUFFER
PR47E209560G1
J1-13
J2-13
CIRCUIT GRD
CR1
CR2
R1 5.11K
R5 100K
Q2 2N871
Q1 2N2906
R3 43.2K
R4 5.11K
Q3 2N2193A
R2 43.2K
A20-U
A21-U
A22-U
-30V

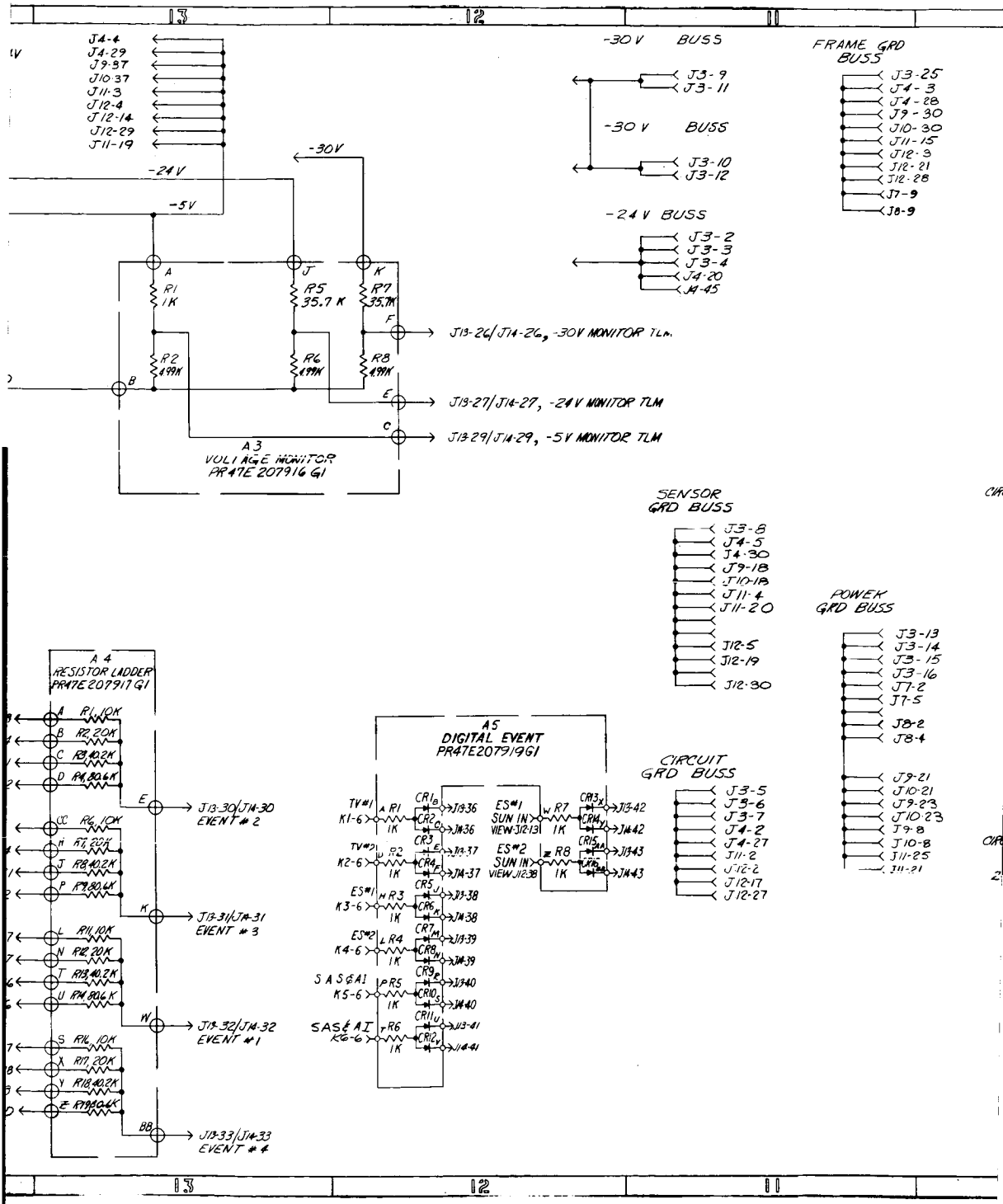
13
12
11
J4-4
J4-29
J9-37
J10-37
J11-3
J12-4
J12-14
J12-29
J11-19
-24V
-5V
-30V
A
J
K
R1
1K
R5
35.7K
R7
35.7K
R2
4.99K
R6
4.99K
R8
4.99K
B
F
E
C
J13-26/J14-26, -30V MONITOR TLM.
J13-27/J14-27, -24V MONITOR TLM
J13-29/J14-29, -5V MONITOR TLM
A3
VOLTAGE MONITOR
PR47E207916G1
-30V BUSS
J3-9
J3-11
-30V BUSS
J3-10
J3-12
-24V BUSS
J3-2
J3-3
J3-4
J4-20
J4-45
FRAME GRD BUSS
J3-25
J4-3
J4-28
J9-30
J10-30
J11-15
J12-3
J12-21
J12-28
J7-9
J8-9
SENSOR GRD BUSS
J3-8
J4-5
J4-30
J9-18
J10-18
J11-4
J11-20
J12-5
J12-19
J12-30
POWER GRD BUSS
J3-13
J3-14
J3-15
J3-16
J7-2
J7-5
J8-2
J8-4
J9-21
J10-21
J9-23
J10-23
J9-8
J10-8
J11-25
J11-21
CIRCUIT GRD BUSS
J3-5
J3-6
J3-7
J4-2
J4-27
J11-2
J12-2
J12-17
J12-27
A4
RESISTOR LADDER
PR47E207917G1
A R1 10K
B R2 20K
C R3 40.2K
D R4 80.6K
CC R5 10K
H R6 20K
J R8 40.2K
P R9 80.6K
L R11 10K
N R12 20K
T R13 40.2K
U R14 80.6K
S R16 10K
X R17 20K
Y R18 40.2K
Z R19 80.6K
E
K
W
BB
J13-30/J14-30
EVENT # 2
J13-31/J14-31
EVENT # 3
J13-32/J14-32
EVENT #1
J13-33/J14-33
EVENT # 4
A5
DIGITAL EVENT
PR47E207919G1
TV#1 K1-6
TV#2 K2-6
ES#1 K3-6
ES#2 K4-6
SASGAI K5-6
SASGAI K6-6
R1
R2
R3
R4
R5
R6
1K
CR1
CR2
CR3
CR4
CR5
CR6
CR7
CR8
CR9
CR10
CR11
CR12
J13-36
J14-36
J13-37
J14-37
J13-38
J14-38
J13-39
J14-39
J13-40
J14-40
J13-41
J14-41
ES#1 SUN IN VIEW J12-13
ES#2 SUN IN VIEW J12-38
R7
R8
1K
CR13
CR14
CR15
CR16
J13-42
J14-42
J13-43
J14-43

19-(2)

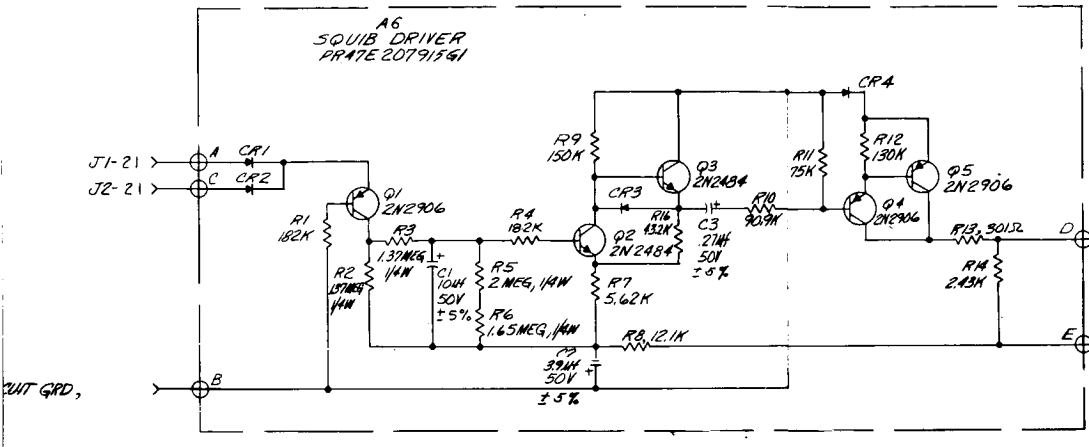
A6
SQUIB DRIVER
PR47E20791561
J1-21
J2-21
CR1
CR2
Q1 2N2906
R1 182K
R2 137MEG 1/4W
R3 1.37MEG 1/4W
C1 10UH 50V ±5%
R4 182K
R5 2.MEG, 1/4W
R6 1.65MEG, 1/4W
Q2 2N2484
R7 5.62K
R8 12.1K
C2 3.9UH 50V ±5%
R9 150K
Q3 2N2484
CR3
R10 90.9K
C3 .27UH 50V ±5%
R11 75K
CR4
R12 130K
Q5 2N2906
Q4 2N2906
R13 30.1Ω
R14 2.43K
D
E
Q9 MNT6331
R97 51.1Ω
CIRCUIT GRD,
B

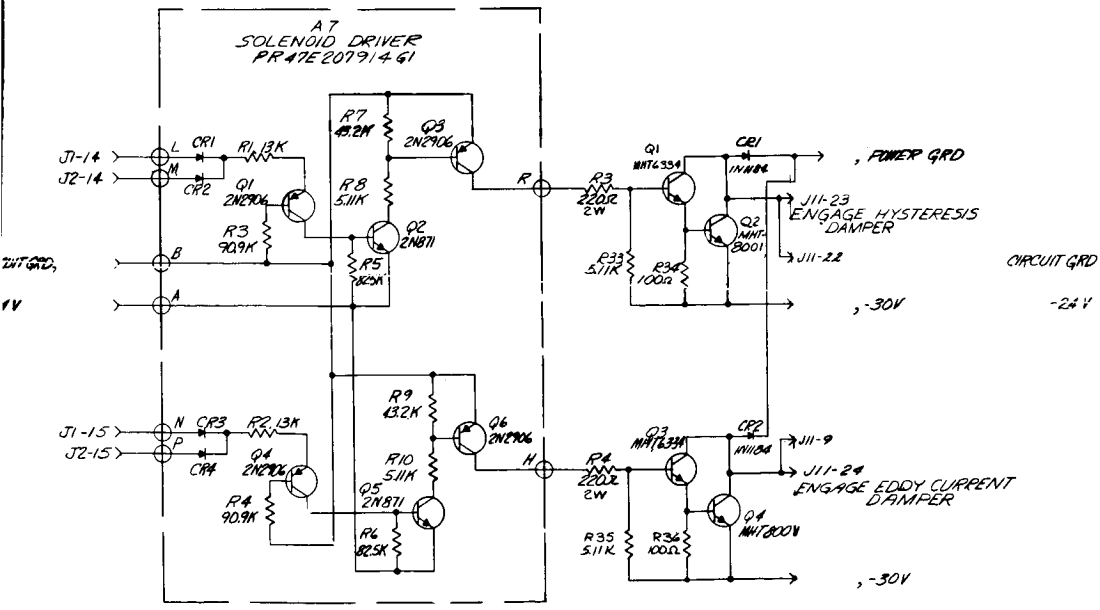
A7
SOLENOID DRIVER
PR47E20791461
J1-14
J2-14
L
M
CR1
CR2
R1 13K
Q1 2N2906
R3 90.9K
R7 49.2M
Q3 2N2906
R8 5.11K
Q2 2N871
R5 82.5K
R
B
A
CIRCUIT GRD,
-24V
J1-15
J2-15
N
P
CR3
CR4
R2 13K
Q4 2N2906
R4 90.9K
R9 43.2K
Q6 2N2906
R10 5.11K
Q5 2N871
R6 82.5K
H
Q1 MNT6334
CR1 IN1184
R3 2.20Ω 2W
R33 5.11K
R34 100Ω
Q2 MNT-8001
, POWER GRD
J11-23 ENGAGE HYSTERESIS DAMPER
J11-22
, -30V
Q3 MNT6334
CR2 IN1184
R4 2.20Ω 2W
R35 5.11K
R36 100Ω
Q4 MNT8001
J11-9
J11-24 ENGAGE EDDY CURRENT DAMPER
, -30V
J1-16
J2-16
CIRCUIT GRD,
-24V,
J1-17
J2-17

19 -(3)

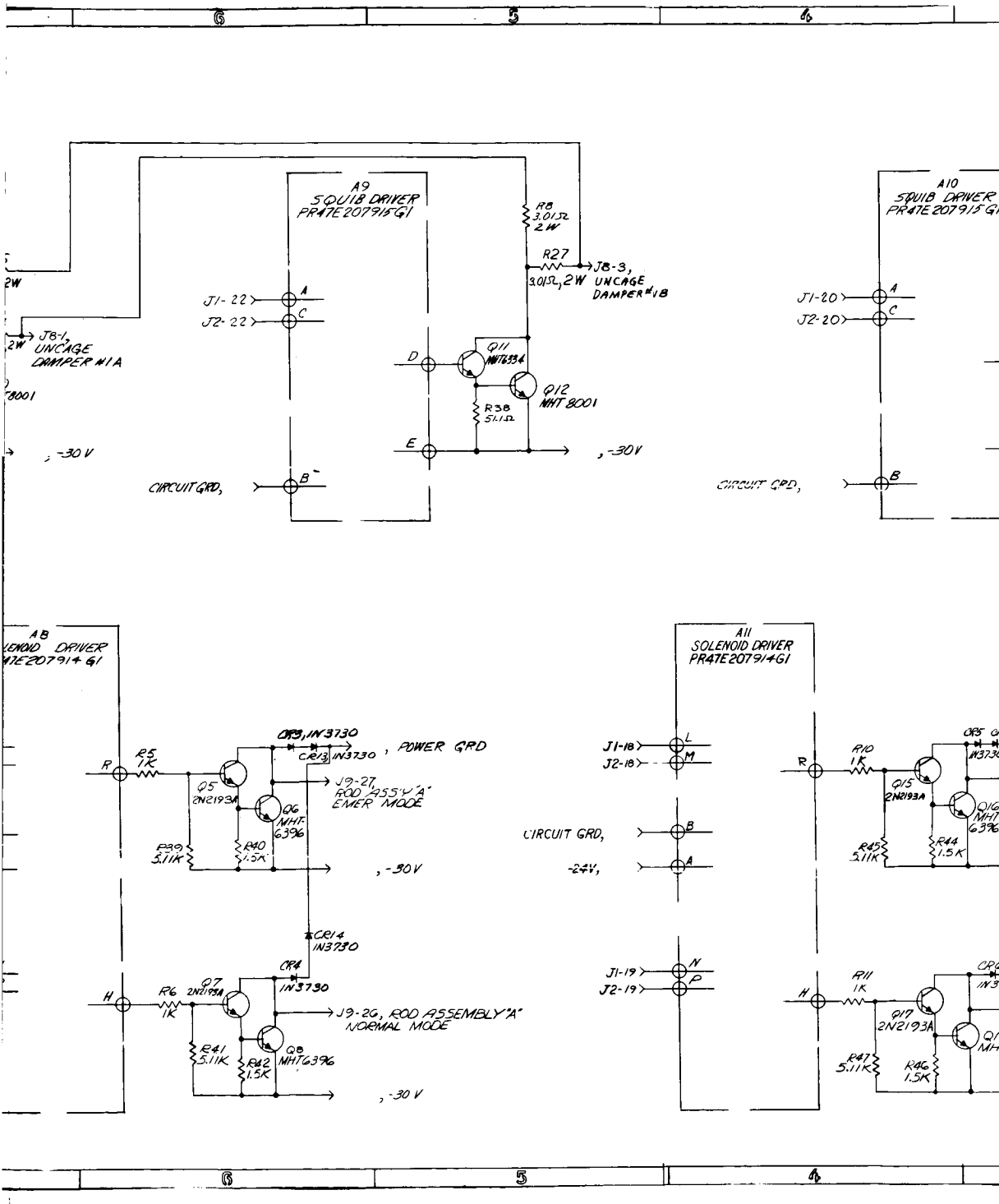
A9
SQUIB DRIVER
PR47E207915G1
R8
3.01Ω
2W
R27
3.01Ω, 2W
J8-3,
UNCAGE
DAMPER #1B
J8-1,
UNCAGE
DAMPER #1A
J1-22
J2-22
A
C
D
E
B
Q11
MHT6396
Q12
MHT8001
R38
51.1Ω
-30V
CIRCUIT GRD,
A10
SQUIB DRIVER
J1-20
J2-20
A8
SOLENOID DRIVER
CR3, IN3730
CR13 IN3730
POWER GRD
R5
1K
Q5
2N2193A
Q6
MHT6396
J9-27,
ROD ASSY "A"
EMER MODE
R39
5.11K
R40
1.5K
CR14
IN3730
CR4
IN3730
Q7
2N2193A
R6
1K
J9-26, ROD ASSEMBLY "A"
NORMAL MODE
R41
5.11K
R42
1.5K
Q8
MHT6396
A11
SOLENOID DRIVER
PR47E207914G1
J1-18
J2-18
L
M
CIRCUIT GRD,
-24V,
J1-19
J2-19
N
P
R10
1K
Q15
2N2193A
R45
5.11K
R44
1.5K
R11
1K
Q17
2N2193A
R47
5.11K
R46
1.5K

19

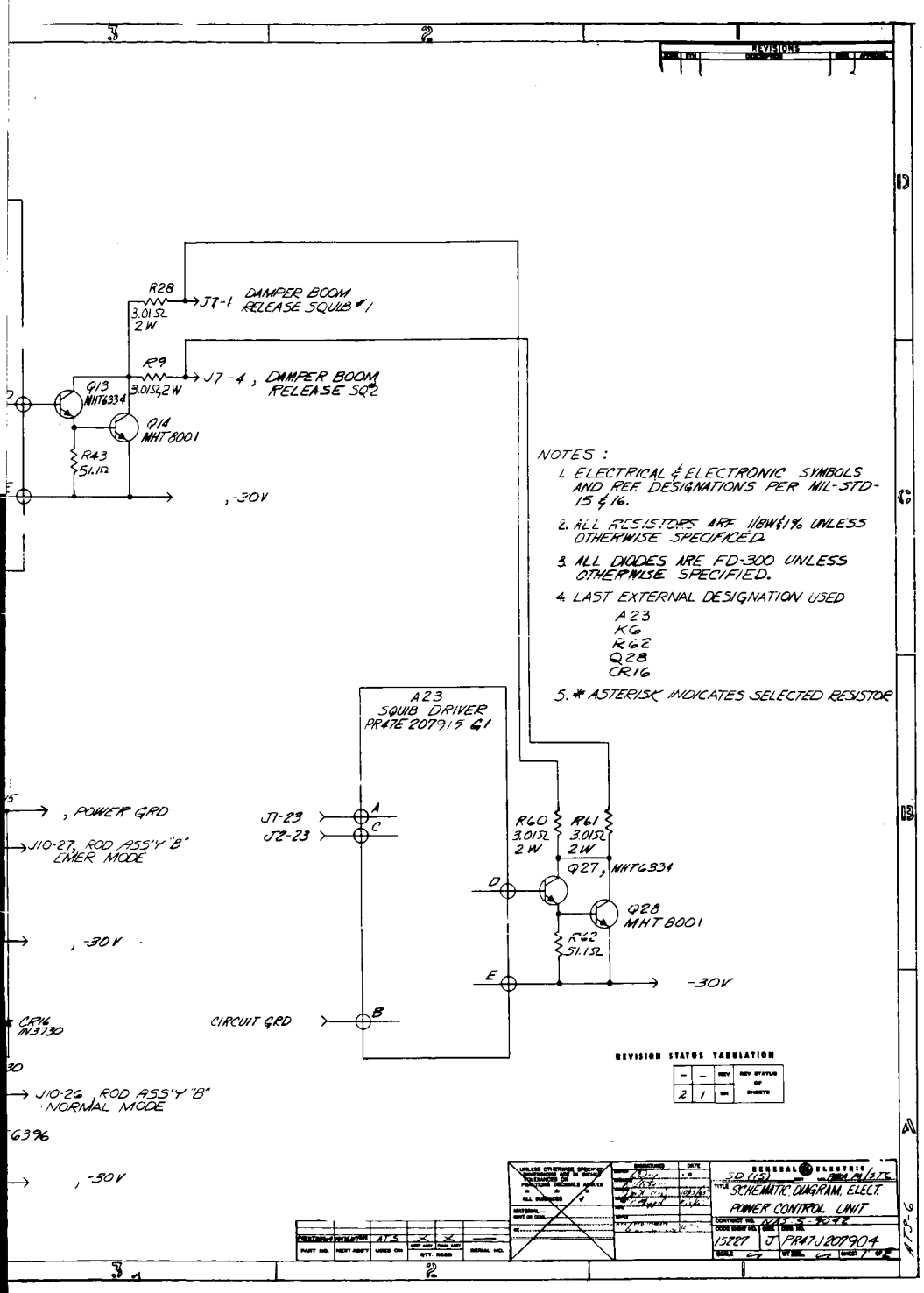

Figure 5-15. Power Control Unit Schematic Diagram (Sheet 1 of 2)

5-19/20

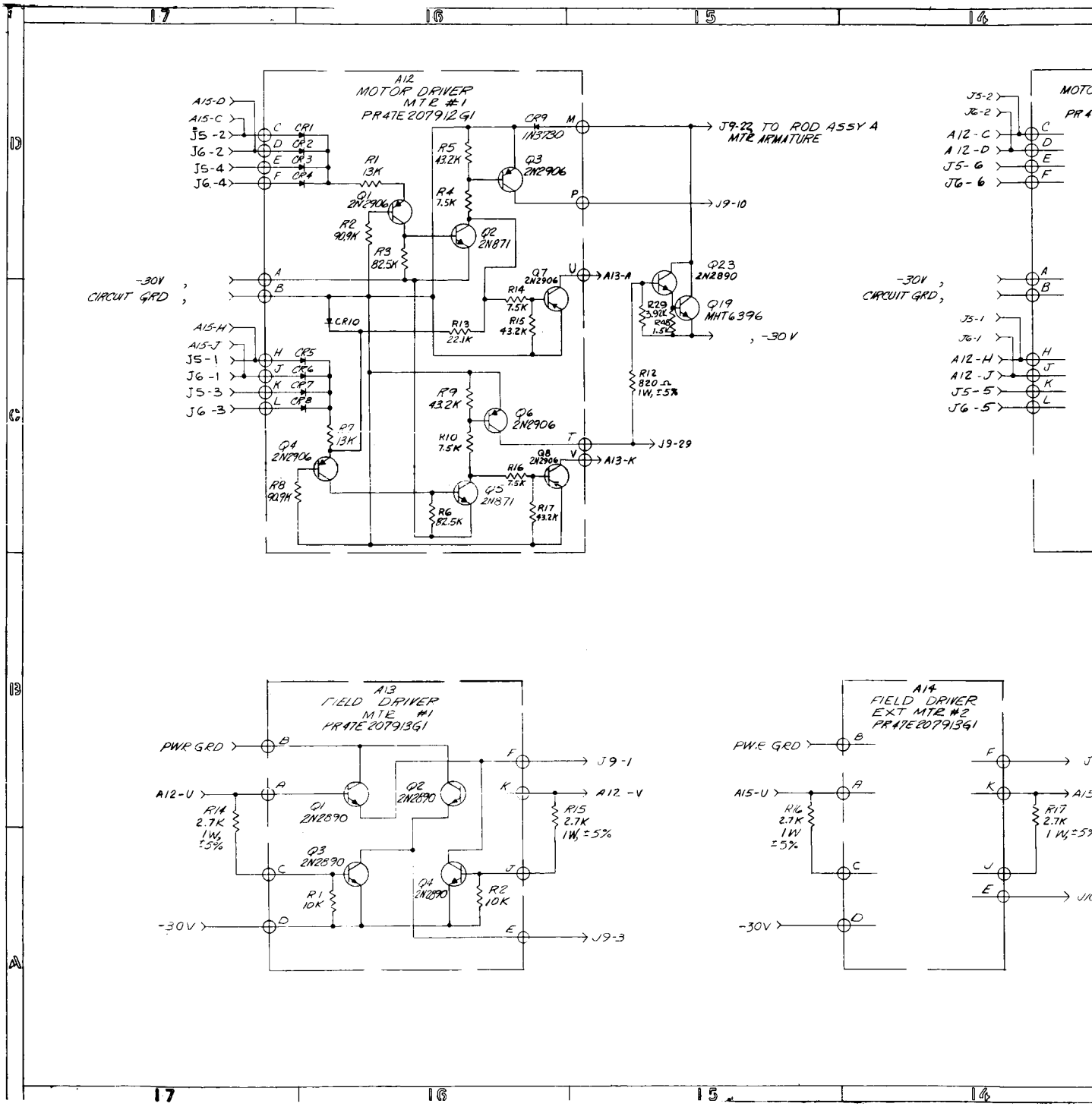
A12
MOTOR DRIVER
MTR #1
PR47E207912G1
A15-D
A15-C
J5-2
J6-2
J5-4
J6-4
CR1
CR2
CR3
CR4
R1 13K
Q1 2N2906
R2 90.9K
R3 82.5K
Q2 2N871
R5 13.2K
Q3 2N2906
R4 7.5K
CR9 1N3730
J9-22 TO ROD ASSY A MTR ARMATURE
J9-10
-30V CIRCUIT GRD
A
B
CR10
R13 22.1K
Q7 2N2906
R14 7.5K
R15 43.2K
A13-A
Q23 2N2890
R23 3.92K
R24 1.5K
Q19 MHT6396
-30 V
A15-H
A15-J
J5-1
J6-1
J5-3
J6-3
H
J
K
L
CR5
CR6
CR7
CR8
R7 13K
Q4 2N2906
R8 90.9K
R9 43.2K
Q6 2N2906
R10 7.5K
R12 820Ω 1W, ±5%
J9-29
Q8 2N2906
A13-K
R16 7.5K
Q5 2N871
R6 82.5K
R17 43.2K
A13
FIELD DRIVER
MTR
#1
PR47E207913G1
PWR GRD
A12-U
R14 2.7K 1W, ±5%
Q1 2N2890
Q2 2N2890
Q3 2N2890
Q4 2N2890
R1 10K
R2 10K
J9-1
A12-V
R15 2.7K 1W, ±5%
-30V
J9-3
A14
FIELD DRIVER
EXT MTR #2
PR47E207913G1
PWR GRD
A15-U
R16 2.7K 1W ±5%
-30V
R17 2.7K 1W, ±5%
J5-2
J6-2
A12-C
A12-D
J5-6
J6-6
-30V CIRCUIT GRD
J5-1
J6-1
A12-H
A12-J
J5-5
J6-5

21-0

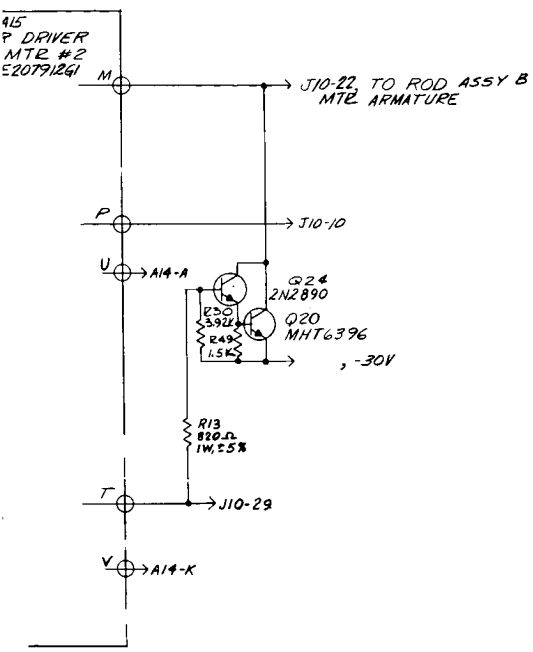
M
J10-22, TO ROD ASSY B MTR ARMATURE
P
J10-10
U
A14-A
Q24 2N2890
R35 3.92K
R49 1.5K
Q20 MHT6396
, -30V
R13 820Ω 1W, ±5%
T
J10-29
V
A14-K

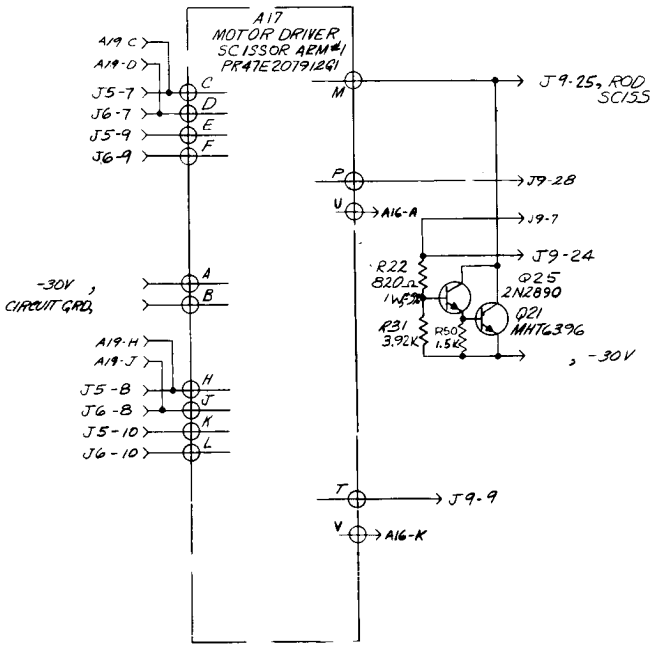
A17
MOTOR DRIVER
SCISSOR ARM #1
PR47E20791261
A19-C
A19-D
J5-7
J6-7
J5-9
J6-9
C
D
E
F
-30V, CIRCUIT GRD,
A
B
A19-H
A19-J
J5-8
J6-8
J5-10
J6-10
H
J
K
L
M
J9-25, ROD SCISS
P
J9-28
U
A16-A
J9-7
J9-24
R22 820Ω 1W, ±5%
Q25 2N2890
R31 3.92K
R50 1.5K
Q21 MHT6396
, -30V
T
J9-9
V
A16-K

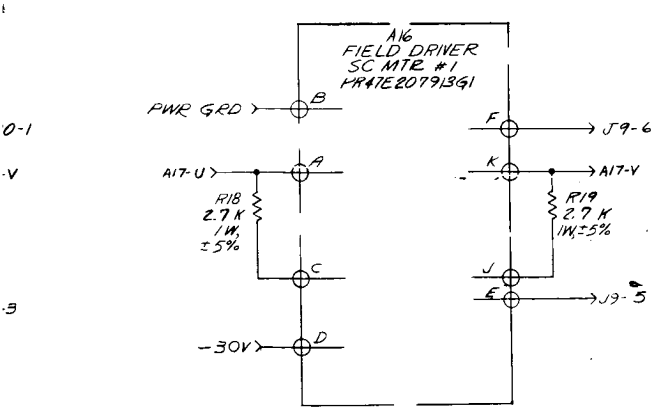
A16
FIELD DRIVER
SC MTR #1
PR47E20791361
PWR GRD
B
A17-U
A
R18 2.7K 1W, ±5%
C
-30V
D
F
J9-6
K
A17-V
R19 2.7K 1W, ±5%
J
E
J9-5

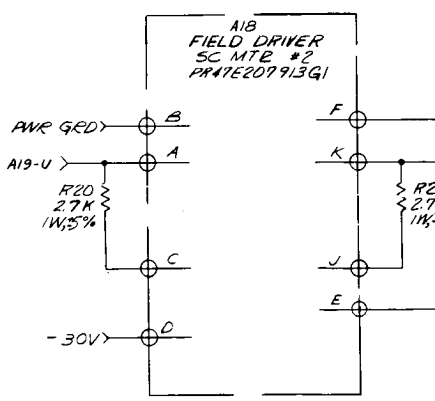
A18
FIELD DRIVER
SC MTR #2
PR47E20791361
PWR GRD
B
A19-U
A
R20 2.7K 1W, ±5%
C
-30V
D
F
K
J
E

21 (2)

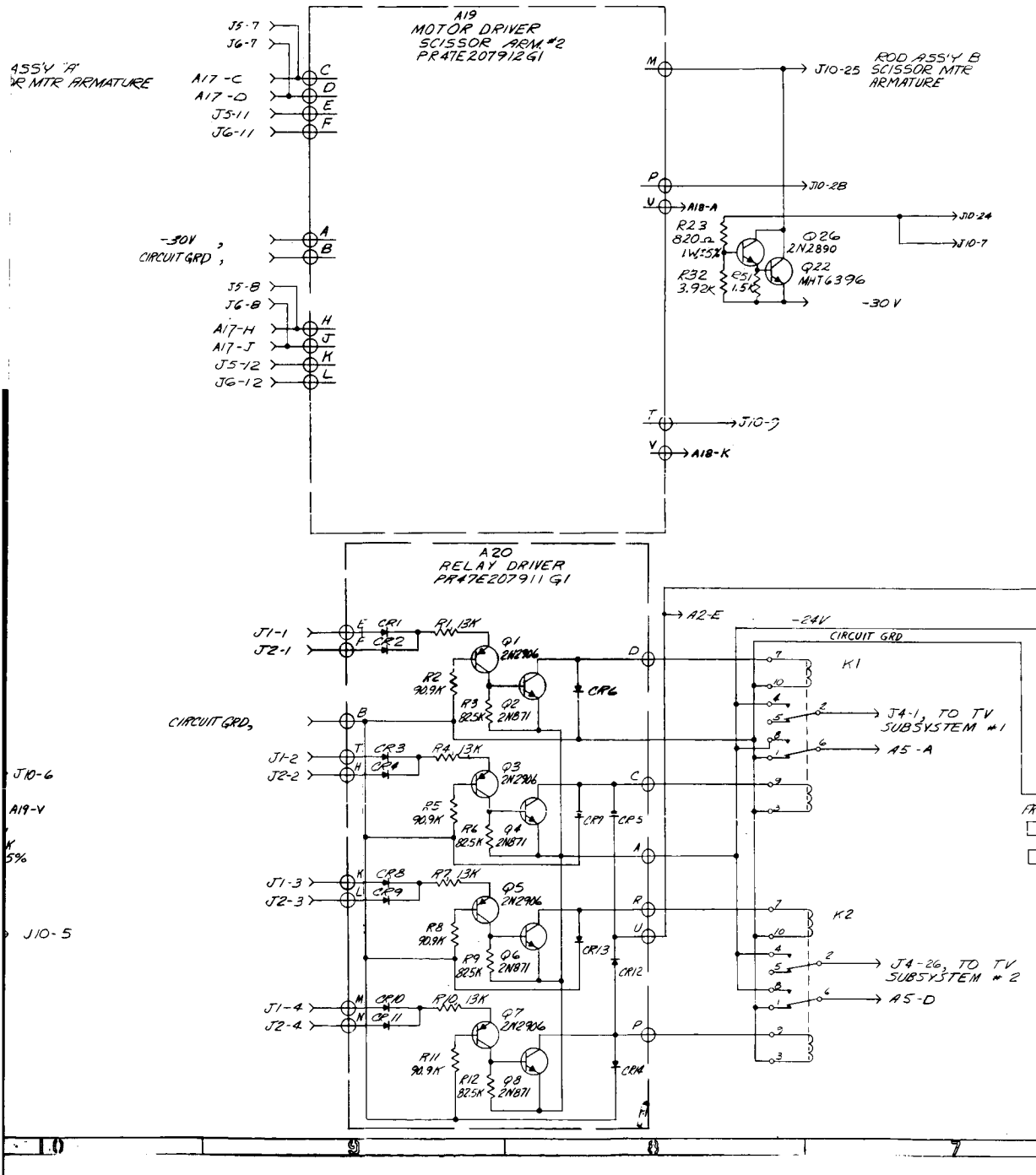
A19
MOTOR DRIVER
SCISSOR ARM #2
PR47E207912G1
J5-7
J6-7
A17-C
A17-D
J5-11
J6-11
-30V, CIRCUIT GRD,
J5-8
J6-8
A17-H
A17-J
J5-12
J6-12
M
J10-25
ROD ASS'Y B
SCISSOR MTR
ARMATURE
P
J10-28
V
A18-A
R23
820Ω
1W 5%
Q26
2N2890
R32
3.92K
Q22
MHT6396
-30V
J10-24
J10-7
T
J10-9
V
A18-K
A20
RELAY DRIVER
PR47E207911G1
J1-1
J2-1
CR1
CR2
R1 13K
Q1
2N2906
R2
90.9K
R3
82.5K
Q2
2N871
CR6
CIRCUIT GRD,
J1-2
J2-2
CR3
CR4
R4 13K
Q3
2N2906
R5
90.9K
R6
82.5K
Q4
2N871
CR7
CR5
J1-3
J2-3
CR8
CR9
R7 13K
Q5
2N2906
R8
90.9K
R9
82.5K
Q6
2N871
CR13
CR12
J1-4
J2-4
CR10
CR11
R10 13K
Q7
2N2906
R11
90.9K
R12
82.5K
Q8
2N871
CR14
A2-E
-24V
CIRCUIT GRD
K1
J4-1, TO TV
SUBSYSTEM #1
A5-A
K2
J4-26, TO TV
SUBSYSTEM #2
A5-D
J10-6
A19-V
J10-5

21-3

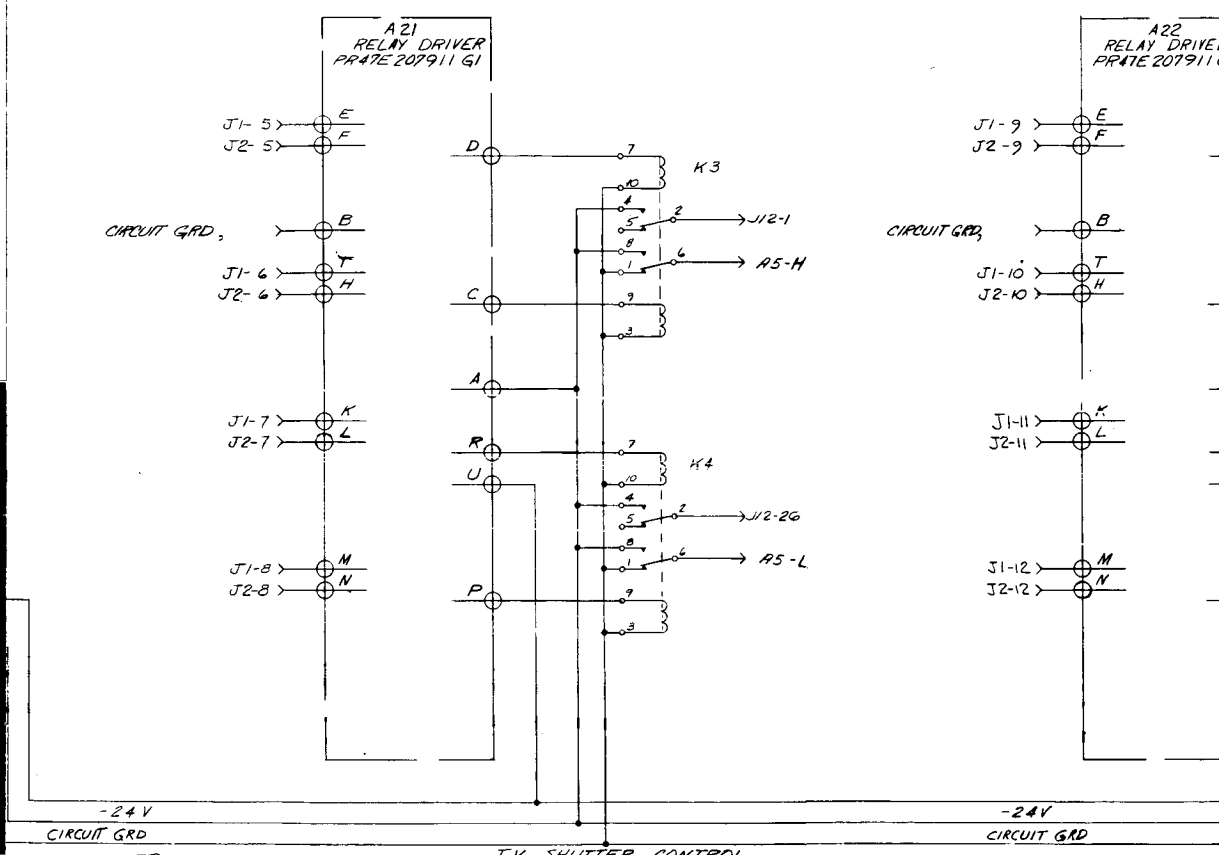
A21
RELAY DRIVER
PR47E207911G1
A22
RELAY DRIVE
PR47E207911
J1-5
J2-5
J1-6
J2-6
J1-7
J2-7
J1-8
J2-8
J1-9
J2-9
J1-10
J2-10
J1-11
J2-11
J1-12
J2-12
CIRCUIT GRD,
K3
K4
J12-1
A5-H
J12-26
A5-L
-24V
CIRCUIT GRD
TV SHUTTER CONTROL
COMMAND INTERFACE
TIME SYNC DISTR.
J13-35
J12-18
J14-55
J12-24
EARTH SENSOR
OUT PUT INTERFACE
J12-9 ES #1 X MEAS.
J12-34 ES #2 X MEAS.
J14-47
J12-10 ES #1 Y MEAS.
J12-35 ES #2 Y MEAS.
J13-48
J14-48
J12-11 ES #1 X' MEAS.
J12-36 ES #2 X' MEAS.
J13-49
J14-49
J12-12 ES #1 Y' MEAS.
J12-37 ES #2 Y' MEAS.
J13-50
J14-50
J1-24
J4-10
J2-24
J4-11
J1-25
J4-12
J2-25
J4-13
J5-14
J4-35
J6-14
J4-36
J5-15
J4-37
J6-15
J4-38
ROD LENGTH AND
ASSEMBLY PRESSURE
INTERFACE
J9-15 ROD ASSY A LG.
J13-1
J14-1
J10-15 ROD ASSY B LG.
J13-2
J14-2
J9-34 ROD ASSY A SC. ANGLE
J13-4
J14-4
J10-34 ROD ASSY B SC. ANGLE
J13-5
J14-5
J9-33 ROD ASSY A PRESSURE
J13-6
J14-6
J10-33 ROD ASSY B PRESSURE
J13-7
J14-7
TEMP. AND

21-40

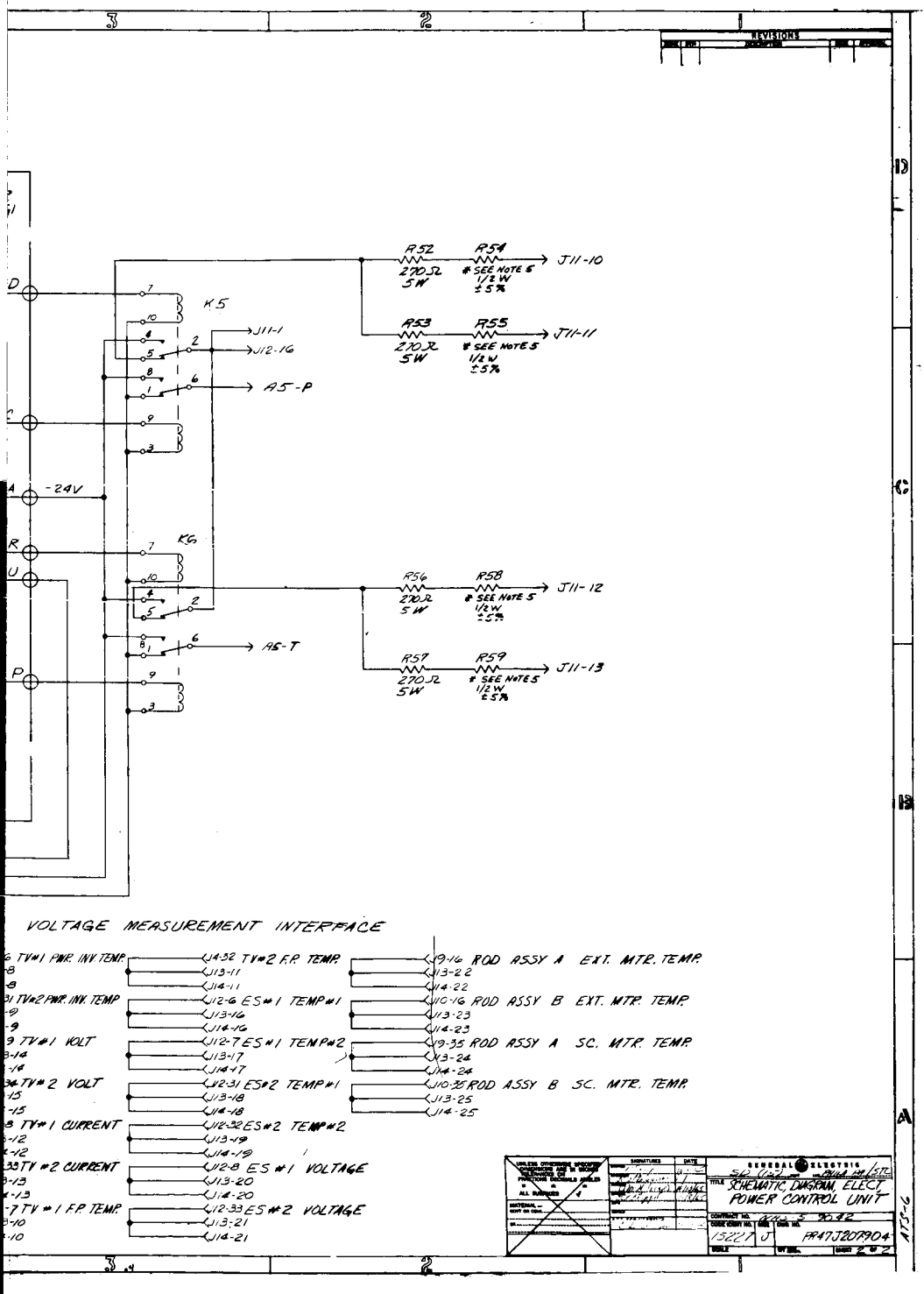

Figure 5-15. Power Control Unit Schematic Diagram (Sheet 2 of 2)

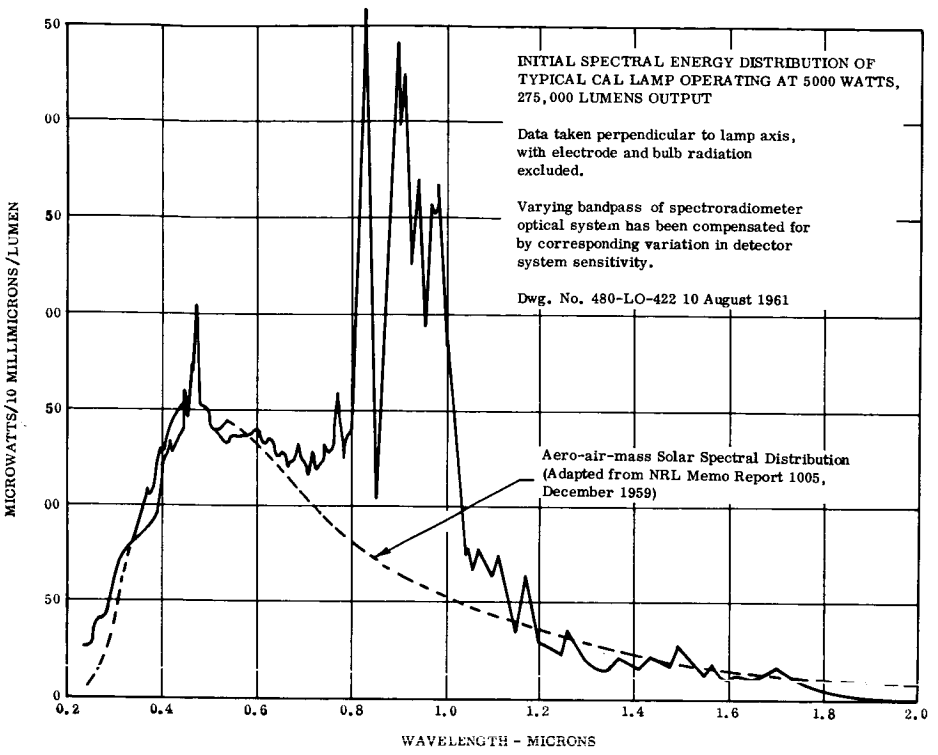

Figure 5-16. GE 5000 Watt Xenon Compact Arc Lamp

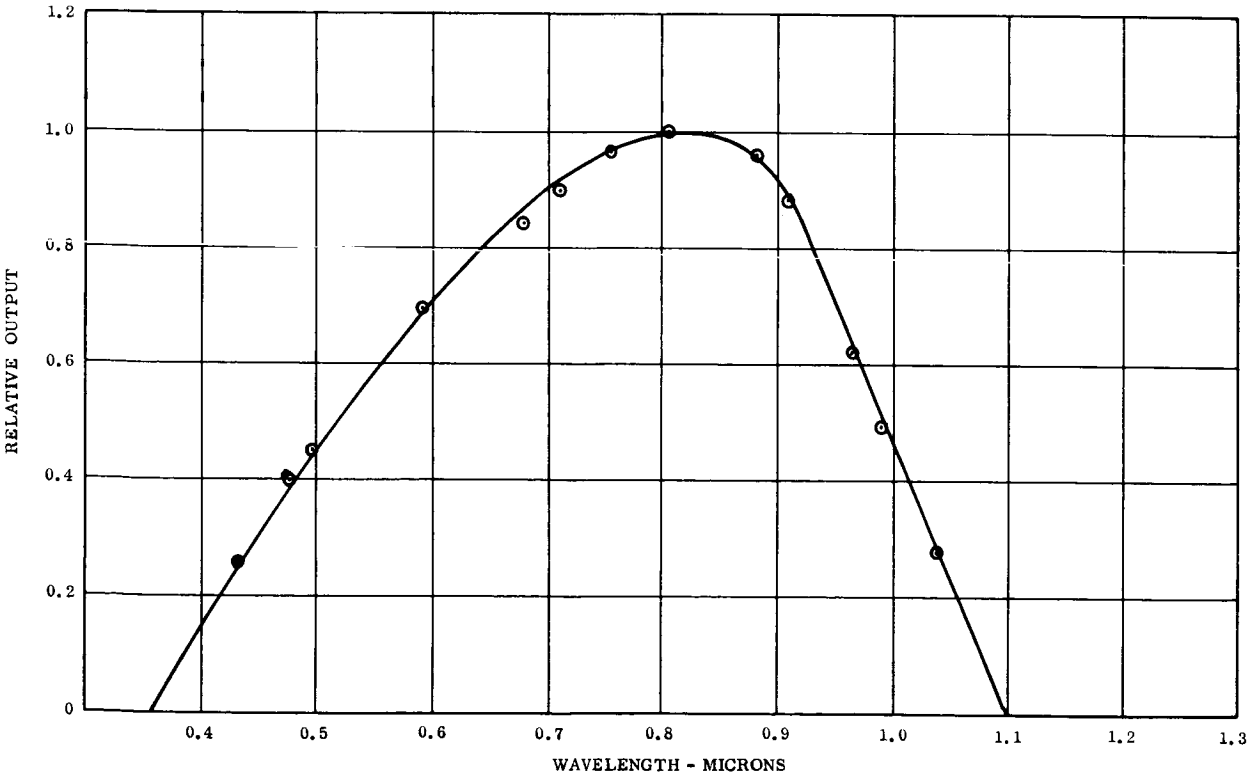

Figure 5-17. Solar Cell Relative Spectral Response

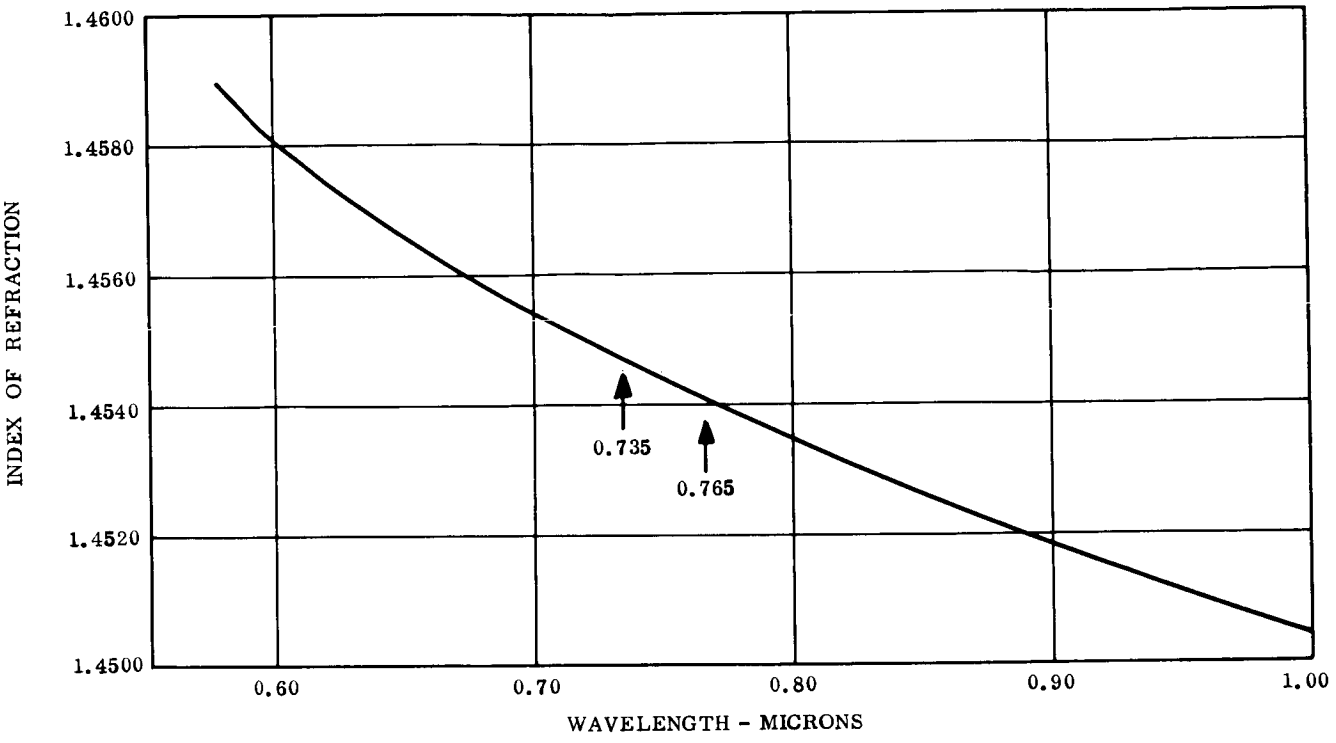

Figure 5-18. Index of Refraction of Fused Quartz

$$\frac{d\theta}{dn} = \frac{d}{\sqrt{t^2 - d^2(n^2 - 1)}}$$

Then to the first order:

$$\theta + \Delta\theta = \frac{nd}{\sqrt{t^2 + d^2}} + \Delta n \frac{d}{\sqrt{t^2 - d^2(n^2-1)}}$$

Where $\Delta\theta$, Δn are small changes in the measured angle of incidence and the index of refraction.

Therefore,

$$\Delta\theta = \frac{d}{\sqrt{t^2 - d^2(n^2-1)}} \Delta n \text{ (in radians)}$$

At 63.5 degrees, near the last transition edge of the SAS detector

$$\frac{d}{\sqrt{t^2 - d^2 (n^2 - 1)}} \approx 1.44$$

$$\Delta \theta_{63.5} \approx 1.44 \times 57.3 \ \Delta n$$

$$\Delta \theta_{63.5} \approx 82.5 \ n \text{ (in degrees)}$$

From this, it is evident that the index of refraction can induce considerable error into the SAS outputs. Also, it is clear that the index of refraction used in the transfer function must be different if the SAS is tested with an illumination source which has a spectral distribution different from that of the sun, e.g., an xenon arc lamp with a spectral distribution shown in Figure 5-16.

Theoretically, the effective index of refraction is the index of quartz at the "median wavelength" of the product of the spectrum of the sun with the response of the detector. The output of the detector is proportional to the area under that product curve and the "median wavelength" is then that point on the abscissa below and beyond which the area under the curve is the same. Figure 5-19 is a graph of the product of the solar spectrum and the typical silicone solar cell response. The "median wavelength" was determined graphically and equals 0.696 micron.

Figure 5-20 shows the product of the xenon arc lamp spectrum and silicon solar cell response. The "median wavelength" here equals 0.826 micron.

Test data from the SAS taken with an xenon arc lamp, however, shows that a best fit is achieved with an index of refraction of 1.4541. This, according to Figure 5-18, corresponds to 0.765 micron rather than the predicted 0.826 micron and indicates that the detector response is significantly different from that shown in Figure 5-17. The xenon arc lamp spectrum is not that of Figure 5-16 since the SAS detector operation was oversimplified and other factors must be considered in the derivation of a transfer function.

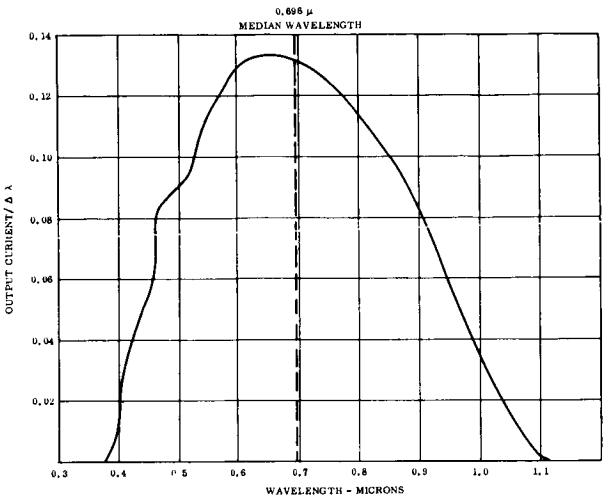

Figure 5-19. Product of Solar Spectrum and Silicon Solar Cell Response

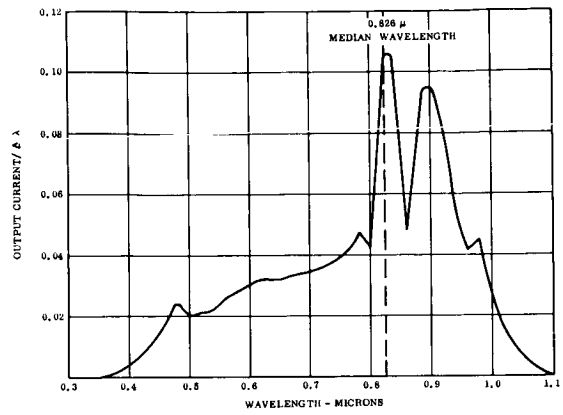

Figure 5-20. Product of Xenon Spectrum

For testing purposes, the problem has been solved empirically. Fifteen different SAS detectors have been tested and an index of refraction of 1.4541 best fits all data taken with the Adcole solar simulator. The magnitude of errors introduced from this source is small in the ATS application (of the order of 0.02 degrees) and no corrective action is presently planned. The following analytical and experimental program would allow such errors to be minimized further.

a. Measure the response of the actual solar cells used.
b. Measure the spectrum of the Adcole solar simulator.
c. Measure the spectrum of a carbon arc solar simulator.
c. Test one SAS detector with a carbon arc solar simulator.

The data from these experiments would then provide additional confidence in the method used to devise the effective index of refraction or would provide points on a graph of calculated versus measured median wavelength which could be used for interpolation.

5.4.2 DETECTOR TESTS

During the last quarter, all points, in the field of view of the detector and in the two planes defined by the slits and normal to the detector where the output of the AGC equals the output of the bit cell, were measured at 25°C. The illumination was by xenon arc solar simulator. The unit was positioned and aligned optically on a rotab so that its surface was normal to the light source. This was accomplished by using the setup shown in Figure 5-21.

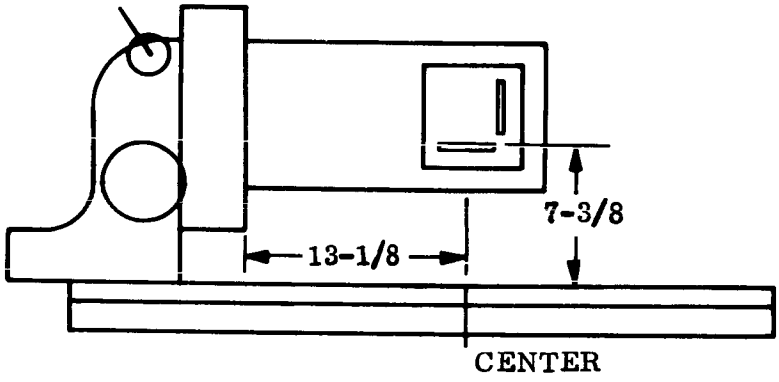

Figure 5-21. Optical Alignment Setup

Alignment was accomplished through the following procedure. The optical axis of the telescope was adjusted to coincide with the optical axis of the xenon lamp. This was done by sighting through the telescope and adjusting the telescope until images of two crosshairs of the lamp (crosshairs are at the geometric center) coincided when viewed through the telescope. The front face of the detector was aligned by autocollimating. The detector was then rotated 90 degrees about a vertical axis and it was again aligned by autocollimating.

The output of a solar cell across the detector varied between 24 and 26.5 millivolts, while one sun equals 25.3 millivolts. This uniformity is due to the position of the xenon

lamp relative to its optics. The intensity of the light is due to the current supplied to the lamp. The power supply for the arc lamp was set at 142 amperes.

The nulling circuit for null point testing is shown in Figure 3-22.

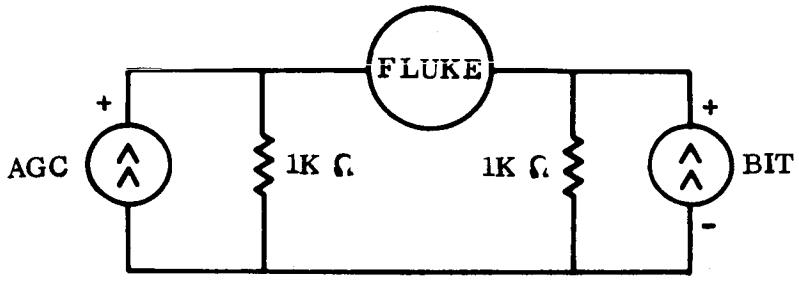

Figure 3-22. Nulling Circuit

The rotab rotated the sensor relative to the incident light; the accuracy of the rotab is ± 1 minute. The points were recorded where the Fluke (a null type voltmeter) showed a null. This would happen when the output of the AGC equalled the output of Bit 1. The test setup is the same for all bits. Bit 1 is the least significant bit and ideally, should null at approximately every degree according to the transfer function. The transfer function for the detector, when the incident sunlight is in the normal planes, is given as follows:

$$\sin \quad = \frac{nd}{\sqrt{t^2 + d^2}}$$

n = index of refraction

d = distance from center of reticle (each 1/2-degree increment = 0.00274")

t = thickness of reticle

This test was repeated at + 100°C and -107°C, however, data were unreliable due to imperfections in the temperature chamber window. Using the same optical setup as

described above, the output of the bits as a function of the angle was recorded. The incident light was in the plane defined by slit B and the normal to the detector. The results for all bits are given in Figures 5-23 through 5-26.

5.4.3 SAS SYSTEM TESTS IN DIRECT SUNLIGHT

This functional test of the SAS demonstrated the ability of the system to measure the angle between the normal of the sensor and the incident sunlight within a specified error band. Transition edges were not measured on this test; instead the output of the electronics unit was monitored every 2 minutes. The output of the electronics unit was compared to what the true angle should be at that particular time. The difference was calculated and recorded.

This was accomplished by the use of the following procedure. To calculate the true angle between the sensor and the incident sunlight, a computer program was written. This program used vector algebra to translate the axis from a reference coordinate system to our latitude and longitude. The angle of the incident sunlight at the reference was taken from the Nautical Almanac of 1965.

Since the output of the electronics unit is in the form of a Gray code, a program was written to transform the output of the electronics unit to the measured angle by the use of the sensors transformation equations. The data for the program was not the Gray code but was the segment number which, through the use of a table, can be converted from the Gray code.

These two programs were combined into one with a further addition that the difference between the two angles (true and measured both at the same time) was calculated. The output of the program had the following form:

Time - True Angle - Measured Angle - Error

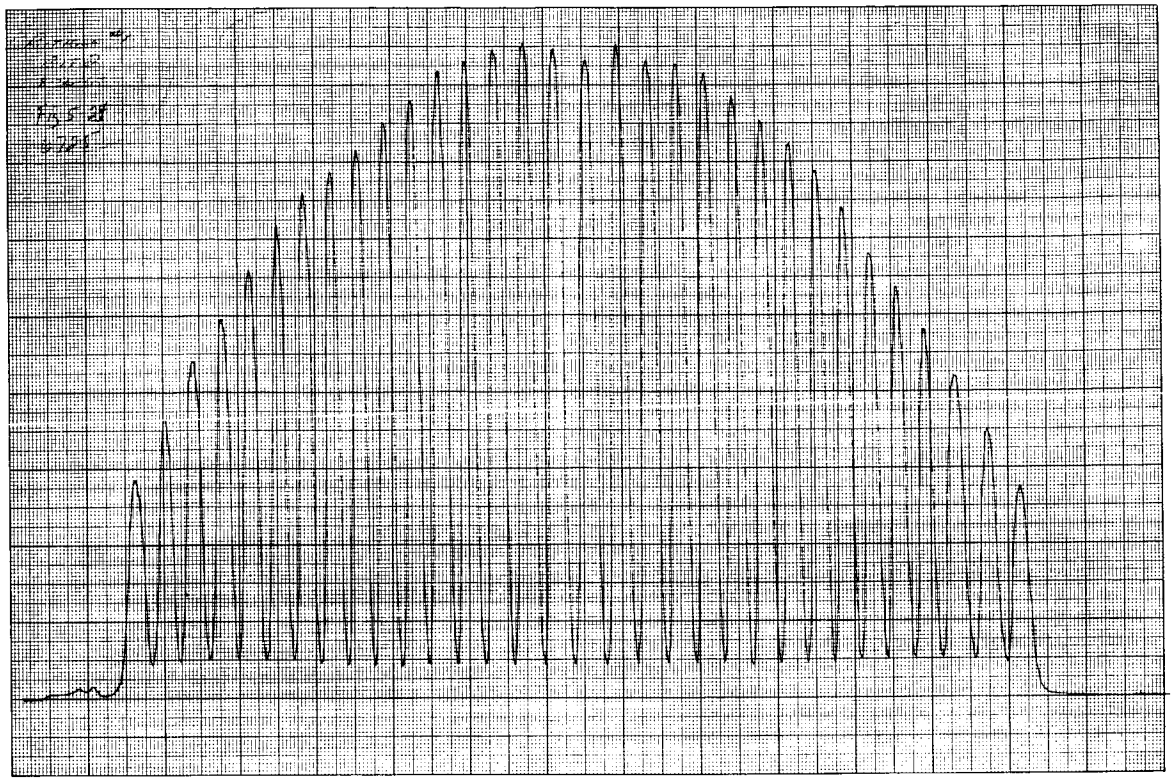

Figure 5-23. Tests Results, Reticle 1 Bit 2

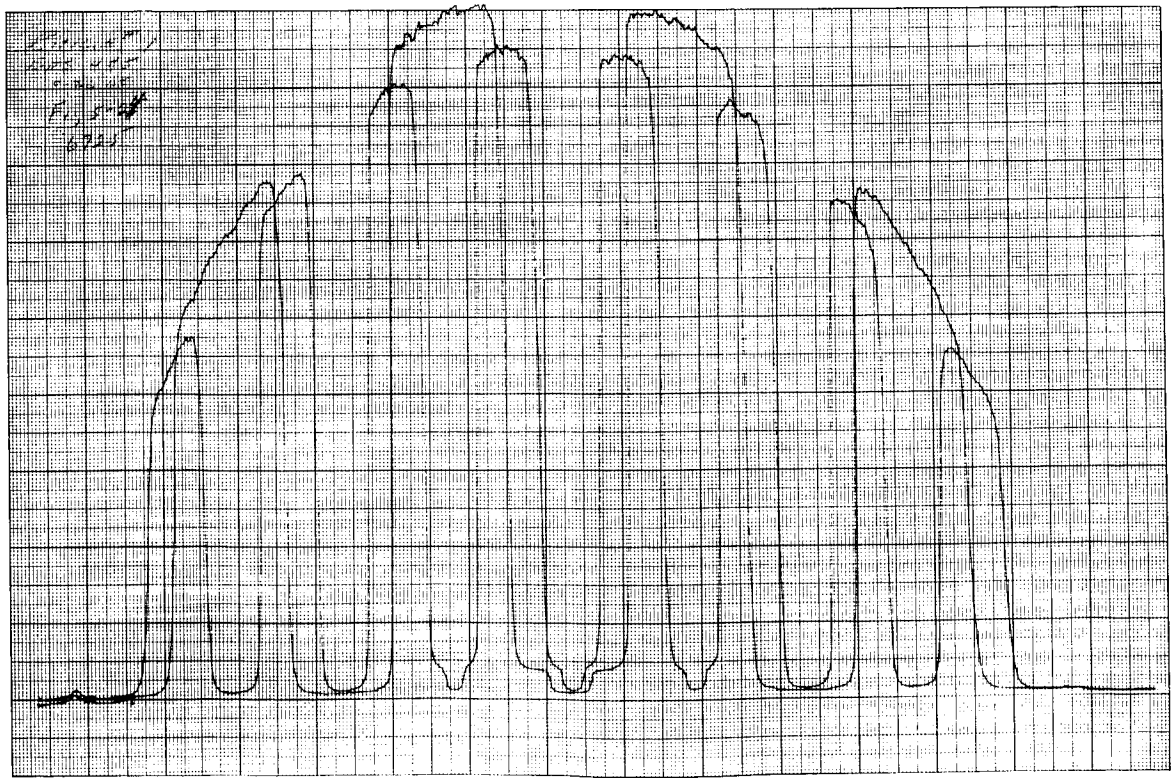

Figure 5-24. Test Results, Reticle 1 Bits 4 and 5

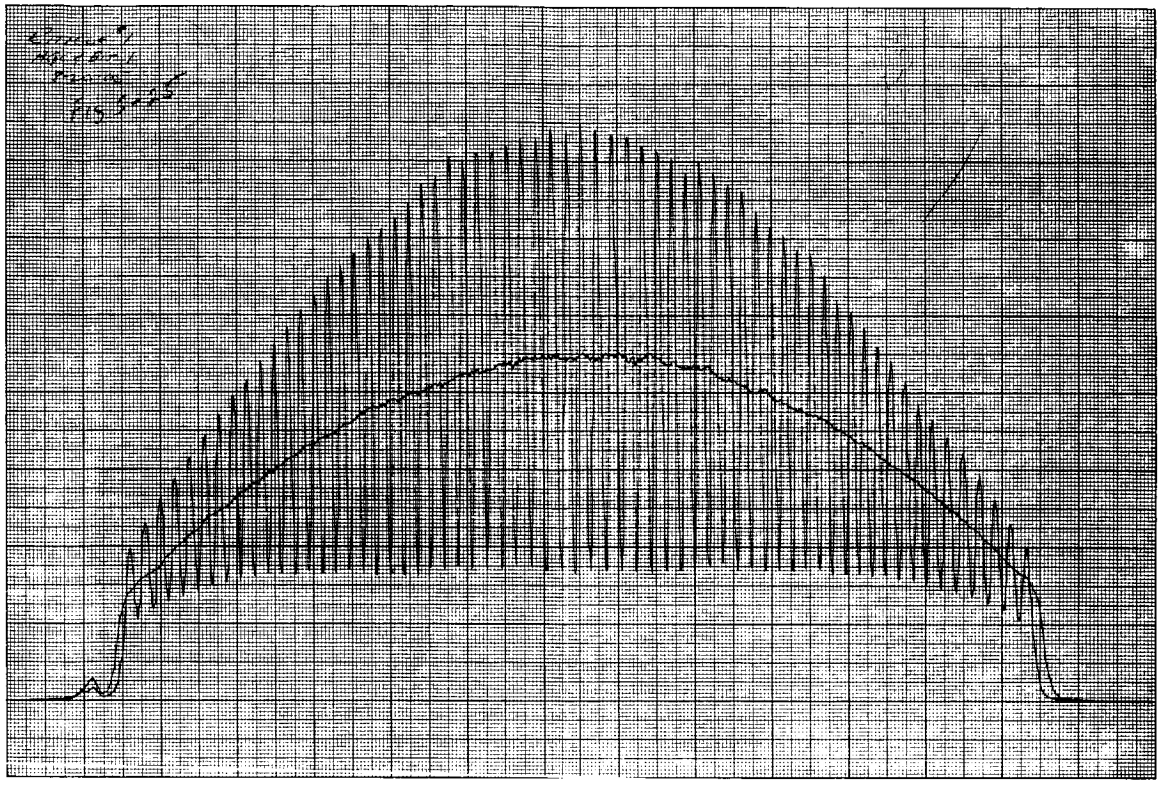

Figure 5-25. Test Results, Reticle 1 AGC and Bit 1

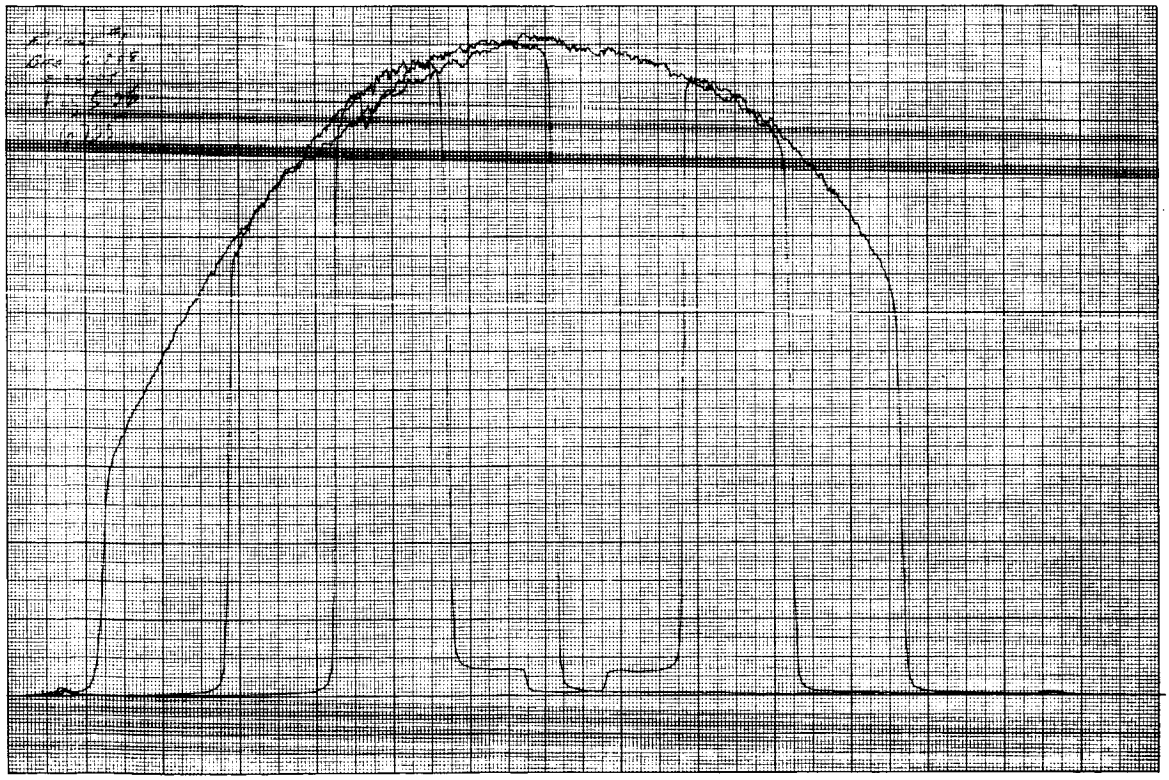

Figure 5-26. Test Results, Reticle 1 Bits 6, 7, and 8

The main difficulty with this test was alignment of the sensor so that the true angle could be calculated. It was convenient to align the sensor to true south and with a declination, to give a large compound angle. True south was obtained by taking optical fixes on two land marks that formed a line having a known direction from south. The direction south was then transfered to the test setup. Once true south was obtained the alignment was accomplished using a flat mirror and an autocollimator. All optical fixes were obtained through the use of the autocollimator.

To record the output of the electronics unit, a multipoint recorder was used which had a two minute cycling time. This presented a problem since the output of the electronics unit at the beginning of the recorder cycle was not necessarily the output at the end of the cycle, since the electronics might have switched at the middle (anywhere throughout the duration) of the cycle. For this reason, the interrogate oscillator (in the test console) was disabled and the electronics unit was given a readout pulse every 2 minutes. This was accomplished by enabling the interrogate oscillator for approximately 3 seconds every 2 minutes. In this manner, once the recorder started its cycle, the readout was fixed for the duration of the cycle.

Data in the form of a computer print-out will be found in Appendix B.

The transformation equations for a translation from the reference coordinate system to our latitude and longitude are given as follows:

$B' = \hat{A}\,\hat{B}$

$\hat{B}'$ -- Represents the direction of the sun in the new system

$\hat{B}$ -- Represents the direction of the sun in the reference system

$\hat{A}$ -- Is the transformation matrix

The elements of $\hat{A}$ and $\hat{B}$ are as follows:

A (1, 1) = Cos (PL) Sin (PD)

A (1, 2) = Cos (PD)

A (1, 3) = Sin (PL) Sin (PD)

A (2, 1) = Cos (PL) Cos (PD)

A (2, 2) = Sin (PD)

A (2, 3) = Sin (PL) Cos (PD)

A (3, 1) = Sin (PL)

A (3, 3) = Cos (PL)

B (1, 1) = Cos (SL) Cos (SD)

B (2, 1) = Sin (SD)

B (3, 1) = Sin (SL) Cos (SD)

O = A (1, 1) B (1, 1) + A (1, 2) B (2, 1) + A (1, 3) B (3, 1)

P = A (2, 1) B (1, 1) + A (2, 2) B (2, 1) + A (2, 3) B (3, 1)

Q = A (3, 1) B (1, 1) + A (3, 3) B (3, 1)

$$\text{Angle A} = \left[\text{Tan}^{-1} \quad (-Q/P)\right] \quad \frac{180.}{3.14157}$$

$$\text{Angle B} = \left[\text{Tan}^{-1} \quad (O/P)\right] \quad \frac{180.}{3.14157}$$

In the above equations, the following symbols were used:

PD - local declination

PL - local longitude

SD - sun declination

SL - sun longitude at reference

The transformation equations for the detector for a compound angle are given as follows:

$$\text{Cot } A = \frac{E + 1/2}{\sqrt{L^2 - (1-N^2)\left[(E + 1/2)^2 + (E_2 + 1/2)^2\right]}}$$

$$\text{Cot } B = \frac{E_2 + 1/2}{\sqrt{L^2 - (1-N^2)\left[(E + 1/2)^2 + (E_2 + 1/2)^2\right]}}$$

$$\text{Where } L = \frac{128\sqrt{1 - N^2}\cos 26^\circ}{\text{Cos } 26^\circ}$$

N = index of refraction

E = segment number for sensor A

E_2 = segment number for sensor B

SECTION 6

GROUND TESTING

6.1 ENGINEERING EVALUATION TESTING

6.1.1 SUBSYSTEM EVALUATION TESTS

In accordance with the program schedule, the engineering units of the ATS Gravity Gradient Stabilization System were subjected to a series of functional performance and environmental tests as prescribed in the test plan for each unit. The objective of these tests is to enable evaluation of the design adequacy and to compare the performance of each subsystem before and after exposure to qualification-level environments. A summary of the tests which were completed by the end of December is presented for each subsystem in the following paragraphs. It is anticipated that evaluation of the engineering units will be completed during the next reporting period. The subsystems tested are listed below together with the applicable test plan and component specification.

Subsystem	Test Plan Documentation (PIR)	Applicable Specification	Engineering Unit No.
Primary Boom	-	SVS-7316	T-1a
Damper Boom	4176-085	SVS-7314	T-1
Combination Passive Damper	4176-085	SVS-7314	Engineering Unit 1
TV Camera and Electronics	4176-441	SVS-7310	S/N5101 & S/N5102
Solar Aspect Sensor and Detector	4176-537	SVS-7306	Engineering Unit 1
Power Control Unit	4172-091	SVS-7307	Engineering Unit 1

6.1.1.1 T-1a Primary Boom Assembly

The T-1a Primary Boom Assembly was shipped from deHavilland on 17 September. It was subjected to pre-environmental testing at GE,preliminary to a series of engineering evaluation tests. However, difficulties were encountered during initial vibration tests and testing was stopped pending rework of the failed components. A complete description of these failures is given in Section 3.

6.1.1.2 T-1 Damper Boom Assembly

The T-1 Damper Boom Assembly was subjected to the following engineering evaluation tests. With the exception of the deployments, which were conducted on the GE test track facility, all testing was conducted with the Damper Boom mounted on the Combination Passive Damper.

a. Three-axis qualification vibration (both simusoidal and random)
b. Single squib/thruster tip mass release
c. Full deployment on the GE test track facility
d. Qualification acceleration
e. Double squib/thruster tip mass release
f. Full deployment on test track
g. Humidity
h. Double squib/thruster tip mass release
i. Full deployment on test track
j. Solar vacuum 24 hours
k. Single squib/thruster tip release in solar-vacuum chamber at -12°F
l. Full deployment on test track.

During the above test sequence, only one problem, other than the previously mentioned secondary tip mass release failures,occurred. Full deployment after vibration testing resulted in 1/2-inch overtravel of one of the tip mass/erection units. This overtravel resulted from a stiff brake lever arm not maintaining pressure against the element during deployment, and not dropping into the spool slot at the end of travel. Only minor crinkling of the element resulted from this overtravel. Considering that the nature of the retrofit necessitated drilling and pinning of the new sides of the tip mass housing to old sides, it is not too unlikely that misalignment of these side plates occurred and caused the stiffness of the brake lever arm. Ordinarily, the sides are drilled and pinned in a matched assembly, therefore this misalignment should not occur. However, to further ensure proper alignment in future units, additional pins are being added to the short side plate. This plate presently is pinned in only two places.

Deployment rates of the retrofitted Damper Boom Assembly tip masses have been within 0.4 ft/sec of each other during deployment tests at deHavilland and GE, and have been within specification for each deployment. All deployments conducted to date have been by either mechanical or manual release. During the electroexplosive releases, the tip masses were restrained from moving more than 1/8 inch by GE built tip mass catchers. Effort is underway to allow electroexplosive release while the Damper Boom Assembly is mounted on the test track. The deployment rates have been decreasing in a normal manner by about 0.1 ft/sec for each successive deployment of the same booms. During the qualification vibration tests, the tip mass response was at about the 100g level and resonances occurred at 150 cps and 170 cps.

6.1.1.3 CPD Engineering Unit 1 Testing Progress

The CPD Engineering Unit 1 was received on 22 November by Engineering from Manufacturing; testing began in accordance with the engineering test plan (PIR 4176-085, Rev A) and the component specification (SVS 7314). The following is a brief discussion of the tests performed and comments on the results of these tests. Weight and center of gravity were measured during the initial inspection. These measurements were made by the weights specialist and will be used by him to update the weight and center-of-gravity reports.

The circuit impedances were checked as well as the insulation resistance and dielectric strength. All results were within the specification limits. Electrical performance was checked by applying power to the instrumentation and mode switching (solenoid) circuits. All circuits worked properly. The CPD boom and Eddy-Current Damper (ECD) were decaged by cutting the caging cable in one place at a time (two cutters are included in the design). The firing of the first cable cutter successfully decaged the boom, ECD, and solenoid. The damping mode was changed by switching the solenoid. Instrumentation read-out and visual inspection noted the proper changes. Illustrations of the released cable are shown in Section 4.

The CPD was placed on the Advanced Damping Test Fixture (ADTF) for evaluation of the angle indicator, eddy-current damping and torsional restraint, and hysteresis damping and torsional restraint. With the CPD in the ECD mode, the tests on the angle indicator and ECD were performed. The performance of the angle indicator was as anticipated. The ECD torsional restraint constant was 23 dyne-cm/deg (specified as 21.0 to 25.2 dyne-cm/deg). The soft stop torsional restraint constant was found to be 700 dyne-cm/deg. It was determined that an error in manufacturing caused this constant to be lower than the specified value of 1000.

The eddy-current damping coefficient was found to be 730,500 dyne-cm-sec (spec is 905,000 nominal) or 18% low. An investigation showed that the use of a "master" disc to set the flux level in the damping magnets resulted in the flux being set too low resulting in the low damping coefficient. Future adjustments of the flux levels in the damping magnets will be performed with the actual damping disc to be installed into the particular CPD rather than with a "master" disc. Thus,a matched set will be used for each damper.

Tests performed on the hysteresis damper (installed in the CPD) indicated high values of damping and torsional restraint torques. Investigation into the cause of this out-of-spec data is continuing. It is anticipated that the explanation of these high values will be found in the alignment of this damper with the CPD and its test equipment, since any deterioration in the wire suspension system could only cause the torsional restraint constant to decrease rather than increase.

The CPD was installed on the force fixture for suspension system tests. The ECD radial forces measured were 7.93 dynes/ 0.001 inch (as compared to 6.2 predicted) in the direction of the torsional restraint magnets and 13.6 dynes/ 0.001 inch (13.0 predicted) in the direction perpendicular to the torsional restraint magnets. The ECD axial suspension forces were measured at 1.6 dynes/ 0.001 inch (4.1 predicted). Since this axial force data varied significantly from the predicted value, an investigation as to the cause is continuing.

The magnetic dipole of the CPD was measured both with and without electrical power applied to the unit. It was found that no difference in the dipole exists between the powered or unpowered condition. The measurements indicate a fundamental and a strong second harmonic. The CPD was uncompensated during the test. The data is presently being analyzed to determine the size and location of compensation magnets which would be required to reduce the dipole to design goal levels.

The CPD was next subjected to vibration, acceleration and humidity tests. Prior to and after each of these tests,the CPD and boom were decaged and the instrumentation and mode changing capabilities checked. All of these tests were performed successfully with no damaging effects upon the functional performance of the unit except the following. The angle indicator encoder disc in the vibration environment and the unpainted magnesium parts in the humidity test. The magnesium parts had been given the Dow 9 surface treatment. These problems and the solutions to them are discussed in Section 8, Materials and Processes.

The CPD and Damper Boom were then subjected to a 3-part solar-vacuum test. Results are presently being reviewed by the thermal analysts. All indications are that it was a very successful test. All functions, caging, solenoid switching, etc., were successfully performed. Based on calculations, the temperature distributions throughout the unit were very close to the predicted values.

The CPD Engineering Unit 1 is presently being prepared for final thermal and ambient functional testing.

6.1.1.4 TV Camera

Engineering evaluation of the TV Camera System began at GE during the week of 27 October. Tests were conducted in accordance with the test plans defined in the GE internal document (PIR 4176-441). Environments were to the qualification requirements defined in the TV Camera System Specification, SVS-7310. Two TV Camera Systems were used in various tests during this evaluation. These systems were assigned serial numbers S/N5101 and S/N5102 by Lear-Siegler Inc. (LSI).

The weight of the control unit for S/N 5102 exceeded the 5-pound maximum by 2 ounces after being conformal coated. The allowable weight was adjusted to 5-1/4 pounds since the total specified weight of 10 pounds for the system was not exceeded. During a functional performance test of S/N5102, distortion was tracted to the vidicon. LSI indicated that the vidicon was marginally acceptable, and the vidicon was later returned to the manufacture (RCA) for evaluation.

Failure of the test console to close the camera shutter upon removal of power from the TV Camera System was traced to undesired disconnect of shutter power when the camera power is switched off. The test console was modified to preclude this difficulty in future testing.

A corona test was next performed with S/N5102 in a 2-foot by 2-foot vacuum chamber. The camera operated normally at pressures greater than 2 mm Hg and less than 0.1 mm Hg. Corona was evident at three different times during the pump down, but proper operation was observed at 1.5×10^{-5} mm Hg. When the chamber was slowly vented, corona occurred several times between 100 and 500 microns and video was lost entirely at 750 microns. It was subsequently determined that a transistor in the vidicon sweep failure protection circuit (Type 2N598) had shorted. The shorted transistor was replaced and a retest of

performance was conducted before the unit was subjected to vibration testing. The camera and control unit were then vibrated to qualification levels in three axes. A functional test was performed between the application of the sinusoidal and random inputs to each plane as well as between planes. The only apparent malfunction was the failure of the sun protection shutter to operate properly between the second and third planes and at the conclusion of the vibration test. The camera shutter was observed to open and close at several different frequencies during the sinusoidal vibration. Also, some shift of the vidicon with respect to the optics was suspected from visual observations between tests in the two planes. A Wollensak representative visited GE to examine the shutter failure that occurred during vibration. Arrangements were made to return the shutter for their analysis.

Unit S/N5102 was next subjected to thermal-vacuum tests, but it was not possible to obtain the large thermal gradient between the optics and the camera that is indicated in the specification. The cold temperatures reached were -38°F at the lens, -16°F on the camera housing,and +20°F on the control unit case. The high temperature values of the specification were limited in order to keep the vidicon face plate below +140°F. All of the temperature limits specified were reviewed following the test. Reports on the corona tests, vibration, and thermal-vacuum tests are presented in Section 5.

6.1.1.5 Solar Aspect Sensor

High temperature tests were completed on the SAS electronics unit to the engineering evaluation test plan requirements in GE internal document PIR 4176-537. The temperature data taken on the system during testing was run through the computer and all results are within specification. Arrangements were made to test the SAS in direct sunlight on the roof of the General Electric facility at Valley Forge. The SAS test rack and a recorder were moved to the roof in advance of these tests. System tests of one detector and the SAS electronics unit were begun in direct sunlight during the week of 6 October. Only minor problems were encountered in surveying the site to establish proper alignment of the detector. An alignment procedure was established for orienting the detector unit

on the roof site, and a mounting fixture was fabricated. Following alignment, the system was operated for 13 hours with the sun in a plane about 8 degrees from the plane of one detector eye. Two or three additional runs will be made with the sun in other planes. A computer program was written and checked to calculate the true position of the sun with respect to the detector coordinate system.

Tests in direct sunlight demonstrated that the system works well within specifications at compound angles. Data was accumulated with the sun in two separate planes, i.e., angle B varying from 18 to 8 degrees with angle A varied from -64 to +64 degrees, and at the edge of the field of view with angle B varying from 61 to 64 degrees and angle A varying from 64 to 53 degrees. The first 12 readings from the extreme edge of the field show an error of less than 0.6 degree, only about half of the maximum allowable error of 1.3 degrees. Data taken with the SAS in direct sunlight was reduced and printed out in tabular form; all readings were within specification.

The SAS electronics unit was next exposed to cold temperature testing at -15°C. Results were so close to the vendor's data that the cold chamber tests were repeated at only a few points. The solar-vacuum test of the SAS engineering unit and one detector were set up and run for 22 hours. However, the test was discontinued after the data indicated that the fixture did not adequately simulate flight conditions. The fixture was reviewed with thermal specialists and a redesign of the fixture was recommended.

6.1.1.6 Power Control Unit

Engineering Unit 1 of the Power Control Unit was exposed to the evaluation as defined for engineering evaluation in GE internal document PIR 4172-091. Temperature testing stated in September was completed. As a result of these tests, one transistor apparently opened, another developed a high leakage path, and one connector module is suspected of loosening. These problems were corrected prior to subjecting the unit to vibration tests to qualification levels. The transistor failure apparently resulted from an excessive current drain. Rework of the failed parts and modules was completed and the new modules were installed.

An exploratory vibration test on the unfoamed PCU engineering unit was performed at the ATS component acceptance levels of NASA/GSFC specification S2-0102, Revision C. The results of the test indicate that the unit would survive the qualification levels of S2-0102 without degradation.

The unfoamed engineering unit of the PCU was subjected to qualification level vibration tests with no observable degradation or failure. The unit then underwent thermal-vacuum tests without failure, except for one of the instrumentation thermocouples which was mounted on the outside. No temperature rise was detected in the specially instrumented power transistors during normal operation, i.e., during the execution of commands for up to two minutes. Operational tests were performed without failure at temperatures of +60°C, +25°C and -20°C.

Preliminary EMI tests on Engineering Unit 1 revealed a potential conducted susceptibility in the motor driver circuits. Further tests to determine the specific nature of the susceptibility resulted in the loss of the four field driver modules as a result of the faulty application of test equipment. New modules were built to replace the damaged modules. With the drive circuits changed to operate from the regulated bus, the conducted susceptibility was reduced to within specification limits.

6.1.2 SYSTEM TESTING

The "ATS System Evaluation Requirements and Test Plan" was completed in October and copies were delivered to NASA/GSFC. The objectives of this system evaluation test are:

a. To demonstrate electrical compatibility of all ATS components after they are interconnected into the gravity-gradient system.
b. To evaluate test procedures and techniques prior to their use on the System Prototype and System Flight Spacecrafts at HAC.

c. To acquaint GE field test personnel with the gravity-gradient hardware under system test conditions.

d. To demonstrate electrical compatibility between the gravity-gradient system and the AGE.

e. To evaluate the gravity-gradient system with respect to electromagnetic interference and susceptibility properties.

A tentative test site has been selected at GE for the system evaluation test. The area will be approximately 20 feet by 20 feet in order to conduct the tests and house the spacecraft components, AGE, and accessories needed during testing. A minimum of five 110-volt ac outlets will be required in the test area. A protective cover will be used for all cabling. The area will have overhead protection in order that no debris, oil, metal chips, etc., fall into the system. A laminar filtered air flow will be provided. The filtered air is required during boom deployment so that a dirt film will not form on the booms. White coats will be worn by all personnel in the area, and white gloves will be used in handling components that have a thermal protective finish.

6.2 QUALIFICATION TESTING

6.2.1 PARTS QUALIFICATION PROGRAM

The Parts Qualification Program is presented in Tables 6-1 and 6-2. The program is shown as revised during the reporting period. Additions to each list are indicated by an asterisk; changes and deletions are lined out.

The status of each item contained in the Parts Qualification Program is given in Table 6-3. ETP-4165-1, issued 11 November 1965, is an engineering test plan for the testing of miniature lamps for the angle indicator. It specifies an operational accelerated life test on a total of 75 lamps. Acceleration levels are 10:1 for 50 lamps and 50:1 for 25 lamps (based on a voltage exponent of 12). Duration of the test is 3000 hours.

TABLE 6-1. GROUP A - PARTS REQUIRING QUALIFICATION TESTING

ITEM	PART	PART/TYPE NO.	VENDOR	WHERE USED	QUANTITY	WHERE TESTED
1	Transformer, ~~Inverter~~	R4610P1	Edgerton	SAS	5	~~GE-SD~~ Adcole
2	Solar Cell Assembly	R4611P1	Hoffman ~~Edgerton~~	SAS	5	Adcole
3	Solenoid	R4612P1	Koontz-Wagner	CPD	~~5~~ 6	Koontz-Wagner
4	Angle Indicator ~~Head~~ Assembly	47E207350	GE-SD	CPD	3	GE-SD
5	Cable Cutter	115C7516 895D724	Holex	CPD	20	Holex
6	Not used					
7	Pressure Transducer	*Model 1000	C.I.C.	Booms	5	*GE-SD
8	Potentiometer, Scissoring	TSPR10K(2)L2	Helipot	Booms	5	*GE-SD
9	Potentiometer, Extension	T223R10K(1)L2	Helipot	Booms	5	*GE-SD
10	Limit Switch, Extension	2HM1-3	Minn. Honey.	Booms	10	*GE-SD
11	Limit Switch, Scissoring	6HM1-1	Minn. Honey.	Booms	10	*GE-SD
12	Motor, Boom Drive	*106A161	Globe Ind.	Booms	~~15~~ 5	*GE-SD
13	Motors, Scissoring	*114A152	Globe Ind.	Booms	~~15~~ 5	*GE-SD
14	Transmission ~~Sealed Drive~~ Unit	*5398E1-1	deHavilland	Booms	2	GE-SD
15	Lamps, Double Filament	47C207314P1	Chicago Miniature	CPD	~~100~~ 75	* Chicago - Miniature
*16	*Linear Actuator Assy	*47C209587G1	*Holex	*Booms	*18	*Holex
*17	*Ball Lock Release Assy	*47D209594G1	*Avdel	*Booms	*18	*GE-SD

Note: Additions are indicated by an asterisk. Changes and deletions are lined out.

TABLE 6-2. GROUP B - PARTS FOR TEAR-DOWN AND ANALYSIS

ITEM	PART	VENDOR	PART/TYPE NUMBER	COMP-ONENT	NUMBER TO BE PURCHASED
1	Transistor	*Texas Inst.	2N2432	SAS	5
2	Not used				
3	Not used				
4	Relay	*GE	R2313	PCU	5
5	~~Temp. Sensors~~	-		~~All~~	~~5~~
6	~~Thermistor~~	~~Fenwal~~		~~Booms~~	~~5~~
7	Solenoid, Rotary	Ledex	RS222-AE4	Booms	5
8	~~Switch - 1HM1~~	~~M. H.~~		~~Booms~~	~~5~~
9	Switch	M. H.	12SM4T	Booms	5
10	Bellows,*Linkage	*Flexonics	5398E12-1	Booms	5
11	~~Capacitor~~	~~Sprague~~	~~118P~~	~~Booms~~	~~5~~
12	Connector	Cannon ~~DEM~~	DDM-50P-NAB OTC	Booms	5
13	Connector	Cannon ~~DCM~~	DCH-37P202	Booms	5
14	~~Connector~~	Cannon ~~DBH~~		~~Booms~~	~~5~~
*15	*Bellows, Eccentric	*Flexonics	*5398D31-1	*Booms	*5

Note: Additions are indicated by an asterisk.
Changes and deletions are lined out.

TABLE 6-3. STATUS OF PARTS QUALIFICATION PROGRAM, 23 DECEMBER 1965

ITEM NO.	DESCRIPTION	STATUS
Group A		
1	Transformer	Parts are completed and on hand at Adcole. Testing will begin upon revision and approval of Adcole test plan.
2	Solar Cell Assembly	Parts are completed and on hand at Adcole. Test plan is needed from Adcole.
3	Solenoid	Parts are completed. Acceptance testing is completed. Test plan by Koontz-Wagner is approved. Qualification testing has begun; failure in test caused redesign and restart of test.
4	Angle Indicator Assembly	Procurement of parts is in process. Resolution of design problem on module is pending.
5	Cable Cutter	Qualification testing is completed. Report is issued
6	Not used	
7	Pressure Transducer	Quotation for hardware is due 1/7/66
8	Potentiometer, Scissoring	Quotation for hardware is due 1/7/66
9	Potentiometer, Extension	Quotation for hardware is due 1/7/66
10	Limit Switch, Extension	Parts are requisitioned. Feedback from Procurement is needed
11	Limit Switch, Scissoring	Parts are requisitioned. Feedback from Procurement is needed
12	Motor, Boom Drive	Quotation for hardware is due 1/7/66
13	Motor, Scissoring	Quotation for hardware is due 1/7/66
14	Transmission Unit	Two primary boom assemblies will be made available upon

	Transmission Unit	Two primary boom assemblies will be made available upon completion of the planned testing for engineering and component qualification purposes
15	Lamps	Parts are on order. Expect delivery 1/27/66 for vibration testing at GE. Test plan ETP-4165-1 is issued. Testing at vendor's plant will follow. Duration of testing is 125 days
Group B		
1	Transistor	Parts were delivered to Spacecraft Materials Research and Development (SMR&D). Evaluation plan is pending
2	Not used	
3	Not used	
4	Relay	Parts were delivered to SMR&D. Evaluation plan is pending
5	Not used	
6	Not used	
7	Solenoid, Rotary	Parts are requisitioned. Feedback from Procurement is needed
8	Not used	
9	Switch	Parts are requisitioned. Feedback from Procurement is needed
10	Bellows, Linkage	Decision to use in-house welding process check specimens for qualification purposes is pending
11	Not used	
12	Connector	Parts are requisitioned. Feedback from Procurement is needed
13	Connector	Parts are requisitioned. Feedback from Procurement is needed
14	Not used	
15	Bellows, Eccentric	Decision to use in-house welding process check specimens for qualification purposes is pending

6.2.2 COMPONENT QUALIFICATION TESTING

Revised qualification test cycles for each component were submitted to NASA for approval. A TWX was received from NASA on 16 November 1965 approving the following cycles:

a. Combination Passive Damper

1. Electrical functional - ambient
2. Force functional - ambient and temperature (T_{max} + 15°C, T_{min} - 15°C)
3. Damping functional - ambient and temperature (T_{max} + 15°C, T_{min} - 15°C)
4. Humidity
5. Electrical functional - ambient
6. Vibration
7. Electrical functional - ambient
8. Acceleration
9. Electrical functional - ambient
10. Vacuum thermal (T_{max} + 10°C, T_{min} - 10°C, hot and cold soak)
11. Force functional - ambient
12. Damping functional - ambient
13. Electrical functional - ambient

b. Primary Boom

1. Functional - ambient
2. Leak
3. Humidity
4. Functional - ambient
5. Vibration
6. Functional - ambient
7. Acceleration
8. Functional - ambient

9. Vacuum thermal (T_{max} + 10°C, T_{min} - 10°C, hot and cold soak)
10. Leak
11. Functional - ambient

c. Damper Boom

1. Functional - ambient
2. Humidity
3. Vibration
4. Acceleration
5. Vacuum thermal (T_{max} + 10°C, T_{min} - 10°C, hot and cold soak)
6. Functional - ambient

Note

The pyrotechnic device must be fired in order to deploy. Functional tests between environments have been waived in order to permit the pyrotechnic device to be processed through the entire qualification cycle. An electrical check (no fire) will be performed on the pyrotechnic device between each environment.

d. TV Camera Subsystem

1. Functional - ambient
2. Humidity
3. Functional - ambient
4. Vibration
5. Functional - ambient
6. Acceleration
7. Functional - ambient
8. Vacuum thermal (T_{max} + 10°C, T_{min} - 10°C, hot and cold soak)
9. Functional - ambient

e. Solar Aspect Sensor

1. Functional - ambient
2. Humidity
3. Functional - ambient
4. Temperature (T_{max} + 15°C, T_{min} - 15°C)
5. Vibration
6. Functional - ambient
7. Acceleration
8. Functional - ambient
9. Vacuum thermal (T_{max} + 10°C, T_{min} - 10°C, hot and cold soak)
10. Functional - ambient

f. Power Control Unit

1. Functional - ambient
2. Humidity
3. Functional - ambient
4. Vibration
5. Functional - ambient
6. Acceleration
7. Functional - ambient
8. Vacuum thermal (T_{max} + 10°c, T_{min} - 10°C, hot and cold soak)
9. Functional - ambient

6.2.3 SYSTEM TESTING

The GE Gravity-Gradient System Prototype Field Test Plan was submitted to NASA on 6 December 1965. The plan includes the following information:

a. Block diagrams of each major test
b. Test parameters and tolerances
c. Special test equipment
d. Alignment requirements
e. Individual test plans for each component
f. Environmental test requirements
g. Facility requirements at HAC.

NASA has reviewed this test plan (GE document 65SD4499-A) and has requested that GE also submit a standing instruction for the system qualification test at HAC. It now appears that HAC will not prepare test instructions for the system test but will work directly from GE test instructions.

6.3 FLIGHT ACCEPTANCE TESTS, AGE

The first set of AGE was completed during October. Checkout of the AGE and its associated harnesses were completed in November utilizing the "ATS System Evaluation Requirements and Test Plan." This AGE set has gone through the calibration lab and has received formal calibration status.

A simulated ATS structure was completed in October. The structure was painted and will be used during the system evaluation tests and subsequent prototype and flight system tests at GE.

SECTION 7
QUALITY CONTROL

7.1 SOLAR ASPECT SENSOR

The in process inspection of five prototype printed circuit boards was witness at Adcole Corporation and the units were accepted for further processing. The Solar Aspect Sensor Test Plan was circulated for comments and updated to include changes requested by Engineering.

7.2 TV CAMERA SUBSYSTEM

A quality audit was conducted at Lear-Sigler Inc., by the vendor surveillance representative and quality control engineer. Comments on the vendors Acceptance Test Plan were forwarded through purchasing. Engineering testing has been supported by QC technicians during the period.

7.3 BOOM SUBSYSTEM

The Quality Control Plan and Acceptance Test Procedure submitted by Holex, Inc., were reviewed and approved by the QC Engineer for the linear actuator. Vendor surveillance consisted of reviewing some in-process parts which were found suitable for shipment to GE. A comprehensive report covering all vendor surveillance activity at deHavilland for the wood mock-up, dynamic and thermal models, Engineering Unit T-1a, and test equipment was issued. All quality problems are summarized and pertinent remarks regarding present status and corrective action are included. Engineering testing at GE was supported with QC test technicians. DeHavilland's Acceptance Test Plan was reviewed and comments, regarding changes which must be incorporated, were forwarded through Purchasing.

7.4 COMBINATION PASSIVE DAMPER

The Acceptance Test Plan and Inspection Procedures submitted by Bausch and Lomb for the fiber optics assembly were reviewed and approved by the Quality Control Engineer.

Process certification was granted to Metal Finishing Company for surface treatment of magnesium alloys in accordance with GE drawing and specification requirements.

Vendor surveillance performed at Ehresmann Machine Company resulted in shipment of six angle indicator heads and a drill jig for some detail parts being made in-house.

In-process assembly was monitored at TRW Systems for the first prototype unit. Test equipment checkout was also witnessed.

Action was initiated to accept the test equipment used in conjunction with the LOFF and ATDF. These items were designed and built by Engineering. Calibration procedures are being provided by Quality Control in addition to assuring that the equipment is satisfactory for QC testing.

Recommendations for obtaining quality control acceptance of the assembly fixture (101T123AF) are contained in PIR 4323-FM-179. Corrective action has been initiated by the Tool Equipment Design and Loft operations.

A procedure for inspecting the encoder disc using the positive and negative masters was issued in PIR 4323-FM-183.

7.5 POWER CONTROL UNIT

The PCU module test equipment designs are essentially complete and fabrication of two module test boxes has been completed. Most of the piece parts for the prototype units have been processed through the Parts Test Laboratory.

7.6 GENERAL

Discussions with NASA - Western Operations Office resulted in an acceptance of the Quality Control Program provided two outstanding items are incorporated. This shall be accomplished during the next reporting period. Component qualification test cycles were revised and the Qualification Test Plans reflect the changes.

SECTION 8

MATERIALS AND PROCESSES

8.1 PRIMARY BOOMS

A procedure has been evolved to braze the drive bellows in the Primary Boom Package to the stainless steel end fittings. A braze alloy will be used which will permit the simultaneous brazing and solution annealing of the beryllium copper. Hardening of the beryllium copper will be done subsequent to the brazing.

8.2 DAMPER BOOM MATERIALS

Two problem areas presently exist in material applications in the Damper Boom. The first of these is breakage of the spindle in the ball-lock mechanism upon acuation. The material used by the vendor for this application, 440C stainless steel,has good tensile strength and hardness for the applications but suffers from very low impact strength. Because the stress analysis indicates that high impact strength is important for survival of this component after repeated pyrotechnic actuation, a material of higher impact strength at the required tensile strength and hardness was selected. The most desirable material appears to be 4340 low alloy steel. It offers a five to tenfold increase in impact strength over 440C stainless steel at the same strength and hardness levels.

The second problem area in the Damper Boom results from the low solar absorbtivity requirement of the finished aluminum surface of the boom housing. A controlled emissivity (short treatment period) alodine 1200 chromate conversion coating was selected to give this optical surface. It did not give adequate protection during the humidity test; some blotching of the finish resulted. Measurements of the optical properties of the surface are now underway to determine whether the change in thermal radiative properties of the finish results in an intolerable change in value.

A summary report has been written on the various tests to determine the decomposition of silver sulfide in space. The results of solar absorptivity tests on samples of plated rod, stored for six months,were also presented. Recommended action with regard to the problem was the storage of the tape on a spool and reasonable bagging were more effective and reliable than depending upon decomposition of silver sulfide in space.

8.3 CPD MATERIALS

Both engineering model vibration tests and humidity tests have been conducted and the performance of the materials evaluated. There was no observable degradation of materials resulting from the vibration test of the CPD dynamic model. The vibration test of the engineering model caused failure of the angle detector encoder disc. There was only a blank disc in the dynamic model. This disc was 0.005-inch thick copper. Analytical calculations indicated that the performance of this disc would be marginal, but to minimize light reflection from the edges of the cutouts, the disc was built. For the second engineering unit, both 0.010-inch thick beryllium copper and aluminum are being considered.

As a result of the humidity test on the first engineering unit, severe pitting was observed on the magnesium parts finished with Dow 9 anodic coating. Other magnesium parts finished with Dow 17 anodic finish plus epoxy paint showed no deterioration from the test. Both finishes had been certified by the vendor to the applicable military specification. Samples of both Dow 9 (produced in the laboratory) and Dow 17 finished magnesium were exposed to the specified humidity test conditions for three days. No corrosion or pitting was observed in either specimen. Resolution of the problem is still underway.

8.4 SOLAR ASPECT SENSOR

Adcole was instructed to vacuum bake the DC675 silicone rubber grating bumpers for 24 hours at 400^{0}F at 10^{-5} mm Hg prior to installation into the Solar Aspect Sensor detector heads.

SECTION 9
MANUFACTURING

Full time technical support was provided by the Manufacturing operation during assembly of Engineering Units 1 and 2 of the Combination Passive Damper. Delays in the assembly cycle of Engineering Unit 2 were reduced to a minimum because of the experience gained during the assembly of Engineering Unit 1. Refinements were made in the assembly sequence, and adjustment of internal components was accomplished. A number of minor design changes were implemented in the manufacturing processes. Complete assembly of Engineering Unit 2 is delayed pending the installation of the redesigned angle indicators encoder disc. The experience gained in the assembly of the two CPD engineering units will make the assembly of the prototype unit a much smoother operation.

The following status is reported for the prototype unit:

a. Prototype 1 - Manufacture of the component parts is about 95% complete.
b. Prototype 2 - Manufacture of the component parts is about 85% complete.
c. Flight Units - Manufacture of the major mechanical parts is progressing per schedule.
d. Ground Support and Test Equipment - The equipment is about 90% complete
e. Tooling - All major tooling is complete.

SECTION 10

RELIABILITY AND PARTS & STANDARDS

10.1 RELIABILITY

10.1.1 EMERGENCY-MODE LIMIT SWITCHING

The Primary Boom package limit-switching configuration has been evaluated,primarily to determine the desirability of including limit switching in the emergency mode of operation. A functional diagram of the present configuration is shown in Figure 10-1. The effects of all possible combinations of limit-switch failure modes (open and shorted) and boom position/status have been tabulated. The results are summarized in Figure 10-2. Two categories of failure effect have been defined: "Catastrophic" (indicated in Figure 10-2 by an "X"), leading to loss of vehicle stabilization capability; and "Gravity Gradient Experiment Critical" (indicated in Figure 10-2 by an "*"), leading to loss of a function or capability necessary to the completion of the orbit test plan. (Depending on boom configuration at the time of failure, an "Experiment Critical" failure may, of course, also result in degradation of the basic stabilization function, i.e., loss of pointing accuracy.) Figure 10-2 indicates the sequence of switch failure events leading to each type of system failure.

The extension limit switch shown in Figure 10-1 is actually a four-switch quad; the "max-angle" switches shown are actually two switches in parallel. The probability of occurrence of a failure-mode path that requires either the failure of an extension limit switch or the combination of an extension limit-switch failure with another failure (e.g., max-angle limit switch) is therefore very small. The three failure-mode paths shown in Figure 10-2 that do not fall into this category require at least one switch failure in addition to what would amount to an incorrect command.

If additional limit switches were added for emergency-mode operation at the points marked "X" in Figure 10-1, for instance, the only reliability improvement would be in the two failure-mode paths that include the combination of a failure in the normal mode and the

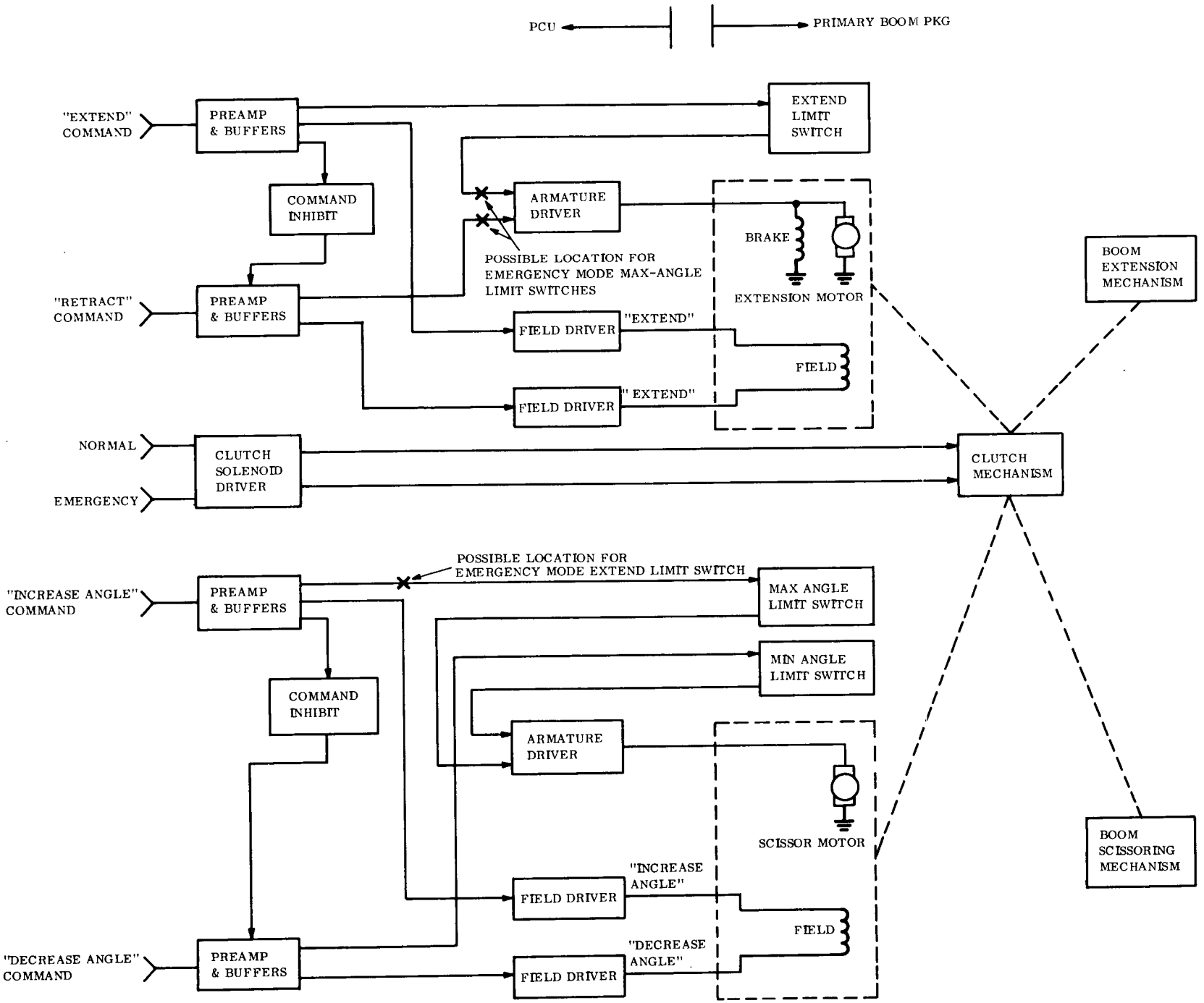

Figure 10-1. Present Emergency Mode Limit Switching Configuration

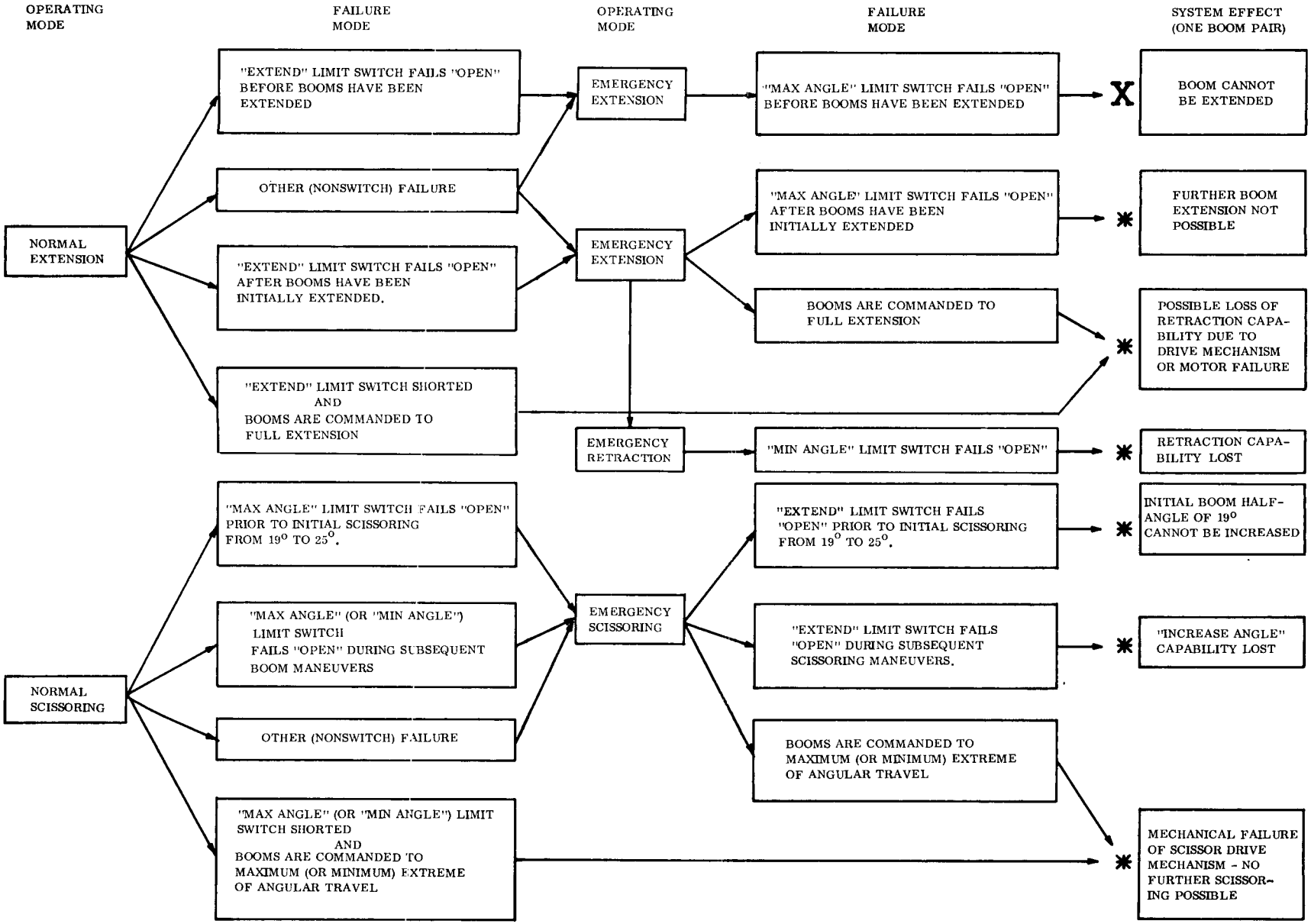

Figure 10-2. Limit-Switching Failure Modes

transmission of an incorrect command in the emergency mode. (The motion of the booms in the emergency extension mode is very slow, so the likelihood of inadvertently driving the booms to the limit is small. Due to uncertainties in controlling the boom angle in the emergency scissoring mode, it is unlikely that any maneuvers will be attempted in this mode other than to return the booms to the nominal optimum half-angle.)

The probability of occurrence of one of the other failure-mode paths would at the same time be increased by the addition of more switches. The overall effect would be to reduce the reliability in the normal mode while increasing slightly the reliability of the backup mode.

On the basis of the foregoing, there does not appear to be significant advantage to be gained by adding emergency-mode limit switches.

10.1.2 ANGLE INDICATOR - PRELIMINARY RELIABILITY ASSESSMENT

A failure mode/effects analysis was performed on the CPD angle indicator, and a preliminary reliability estimate obtained. Quantitative evaluation of this device has been hampered by the lack of adequate reliability data on two low-usage parts: the dual-filament lamps and the phototransistors. It was necessary to make estimates of the failure rates of these two items, based on extrapolation of existing test data and on other supplementary information. The numerical results in Table 10-1 are based on these estimates, and will be updated as more data becomes available.

The reliability of the angle indicator is estimated to be 0.99 for the first thirty days, 0.94 for the first year, and 0.82 for the full three years. The most probable mode of failure, by a wide margin, is a continuous "1" in one bit of the gray-coded output. The predominant failure modes of all piece-parts in the circuit lead to this result.

TABLE 10-1. ANGLE INDICATOR RELIABILITY ASSESSMENT

PART IDENT.	PART DESCRIPTION	CIRCUIT FUNCTION	FAILURE MODES	PRINCIPAL FAILURE EFFECTS (FAILURE MODE RATES X 10^{-9}/HR) CONTINUOUS "1" OUTPUT	CONTINUOUS "0" OUTPUT	LOSS OF HAC INPUT PROTECT	PROBABLY NONE DUE TO EXTENSIVE DERATING
V1	Phototransistor, (TI LS433)	Sense light passing through Gray-code apertures in angle-indicator disk.	Open (E, C) Short High I_D Low I_L	300	120		 100 100
Q1	Transistor (2N2907), PNP Si, Epit. Planar Sw, 400mw.	Switch providing "Light-On" ("0") signal to HAC encoders	Open (E, B, C) Short (CB) Short (EB) Low β High I_{CBO}	5 1	1		 1 3
CR1, 2	Diode (1N3595) Si Planar Sw, 500 mw	Conduct Q1 I_C for "ON" ("0") signal; blocks failure interaction between HAC encoders.	Open Short High I_R	8 (2)		4(2)	 8 (2)
R1	Resistor (NF170N), Carbon Film, 1/8w, 90.9K, 1%	V1 current limiting.	Open Drift	5			 0.5
R6	Resistor (NF170N), Carbon Film, 1/8w, 22. 1K, 1%	V1 Bias, Q1 leakage protection	Open Drift	5			 0.5
			TOTALS	324	121	4	213

10.1.3 BOOM SUBSYSTEM FAILURE-MODE RISK ASSESSMENT

The current estimates of the risk (likelihood of occurrence) associated with significant failure modes in the Boom Subsystem are summarized in Table 10-2. This analysis is restricted to those functions critical to the basic vehicle stabilization mission, i.e., deployment of "X"-booms and damper booms, and scissoring from 19 to 25 degrees. A more detailed study is in progress (in connection with optimizing the orbit test plan), covering also those functions and additional components required for the gravity-gradient experiment.

The probability of success (reliability) of the initial boom deployment function may be approximated by R = 1-Q. Where Q is the total of the first, third, fifth, sixth, and seventh columns in Table 10-2, i.e., the total failure probabilities of those functions for which no backup exists. The total Q for these five columns is 0.042, yielding R = 0.958.

10.2 PARTS AND STANDARDS

10.2.1 INTRODUCTION

The activities in Parts and Standards during the quarter have continued as reported in the Fifth Quarterly Report. Increased emphasis was directed to the revision and updating of parts drawings. Also emphasized were the selection and processing of part substitutions and waivers, as required to meet prototype program schedules. In addition, the degradation analysis of parts for flight hardware is progressing as parts and data are delivered.

Questions which existed regarding the "Reliability Program Plan" were resolved in meetings with NASA representatives. Documents which were requested by NASA were collected for submittal.

TABLE 10-2. BOOM SUBSYSTEM FAILURE-MODE RISK ASSESSMENT

COMPONENT/SUBASS'Y [NO.]	SYSTEM FUNCTION	PRINCIPAL FAILURE MODE (S)	PRINCIPAL FAILURE EFFECT (S) WITH ESTIMATED PROBABILITY OF OCCURANCE (IN Q X 10^{-2}): FAILURE TO EXTEND A PRIMARY BOOM PAIR	LOSS OF NORMAL EXTENSION CAPABILITY, ONE PAIR	LOSS OF ALL SCISSORING CAPABILITY, ONE PAIR	LOSS OF NORMAL SCISSORING CAPABILITY, ONE PAIR	LOSS OF EMERGENCY-MODE CAPABILITY	FAILURE TO DEPLOY DAMPER BOOMS	LOSS OF TELEMETRY DATA ON BOOM STATUS	DATA SOURCE	REMARKS
Primary boom assemblies [4] element, tip mass/ target, storage drum, spring belt, etc.	Storage & deployment of stem elements for primary ("X") booms.	Jamming of element or spring belt, bearing siezure, etc.	1.36							DeH. test data	
Extension motors [2]	Primary power to extend booms	Bearing siezure, winding short/open.		0.02						IHA*	+loss of scissor backup
PCU-Armature/field drivers (A12/13/14/15)	Excitation to armature, field and brake windings of extension motors.	No/low output, premature output		0.0004						PIR 4144-237	+loss of scissor backup
Transmission (partial) [2]	Transmit power from extension motor to clutch	Bearing siezure, jammed gears		0.006						IHA	+loss of scissor backup
Transmission (partial) [2]	Transmit power from "normal external" clutch to extend output shaft - also from "emergency extend" clutch - also from extend output shaft to extend potentiometer - also eccentric drive and bellows.	Bearing siezure, jammed gears, jammed eccentric drive, siezed pot.	0.048							IHA	+loss of scissor backup
Scissoring Motors [2]	Primary power to scissor booms; backup power to extend/retract booms.	Bearing siezure, winding short/open.				0.032				IHA	+ loss of ext. backup
PCU-Armature/field drivers (A16/17/18/19)	Excitation to armature & field windings of scissoring motors.	No/low output, premature output.				0.0004				PIR 4144-237	+ loss of ext. backup
Transmission (partial) [2]	Transmit power from scissor motor to clutch	Bearing siezure, jammed gears.				0.006				IHA	+ loss of ext. backup
Transmission (partial) [2]	Transmit power from "normal scissor" clutch to scissor output shaft - also from "emergency scissor" clutch - also from scissor output shaft to scissor-angle potentiometer	Bearing siezure, jammed gears, siezed potentiometer			0.034					IHA	+ loss of ext. backup
Clutch Mechanism [2]	Transfer power train paths to reverse functions of motors.	Open, shorted, or jammed solenoid, bearing siezed.					0.02			IHA	
PCU-Clutch driver (A8) [2]	Excitation to rotary solenoid that actuates clutch.	No or low output					0.0004			PIR 4144-237	
Damper-boom release mechanism.	Secures self-extending damper booms during launch-boost phase; releases on command to allow deployment	Squibs fail to fire, mechanism jammed.						0.70		PIR 4E20-1	Squibs redundant
PCU-Squib drivers [2] (AID/23 - redundant)	Provides firing pulse to release-mechanism squibs.	No/low output (Premature negl.)						Negl.		PIR 4144-237	
PCU-T/M power supply (A1)	Provides -5 vdc excitation for boom-status transducers.	No output, unregulated output, unstable.							0.0003	PIR 4144-237	
Boom status transducers (extention & angle potentrometers, temperature & pressure transducers)	Provide telemetry data on boom extension, angle; sealed unit pressure, temperature; etc.	No output, drift							0.026	IHA	
Damper boom assemblies [2]	Storage and deployment of STEM elements for damper booms	Jamming of element guides, etc. Hang-up of brake						2.0		DeH. test data	
TOTAL RISK (Q X 10^{-2}):			1.408	0.0264	0.034	0.0384	0.0204	2.7	0.0263		

*In-house analysis (not yet published)

10.2.2 PART DRAWINGS AND PARTS LISTS

The following GE drawings and parts lists were revised and updated during the reporting period:

R4504, Rev. B
R4510, Rev. A
R4515, Rev. B
R4518, Rev. B
R4521, Rev. B
R4526, Rev. A
R4528, Rev. A
R4535, Rev. A
R4536, Rev. A
R4540, Rev. A
R4548, Rev. B
R4562, Rev. B
R4573, Rev. B
R4581, Rev. A
R4582, Rev. A
R4583, Rev. B
R4590, Rev. A
R4602, Rev. B
R4604, Rev. B
R4605, Rev. A
R4612, Rev. B
490L106, Rev. E
490L107, Rev. B
490L113, Rev. A
490L116, Orig. Issue and Rev. A

In addition, the referenced HAC drawings were updated.

10.2.3 PARTS QUALIFICATION PROGRAM

Details of parts qualification are discussed in Section 6.2.1.

10.2.4 DEGRADATION ANALYSIS

The degradation analysis of parts to select the most stable specimens for flight use is continuing. Parts purchased by GE are 63% completed; parts purchased by Adcole Corporation are 85% completed. (See Table 10-3 for details.) Of the items noted in Table 10-3 as not yet received by GE, 10 lots are on hand with incomplete or questioned data. Since they cannot be processed at this time, they are listed as not yet received. The processing is completed for all other items that have been received to date. The range of sizes of delivered lots is indicated in the table.

TABLE 10-3. DEGRADATION ANALYSIS SUMMARY

PARTS ORDERED BY	PART TYPE	NO. OF RATINGS ORDERED	NO. OF RATINGS NOT YET RECEIVED	RANGE OF QUANTITIES PER RATING
GE	Resistors	56	15	8-192
	Capacitors	5	4	9-36
	Diodes	4	3	10-936
	Transistors	9	5	15-366
Adcole Corp.	All	20	3	7-712

SECTION 11

NEW TECHNOLOGIES

Three items are reported as new technologies as a result of development of the passive stabilization system for the NASA Applications Technology Satellite. All three items were developed as part of implementing the Combination Passive Damper. The first item concerns the damper boom angle indicator readout device. The principle on which this device operates was first reported as a new technology in the Fourth Quarterly Progress Report. The information reported here implements that principle.

The second item describes the CPD clutch that is used for transferring either one of the two damper systems of the CPD to the damper boom. The third item discusses the development of a material for providing torsional restraint of the eddy-current damper.

11.1 ANGLE INDICATOR READOUT DEVICE

The encoder in the boom angle indicator provides an angular position readout which is independent of small displacements of a rotating member in relation to a fixed member. Fundamentally, the device is a simple Gray-code encoder which has a slit pattern on a thin disc. The disc is attached to the rotating member (damper boom) that is to be monitored. The disc is shown in Figure 11-1 (GE dwg PR47C 207272). A collimated slit-beam of light either passes through or is interrupted by pattern lines on the disc; the light is detected by photodetectors which are located below the disc. Use of the Gray code pattern provides a digitized readout while minimizing error at the code change point.

For ATS application, it was necessary to devise a readout device capable of $\pm$ 1 degree accuracy within $\pm$ 10 degrees of a zero point and approximately $\pm$10% accuracy between 10 and 50 degrees on either side of zero. The device must provide these accuracies independently of nonrotary motion of the fixed and movable members within constraining limits. It must also operate with high reliability during a large lifetime and over the relatively wide temperature ranges expected in the ATS mission.

The Gray-code encoder is a simple, digital device which inherently meets the reliability and temperature specifications easier than a typical analog device. Ordinarily the code pattern is designed to provide equal accuracy over the entire range. However, the pattern can be readily modified so that the lower accuracy is provided at larger angles in accordance with the requirements of the ATS application. Such a nonlinear device has been designed for this application. The advantage gained as compared with the $\pm$ 1 degree accuracy over the entire range is a decreased number of digital bits and the associated detector channels to provide them.

Nonrotational relative motion can be divided into three types: axial, lateral (or radial) and tilt. In the design application the axial shift can be relatively large, up to $\pm$0.22 inch. However, with a collimated slit light beam, the encoder is inherently insensitive to this shift. Tilt is confined to about 1 degree of arc, since this error projected into the plane of the disc is proportional to the consine of the tilt angle, it will have negligible affect an accuracy.

Lateral or radial motions are significant. The design application permits up to 0.07 inch lateral motion. With the encoder disc size proposed this could result in a readout error of nearly 2 degrees. However, by providing a second, identical code pattern and reading this out as well, the necessary information for lateral shift compensation is provided. This pattern is illustrated in Figure 11-1.

With pure rotational motion about the center of the disc, the light slit and detectors will be along line A. Note that in this case, the coded word on one side of the disc will be identical to the word on the other side.

Line B represents the detector line with the same rotation plus a small lateral displacement. In this case there will be one bit different in the two words as read out from opposite sides of the disc. If the angle is now read as the value at which a nonshifted detector line would just change from one to the other of the indicated code patterns, the assumed value will be within 1 degree of the true angle. Note that this will be the true even at the larger angles even though the Gray code is providing larger, less accurate steps. This is an unnecessary, though interesting dividend.

Having added the additional code pattern and optical pickoff system for lateral shift compensation, a reliability bonus is also achieved. The second code pattern effectively adds a redundancy improvement in reliability. Individual channels can fail in any combination provided that, between the two disc sides, a complete channel set still exists. Of course, in this case, lateral displacement compensation may be lost, but an angle reading with less accuracy is still available.

11.2 CPD CLUTCH MECHANISM

11.2.1 PURPOSE

The diaphragm spring device and the associated clutch arrangement was designed for use in the Combination Passive Damper. The CPD contains two dampers -- an eddy current damper and a hysteresis damper. These dampers are alternately coupled to a single damping boom shaft in orbit to test the relative merits of the two dampers to damp the libratory

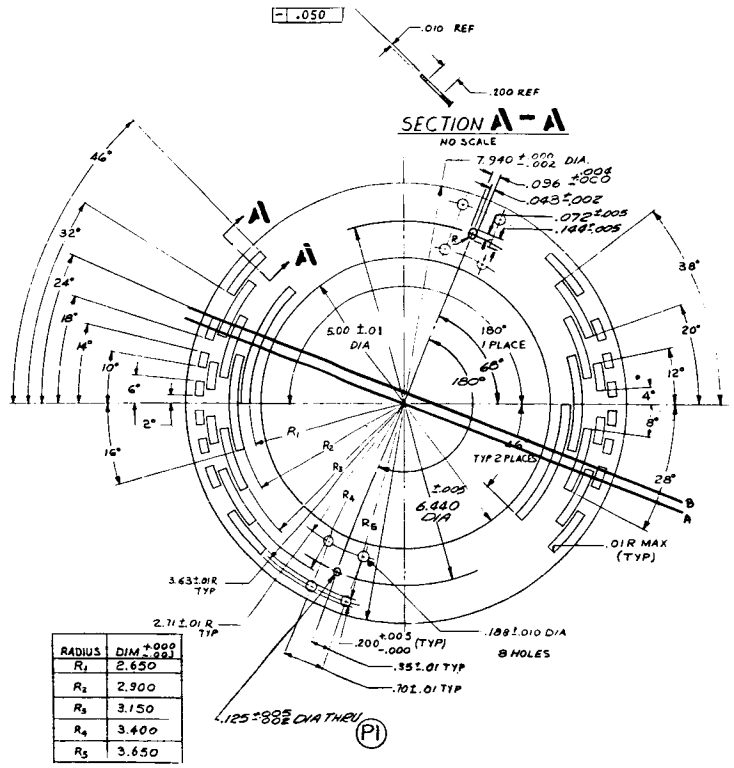

Figure 11-1. Encoder Disc (GE Dwg PR47C207272)

motion of an actual spacecraft. A coupling arrangement free of external forces in all axes (including rotational) was mandatory because of the very small damping forces involved, and also, because of the very weak axial forces produced by the diamagnetic suspension method, no external axial forces were allowed. The requirement that the inoperative damper be completely isolated from the damper boom during test of the other damper was a major factor in the design. The new technology described here was the solution to the problem.

11.2.2 DESCRIPTION (SEE FIGURE 11-2)

The coned diaphragm spring (Figure 11-2, 1) is mounted within a ring (2) centrally located within an integral housing of the output shaft (3). The ring (2) provides a surface about which the spring pivots during "snap through." The integral housing forms an upper clutch face (4) and a lower clutch face (5). Shaft one (6) contains a circular V-groove (7) which matches the lower clutch face (5). Shaft two (8) contains a circular V-grove (9) which matches the upper clutch face (4). The actuator shaft (10) is positioned through the open center of the diaphragm spring (1) and faces (11) and (12) form a spool on the end of the actuator shaft which contact the surface of the diaphragm spring during actuation only.

The coned diaphragm spring (1) has two stable positions, and is used as an over-center toggle. The diaphragm spring is coned so that it exerts a force on shaft one (6) such that V-groove (7) contacts the lower clutch face (5) of the output shaft (3). The mating of these surfaces under the compressive load provided by the diaphragm spring (1) produces a friction coupling torque which allows shaft one (6) to drive the output shaft (3) rotationally with no restraining external force present. The V-shape of the engaging surfaces ensures that the mating shafts will be properly aligned axially and radially.

In transferring the output shaft (4) to shift two (8), the actuator (10) is displaced linearly upward. This displacement causes spool face (11) to contact the surface of the diaphragm spring, driving it flat and then over-center so that the diaphragm spring (1) assumes a conical shape in the other direction as shown in Figure 11-2c. The actuator (10) is further displaced such that the upper face (12) and the lower face (11) of the spool are clear of the

the spring, thereby eliminating any external forces which would retard rotation of the output shaft (3). With the diaphragm spring (1) coned in the position shown in Figure 11-2c, it forces clutch surfaces (4) and (9) together which couples shaft two (8) to the output shaft (3), resulting in the CPD being changed to the Hysteresis Damper Mode.

Reversing the direction of linear displacement of actuator (10) will shift the diaphragm spring (1) back to the position shown in Figure 11-2b, where shaft one (6) is again coupled to the output shaft (3). Note in Figure 11-2b and c, that the inoperative shaft has a nominal clearance to the output shaft V-surface. Because of this clearance which is necessary to isolate the inoperative shaft, the output shaft (9) is displaced axially this same distance during switchover.

11.2.3 FEATURES OF DESIGN:

The novel features of the new technology are as follows:

a. The overall clutch mechanism provides in a compact package a dual coupling method which eliminates all external forces that would tend to retard rotation or cause axial displacement. When the clutch is engaged in one direction, it is essentially floating and is completely free from the actuator and the disengaged component parts.

b. The fluted configuration (Figure 11-2a) of the diaphragm spring lends itself to a wide range of load-deflection combinations which are readily predictable. The spring, in combination with the pivot ring, has the properties of an over-center toggle device but with fewer parts. The spring has a larger "throw" than a plain Belleville washer plus the advantage of having essentially equal force/deflection characteristics in each of the two operating directions. It also occupies less space than other similar over-center devices. The spring is formed in a flat (on-center) position, and is coned at assembly by the fact that the diameter of the holding ring

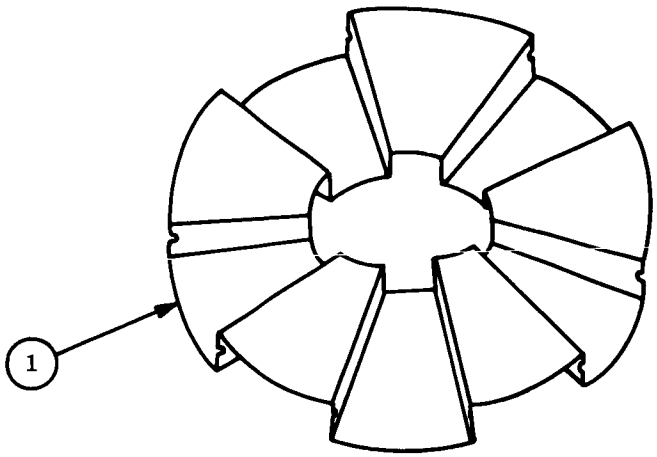

(a) DIAPHRAGM SPRING

1. Diaphram spring
2. Ring
3. Output shaft
4. Upper clutch face
5. Lower clutch face
6. Shaft one
7. Circular V-groove
8. Shaft two
9. Circular V-groove
10. Actuator
11. Lower spool face
12. Upper spool face

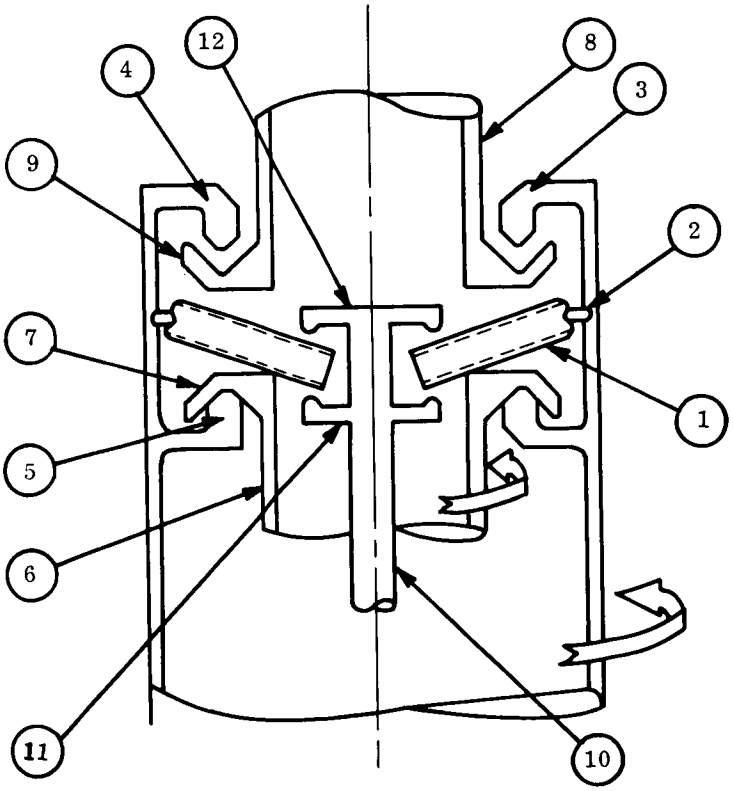

(b) EDDY-CURRENT DAMPER MODE

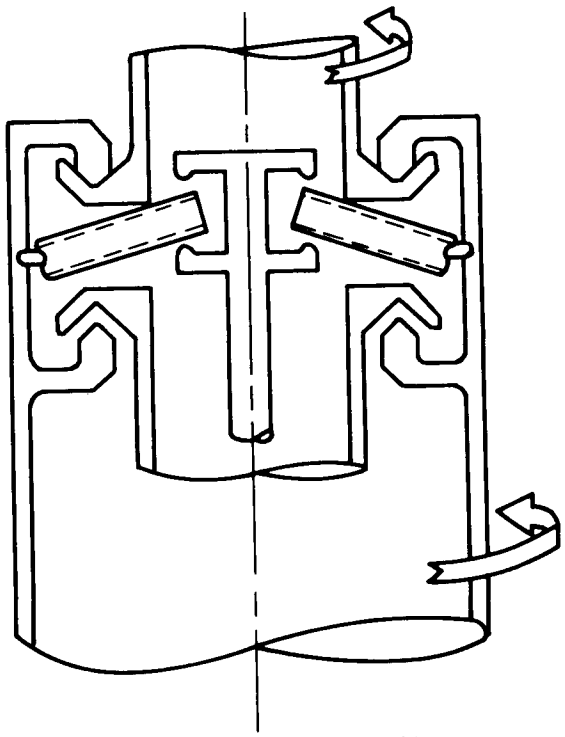

(c) HYSTERESIS DAMPER MODE

Figure 11-2. CPD Clutch Mechanism

is smaller than the free diameter of the flat spring. The deformation of the spring during coning and during subsequent over-center actuations is accounted for through simple bending of the sides and faces of the flutes. Stresses and loads resulting from such bending are readily calculable and any desired load-deflection characteristics can be easily obtained. Load-deflection characteristics of other similar devices (i.e., Belleville washer and variations thereof) are more restrictive and less amenable to accurate prediction. Another advantage of the fluted configuration of the spring is that it can be manufactured without resorting to exotic manufacturing techniques.

c. The self-centering feature of the V-groove clutch surfaces as forced together by the spring is an integral advantage of the overall design. The V-groove arrangement ensures that the mating parts will repeatedly engage in the concentric position and with parallel faces for any location of clamping force within the engagement circle.

SECTION 12

GLOSSARY

The following is a list of abbreviations and definitions for terms used throughout this report:

ADTF	Advanced Damping Test Fixture (used for CPD testing)
ATS-A	Medium Altitude Gravity Gradient Experiment (6000-nautical mile orbit flight)
ATS-D/E	Synchronous Altitude Gravity Gradient Experiment (24-hour orbit flight)
CPD	Combination Passive Damper
Crab Angle	Out-of-orbit angle flight caused by changes in X-rod angle
DME	Dynamic Mission Equivalent (Accelerated Functional Program)
GE-MSD	General Electric Company Missile and Space Division
GGS/ATS	Gravity Gradient System/Applications Technology Satellite
HAC	Hughes Aircraft Company
ITPB	Integrated Test Program Board
Local Vertical	Imaginary line extending from the satellite center of mass to the center of mass of the earth
LOFF	Low Order Force Fixture (used for CPD testing)
MTBF	Mean Time Before Failure
MTTF	Mean Time to Failure
PCU	Power Control Unit
PIR	Program Information Request/Release, GE documentation
SAS	Solar Aspect Sensor
Scissoring	Changing the angle included between the primary booms in a manner that maintains a symmetrical configuration about the satellite yaw axis
STEM	Storable Tubular Extendable Member
Stiction Torque	That amount of torque required to overcome the initial effects of friction
SVA Fixture	Shock and Vibration Attachment Fixture
Thermal Twang	Sudden thermal bending which the booms experience in passing from a region of total eclipse into a region of continuous sunlight or vice versa
TR	Torsional restraint
TVCS	TV Camera Subsystem

APPENDIXES

APPENDIX A

FRACTURE ANALYSIS OF BERYLCO 25 OVERLAP TUBES

This appendix presents data gathered during metallurgical analysis subsequent to the reverse wind failure (discussed under Rod 1) and the cracking at the drum support roller (discussed underRod 2) that are described in Section 3.3.1 of this report. The analysis was originally published in GE PIR 4493-028, dated 24 November 1965. With regard to the statements made about Rod 2, it should be pointed out that the possibility that fatigue crack occurred first (due to cycling of the highly stressed dimpled area during vibration testing).

A.1 PART DESCRIPTION

Two 1/2 tubes with 100 degree overlap were fabricated from 0.001 x 2 inch BeCu foil. The specific chemistry of the alloy was:

Be = 1.80 - 2.05%
Co = 0.20 - 0.30%
Cu = Balance

The two lengths of tubing failed by tearing during the operation of the deployment mechanism supplied by an outside vendor. The lengths of tubing were sent to the laboratory for an analysis of the failures. For purposes of identification, the rods are designated as Rod 1 and 2,respectively.

A.2 DESCRIPTION OF THE FAILURES

A.2.1 ROD 1

The overall view of the failed section is shown in Figures A-1 thru A-4. Figure A-1 is a

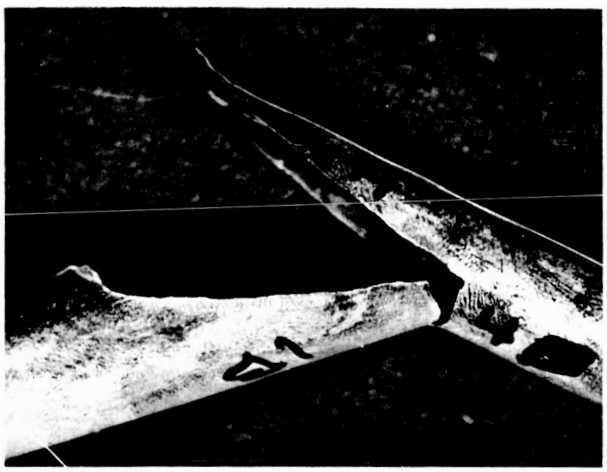

Figure A-1. Overall View of Failure Section Rod 1 (Magnification 1.5X)

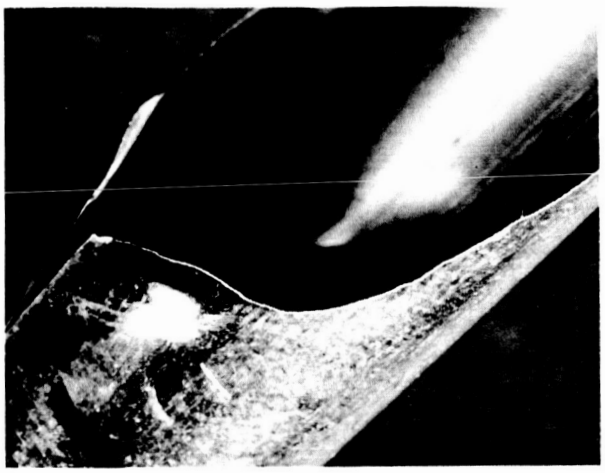

Figure A-2. Edges of Rod 2 Showing Origin of Failure (Magnification 4X)

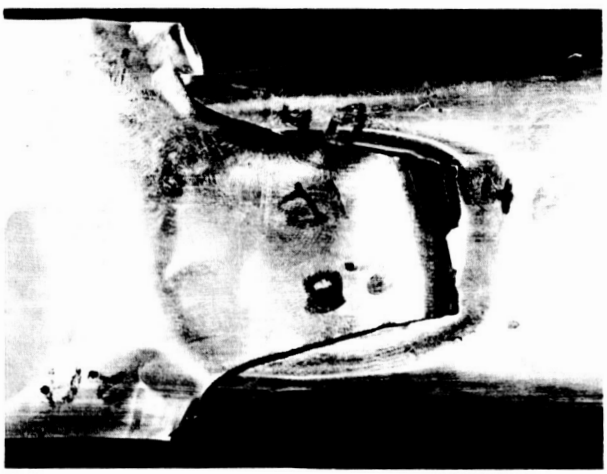

Figure A-3. View of Fractured Area, Tube Flattened Out (Magnification 1.5X)

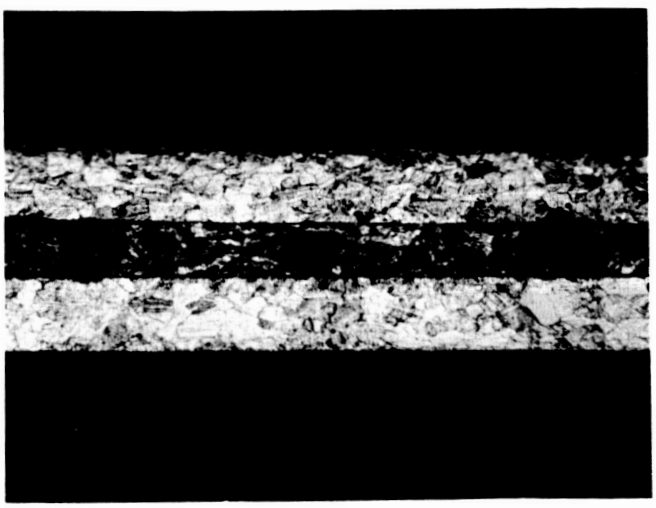

Figure A-4. Photomicrograph Along Edge of Tube Cross-Section (Magnification 250X)

general view of the tube, opened up to show the extent of the tear. Figure A-2 is an enlargement of the area in which the tear was initiated. Figure A-3 is a view of the failed area after the tube has been flattened out. Examination of the failed area shows that the tube was torn along the two opposite edges and that the tears propagated symetrically toward the center of the tube (See Figures A-2 and A-3). The edges of the tubes were examined for evidence of cracking; however, none was observed. A cross-sectional photomicrograph was taken along the edges of the failed tube. The microstructure was considered to be normal for this alloy. The structure is shown in Figure A-4.

A.2.2 ROD 2

This rod failed by tearing from a point approximately 1/2 inch from the edge. At the point of initiation, the foil is dimpled. At this point, the tear progressed in two directions (See Figure A-5). The edge of the tube was examined for evidence of edge cracking. It was observed that several cracks were present along the edges. One such typical crack is shown in Figure A-6. A photomicrograph was taken in the region of one of these cracks and is shown in Figure A-7. Examination of this micrograph shows that the nature of the fracture is transgranular from the edge to about the midpoint of the micrograph. This is considered to be the extent of damage due to the initial tear. From that point on, the nature of the failure is intergranular; this is characteristic of the fatigue mode of failure and is attributed to cycling of the material due to handling.

A.3 CONCLUSIONS

The fracture surfaces indicated an origin of failure in Rod 1, at two points on opposite sides of the rod. The nature of the tear and the symmetry of the tears indicate that the material was subjected to an equal stress on both edges.

The fracture surfaces indicated an origin of fracture in Rod 2 at a point 1/2 inch from the edge of the tube. At this point, the material contained a dimple approximately 1/4 inch in diameter. It is concluded that this dimple represented a point of overload. The material

Figure A-5. Area Showing Origin of Failure (Magnification 4X)

Figure A-6. Edge of Tube Overlap Showing Cracks Along Edge (Magnification 25X)

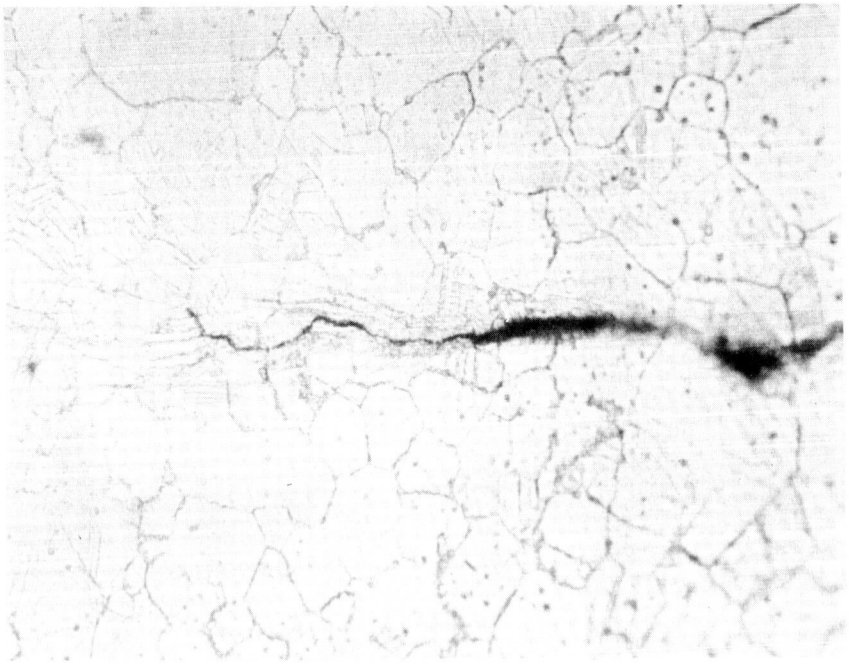

Figure A-7. Photomicrograph Taken in Region of Crack Shown in Figure A-6

failed at this point and the tear progressed in two directions from that point.

The microstructure of this alloy appears normal according to thermal treatments and manufacturer's specifications. After examining both of the failed rods, it can be concluded that no material or manufacturing defect was associated with the origin and that the tubes were apparently overstressed in the area of primary failure.

APPENDIX B

COMPUTER PRINTOUT DATA FROM SAS SYSTEMS TESTS

12 October 1965

LOCAL TIME	TRUE A	TRUE B	MEAS A	MEAS B	ERROR A	ERROR B
13,278	-7.574	8.653	-7,436	8.447	0.139	-0,206
13,311	-8.076	8.663	-7,947	8.453	0.129	-0,210
13,345	-8.577	8.673	-8,459	8.459	0.119	-0,214
13,378	-9.079	8.684	-8,970	8.465	0.109	-0,219
13,411	-9.580	8.695	-9,480	8.471	0.100	-0,224
13,445	-10.082	8.707	-9,991	8.478	0.091	-0,229
13,478	-10.583	8.719	-10,501	8.485	0.082	-0,234
13,511	-11.085	8.733	-11,011	8.493	0.074	-0,240
13,545	-11.586	8.746	-11,520	8.501	0.066	-0,245
13,578	-12.087	8.761	-12,029	8.509	0.058	-0,251
13,611	-12.589	8.776	-12,538	8.518	0.051	-0,258
13,645	-13.090	8.791	-13,047	8.527	0.044	-0,264
13,678	-13.592	8.808	-13,555	8.537	0.037	-0,271
13,711	-14.093	8.825	-14,062	8.547	0.031	-0,278
13,745	-14.594	8.842	-14,570	8.557	0.025	-0,285
13,778	-15.096	8.861	-15,076	8.568	0.019	-0,292
13,811	-15.597	8.880	-15,583	8.579	0.014	-0,300
13,845	-16.099	8.899	-16,089	8.591	0.010	-0,308
13,878	-16.600	8.919	-16,594	8.603	0.006	-0,316
13,911	-17.101	8.941	-17,099	8.616	0.002	-0,325
13,945	-17.603	8.962	-17,604	8.629	-0.001	-0,334
13,978	-18.104	8.985	-18,121	9.164	-0.017	0,179
14,011	-18.605	9.008	-18,625	9.179	-0.019	0,171
14,045	-19.107	9.032	-19,128	9.194	-0.021	0,162
14,078	-19.608	9.056	-19,631	9.210	-0.023	0,153
14,111	-20.110	9.082	-20,134	9.226	-0.024	0,144
14,145	-20.611	9.108	-20,636	9.242	-0.025	0,135
14,178	-21.112	9.135	-21,137	9.260	-0.025	0,125
14,211	-21.614	9.162	-21,638	9.277	-0.025	0,115
14,245	-22.115	9.191	-22,139	9.295	-0.024	0,105
14,278	-22.616	9.220	-22,639	9.314	-0.023	0,095
14,311	-23.117	9.250	-23,138	9.333	-0.021	0,084
14,345	-23.618	9.281	-23,637	9.353	-0.019	0,073
14,378	-24.120	9.312	-24,135	9.374	-0.016	0,061
14,411	-24.621	9.345	-24,633	9.395	-0.012	0,050
14,445	-25.122	9.378	-25,130	9.416	-0.008	0,038
14,478	-25.623	9.413	-25,627	9.438	-0.004	0,025
14,511	-26.125	9.448	-26,123	9.461	0.001	0,013
14,545	-26.626	9.484	-26,619	9.484	0.007	0,000
14,578	-27.127	9.521	-27,114	9.508	0.013	-0,013
14,611	-27.628	9.560	-27,609	9.533	0.019	-0,027
14,645	-28.130	9.599	-28,103	9.558	0.026	-0,040
14,678	-28.631	9.639	-28,597	9.584	0.034	-0,055
14,711	-29.132	9.680	-29,090	9.611	0.042	-0,069
14,745	-29.633	9.722	-29,583	9.638	0.050	-0,084

12 October 1965 (Cont'd)

LOCAL TIME	TRUE A	TRUE B	MEAS A	MEAS B	ERROR A	ERROR B
14,778	-30.134	9.765	-30,075	9.666	0.059	-0,099
14,811	-30.636	9.809	-30,567	9.695	0.069	-0,115
14,845	-31.137	9.855	-31,058	9.724	0.078	-0,131
14,878	-31.638	9.901	-31,549	9.755	0.089	-0,147
14,911	-32.139	9.949	-32,039	9.786	0.100	-0,163
14,945	-32.640	9.998	-32,529	9.817	0.111	-0,181
14,978	-33.141	10.048	-33,019	9,850	0.122	-0,198
15,011	-33.642	10.099	-33,508	9,884	0.134	-0,216
15,045	-34.144	10.152	-33,997	9.918	0.147	-0,234
15,078	-34.645	10.206	-34,485	9,953	0.160	-0,253
15,111	-35.146	10.261	-34,973	9,989	0.173	-0,272
15,145	-35.647	10.318	-35,461	10,026	0.186	-0,291
15,178	-36.148	10.375	-35,948	10.064	0.200	-0,311
15,211	-36,649	10.435	-36,462	10.678	0.187	0,243
15,245	-37.150	10.496	-36,950	10.720	0.201	0.225
15,278	-37.652	10.558	-37,436	10.764	0,215	0,206
15,311	-38.153	10.622	-37,923	10.808	0.230	0,187
15,345	-38,654	10.687	-38,410	10,854	0.245	0,167
15,378	-39.155	10.754	-38,896	10.901	0.259	0,147
15,411	-39.656	10.823	-39,382	10.949	0.274	0,126
15,445	-40.157	10.893	-39,868	10.998	0.289	0,105
15,478	-40.658	10.965	-40,354	11.049	0.305	0,084
15,511	-41.160	11.039	-40,840	11.101	0.320	0,062
15,545	-41.661	11.115	-41,326	11.154	0.335	0,039
15,578	-42.162	11.193	-41,811	11.209	0.350	0,016
15,611	-42.663	11.272	-42,297	11.266	0.366	-0,007
15,645	-43.164	11.354	-42,783	11.323	0.381	-0,031
15,678	-43.665	11.438	-43,269	11.383	0.396	-0,055
15,711	-44,166	11.524	-44,242	11.507	-0.076	-0,017
15,745	-44.667	11.612	-44,242	11.507	0.425	-0,105
15,778	-45.168	11.702	-45,216	11,638	-0.048	-0,064
15,811	-45.669	11.795	-45,703	11.707	-0.034	-0,088
15,845	-46.170	11.890	-46,191	11.777	-0.021	-0,113
15,878	-46.671	11.987	-46,679	11.849	-0.008	-0,138
15,911	-47.172	12.087	-47,168	11,924	0.004	-0,163
15,945	-47.673	12.190	-47,658	12.001	0.015	-0,189
15,978	-48.174	12.296	-48,148	12.080	0.026	-0,215
16,011	-48.675	12.404	-48,638	12.162	0,036	-0,242
16,045	-49.176	12.515	-49,169	12.904	0.006	0,389
16,078	-49.677	12.629	-49,662	12,995	0.014	0,366
16,111	-50.177	12.747	-50,156	13.090	0.021	0,343
16,145	-50.678	12.868	-50,651	13,187	0.027	0,320
16,178	-51.179	12.992	-51,147	13.288	0.032	0,296
16,211	-51.680	13.119	-51,644	13.392	0,036	0,273
16,245	-52.181	13.250	-52,143	13,500	0.038	0,249

13 October 1965

No. 1

LOCAL TIME	TRUE A	TRUE B	MEAS A	MEAS B	ERROR A	ERROR B
8.500	64.204	18.485	64,305	17.633	0.101	-0.852
8.533	63.704	18.198	63,730	17.344	0.026	-0.854
8.567	63.203	17.921	63,162	17.071	-0.041	-0.850
8.600	62.702	17.654	62,599	16.812	-0.103	-0.842
8.633	62.202	17.396	62,042	16.567	-0.160	-0.829
8.667	61.701	17.147	61,490	16.334	-0.211	-0.814
8.700	61.200	16.907	60,943	16.112	-0.257	-0.795
8.733	60.700	16.674	60,943	16.112	0.244	-0.562
8.767	60.199	16.450	59,863	15.699	-0.336	-0.750
8.800	59.698	16.232	59,863	15.699	0.164	-0.533
8.833	59.198	16.022	59,328	15.507	0.131	-0.515
8.867	58.697	15.818	58,798	15.323	0.101	-0.495
8.900	58.196	15.621	58,270	15.147	0.074	-0.474
8.933	57.695	15.430	57,746	14.978	0.051	-0.452
8.967	57.195	15.245	57,225	14.816	0.031	-0.429
9.000	56.694	15.066	56,707	14.661	0.013	-0.405
9.033	56.193	14.892	56,191	14.512	-0.002	-0.380
9.067	55.692	14.723	55,678	14.368	-0.014	-0.354
9.100	55.191	14.559	55,167	14.230	-0.024	-0.329
9.133	54.691	14.400	54,659	14.097	-0.032	-0.303
9.167	54.190	14.245	54,152	13.969	-0.038	-0.276
9.200	53.689	14.095	53,647	13.845	-0.042	-0.250
9.233	53.188	13.950	53,144	13.726	-0.044	-0.224
9.267	52.687	13.808	52,643	13.611	-0.045	-0.197
9.300	52.186	13.671	52,143	13.500	-0.044	-0.171
9.333	51.685	13.537	51,644	13.392	-0.041	-0.145
9.367	51.185	13.407	51,147	13.288	-0.038	-0.119
9.400	50.684	13.280	50,651	13.187	-0.033	-0.093
9.433	50.183	13.157	50,156	13.090	-0.027	-0.067
9.467	49.682	13.037	49,622	12.333	-0.059	-0.704
9.500	49.182	12.922	49,130	12.246	-0.052	-0.676
9.533	48.681	12.809	48,638	12.162	-0.043	-0.647
9.567	48.180	12.698	48,148	12.080	-0.032	-0.618
9.600	47.679	12.591	47,658	12.001	-0.022	-0.590
9.633	47.178	12.486	47,168	11.924	-0.010	-0.562
9.667	46.677	12.384	46,679	11.849	0.002	-0.535
9.700	46.176	12.285	46,191	11.777	0.015	-0.508
9.733	45.675	12.188	45,703	11.707	0.028	-0.481
9.767	45.174	12.093	45,216	11.638	0.041	-0.455
9.800	44.673	12.001	44,729	11.572	0.055	-0.430
9.833	44.172	11.912	44,242	11.507	0.070	-0.405
9.867	43.671	11.824	43,756	11.444	0.084	-0.380
9.900	43.170	11.739	43,269	11.383	0.099	-0.356
9.933	42.669	11.656	42,783	11.323	0.114	-0.333
9.967	42.168	11.575	42,297	11.266	0.129	-0.309

13 October 1965

No. 1 (Cont'd)

LOCAL TIME	TRUE A	TRUE B	MEAS A	MEAS B	ERROR A	ERROR B
10.000	41.667	11.496	41,811	11.209	0.144	-0.287
10.033	41.166	11.419	41,326	11.154	0.159	-0.264
10.067	40.665	11.344	40,840	11.101	0.174	-0.243
10.100	40.164	11.270	39,868	10.998	-0.296	-0.272
10.133	39.663	11.199	39,868	10.998	0.205	-0.200
10.167	39.162	11.129	38,896	10.901	-0.266	-0.228
10.200	38.661	11.061	38,410	10.854	-0.252	-0.207
10.233	38.160	10.994	37,923	10.808	-0.237	-0.186
10.267	37.659	10.929	37,923	10.808	0.264	-0.121
10.300	37.158	10.866	37,923	10.808	0.765	-0.057
10.333	36.657	10.804	37,923	10.808	1.266	0.004
10.367	36.156	10.744	37,923	10.808	1.768	0.065
10.400	35.654	10.685	37,923	10.808	2.269	0.123
10.433	35.153	10.627	37,923	10.808	2.770	0.181
10.467	34.652	10.571	37,923	10.808	3.271	0.237

13 October 1965
No. 2

LOCAL TIME	TRUE A	TRUE B	MEAS A	MEAS B	ERROR A	ERROR B
10,336	36.616	10.798	36,452	10.678	-0.154	-0,120
10,369	36.115	10.738	35,975	10.637	-0.140	-0,101
10,403	35.614	10.679	35,487	10.597	-0.126	-0,082
10,436	35.112	10.622	34,999	10.558	-0.113	-0,064
10,469	34.611	10.566	34,511	10.520	-0.100	-0,046
10,503	34.110	10.511	34,022	10.482	-0.088	-0,029
10,536	33.609	10.458	33,533	10.446	-0.076	-0,012
10,569	33.107	10.406	33,044	10.411	-0.064	0,005
10,603	32.606	10.355	32,554	10.376	-0.053	0,021
10,636	32.105	10.306	32,063	10.342	-0.042	0,037
10,669	31.604	10.257	31,573	10.310	-0.031	0,052
10,703	31.102	10.210	31,058	9,724	-0.044	-0,486
10,736	30.601	10.164	30,567	9.695	-0.034	-0,470
10,769	30.100	10.120	30,075	9.666	-0.025	-0,454
10,803	29.599	10.076	29,583	9.638	-0.016	-0,438
10,836	29.097	10.033	29,090	9.611	-0.007	-0,423
10,869	28.596	9.992	28,597	9.584	0.001	-0,408
10,903	28.095	9.951	28,103	9.558	0.009	-0,393
10,936	27.593	9.912	27,609	9.533	0.016	-0,379
10,969	27.092	9.873	27,114	9.508	0.022	-0,365
11,003	26.591	9.836	26,619	9,484	0.028	-0,352
11,036	26.089	9.799	26,123	9.461	0.034	-0,338
11,069	25.588	9.764	25,627	9.438	0.039	-0,326
11,103	25.087	9.729	25,130	9.416	0.044	-0,313
11,136	24.585	9.696	24,633	9.395	0.048	-0,301
11,169	24.084	9.663	24,135	9.374	0.051	-0,289
11,203	23.583	9.631	23,637	9.353	0.054	-0,278
11,236	23.081	9.600	23,138	9.333	0.057	-0,267
11,269	22.580	9.570	22,639	9.314	0.059	-0,256
11,303	22.079	9.540	22,139	9.295	0.060	-0,245
11,336	21.578	9.512	21,638	9.277	0.060	-0,235
11,369	21.076	9.484	21,137	9.260	0.061	-0,225
11,403	20.575	9.458	20,636	9.242	0.061	-0,215
11,436	20.074	9.432	20,134	9.226	0.060	-0,206
11,469	19.572	9.406	19,631	9.210	0.059	-0,197
11,503	19.071	9.382	19,128	9.194	0.057	-0,188
11,536	18.570	9.358	18,625	9.179	0.055	-0,179
11,569	18.068	9.335	18,121	9.164	0.053	-0,171
11,603	17.567	9.313	17,616	9.150	0.049	-0,163
11,636	17.066	9.291	17,111	9.136	0.046	-0,155
11,669	16.564	9.271	16,606	9.123	0.042	-0,148
11,703	16.063	9.251	16,100	9.110	0.037	-0,141
11,736	15.561	9.231	15,594	9.098	0.032	-0,134
11,769	15.060	9.213	15,087	9.086	0.027	-0,127
11,803	14.559	9.195	14,580	9.074	0.021	-0,120

13 October 1965
No. 2 (Cont'd)

LOCAL TIME	TRUE A	TRUE B	MEAS A	MEAS B	ERROR A	ERROR B
11,836	14.057	9.178	14,072	9.063	0.015	-0,114
11,869	13.556	9.161	13,564	9.053	0.009	-0,108
11,903	13.054	9.145	13,056	9.043	0.002	-0,103
11,936	12.553	9.130	12,547	9.033	-0.006	-0,097
11,969	12.052	9.115	12,038	9.023	-0.014	-0,092
12,003	11.550	9.102	11,529	9.015	-0.022	-0,087
12,036	11.049	9.088	11,019	9.006	-0,030	-0,082
12,069	10.547	9.076	10,509	8.998	-0.039	-0,078
12,103	10.046	9.064	9,998	8.990	-0.048	-0,073
12,136	9.545	9.052	9,487	8.983	-0.057	-0,069
12,169	9.043	9.042	8,976	8,976	-0.067	-0,066
12,203	8.542	9.032	8,465	8.970	-0.077	-0,062
12,236	8.040	9.022	7,953	8.964	-0.087	-0,059
12,269	7.539	9.013	7,441	8.958	-0.098	-0,056
12,303	7.037	9.005	6,929	8.953	-0.108	-0,053
12,336	6.536	8.998	6,417	8.948	-0.119	-0,051
12,369	6.034	8.991	5,904	8.943	-0.130	-0,048
12,403	5.533	8.985	5,904	8.943	0.371	-0,042
12,436	5.032	8.979	4,878	8.935	-0.153	-0,044
12,469	4.530	8.974	4,878	8.935	0.348	-0,039
12,503	4.029	8.970	3,852	8,929	-0.177	-0,041
12,536	3.527	8.966	3,852	8.929	0.325	-0,037
12,569	3.026	8.962	3,339	8.926	0.313	-0,036
12,603	2.524	8.960	2,825	8.924	0.301	-0,036
12,636	2.023	8.958	1,798	8.920	-0.225	-0,037
12,669	1.521	8.956	1,798	8.920	0.277	-0,036
12,703	1.020	8.955	1,284	8.919	0.264	-0,036
12,736	0.519	8.955	0,771	8.919	0.252	-0,036
12,769	0.017	8.955	-0,257	8.918	-0.274	-0,037
12,803	-0.484	8.956	-0,257	8.918	0.228	-0,038
12,836	-0.986	8.957	-0,771	8.919	0.215	-0,039
12,869	-1.487	8.959	-1,284	8.919	0.203	-0,040
12,903	-1.989	8.962	-1,798	8.920	0.191	-0,041
12,936	-2.490	8.965	-2,312	8.922	0.179	-0,043
12,969	-2.992	8.969	-2,825	8.924	0.166	-0,045
13,003	-3.493	8.973	-3,339	8.926	0.154	-0,047
13,036	-3.995	8.978	-3,852	8.929	0.143	-0,049
13,069	-4.496	8.984	-4,365	8.932	0.131	-0,052
13,103	-4.997	8.990	-4,878	8.935	0.119	-0,055
13,136	-5.499	8.997	-5,391	8.939	0.108	-0,058
13,169	-6.000	9.004	-5,904	8.943	0.096	-0,061
13,203	-6.502	9.012	-6,417	8.948	0.085	-0,065
13,236	-7.003	9.021	-6,929	8.953	0.074	-0,068
13,269	-7.505	9.030	-7,441	8.958	0.064	-0,072
13,303	-8.006	9.040	-7,953	8.964	0.053	-0,076

13 October 1965
No. 2 (Cont'd)

LOCAL TIME	TRUE A	TRUE B	MEAS A	MEAS B	ERROR A	ERROR B
13,336	-8.508	9.050	=8,465	8.970	0.043	=0,080
13,369	-9.010	9.061	=8,976	8.976	0.034	=0,085
13,403	-9.511	9.073	=9,487	8.983	0.024	=0,090
13,436	=10.013	9.085	=9,998	8.990	0.015	=0,095
13,469	=10.514	9.098	-10,509	8.998	0.006	=0,100
13,503	=11.016	9.112	-11,019	9.006	-0.003	=0,105
13,536	=11.517	9.126	-11,529	9.015	-0.011	=0,111
13,569	=12.019	9.141	-12,038	9.023	-0.019	=0,117
13,603	-12.520	9.156	-12,547	9.033	-0.027	=0,123
13,636	=13.022	9.172	-13,056	9.043	-0.034	=0,130
13,669	=13.523	9.189	-13,564	9.053	-0.041	=0,137
13,703	=14.025	9.207	-14,072	9.063	-0.048	=0,144
13,736	=14.526	9.225	-14,580	9.074	-0.054	=0,151
13,769	=15.027	9.244	-14,580	9.074	0.447	=0,170
13,803	=15.529	9.264	-15,594	9.098	-0.065	=0,166
13,836	=16.030	9.284	-16,100	9.110	-0.070	=0,174
13,869	=16.532	9.305	-16,606	9.123	-0.074	=0,183
13,903	=17.033	9.327	-16,606	9.123	0.427	=0,204
13,936	=17.535	9.350	-17,111	9.136	0.423	-0,214
13,969	=18,036	9.373	-18,121	9,164	-0,085	=0,209
14,003	=18.538	9.397	-18,121	9.164	0.417	=0,233
14,036	=19.039	9.422	-18,625	9,179	0.414	=0,243
14,069	=19.540	9.448	-19,631	9.210	-0.091	=0,238
14,103	=20.042	9.474	=19,631	9.210	0.411	=0,264
14,136	=20.543	9.501	-20,134	9.226	0.409	=0,276
14,169	=21.045	9.529	-20,651	9,769	0.393	0,239
14,203	=21.546	9.558	-21,153	9.787	0.393	0,229
14,236	=22.047	9.588	=21,655	9.805	0.393	0,218
14,269	=22.549	9.618	=22,656	9.844	-0.107	0.226
14,303	=23.050	9.650	=22,656	9.844	0.395	0,195
14,336	=23.551	9.682	=23,655	9.886	-0.104	0,204
14,369	=24.052	9.715	=23,655	9,886	0.398	0,171
14,403	=24.554	9.749	=24,652	9.929	-0.098	0,180
14,436	=25.055	9.784	=24,652	9.929	0.403	0,145
14,469	=25.556	9.820	=25,149	9.952	0.407	0,132
14,503	=26.058	9.857	=25,647	9,975	0.411	0,119
14,536	=26.559	9.894	=26,143	9,999	0.416	0,105
14,569	=27.060	9.933	=26,639	10.024	0.421	0,091
14,603	=27.561	9.973	=27,630	10.075	-0.068	0,103
14,636	=28.063	10.014	=28,124	10.102	-0.062	0,089
14,669	=28.564	10.055	=28,618	10.130	-0.054	0,074
14,703	=29.065	10.098	=28,618	10.130	0.447	0,031
14,736	=29.567	10.142	=29,112	10.158	0.454	0,015
14,769	=30.068	10.187	=30,098	10,216	=0,030	0,029
14,803	=30.569	10.234	=30,590	10.247	-0.021	0,013

13 October 1965
No. 2 (Cont'd)

LOCAL TIME	TRUE A	TRUE B	MEAS A	MEAS B	ERROR A	ERROR B
14,836	-31.070	10.281	-30,590	10.247	0.480	-0,035
14,869	-31.571	10.330	-31,573	10.310	-0.001	-0,020
14,903	-32.073	10.379	-32,063	10.342	0.009	-0,037
14,936	-32.574	10.430	-32,554	10.376	0.020	-0,054
14,969	-33.075	10.483	-33,044	10.411	0.032	-0,072
15,003	-33.576	10.536	-33,533	10.446	0.043	-0,090
15,036	-34.077	10.591	-34,022	10.482	0.055	-0,109
15,069	-34.579	10.647	-34,511	10.520	0.068	-0,128
15,103	-35.080	10.705	-34,999	10.558	0.081	-0,147
15,136	-35.581	10.764	-35,487	10.597	0.094	-0,167
15,169	-36.082	10.824	-35,975	10.637	0.107	-0,187
15,203	-36.583	10.886	-36,462	10.678	0.121	-0,208
15,236	-37.084	10.950	-36,950	10.720	0.135	-0,229
15,269	-37.586	11.015	-37,436	10.764	0.149	-0,251
15,303	-38.087	11.081	-37,923	10.808	0.164	-0,273
15,336	-38.588	11.150	-38,440	11.438	0.149	0,288
15,369	-39.090	11.220	-39,413	11.538	-0.323	0,318
15,403	-39.591	11.292	-39,899	11.590	-0.309	0,298
15,436	-40.092	11.365	-39,899	11.590	0.193	0,224
15,469	-40.593	11.441	-40,386	11.643	0.207	0,202
15,503	-41.094	11.518	-40,872	11.698	0.222	0,180
15,536	-41.595	11.597	-41,358	11.754	0.237	0,157
15,569	-42.096	11.678	-41,844	11.812	0.252	0,134
15,603	-42.597	11.761	-42,331	11.871	0.267	0,110
15,636	-43.099	11.846	-42,817	11.932	0.282	0,086
15,669	-43.600	11.934	-43,303	11.995	0.296	0,061
15,703	-44.101	12.023	-44,277	12.125	-0.176	0,102
15,736	-44.602	12.115	-44,277	12.125	0.325	0,010
15,769	-45.103	12.209	-44,764	12.194	0.339	-0,016
15,803	-45.604	12.306	-45,252	12.264	0.352	-0,043
15,836	-46.105	12.405	-46,228	12.410	-0.123	0,005
15,869	-46.606	12.507	-46,228	12.410	0.378	-0,097
15,903	-47.107	12,611	-46,716	12.486	0.390	-0,125
15,936	-47.608	12.719	-47,206	12.565	0.402	-0,154
15,969	-48.109	12.829	-48,186	12.729	-0.077	-0,099
16,003	-48.610	12.942	-48,186	12.729	0.424	-0,212
16,036	-49.111	13.058	-48,677	12.815	0.434	-0,242
16,069	-49.612	13.177	-49,652	12.995	-0.050	-0,181
16,103	-50.113	13.299	-50,156	13.090	-0.043	-0,209
16,136	-50.614	13.425	-50,156	13.090	0.458	-0,335
16,169	-51.115	13.554	-51,147	13.288	-0.032	-0,266
16,203	-51.616	13.687	-51,644	13.392	-0.029	-0,295
16,236	-52.117	13.824	-52,143	13.500	-0.026	-0,324
16,269	-52.617	13.964	-52,188	14.187	0.430	0,222
16,303	-53.118	14.109	-52,688	14.303	0.430	0,195

13 October 1965
No. 2 (Cont'd)

LOCAL TIME	TRUE A	TRUE B	MEAS A	MEAS B	ERROR A	ERROR B
16,336	-53.619	14.256	-53,694	14.550	-0.075	0,293
16,369	-54.119	14.409	-54,199	14.679	-0,080	0,270
16.403	-54.620	14.567	-54,199	14.679	0.421	0,113
16,436	-55.121	14.729	-55,216	14.954	-0,095	0,225
16.469	-55.622	14.896	-55,216	14.954	0,406	0,058
16,503	-56.123	15.068	-55,727	15.099	0.395	0,031
16,536	-56.623	15.245	-56,241	15.249	0.382	0,004
16,569	-57.124	15.428	-56,757	15.406	0.367	-0,022
16,603	-57.625	15.616	-57,276	15.569	0.349	-0,047
16,636	-58.126	15.811	-57,798	15.739	0.327	-0,072
16,669	-58.626	16.012	-58,323	15.916	0.303	-0,095
16,703	-59.127	16.219	-58,851	16.101	0.276	-0,118
16,736	-59.628	16.433	-59,382	16.294	0.245	-0,139
16,769	-60.128	16.654	-59,918	16.496	0,211	-0,158
16,803	-60.629	16.883	-60,457	16.708	0.172	-0,175
16,836	-61.130	17.119	-61,000	16,929	0,130	-0,190
16.869	-61.630	17.364	-61,548	17.162	0.082	-0,202
16,903	-62.131	17.617	-62,101	17.407	0.030	-0,210
16,936	-62.632	17.879	-62,659	17.664	-0.027	-0,214
16,969	-63.132	18.150	-63,222	17.936	-0,090	-0,214
17,003	-63.633	18.432	-63,792	18.223	-0.159	-0,209
17,036	-64.133	18.723	-63,792	18.223	0.341	-0.501
17,069	-64.634	19.026	-64,435	19.418	0.199	0,392
17,103	-65.135	19.340	-64,435	19.418	0,699	0,078
17,136	-65.635	19.666	-64,435	19,418	1,200	-0,248
17,169	-66.136	20.005	-66,731	37.780	-0,595	17,775
17,203	-66.636	20.357	22,354	22.354	88,990	1,997
17,236	-67.137	20.724	22,354	22.354	89,491	1,630
17,269	-67.637	21.106	22,354	22.354	89,991	1,248
17,303	-68.138	21.503	22,354	22.354	90,492	0,851

20 October 1965

LOCAL TIME	TRUE A	TRUE B	MEAS A	MEAS B	ERROR A	ERROR B
9.973	64.354	65.540	64.171	65.288	-0.183	-0.252
10.007	63.881	65.439	63.969	65.532	0.088	0.093
10.040	63.403	65.341	63.211	65.039	-0.191	-0.302
10.073	62.920	65.245	63.014	65.297	0.094	0.052
10.107	62.431	65.151	62.264	64.830	-0.168	-0.321
10.140	61.938	65.059	62.070	65.100	0.132	0.041
10.173	61.440	64.970	61.326	64.657	-0.113	-0.313
10.207	60.936	64.883	61.136	64.939	0.201	0.056
10.240	60.426	64.798	60.954	65.227	0.528	0.429
10.273	59.911	64.715	59.474	64.409	-0.437	-0.305
10.307	59.390	64.634	59.290	64.713	-0.100	0.079
10.340	58.863	64.555	58.556	64.330	-0.307	-0.225
10.373	58.330	64.477	57.829	63.960	-0.501	-0.517
10.407	57.792	64.402	57.643	64.278	-0.149	-0.124
10.440	57.247	64.328	56.916	63.924	-0.331	-0.404
10.473	56.695	64.257	56.731	64.250	0.036	-0.006
10.507	56.137	64.187	56.004	63.912	-0.133	-0.274
10.540	55.573	64.118	55.821	64.247	0.248	0.129
10.573	55.002	64.051	55.093	63.923	0.092	-0.128
10.607	54.424	63.986	54.182	63.956	-0.242	-0.030
10.640	53.839	63.923	53.456	63.655	-0.383	-0.267
10.673	53.247	63.861	53.268	64.009	0.021	0.148
10.707	52.648	63.800	52.540	63.721	-0.108	-0.079
10.740	52.041	63.741	51.815	63.441	-0.227	-0.300
10.773	51.427	63.683	51.620	63.805	0.193	0.122
10.807	50.806	63.627	50.891	63.537	0.085	-0.091
10.840	50.177	63.572	50.696	63.908	0.520	0.335
10.873	49.539	63.519	49.231	63.400	-0.309	-0.119
10.907	48.894	63.467	48.501	63.157	-0.393	-0.310
10.940	48.241	63.416	48.290	63.540	0.049	0.123
10.973	47.580	63.367	47.555	63.306	-0.025	-0.061
11.007	46.911	63.319	46.821	63.080	-0.090	-0.239
11.040	46.233	63.272	46.600	63.472	0.368	0.200
11.073	45.546	63.226	45.120	63.042	-0.426	-0.184
11.107	44.851	63.181	44.381	62.837	-0.470	-0.345
11.140	44.147	63.138	44.140	63.240	-0.007	0.101
11.173	43.434	63.096	43.393	63.042	-0.041	-0.054
11.207	42.713	63.055	42.647	62.850	-0.066	-0.205
11.240	41.982	63.015	42.394	63.262	0.412	0.247
11.273	41.242	62.976	41.638	63.078	0.396	0.101
11.307	40.493	62.939	40.128	62.725	-0.365	-0.213
11.340	39.735	62.902	39.851	63.147	0.116	0.245
11.373	38.967	62.867	39.086	62.980	0.119	0.114
11.407	38.190	62.832	38.321	62.819	0.131	-0.013
11.440	37.403	62.799	37.555	62.662	0.152	-0.137

LOCAL TIME	TRUE A	TRUE B	MEAS A	MEAS B	ERROR A	ERROR B
11.473	36.607	62.766	36.474	62.944	-0.133	0.178
11.507	35.802	62.735	35.697	62.798	-0.104	0.063
11.540	34.987	62.704	34.920	62.657	-0.067	-0.048
11.573	34.162	62.675	34.141	62.520	-0.021	-0.155
11.607	33.328	62.646	33.361	62.387	0.034	-0.259
11.640	32.484	62.619	32.213	62.707	-0.271	0.088
11.673	31.630	62.592	31.420	62.584	-0.210	-0.008
11.707	30.767	62.567	30.627	62.466	-0.141	-0.101
11.740	29.895	62.542	29.831	62.351	-0.063	-0.191
11.773	29.013	62.518	29.035	62.240	0.022	-0.278
11.807	28.122	62.495	28.238	62.133	0.116	-0.362
11.840	27.221	62.473	27.000	62.495	-0.221	0.022
11.873	26.312	62.452	26.188	62.397	-0.124	-0.055
11.907	25.393	62.432	25.374	62.303	-0.019	-0.129
11.940	24.465	62.412	24.559	62.212	0.094	-0.200
11.973	23.528	62.394	23.250	62.603	-0.280	0.209
12.007	22.584	62.376	22.419	62.521	-0.165	0.145
12.040	21.631	62.359	21.587	62.443	-0.044	0.084
12.073	20.670	62.343	20.754	62.368	0.084	0.025
12.107	19.701	62.328	19.919	62.296	0.218	-0.032
12.140	18.724	62.314	19.083	62.228	0.359	-0.086
12.173	17.740	62.300	17.407	62.101	-0.333	-0.199
12.207	16.748	62.287	16.567	62.042	-0.182	-0.245
12.240	15.750	62.276	15.725	61.986	-0.025	-0.289
12.273	14.745	62.264	15.104	62.489	0.358	0.224
12.307	13.734	62.254	14.247	62.439	0.513	0.184
12.340	12.718	62.245	12.532	62.347	-0.186	0.102
12.373	11.696	62.236	11.672	62.306	-0.023	0.070
12.407	10.668	62.228	10.812	62.268	0.143	0.040
12.440	9.637	62.221	9.951	62.233	0.314	0.012
12.473	8.600	62.215	9.088	62.201	0.488	-0.014
12.507	7.561	62.209	7.361	62.146	-0.199	-0.064
12.540	6.517	62.205	6.497	62.122	-0.020	-0.082
12.573	5.471	62.201	5.632	62.102	0.161	-0.099
12.607	4.422	62.198	4.766	62.085	0.344	-0.113
12.640	3.371	62.195	3.900	62.070	0.529	-0.125
12.673	2.319	62.194	2.167	62.050	-0.152	-0.144
12.707	1.266	62.193	1.300	62.044	0.035	-0.148
12.740	0.212	62.193	0.434	62.041	0.222	-0.151
12.773	-0.843	62.193	-0.434	62.041	0.409	-0.152
12.807	-1.896	62.195	-2.167	62.050	-0.271	-0.145
12.840	-2.949	62.197	-3.034	62.059	-0.085	-0.139
12.873	-4.001	62.200	-3.900	62.070	0.101	-0.130
12.907	-5.051	62.204	-4.766	62.085	0.285	-0.119
12.940	-6.099	62.209	-5.632	62.102	0.467	-0.107

20 October 1965 (Cont'd)

LOCAL TIME	TRUE A	TRUE B	MEAS A	MEAS B	ERROR A	ERROR B
12.973	-7.143	62.214	-7.361	62.146	-0.218	-0.069
13.007	-8.185	62.220	-8.225	62.172	-0.040	-0.049
13.040	-9.224	62.227	-9.088	62.201	0.135	-0.026
13.073	-10.258	62.235	-9.951	62.233	0.307	-0.002
13.107	-11.288	62.244	-11.672	62.306	-0.385	0.062
13.140	-12.313	62.253	-12.532	62.347	-0.219	0.094
13.173	-13.333	62.263	-13.390	62.391	-0.058	0.128
13.207	-14.347	62.274	-14.247	62.439	0.099	0.164
13.240	-15.355	62.286	-15.104	62.489	0.251	0.203
13.273	-16.357	62.299	-15.958	62.542	0.398	0.244
13.307	-17.352	62.312	-17.407	62.101	-0.055	-0.211
13.340	-18.340	62.326	-18.246	62.163	0.094	-0.163
13.373	-19.321	62.341	-19.083	62.228	0.238	-0.113
13.407	-20.294	62.357	-19.919	62.296	0.375	-0.061
13.440	-21.260	62.374	-21.587	62.443	-0.327	0.069
13.473	-22.218	62.391	-22.419	62.521	-0.201	0.130
13.507	-23.167	62.410	-23.250	62.603	-0.082	0.193
13.540	-24.108	62.429	-24.079	62.688	0.029	0.259
13.573	-25.040	62.449	-24.559	62.212	0.481	-0.237
13.607	-25.964	62.470	-26.188	62.397	-0.224	-0.073
13.640	-26.878	62.492	-27.000	62.495	-0.122	0.003
13.673	-27.784	62.515	-27.811	62.596	-0.027	0.081
13.707	-28.680	62.538	-28.238	62.133	0.443	-0.405
13.740	-29.567	62.563	-29.035	62.240	0.532	-0.323
13.773	-30.445	62.588	-30.627	62.466	-0.182	-0.123
13.807	-31.313	62.615	-31.420	62.584	-0.108	-0.031
13.840	-32.171	62.642	-32.213	62.707	-0.042	0.065
13.873	-33.021	62.670	-33.005	62.834	0.016	0.163
13.907	-33.860	62.700	-33.361	62.387	0.499	-0.313
13.940	-34.690	62.730	-34.141	62.520	0.549	-0.210
13.973	-35.510	62.761	-35.697	62.798	-0.187	0.037
14.007	-36.321	62.793	-36.474	62.944	-0.153	0.150
14.040	-37.122	62.827	-37.251	63.094	-0.129	0.268
14.073	-37.914	62.861	-37.555	62.662	0.359	-0.199
14.107	-38.696	62.896	-38.321	62.819	0.375	-0.077
14.140	-39.469	62.932	-39.851	63.147	-0.382	0.215
14.173	-40.232	62.970	-40.615	63.319	-0.383	0.349
14.207	-40.986	63.008	-40.883	62.899	0.103	-0.109
14.240	-41.731	63.048	-41.638	63.078	0.092	0.030
14.273	-42.466	63.088	-42.394	63.262	0.073	0.173
14.307	-43.193	63.130	-43.393	63.042	-0.201	-0.088
14.340	-43.910	63.173	-44.140	63.240	-0.230	0.066
14.373	-44.619	63.217	-44.888	63.443	-0.269	0.226
14.407	-45.319	63.263	-45.120	63.042	0.199	-0.220
14.440	-46.010	63.309	-45.859	63.254	0.151	-0.055

20 October 1965 (Cont'd)

LOCAL TIME	TRUE A	TRUE B	MEAS A	MEAS B	ERROR A	ERROR B
14.473	-46.693	63.357	-46.600	63.472	0.092	0.115
14.507	-47.367	63.406	-46.821	63.080	0.546	-0.326
14.540	-48.032	63.456	-47.555	63.306	0.477	-0.150
14.573	-48.690	63.508	-49.028	63.780	-0.338	0.272
14.607	-49.339	63.561	-49.231	63.400	0.108	-0.161
14.640	-49.981	63.615	-49.962	63.650	0.018	0.035
14.673	-50.614	63.671	-50.696	63.908	-0.082	0.237
14.707	-51.240	63.728	-50.891	63.537	0.349	-0.191
14.740	-51.858	63.786	-51.620	63.805	0.238	0.019
14.773	-52.469	63.846	-52.540	63.721	-0.071	-0.125
14.807	-53.072	63.907	-53.268	64.009	-0.197	0.101
14.840	-53.668	63.970	-54.000	64.307	-0.333	0.336
14.873	-54.256	64.035	-54.182	63.956	0.075	-0.079
14.907	-54.838	64.101	-54.911	64.266	-0.073	0.165
14.940	-55.413	64.169	-55.093	63.923	0.320	-0.245
14.973	-55.981	64.238	-55.821	64.247	0.160	0.009
15.007	-56.543	64.309	-56.004	63.912	0.538	-0.397
15.040	-57.097	64.382	-57.463	64.600	-0.366	0.218
15.073	-57.646	64.456	-58.201	64.961	-0.555	0.505
15.107	-58.188	64.533	-58.375	64.643	-0.187	0.110
15.140	-58.724	64.611	-59.114	65.022	-0.389	0.411
15.173	-59.254	64.691	-59.290	64.713	-0.036	0.022
15.207	-59.779	64.773	-60.031	65.110	-0.252	0.337
15.240	-60.297	64.857	-60.210	64.811	0.087	-0.046
15.273	-60.810	64.943	-60.954	65.227	-0.145	0.284
15.307	-61.317	65.031	-61.136	64.939	0.180	-0.092
15.340	-61.818	65.121	-61.885	65.377	-0.066	0.255
15.373	-62.315	65.214	-62.070	65.100	0.244	-0.114
15.407	-62.806	65.309	-62.824	65.561	-0.019	0.252
15.440	-63.292	65.406	-63.014	65.297	0.278	-0.109
15.473	-63.772	65.505	-63.211	65.039	0.561	-0.466
15.507	-64.248	65.607	-63.969	65.532	0.280	-0.075
15.540	-64.719	65.711	-64.937	65.810	-0.218	0.099
15.573	-65.186	65.818	-65.717	66.355	-0.531	0.537
15.607	-65.648	65.928	-65.144	65.581	0.503	-0.347
15.640	-66.105	66.040	-66.715	66.715	-0.610	0.674
15.673	-66.558	66.156	-66.926	66.512	-0.368	0.356
15.707	-67.006	66.274	-66.355	65.717	0.651	-0.556
15.740	-67.451	66.395	-67.145	66.318	0.305	-0.077
15.773	-67.891	66.519	-68.179	66.774	-0.289	0.255
15.807	-68.327	66.646	-69.006	67.450	-0.679	0.804
15.840	-68.759	66.776	-68.658	66.456	0.100	-0.320
15.873	-69.187	66.910	-68.658	66.456	0.529	-0.454
15.907	-69.612	67.048	-68.911	66.312	0.701	-0.735
15.940	-70.032	67.188	-70.592	67.793	-0.560	0.605